



$$J = 0$$

was  $H^0$

In the following  $H$  refers to the signal that has been discovered in the Higgs searches. Whereas the observed signal is labeled as a spin 0 particle and is called a Higgs Boson, the detailed properties of  $H$  and its role in the context of electroweak symmetry breaking need to be further clarified. These issues are addressed by the measurements listed below.

Concerning mass limits and cross section limits that have been obtained in the searches for neutral and charged Higgs bosons, see the sections "Searches for Neutral Higgs Bosons" and "Searches for Charged Higgs Bosons ( $H^\pm$  and  $H^{\pm\pm}$ )", respectively.

NODE=S126

NODE=S126

## $H$ MASS

NODE=S126M

VALUE (GeV)	DOCUMENT ID	TECN	COMMENT
<b>125.13±0.11 OUR AVERAGE</b>	Error includes scale factor of 1.5. See the ideogram below. [125.20 ± 0.11 GeV OUR 2025 AVERAGE Scale factor = 1.4]		
125.04±0.12	<sup>1</sup> HAYRAPETY...25L	CMS	$pp$ , 13 TeV, $ZZ^* \rightarrow 4\ell$
125.10±0.11	<sup>2</sup> AAD	23BP ATLS	$pp$ , 13 TeV, $\gamma\gamma$ , $ZZ^* \rightarrow 4\ell$
125.78±0.26	<sup>3</sup> SIRUNYAN	20L CMS	$pp$ , 13 TeV, $\gamma\gamma$
125.09±0.21±0.11	<sup>4,5</sup> AAD	15B LHC	$pp$ , 7, 8 TeV
● ● ● We do not use the following data for averages, fits, limits, etc. ● ● ●			
124.99±0.18±0.04	<sup>6</sup> AAD	23AU ATLS	$pp$ , 13 TeV, $ZZ^* \rightarrow 4\ell$
124.94±0.17±0.03	<sup>7</sup> AAD	23AU ATLS	$pp$ , 7, 8, 13 TeV, $ZZ^* \rightarrow 4\ell$
125.11±0.11	<sup>8</sup> AAD	23BP ATLS	$pp$ , 7, 8, 13 TeV, $\gamma\gamma$ , $ZZ^* \rightarrow 4\ell$
125.17±0.11±0.09	<sup>9</sup> AAD	23BU ATLS	$pp$ , 13 TeV, $\gamma\gamma$
125.22±0.11±0.09	<sup>10</sup> AAD	23BU ATLS	$pp$ , 7, 8, 13 TeV, $\gamma\gamma$
125.46±0.16	<sup>11</sup> SIRUNYAN	20L CMS	$pp$ , 13 TeV, $\gamma\gamma$ , $ZZ^* \rightarrow 4\ell$
125.38±0.14	<sup>12</sup> SIRUNYAN	20L CMS	$pp$ , 7, 8, 13 TeV, $\gamma\gamma$ , $ZZ^* \rightarrow 4\ell$
124.79±0.37	<sup>13</sup> AABOUD	18BMATLS	$pp$ , 13 TeV, $ZZ^* \rightarrow 4\ell$
124.93±0.40	<sup>14</sup> AABOUD	18BMATLS	$pp$ , 13 TeV, $\gamma\gamma$
124.86±0.27	<sup>4</sup> AABOUD	18BMATLS	$pp$ , 13 TeV, $\gamma\gamma$ , $ZZ^* \rightarrow 4\ell$
124.97±0.24	<sup>4,15</sup> AABOUD	18BMATLS	$pp$ , 7, 8, 13 TeV, $\gamma\gamma$ , $ZZ^* \rightarrow 4\ell$
125.26±0.20±0.08	<sup>16</sup> SIRUNYAN	17AV CMS	$pp$ , 13 TeV, $ZZ^* \rightarrow 4\ell$
125.07±0.25±0.14	<sup>5</sup> AAD	15B LHC	$pp$ , 7, 8 TeV, $\gamma\gamma$
125.15±0.37±0.15	<sup>5</sup> AAD	15B LHC	$pp$ , 7, 8 TeV, $ZZ^* \rightarrow 4\ell$
126.02±0.43±0.27	AAD	15B ATLS	$pp$ , 7, 8 TeV, $\gamma\gamma$
124.51±0.52±0.04	AAD	15B ATLS	$pp$ , 7, 8 TeV, $ZZ^* \rightarrow 4\ell$
125.59±0.42±0.17	AAD	15B CMS	$pp$ , 7, 8 TeV, $ZZ^* \rightarrow 4\ell$
125.02 <sup>+0.26+0.14</sup> <sub>-0.27-0.15</sub>	<sup>17</sup> KHACHATRY...15AM	CMS	$pp$ , 7, 8 TeV
125.36±0.37±0.18	<sup>4,18</sup> AAD	14W ATLS	$pp$ , 7, 8 TeV
125.98±0.42±0.28	<sup>18</sup> AAD	14W ATLS	$pp$ , 7, 8 TeV, $\gamma\gamma$
124.51±0.52±0.06	<sup>18</sup> AAD	14W ATLS	$pp$ , 7, 8 TeV, $ZZ^* \rightarrow 4\ell$
125.6 ±0.4 ±0.2	<sup>19</sup> CHATRCHYAN14AA	CMS	$pp$ , 7, 8 TeV, $ZZ^* \rightarrow 4\ell$
122 ±7	<sup>20</sup> CHATRCHYAN14K	CMS	$pp$ , 7, 8 TeV, $\tau\tau$
124.70±0.31±0.15	<sup>21</sup> KHACHATRY...14P	CMS	$pp$ , 7, 8 TeV, $\gamma\gamma$
125.5 ±0.2 <sup>+0.5</sup> <sub>-0.6</sub>	<sup>4,22</sup> AAD	13AK ATLS	$pp$ , 7, 8 TeV
126.8 ±0.2 ±0.7	<sup>22</sup> AAD	13AK ATLS	$pp$ , 7, 8 TeV, $\gamma\gamma$
124.3 <sup>+0.6+0.5</sup> <sub>-0.5-0.3</sub>	<sup>22</sup> AAD	13AK ATLS	$pp$ , 7, 8 TeV, $ZZ^* \rightarrow 4\ell$
125.8 ±0.4 ±0.4	<sup>4,23</sup> CHATRCHYAN13J	CMS	$pp$ , 7, 8 TeV
126.2 ±0.6 ±0.2	<sup>23</sup> CHATRCHYAN13J	CMS	$pp$ , 7, 8 TeV, $ZZ^* \rightarrow 4\ell$
126.0 ±0.4 ±0.4	<sup>4,24</sup> AAD	12AI ATLS	$pp$ , 7, 8 TeV
125.3 ±0.4 ±0.5	<sup>4,25</sup> CHATRCHYAN12N	CMS	$pp$ , 7, 8 TeV

NODE=S126M

NEW

OCCUR=2

OCCUR=2

OCCUR=2

OCCUR=2

OCCUR=3

OCCUR=2

OCCUR=3

OCCUR=4

OCCUR=2

OCCUR=3

OCCUR=4

OCCUR=5

OCCUR=6

OCCUR=2

OCCUR=3

OCCUR=2

OCCUR=3

OCCUR=2

- <sup>1</sup> HAYRAPETYAN 25L use 138 fb<sup>-1</sup> of  $pp$  collisions at  $E_{\text{cm}} = 13$  TeV with  $H \rightarrow ZZ^* \rightarrow 4\ell$  where  $\ell = e, \mu$ .
- <sup>2</sup> AAD 23BP combine 13 TeV results of  $H \rightarrow \gamma\gamma$  (AAD 23BU) and  $H \rightarrow ZZ^* \rightarrow 4\ell$  where  $\ell = e, \mu$  (AAD 23AU) using 140 fb<sup>-1</sup> of  $pp$  collision data. The result is  $125.10 \pm 0.09(\text{stat}) \pm 0.07(\text{syst})$  GeV.
- <sup>3</sup> SIRUNYAN 20L use 35.9 fb<sup>-1</sup> of  $pp$  collisions at  $E_{\text{cm}} = 13$  TeV with  $H \rightarrow \gamma\gamma$ .
- <sup>4</sup> Combined value from  $\gamma\gamma$  and  $ZZ^* \rightarrow 4\ell$  final states.
- <sup>5</sup> ATLAS and CMS data are fitted simultaneously.
- <sup>6</sup> AAD 23AU use 139 fb<sup>-1</sup> of  $pp$  collisions at  $E_{\text{cm}} = 13$  TeV with  $H \rightarrow ZZ^* \rightarrow 4\ell$  where  $\ell = e, \mu$ .
- <sup>7</sup> AAD 23AU combine 13 TeV results with 7 and 8 TeV results (AAD 14W).
- <sup>8</sup> AAD 23BP combine 13 TeV results with 7 and 8 TeV results. The result is  $125.11 \pm 0.09(\text{stat}) \pm 0.06(\text{syst})$  GeV.
- <sup>9</sup> AAD 23BU use 140 fb<sup>-1</sup> of  $pp$  collisions at  $E_{\text{cm}} = 13$  TeV with  $H \rightarrow \gamma\gamma$ .
- <sup>10</sup> AAD 23BU combine 13 TeV results with 7 and 8 TeV results (AAD 15B).
- <sup>11</sup> SIRUNYAN 20L result of  $H \rightarrow \gamma\gamma$  is combined with that of  $H \rightarrow ZZ^* \rightarrow 4\ell$  where  $\ell = e, \mu$  (SIRUNYAN 17AV).
- <sup>12</sup> SIRUNYAN 20L combine 13 TeV results with 7 and 8 TeV results (KHACHATRYAN 15AM).
- <sup>13</sup> AABOUD 18BM use 36.1 fb<sup>-1</sup> of  $pp$  collisions at  $E_{\text{cm}} = 13$  TeV with  $H \rightarrow ZZ^* \rightarrow 4\ell$  where  $\ell = e, \mu$ .
- <sup>14</sup> AABOUD 18BM use 36.1 fb<sup>-1</sup> of  $pp$  collisions at  $E_{\text{cm}} = 13$  TeV with  $H \rightarrow \gamma\gamma$ .
- <sup>15</sup> AABOUD 18BM combine 13 TeV results with 7 and 8 TeV results. Other combined results are summarized in their Fig. 4.
- <sup>16</sup> SIRUNYAN 17AV use 35.9 fb<sup>-1</sup> of  $pp$  collisions at  $E_{\text{cm}} = 13$  TeV with  $H \rightarrow ZZ^* \rightarrow 4\ell$  where  $\ell = e, \mu$ .
- <sup>17</sup> KHACHATRYAN 15AM use up to 5.1 fb<sup>-1</sup> of  $pp$  collisions at  $E_{\text{cm}} = 7$  TeV and up to 19.7 fb<sup>-1</sup> at  $E_{\text{cm}} = 8$  TeV.
- <sup>18</sup> AAD 14W use 4.5 fb<sup>-1</sup> of  $pp$  collisions at  $E_{\text{cm}} = 7$  TeV and 20.3 fb<sup>-1</sup> at 8 TeV.
- <sup>19</sup> CHATRCHYAN 14AA use 5.1 fb<sup>-1</sup> of  $pp$  collisions at  $E_{\text{cm}} = 7$  TeV and 19.7 fb<sup>-1</sup> at  $E_{\text{cm}} = 8$  TeV.
- <sup>20</sup> CHATRCHYAN 14K use 4.9 fb<sup>-1</sup> of  $pp$  collisions at  $E_{\text{cm}} = 7$  TeV and 19.7 fb<sup>-1</sup> at  $E_{\text{cm}} = 8$  TeV.
- <sup>21</sup> KHACHATRYAN 14P use 5.1 fb<sup>-1</sup> of  $pp$  collisions at  $E_{\text{cm}} = 7$  TeV and 19.7 fb<sup>-1</sup> at  $E_{\text{cm}} = 8$  TeV.
- <sup>22</sup> AAD 13AK use 4.7 fb<sup>-1</sup> of  $pp$  collisions at  $E_{\text{cm}} = 7$  TeV and 20.7 fb<sup>-1</sup> at  $E_{\text{cm}} = 8$  TeV. Superseded by AAD 14W.
- <sup>23</sup> CHATRCHYAN 13J use 5.1 fb<sup>-1</sup> of  $pp$  collisions at  $E_{\text{cm}} = 7$  TeV and 12.2 fb<sup>-1</sup> at  $E_{\text{cm}} = 8$  TeV.
- <sup>24</sup> AAD 12AI obtain results based on 4.6–4.8 fb<sup>-1</sup> of  $pp$  collisions at  $E_{\text{cm}} = 7$  TeV and 5.8–5.9 fb<sup>-1</sup> at  $E_{\text{cm}} = 8$  TeV. An excess of events over background with a local significance of  $5.9 \sigma$  is observed at  $m_H = 126$  GeV. See also AAD 12DA.
- <sup>25</sup> CHATRCHYAN 12N obtain results based on 4.9–5.1 fb<sup>-1</sup> of  $pp$  collisions at  $E_{\text{cm}} = 7$  TeV and 5.1–5.3 fb<sup>-1</sup> at  $E_{\text{cm}} = 8$  TeV. An excess of events over background with a local significance of  $5.0 \sigma$  is observed at about  $m_H = 125$  GeV. See also CHATRCHYAN 12BY and CHATRCHYAN 13Y.

NODE=S126M;LINKAGE=T

NODE=S126M;LINKAGE=P

NODE=S126M;LINKAGE=J  
 NODE=S126M;LINKAGE=AA  
 NODE=S126M;LINKAGE=LC  
 NODE=S126M;LINKAGE=N

NODE=S126M;LINKAGE=O  
 NODE=S126M;LINKAGE=Q

NODE=S126M;LINKAGE=R  
 NODE=S126M;LINKAGE=S  
 NODE=S126M;LINKAGE=K

NODE=S126M;LINKAGE=M

NODE=S126M;LINKAGE=G

NODE=S126M;LINKAGE=H  
 NODE=S126M;LINKAGE=I

NODE=S126M;LINKAGE=F

NODE=S126M;LINKAGE=E

NODE=S126M;LINKAGE=A  
 NODE=S126M;LINKAGE=B

NODE=S126M;LINKAGE=D

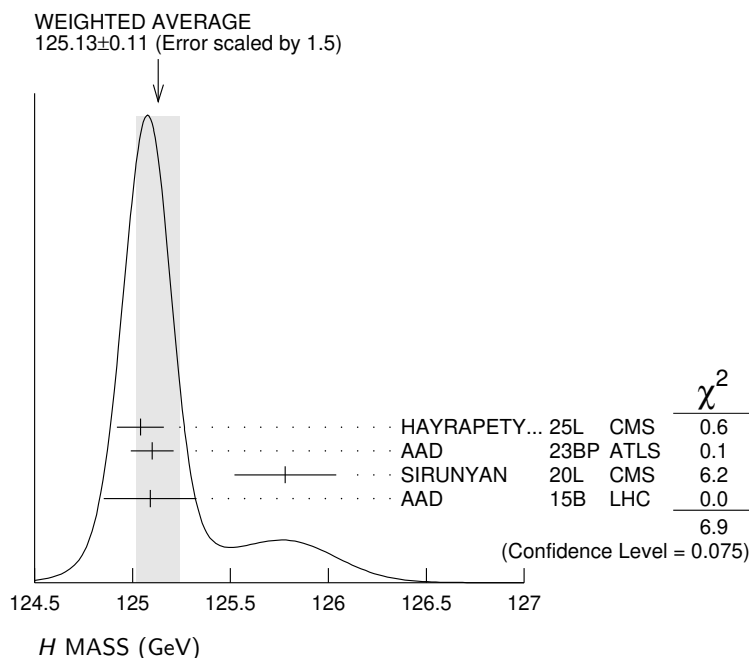
NODE=S126M;LINKAGE=C

NODE=S126M;LINKAGE=LH

NODE=S126M;LINKAGE=CT

NODE=S126M;LINKAGE=AI

NODE=S126M;LINKAGE=CH



## H SPIN AND CP PROPERTIES

NODE=S126CP

NODE=S126CP

The observation of the signal in the  $\gamma\gamma$  final state rules out the possibility that the discovered particle has spin 1, as a consequence of the Landau-Yang theorem. This argument relies on the assumptions that the decaying particle is an on-shell resonance and that the decay products are indeed two photons rather than two pairs of boosted photons, which each could in principle be misidentified as a single photon.

Concerning distinguishing the spin 0 hypothesis from a spin 2 hypothesis, some care has to be taken in modelling the latter in order to ensure that the discriminating power is actually based on the spin properties rather than on unphysical behavior that may affect the model of the spin 2 state.

Under the assumption that the observed signal consists of a single state rather than an overlap of more than one resonance, it is sufficient to discriminate between distinct hypotheses in the spin analyses. On the other hand, the determination of the  $CP$  properties is in general much more difficult since in principle the observed state could consist of any admixture of  $CP$ -even and  $CP$ -odd components. As a first step, the compatibility of the data with distinct hypotheses of pure  $CP$ -even and pure  $CP$ -odd states with different spin assignments has been investigated. In order to treat the case of a possible mixing of different  $CP$  states, certain cross section ratios are considered. Those cross section ratios need to be distinguished from the amount of mixing between a  $CP$ -even and a  $CP$ -odd state, as the cross section ratios depend in addition also on the coupling strengths of the  $CP$ -even and  $CP$ -odd components to the involved particles. A small relative coupling implies a small sensitivity of the corresponding cross section ratio to effects of  $CP$  mixing.

VALUE	DOCUMENT ID	TECN	COMMENT
● ● ● We do not use the following data for averages, fits, limits, etc. ● ● ●			
1	HAYRAPETY...25R	CMS	$t\bar{t}H, tH, H \rightarrow b\bar{b}, 13 \text{ TeV}$
2	AAD 24AG	ATLS	$H \rightarrow ZZ^* \rightarrow 4\ell, \text{VBF}, 13 \text{ TeV}$
3	AAD 24J	ATLS	$t\bar{t}H, tH, H \rightarrow b\bar{b}, 13 \text{ TeV}$
4	AAD 23AK	ATLS	$H \rightarrow \tau\tau, 13 \text{ TeV}$
5	AAD 23AN	ATLS	$H \rightarrow \gamma\gamma, \text{VBF}, 13 \text{ TeV}$
6	TUMASYAN 23AJ	CMS	$H \rightarrow \tau\tau, 13 \text{ TeV}$
7	TUMASYAN 23P	CMS	$t\bar{t}H, H \rightarrow WW^*, \tau\tau, 13 \text{ TeV}$
8	AAD 22V	ATLS	$WW^* (\rightarrow e\nu\mu\nu)+2j, 13 \text{ TeV}$
9	TUMASYAN 22Y	CMS	$H \rightarrow \tau\tau, 13 \text{ TeV}$
10	AAD 20N	ATLS	$H \rightarrow \tau\tau, \text{VBF}, 13 \text{ TeV}$
11	AAD 20Z	ATLS	$t\bar{t}H, H \rightarrow \gamma\gamma, 13 \text{ TeV}$
12	SIRUNYAN 20AS	CMS	$t\bar{t}H, H \rightarrow \gamma\gamma, 13 \text{ TeV}$
13	SIRUNYAN 19BL	CMS	$pp, 7, 8, 13 \text{ TeV}, ZZ^*/ZZ \rightarrow 4\ell$
14	SIRUNYAN 19BZ	CMS	$pp \rightarrow H+2\text{jets (VBF, ggF, VH)}, H \rightarrow \tau\tau, 13 \text{ TeV}$
15	AABOUD 18AJ	ATLS	$H \rightarrow ZZ^* \rightarrow 4\ell (\ell = e, \mu), 13\text{TeV}$
16	SIRUNYAN 17AM	CMS	$pp \rightarrow H+\geq 2j, H \rightarrow 4\ell (\ell = e, \mu)$
17	AAD 16	ATLS	$H \rightarrow \gamma\gamma$
18	AAD 16BL	ATLS	$pp \rightarrow HjjX (\text{VBF}), H \rightarrow \tau\tau, 8 \text{ TeV}$
19	KHACHATRY...16AB	CMS	$pp \rightarrow WH, ZH, H \rightarrow b\bar{b}, 8 \text{ TeV}$
20	AAD 15AX	ATLS	$H \rightarrow WW^*$
21	AAD 15CI	ATLS	$H \rightarrow ZZ^*, WW^*, \gamma\gamma$
22	AALTONEN 15	TEVA	$p\bar{p} \rightarrow WH, ZH, H \rightarrow b\bar{b}$
23	AALTONEN 15B	CDF	$p\bar{p} \rightarrow WH, ZH, H \rightarrow b\bar{b}$
24	KHACHATRY...15Y	CMS	$H \rightarrow 4\ell, WW^*, \gamma\gamma$
25	ABAZOV 14F	D0	$p\bar{p} \rightarrow WH, ZH, H \rightarrow b\bar{b}$
26	CHATRCHYAN 14AA	CMS	$H \rightarrow ZZ^*$
27	CHATRCHYAN 14G	CMS	$H \rightarrow WW^*$
28	KHACHATRY...14P	CMS	$H \rightarrow \gamma\gamma$
29	AAD 13AJ	ATLS	$H \rightarrow \gamma\gamma, ZZ^* \rightarrow 4\ell, WW^* \rightarrow \ell\nu\ell\nu$
30	CHATRCHYAN 13J	CMS	$H \rightarrow ZZ^* \rightarrow 4\ell$

NODE=S126CP

- 1 HAYRAPETYAN 25R measure the  $t\bar{t}H$  and  $tH$  productions with  $H \rightarrow b\bar{b}$  decay channel using  $138 \text{ fb}^{-1}$  of data at  $E_{\text{cm}} = 13 \text{ TeV}$ . Two-dimensional likelihood scan of  $(\kappa_t, \tilde{\kappa}_t)$  to measure the  $CP$  structure of the top Yukawa coupling is shown in their Fig. 16, where  $\kappa_V = 1$ . With other channels (SIRUNYAN 20AS, SIRUNYAN 21AE, TUMASYAN 23P), the  $CP$ -odd fraction  $f_{CP}^{\text{odd}}$  and the  $CP$  mixing angle  $\alpha$  are constrained to be  $|f_{CP}^{\text{odd}}| < 0.85$  and  $\cos\alpha > 0.39$  at 95% CL. NODE=S126CP;LINKAGE=CA
- 2 AAD 24AG search for  $CP$  violation in the decay kinematics and VBF production of the Higgs boson using  $H \rightarrow ZZ^* \rightarrow 4\ell$  decay channel ( $\ell = e, \mu$ ) with  $139 \text{ fb}^{-1}$  at  $E_{\text{cm}} = 13 \text{ TeV}$ . By using the optimal observables, the data constrain six  $CP$ -odd Wilson coefficients in two effective field theory bases: the Warsaw basis and the Higgs basis. The result is given in their Table 5 and Figs. 7–11. The differential fiducial cross sections for the four optimal observables are measured as shown in their Fig. 13. The VBF fiducial cross sections are given in their Table 6. NODE=S126CP;LINKAGE=BA
- 3 AAD 24J measure the  $CP$  structure of the top Yukawa coupling using  $139 \text{ fb}^{-1}$  of data at  $E_{\text{cm}} = 13 \text{ TeV}$ . The  $CP$ -mixing angle  $\alpha$  for top Yukawa coupling is measured to be  $(11^{+52}_{-73})^\circ$  with the top Yukawa coupling strength modifier  $\kappa_t$ . See their Fig. 3. The data disfavour the pure  $CP$ -odd ( $\alpha = 90^\circ$ ) at  $1.2 \sigma$ . NODE=S126CP;LINKAGE=Z
- 4 AAD 23AK measure the  $CP$  structure of the  $\tau$  Yukawa coupling using  $139 \text{ fb}^{-1}$  of data at  $E_{\text{cm}} = 13 \text{ TeV}$ . The  $CP$ -mixing angle  $\alpha$  for  $\tau$  Yukawa coupling is measured to be  $9 \pm 16^\circ$ . The data disfavour the pure  $CP$ -odd ( $\alpha = 90^\circ$ ) at  $3.4 \sigma$ . NODE=S126CP;LINKAGE=V
- 5 AAD 23AN test  $CP$  invariance in  $H$  production via VBF using  $H \rightarrow \gamma\gamma$  decay channel with  $139 \text{ fb}^{-1}$  at  $E_{\text{cm}} = 13 \text{ TeV}$ . By using the Optimal Observable method, the data constrain parameters describing the strength of the  $CP$ -odd component in the coupling between Higgs and  $W/Z$  in effective field theory bases:  $\tilde{d}$  in the HISZ basis and  $c_{H\tilde{W}}$  in the Warsaw basis. The result is  $-0.010 \leq \tilde{d} \leq 0.040$  and  $-0.15 \leq c_{H\tilde{W}} \leq 0.67$  at 68% CL. See their Table I, which shows the result combined with  $H \rightarrow \tau\tau$  (AAD 20N):  $-0.012 \leq \tilde{d} \leq 0.030$  at 68% CL. NODE=S126CP;LINKAGE=X
- 6 TUMASYAN 23AJ constraint anomalous couplings of the Higgs to vector bosons and fermions using  $pp \rightarrow H \rightarrow \tau\tau$  at  $E_{\text{cm}} = 13 \text{ TeV}$  with  $138 \text{ fb}^{-1}$  data. The  $CP$ -violating parameter in gluon-fusion production  $f_{a3}^{ggH}$  and the effective mixing angle  $\alpha^{Hff}$  are given in their Table VII with  $H \rightarrow \tau\tau$  and  $f_{a3}^{ggH}$  in their Table X with  $H \rightarrow \tau\tau$  and  $H \rightarrow 4\ell$ . Using the VBF production analysis, the  $CP$ -violating parameter  $f_{a3}$  and the  $CP$ -conserving parameters  $f_{a2}$ ,  $f_{\Lambda 1}$  and  $f_{\Lambda 1}^{Z\gamma}$  are given in their Table VIII with  $H \rightarrow \tau\tau$  and Table IX with  $H \rightarrow \tau\tau$  and  $H \rightarrow 4\ell$ . The  $CP$ -violating parameter  $f_{CP}^{Htt}$  is constrained to be  $0.03^{+0.17}_{-0.03}$  using  $H \rightarrow \tau\tau$ ,  $H \rightarrow 4\ell$  and  $H \rightarrow \gamma\gamma$ . NODE=S126CP;LINKAGE=W
- 7 TUMASYAN 23P constrain  $\tilde{\kappa}_t$  from  $t\bar{t}H$  and  $tH$  decaying  $H \rightarrow WW^*$  and  $H \rightarrow \tau\tau$  (multilepton decay mode) with  $138 \text{ fb}^{-1}$   $pp$  collision data at  $E_{\text{cm}} = 13 \text{ TeV}$ . The  $\tilde{\kappa}_t$  is constrained to be  $|\tilde{\kappa}_t| \leq 1.4$  at 95% CL by fixing  $\kappa_t = 1$  and other couplings ( $\kappa_V$  etc.) to the SM values, see their Table 6 (see their Fig. 9 for 2-dim contours). The fractional contribution of the  $CP$ -odd component  $|f_{CP}^{Htt}|$  is constrained to  $(0.24, 0.81)$  at 68% CL with a best fit value of 0.59. The combination with other  $t\bar{t}H$  decaying  $H \rightarrow \gamma\gamma$  (SIRUNYAN 20AS) and  $H \rightarrow 4\ell$  (SIRUNYAN 21AE) constraints to be  $|\tilde{\kappa}_t| \leq 1.07$  at 95% CL and  $|f_{CP}^{Htt}| < 0.55$  at 68% CL with a best fit value of 0.28. NODE=S126CP;LINKAGE=Y
- 8 AAD 22V measure the  $CP$  properties of the effective Higgs-gluon interaction using gluon fusion  $H \rightarrow WW^* \rightarrow e\nu\mu\nu$  plus two jets with  $36.1 \text{ fb}^{-1}$  of data at  $E_{\text{cm}} = 13 \text{ TeV}$ . The measured tangent of the  $CP$ -mixing angle  $\tan\alpha$  is  $0.0 \pm 0.4 \pm 0.3$  assuming the standard model  $HVV$  couplings. See their Fig. 6. NODE=S126CP;LINKAGE=U
- 9 TUMASYAN 22Y measure the  $CP$  structure of the  $\tau$  Yukawa coupling using  $137 \text{ fb}^{-1}$  of data at  $E_{\text{cm}} = 13 \text{ TeV}$ . The  $CP$ -mixing angle  $\alpha$  for  $\tau$  Yukawa coupling is measured to be  $-1 \pm 19^\circ$ . The data disfavour the pure  $CP$ -odd ( $\alpha = 90^\circ$ ) at  $3.0 \sigma$ . NODE=S126CP;LINKAGE=T
- 10 AAD 20N test  $CP$  invariance in  $H$  production via VBF using  $H \rightarrow \tau\tau$  decay channel with  $36.1 \text{ fb}^{-1}$  at  $E_{\text{cm}} = 13 \text{ TeV}$ . By using the Optimal Observable method, the data constrain a parameter  $\tilde{d}$ , which is for the strength of  $CP$  violation in an effective field theory, to be  $-0.090 \leq \tilde{d} \leq 0.035$  at 68% CL (see their Fig. 6). NODE=S126CP;LINKAGE=Q
- 11 AAD 20Z exclude a  $CP$ -mixing angle  $\alpha$ ,  $|\alpha| > 43^\circ$  at 95% CL, where  $\alpha = 0$  represents the Standard Model, in  $139 \text{ fb}^{-1}$  of data at  $E_{\text{cm}} = 13 \text{ TeV}$ . The pure  $CP$ -odd structure of the top Yukawa coupling ( $\alpha = 90^\circ$ ) is excluded at  $3.9 \sigma$ . NODE=S126CP;LINKAGE=S
- 12 SIRUNYAN 20AS exclude the pure  $CP$ -odd structure of the top Yukawa coupling at  $3.2 \sigma$  using  $t\bar{t}H$ ,  $H \rightarrow \gamma\gamma$  in  $137 \text{ fb}^{-1}$  of data at  $E_{\text{cm}} = 13 \text{ TeV}$ . The fractional contribution of the  $CP$ -odd component  $f_{CP}^{t\bar{t}H}$  is measured to be  $0.00 \pm 0.33$ . NODE=S126CP;LINKAGE=R
- 13 SIRUNYAN 19BL measure the anomalous  $HVV$  couplings from on-shell and off-shell production in the  $4\ell$  final state. Data of  $80.2 \text{ fb}^{-1}$  at 13 TeV,  $19.7 \text{ fb}^{-1}$  at 8 TeV, and  $5.1 \text{ fb}^{-1}$  at 7 TeV are used. See their Tables VI and VII for anomalous  $HVV$  couplings of  $CP$ -violating and  $CP$ -conserving parameters with on- and off-shells. NODE=S126CP;LINKAGE=P
- 14 SIRUNYAN 19BZ constrain anomalous  $HVV$  couplings of the Higgs boson with data of  $35.9 \text{ fb}^{-1}$  at  $E_{\text{cm}} = 13 \text{ TeV}$  using Higgs boson candidates with two jets produced in VBF, ggF, and  $VH$  that decay to  $\tau\tau$ . See their Table 2 and Fig. 10, which show 68% NODE=S126CP;LINKAGE=O

CL and 95% CL intervals. Combining those with the  $H \rightarrow 4\ell$  (SIRUNYAN 19BL, on-shell scenario), results shown in their Tables 3, 4, and Fig. 11 are obtained. A  $CP$ -violating parameter is set to be  $f_{a3}\cos(\phi_{a3}) = (0.00 \pm 0.27) \times 10^{-3}$  and  $CP$ -conserving parameters are  $f_{a2}\cos(\phi_{a2}) = (0.08^{+1.04}_{-0.21}) \times 10^{-3}$ ,  $f_{\Lambda 1}\cos(\phi_{\Lambda 1}) = (0.00^{+0.53}_{-0.09}) \times 10^{-3}$ , and  $f_{\Lambda 1}^Z \gamma \cos(\phi_{\Lambda 1}^Z \gamma) = (0.0^{+1.1}_{-1.3}) \times 10^{-3}$ .

- 15 AABOUD 18AJ study the tensor structure of the Higgs boson couplings using an effective Lagrangian using  $36.1 \text{ fb}^{-1}$  of  $pp$  collision data at  $E_{\text{cm}} = 13 \text{ TeV}$ . Constraints are set on the non-Standard-Model  $CP$ -even and  $CP$ -odd couplings to  $Z$  bosons and on the  $CP$ -odd coupling to gluons. See their Figs. 9 and 10, and Tables 10 and 11. NODE=S126CP;LINKAGE=N
- 16 SIRUNYAN 17AM constrain anomalous couplings of the Higgs boson with  $5.1 \text{ fb}^{-1}$  of  $pp$  collisions at  $E_{\text{cm}} = 7 \text{ TeV}$ ,  $19.7 \text{ fb}^{-1}$  at  $E_{\text{cm}} = 8 \text{ TeV}$ , and  $38.6 \text{ fb}^{-1}$  at  $E_{\text{cm}} = 13 \text{ TeV}$ . See their Table 3 and Fig. 3, which show 68% CL and 95% CL intervals. A  $CP$  violation parameter  $f_{a3}$  is set to be  $f_{a3}\cos(\phi_{a3}) = [-0.38, 0.46]$  at 95% CL ( $\phi_{a3} = 0$  or  $\pi$ ). NODE=S126CP;LINKAGE=M
- 17 AAD 16 study  $H \rightarrow \gamma\gamma$  with an effective Lagrangian including  $CP$  even and odd terms in  $20.3 \text{ fb}^{-1}$  of  $pp$  collisions at  $E_{\text{cm}} = 8 \text{ TeV}$ . The data is consistent with the expectations for the Higgs boson of the Standard Model. Limits on anomalous couplings are also given. NODE=S126CP;LINKAGE=J
- 18 AAD 16BL study VBF  $H \rightarrow \tau\tau$  with an effective Lagrangian including a  $CP$  odd term in  $20.3 \text{ fb}^{-1}$  of  $pp$  collisions at  $E_{\text{cm}} = 8 \text{ TeV}$ . The measurement is consistent with the expectation of the Standard Model. The  $CP$ -mixing parameter  $\tilde{d}$  (a dimensionless coupling  $\tilde{d} = -(m_W^2/\Lambda^2)f_{WW}^{\sim}$ ) is constrained to the interval of  $(-0.11, 0.05)$  at 68% CL under the assumption of  $\tilde{d} = \tilde{d}_B$ . NODE=S126CP;LINKAGE=L
- 19 KHACHATRYAN 16AB search for anomalous pseudoscalar couplings of the Higgs boson to  $W$  and  $Z$  with  $18.9 \text{ fb}^{-1}$  of  $pp$  collisions at  $E_{\text{cm}} = 8 \text{ TeV}$ . See their Table 5 and Figs 5 and 6 for limits on possible anomalous pseudoscalar coupling parameters. NODE=S126CP;LINKAGE=K
- 20 AAD 15AX compare the  $J^{CP} = 0^+$  Standard Model assignment with other  $J^{CP}$  hypotheses in  $20.3 \text{ fb}^{-1}$  of  $pp$  collisions at  $E_{\text{cm}} = 8 \text{ TeV}$ , using the process  $H \rightarrow WW^* \rightarrow e\nu\mu\nu$ .  $2^+$  hypotheses are excluded at 84.5–99.4%CL,  $0^-$  at 96.5%CL,  $0^+$  (field strength coupling) at 70.8%CL. See their Fig. 19 for limits on possible  $CP$  mixture parameters. NODE=S126CP;LINKAGE=F
- 21 AAD 15CI compare the  $J^{CP} = 0^+$  Standard Model assignment with other  $J^{CP}$  hypotheses in  $4.5 \text{ fb}^{-1}$  of  $pp$  collisions at  $E_{\text{cm}} = 7 \text{ TeV}$  and  $20.3 \text{ fb}^{-1}$  at  $E_{\text{cm}} = 8 \text{ TeV}$ , using the processes  $H \rightarrow ZZ^* \rightarrow 4\ell$ ,  $H \rightarrow \gamma\gamma$  and combine with AAD 15AX data.  $0^+$  (field strength coupling),  $0^-$  and several  $2^+$  hypotheses are excluded at more than 99.9% CL. See their Tables 7–9 for limits on possible  $CP$  mixture parameters. NODE=S126CP;LINKAGE=G
- 22 AALTONEN 15 combine AALTONEN 15B and ABAZOV 14F data. An upper limit of 0.36 of the Standard Model production rate at 95% CL is obtained both for a  $0^-$  and a  $2^+$  state. Assuming the SM event rate, the  $J^{CP} = 0^-$  ( $2^+$ ) hypothesis is excluded at the  $5.0\sigma$  ( $4.9\sigma$ ) level. NODE=S126CP;LINKAGE=E
- 23 AALTONEN 15B compare the  $J^{CP} = 0^+$  Standard Model assignment with other  $J^{CP}$  hypotheses in  $9.45 \text{ fb}^{-1}$  of  $p\bar{p}$  collisions at  $E_{\text{cm}} = 1.96 \text{ TeV}$ , using the processes  $ZH \rightarrow \ell\ell b\bar{b}$ ,  $WH \rightarrow \ell\nu b\bar{b}$ , and  $ZH \rightarrow \nu\nu b\bar{b}$ . Bounds on the production rates of  $0^-$  and  $2^+$  (graviton-like) states are set, see their tables II and III. NODE=S126CP;LINKAGE=D
- 24 KHACHATRYAN 15Y compare the  $J^{CP} = 0^+$  Standard Model assignment with other  $J^{CP}$  hypotheses in up to  $5.1 \text{ fb}^{-1}$  of  $pp$  collisions at  $E_{\text{cm}} = 7 \text{ TeV}$  and up to  $19.7 \text{ fb}^{-1}$  at  $E_{\text{cm}} = 8 \text{ TeV}$ , using the processes  $H \rightarrow 4\ell$ ,  $H \rightarrow WW^*$ , and  $H \rightarrow \gamma\gamma$ .  $0^-$  is excluded at 99.98% CL, and several  $2^+$  hypotheses are excluded at more than 99% CL. Spin 1 models are excluded at more than 99.999% CL in  $ZZ^*$  and  $WW^*$  modes. Limits on anomalous couplings and several cross section fractions, treating the case of  $CP$ -mixed states, are also given. NODE=S126CP;LINKAGE=I
- 25 ABAZOV 14F compare the  $J^{CP} = 0^+$  Standard Model assignment with  $J^{CP} = 0^-$  and  $2^+$  (graviton-like coupling) hypotheses in up to  $9.7 \text{ fb}^{-1}$  of  $p\bar{p}$  collisions at  $E_{\text{cm}} = 1.96 \text{ TeV}$ . They use kinematic correlations between the decay products of the vector boson and the Higgs boson in the final states  $ZH \rightarrow \ell\ell b\bar{b}$ ,  $WH \rightarrow \ell\nu b\bar{b}$ , and  $ZH \rightarrow \nu\nu b\bar{b}$ . The  $0^-$  ( $2^+$ ) hypothesis is excluded at 97.6% CL (99.0% CL). In order to treat the case of a possible mixture of a  $0^+$  state with another  $J^{CP}$  state, the cross section fractions  $f_X = \sigma_X/(\sigma_{0^+} + \sigma_X)$  are considered, where  $X = 0^-, 2^+$ . Values for  $f_{0^-}$  ( $f_{2^+}$ ) above 0.80 (0.67) are excluded at 95% CL under the assumption that the total cross section is that of the SM Higgs boson. NODE=S126CP;LINKAGE=AB
- 26 CHATRCHYAN 14AA compare the  $J^{CP} = 0^+$  Standard Model assignment with various  $J^{CP}$  hypotheses in  $5.1 \text{ fb}^{-1}$  of  $pp$  collisions at  $E_{\text{cm}} = 7 \text{ TeV}$  and  $19.7 \text{ fb}^{-1}$  at  $E_{\text{cm}} = 8 \text{ TeV}$ .  $J^{CP} = 0^-$  and  $1^\pm$  hypotheses are excluded at 99% CL, and several  $J = 2$  hypotheses are excluded at 95% CL. In order to treat the case of a possible mixture of a  $0^+$  state with another  $J^{CP}$  state, the cross section fraction  $f_{a3} = |a_3|^2 \sigma_3 / (|a_1|^2 \sigma_1 + |a_2|^2 \sigma_2 + |a_3|^2 \sigma_3)$  is considered, where the case  $a_3 = 1$ ,  $a_1 = a_2 = 0$  corresponds to a pure  $CP$ -odd state. Assuming  $a_2 = 0$ , a value for  $f_{a3}$  above 0.51 is excluded at 95% CL. NODE=S126CP;LINKAGE=A

- 27 CHATRCHYAN 14G compare the  $J^{CP} = 0^+$  Standard Model assignment with  $J^{CP} = 0^-$  and  $2^+$  (graviton-like coupling) hypotheses in  $4.9 \text{ fb}^{-1}$  of  $pp$  collisions at  $E_{\text{cm}} = 7 \text{ TeV}$  and  $19.4 \text{ fb}^{-1}$  at  $E_{\text{cm}} = 8 \text{ TeV}$ . Varying the fraction of the production of the  $2^+$  state via  $gg$  and  $q\bar{q}$ ,  $2^+$  hypotheses are disfavored at CL between 83.7 and 99.8%. The  $0^-$  hypothesis is disfavored against  $0^+$  at the 65.3% CL.
- 28 KHACHATRYAN 14P compare the  $J^{CP} = 0^+$  Standard Model assignment with a  $2^+$  (graviton-like coupling) hypothesis in  $5.1 \text{ fb}^{-1}$  of  $pp$  collisions at  $E_{\text{cm}} = 7 \text{ TeV}$  and  $19.7 \text{ fb}^{-1}$  at  $E_{\text{cm}} = 8 \text{ TeV}$ . Varying the fraction of the production of the  $2^+$  state via  $gg$  and  $q\bar{q}$ ,  $2^+$  hypotheses are disfavored at CL between 71 and 94%.
- 29 AAD 13AJ compare the spin 0,  $CP$ -even hypothesis with specific alternative hypotheses of spin 0,  $CP$ -odd, spin 1,  $CP$ -even and  $CP$ -odd, and spin 2,  $CP$ -even models using the Higgs boson decays  $H \rightarrow \gamma\gamma$ ,  $H \rightarrow ZZ^* \rightarrow 4\ell$  and  $H \rightarrow WW^* \rightarrow \ell\nu\ell\nu$  and combinations thereof. The data are compatible with the spin 0,  $CP$ -even hypothesis, while all other tested hypotheses are excluded at confidence levels above 97.8%.
- 30 CHATRCHYAN 13J study angular distributions of the lepton pairs in the  $ZZ^*$  channel where both  $Z$  bosons decay to  $e$  or  $\mu$  pairs. Under the assumption that the observed particle has spin 0, the data are found to be consistent with the pure  $CP$ -even hypothesis, while the pure  $CP$ -odd hypothesis is disfavored.

NODE=S126CP;LINKAGE=C

NODE=S126CP;LINKAGE=B

NODE=S126CP;LINKAGE=AA

NODE=S126CP;LINKAGE=CH

## H DECAY WIDTH

NODE=S126W

NODE=S126W

The total decay width for a light Higgs boson with a mass in the observed range is not expected to be directly observable at the LHC. For the case of the Standard Model the prediction for the total width is about 4 MeV, which is three orders of magnitude smaller than the experimental mass resolution. There is no indication from the results observed so far that the natural width is broadened by new physics effects to such an extent that it could be directly observable. Furthermore, as all LHC Higgs channels rely on the identification of Higgs decay products, the total Higgs width cannot be measured indirectly without additional assumptions. The different dependence of on-peak and off-peak contributions on the total width in Higgs decays to  $ZZ^*$  and interference effects between signal and background in Higgs decays to  $\gamma\gamma$  can provide additional information in this context. Constraints on the total width from the combination of on-peak and off-peak contributions in Higgs decays to  $ZZ^*$  rely on the assumption of equal on- and off-shell effective couplings. Without an experimental determination of the total width or further theoretical assumptions, only ratios of couplings can be determined at the LHC rather than absolute values of couplings.

VALUE (MeV)	CL%	DOCUMENT ID	TECN	COMMENT
<b><math>3.5^{+1.6}_{-1.2}</math> OUR AVERAGE</b>				
[ $3.7^{+1.9}_{-1.4}$ MeV OUR 2025 AVERAGE]				
$4.3^{+2.7}_{-1.9}$		1 AAD	25AQ ATLS	$pp, 13 \text{ TeV}, ZZ^*/ZZ \rightarrow 4\ell, ZZ \rightarrow 2\ell 2\nu$
$3.0^{+2.0}_{-1.5}$		2 HAYRAPETY...25L	CMS	$pp, 13 \text{ TeV}, ZZ^*/ZZ \rightarrow 4\ell, ZZ \rightarrow 2\ell 2\nu$
● ● ● We do not use the following data for averages, fits, limits, etc. ● ● ●				
< 160	95	3 AAD	25E ATLS	$pp, 13 \text{ TeV}, \text{on-shell Higgs and } t\bar{t}t\bar{t}$
< 330	95	4 HAYRAPETY...25L	CMS	$pp, 13 \text{ TeV}, ZZ^* \rightarrow 4\ell$
$2.9^{+2.3}_{-1.7}$		5 HAYRAPETY...25L	CMS	$pp, 13 \text{ TeV}, ZZ^* \rightarrow 4\ell$
$4.4^{+3.0}_{-2.2}$		6 AAD	23BR ATLS	$pp, 13 \text{ TeV}, ZZ^*/ZZ \rightarrow 4\ell, ZZ \rightarrow 2\ell 2\nu$
$3.2^{+2.4}_{-1.7}$		7 TUMASYAN	22AMCMS	$pp, 13 \text{ TeV}, ZZ^*/ZZ \rightarrow 4\ell, ZZ \rightarrow 2\ell 2\nu$
$3.2^{+2.8}_{-2.2}$		8 SIRUNYAN	19BL CMS	$pp, 7, 8, 13 \text{ TeV}, ZZ^*/ZZ \rightarrow 4\ell$
< 14.4	95	9 AABOUD	18BP ATLS	$pp, 13 \text{ TeV}, ZZ \rightarrow 4\ell, 2\ell 2\nu$
< 1100	95	10 SIRUNYAN	17AV CMS	$pp, 13 \text{ TeV}, ZZ^* \rightarrow 4\ell$
< 26	95	11 KHACHATRY...16BA	CMS	$pp, 7, 8 \text{ TeV}, WW^{(*)}$
< 13	95	12 KHACHATRY...16BA	CMS	$pp, 7, 8 \text{ TeV}, ZZ^{(*)}, WW^{(*)}$
< 22.7	95	13 AAD	15BE ATLS	$pp, 8 \text{ TeV}, ZZ^{(*)}, WW^{(*)}$
< 1700	95	14 KHACHATRY...15AM	CMS	$pp, 7, 8 \text{ TeV}$
> $3.5 \times 10^{-9}$	95	15 KHACHATRY...15BA	CMS	$pp, 7, 8 \text{ TeV}, \text{flight distance}$

NODE=S126W

NEW

OCCUR=3

OCCUR=2

OCCUR=2

< 46	95	16 KHACHATRY...15BA CMS	$pp, 7, 8 \text{ TeV}, ZZ^{(*)} \rightarrow 4\ell$	OCCUR=2
<5000	95	17 AAD 14W ATLS	$pp, 7, 8 \text{ TeV}, \gamma\gamma$	
<2600	95	17 AAD 14W ATLS	$pp, 7, 8 \text{ TeV}, ZZ^* \rightarrow 4\ell$	OCCUR=2
<3400	95	18 CHATRCHYAN14AA CMS	$pp, 7, 8 \text{ TeV}, ZZ^* \rightarrow 4\ell$	
< 22	95	19 KHACHATRY...14D CMS	$pp, 7, 8 \text{ TeV}, ZZ^{(*)}$	
<2400	95	20 KHACHATRY...14P CMS	$pp, 7, 8 \text{ TeV}, \gamma\gamma$	
<sup>1</sup> AAD 25AQ use $140 \text{ fb}^{-1}$ at $E_{\text{cm}} = 13 \text{ TeV}$ . The off-shell Higgs boson production in the $ZZ \rightarrow 4\ell$ ( $\ell = e, \mu$ ) decay channel is combined with the on-shell production in the $ZZ^* \rightarrow 4\ell$ (AAD 20AQ) decay channel and the off-shell production in the $ZZ \rightarrow 2\ell 2\nu$ decay channel (AAD 23BR, AAD 25AP) to measure the total width assuming the same on-shell and off-shell coupling modifiers for gluon-fusion and for gauge-boson ( $\kappa_{g,\text{on-shell}}^2 \kappa_{V,\text{on-shell}}^2 = \kappa_{V,\text{on-shell}}^4 = \kappa_{g,\text{off-shell}}^2 \kappa_{V,\text{off-shell}}^2 = \kappa_{V,\text{off-shell}}^4$ ). $R_{gg} = \kappa_{g,\text{on-shell}}^2 / \kappa_{g,\text{off-shell}}^2$ and $R_{VV} = \kappa_{V,\text{on-shell}}^2 / \kappa_{V,\text{off-shell}}^2$ are measured to be $1.19^{+0.89}_{-0.66}$ and $0.95^{+0.44}_{-0.35}$ , respectively. Using AAD 25AQ and AAD 23BR, $\kappa_{g,\text{off-shell}}$ and $\kappa_{V,\text{off-shell}}$ are measured to be $1.09^{+0.39}_{-0.35}$ and $0.99^{+0.16}_{-0.19}$ , respectively. The quoted errors are values at 68%CL.				NODE=S126W;LINKAGE=S
<sup>2</sup> HAYRAPETYAN 25L use $138 \text{ fb}^{-1}$ at $E_{\text{cm}} = 13 \text{ TeV}$ . The on- and off-shell Higgs boson production in the $ZZ \rightarrow 4\ell$ ( $\ell = e, \mu$ ) decay channel is combined with the off-shell Higgs boson production in the $ZZ \rightarrow 2\ell 2\nu$ (TUMASYAN 22AM) decay channel to measure the total width. The off-shell Higgs signal strength is measured to be $0.67^{+0.42}_{-0.32}$ . The scenario of no off-shell contribution is excluded at $3.8 \sigma$ .				NODE=S126W;LINKAGE=Q
<sup>3</sup> AAD 25E constrain the total width using on-shell Higgs measurements and the four top quarks production with 13 TeV data. The tree-level Higgs-top Yukawa coupling is assumed to be the same for on-shell and off-shell Higgs boson production processes. Another assumption is that no BSM contributions affect the $t\bar{t}t\bar{t}$ production. The quoted value is obtained by assuming the loop-induced $ggF$ , $H \rightarrow \gamma\gamma$ , and $H \rightarrow Z\gamma$ rates can be modeled as a function of $\kappa_t$ and other SM couplings. Otherwise, $\Gamma_H < 450 \text{ MeV}$ is obtained at 95% CL. Two-dimensional likelihood scan of $(\Gamma_H/\Gamma_H^{\text{SM}}, \kappa_t)$ is shown in their Fig. 3.				NODE=S126W;LINKAGE=R
<sup>4</sup> HAYRAPETYAN 25L obtain an upper limit on the width from the on-shell $H \rightarrow ZZ^* \rightarrow 4\ell$ ( $\ell = e, \mu$ ) decays. Data of $138 \text{ fb}^{-1}$ $pp$ collisions at $E_{\text{cm}} = 13 \text{ TeV}$ is used.				NODE=S126W;LINKAGE=O
<sup>5</sup> HAYRAPETYAN 25L use $138 \text{ fb}^{-1}$ at $E_{\text{cm}} = 13 \text{ TeV}$ . The on- and off-shell Higgs boson production in the $ZZ \rightarrow 4\ell$ ( $\ell = e, \mu$ ) decay channel is used assuming that no new particles affect the gluon fusion production. The scenario of no off-shell contribution is excluded at $3.0 \sigma$ .				NODE=S126W;LINKAGE=P
<sup>6</sup> AAD 23BR use $139 \text{ fb}^{-1}$ at $E_{\text{cm}} = 13 \text{ TeV}$ . The off-shell Higgs boson production in the $ZZ \rightarrow 4\ell$ and $ZZ \rightarrow 2\ell 2\nu$ decay channels and the on-shell production in the $ZZ^* \rightarrow 4\ell$ ( $\ell = e, \mu$ , AAD 20AQ) decay channels are used to measure the total width. The off-shell Higgs signal strength is measured to be $1.1^{+0.7}_{-0.6}$ assuming the same on-shell and off-shell coupling modifiers are used individually for gluon-fusion and for gauge-boson modes. The scenario of no off-shell contribution is excluded at $3.3 \sigma$ . Combining with the on-shell signal strength measurement, the total width normalized to its SM expectation $\Gamma_H/\Gamma_H^{\text{SM}}$ is measured to be $1.1^{+0.7}_{-0.5}$ assuming the same on-shell and off-shell coupling modifiers are used individually for gluon-fusion and for gauge-boson modes. The observed upper limit on the total width is 10.1 MeV at 95% CL. See their Fig. 7. See corrected width values in their erratum AAD 25AP.				NODE=S126W;LINKAGE=N
<sup>7</sup> TUMASYAN 22AM use up to $140 \text{ fb}^{-1}$ at $E_{\text{cm}} = 13 \text{ TeV}$ . The off-shell Higgs boson production in the $ZZ \rightarrow 4\ell$ and $ZZ \rightarrow 2\ell 2\nu$ decay channels and the on-shell production in the $ZZ^* \rightarrow 4\ell$ ( $\ell = e, \mu$ ) decay channels are used to measure the total width. The off-shell Higgs signal strength is measured to be $0.62^{+0.68}_{-0.45}$ without the constraint on the ratio of the off-shell signal strengths for gluon-fusion and gauge-boson modes. The scenario of no off-shell contribution is excluded at $3.6 \sigma$ . The results are shown in their Table 1 with other constraint scenarios and the decay widths assuming the same coupling modifiers for on- and off-shell couplings ( $g_p$ and $g_d$ in their notation). The measurement of anomalous $HVV$ couplings is shown in their Extended Data Table 1 and Fig. 8.				NODE=S126W;LINKAGE=M
<sup>8</sup> SIRUNYAN 19BL measure the width and anomalous $HVV$ couplings from on-shell and off-shell production in the $4\ell$ final state. Data of $80.2 \text{ fb}^{-1}$ at 13 TeV, $19.7 \text{ fb}^{-1}$ at 8 TeV, and $5.1 \text{ fb}^{-1}$ at 7 TeV are used. The total width for the SM-like couplings is measured to be also [0.08, 9.16] MeV with 95% CL, assuming SM-like couplings for on- and off-shells (see their Table VIII). Constraints on the total width for anomalous $HVV$ interaction cases are found in their Table IX. See their Table X for the Higgs boson signal strength in the off-shell region.				NODE=S126W;LINKAGE=L
<sup>9</sup> AABOUD 18BP use $36.1 \text{ fb}^{-1}$ at $E_{\text{cm}} = 13 \text{ TeV}$ . An observed upper limit on the off-shell Higgs signal strength of 3.8 is obtained at 95% CL using off-shell Higgs boson production in the $ZZ \rightarrow 4\ell$ and $ZZ \rightarrow 2\ell 2\nu$ decay channels ( $\ell = e, \mu$ ). Combining with the on-shell signal strength measurements, the quoted upper limit on the Higgs boson total width is obtained, assuming the ratios of the relevant Higgs-boson couplings to the SM predictions are constant with energy from on-shell production to the high-mass range.				NODE=S126W;LINKAGE=K

- 10 SIRUNYAN 17AV obtain an upper limit on the width from the  $m_{4\ell}$  distribution in  $Z Z^* \rightarrow 4\ell$  ( $\ell = e, \mu$ ) decays. Data of  $35.9 \text{ fb}^{-1}$   $pp$  collisions at  $E_{\text{cm}} = 13 \text{ TeV}$  is used. The expected limit is  $1.60 \text{ GeV}$ .
- 11 KHACHATRYAN 16BA derive constraints on the total width from comparing  $W W^{(*)}$  production via on-shell and off-shell  $H$  using  $4.9 \text{ fb}^{-1}$  of  $pp$  collisions at  $E_{\text{cm}} = 7 \text{ TeV}$  and  $19.4 \text{ fb}^{-1}$  at  $8 \text{ TeV}$ .
- 12 KHACHATRYAN 16BA combine the  $W W^{(*)}$  result with  $Z Z^{(*)}$  results of KHACHATRYAN 15BA and KHACHATRYAN 14D.
- 13 AAD 15BE derive constraints on the total width from comparing  $Z Z^{(*)}$  and  $W W^{(*)}$  production via on-shell and off-shell  $H$  using  $20.3 \text{ fb}^{-1}$  of  $pp$  collisions at  $E_{\text{cm}} = 8 \text{ TeV}$ . The K factor for the background processes is assumed to be equal to that for the signal.
- 14 KHACHATRYAN 15AM combine  $\gamma\gamma$  and  $Z Z^* \rightarrow 4\ell$  results. The expected limit is  $2.3 \text{ GeV}$ .
- 15 KHACHATRYAN 15BA derive a lower limit on the total width from an upper limit on the decay flight distance  $\tau < 1.9 \times 10^{-13} \text{ s}$ .  $5.1 \text{ fb}^{-1}$  of  $pp$  collisions at  $E_{\text{cm}} = 7 \text{ TeV}$  and  $19.7 \text{ fb}^{-1}$  at  $8 \text{ TeV}$  are used.
- 16 KHACHATRYAN 15BA derive constraints on the total width from comparing  $Z Z^{(*)}$  production via on-shell and off-shell  $H$  with an unconstrained anomalous coupling.  $4\ell$  final states in  $5.1 \text{ fb}^{-1}$  of  $pp$  collisions at  $E_{\text{cm}} = 7 \text{ TeV}$  and  $19.7 \text{ fb}^{-1}$  at  $E_{\text{cm}} = 8 \text{ TeV}$  are used.
- 17 AAD 14W use  $4.5 \text{ fb}^{-1}$  of  $pp$  collisions at  $E_{\text{cm}} = 7 \text{ TeV}$  and  $20.3 \text{ fb}^{-1}$  at  $8 \text{ TeV}$ . The expected limit is  $6.2 \text{ GeV}$ .
- 18 CHATRCHYAN 14AA use  $5.1 \text{ fb}^{-1}$  of  $pp$  collisions at  $E_{\text{cm}} = 7 \text{ TeV}$  and  $19.7 \text{ fb}^{-1}$  at  $E_{\text{cm}} = 8 \text{ TeV}$ . The expected limit is  $2.8 \text{ GeV}$ .
- 19 KHACHATRYAN 14D derive constraints on the total width from comparing  $Z Z^{(*)}$  production via on-shell and off-shell  $H$ .  $4\ell$  and  $\ell\ell\nu\nu$  final states in  $5.1 \text{ fb}^{-1}$  of  $pp$  collisions at  $E_{\text{cm}} = 7 \text{ TeV}$  and  $19.7 \text{ fb}^{-1}$  at  $E_{\text{cm}} = 8 \text{ TeV}$  are used.
- 20 KHACHATRYAN 14P use  $5.1 \text{ fb}^{-1}$  of  $pp$  collisions at  $E_{\text{cm}} = 7 \text{ TeV}$  and  $19.7 \text{ fb}^{-1}$  at  $E_{\text{cm}} = 8 \text{ TeV}$ . The expected limit is  $3.1 \text{ GeV}$ .

NODE=S126W;LINKAGE=J

NODE=S126W;LINKAGE=H

NODE=S126W;LINKAGE=I

NODE=S126W;LINKAGE=G

NODE=S126W;LINKAGE=D

NODE=S126W;LINKAGE=E

NODE=S126W;LINKAGE=F

NODE=S126W;LINKAGE=AA

NODE=S126W;LINKAGE=B

NODE=S126W;LINKAGE=A

NODE=S126W;LINKAGE=C

## H DECAY MODES

NODE=S126220;NODE=S126

Mode	Fraction ( $\Gamma_i/\Gamma$ )	Confidence level	
$\Gamma_1$ $W W^*$	$(25.7 \pm 2.5) \%$		DESIG=1
$\Gamma_2$ $Z Z^*$	$(2.80 \pm 0.30) \%$		DESIG=2
$\Gamma_3$ $\gamma\gamma$	$(2.50 \pm 0.20) \times 10^{-3}$		DESIG=3
$\Gamma_4$ $b\bar{b}$	$(53 \pm 8) \%$		DESIG=4
$\Gamma_5$ $e^+ e^-$	$< 3.0 \times 10^{-4}$	95%	DESIG=10
$\Gamma_6$ $\mu^+ \mu^-$	$(2.6 \pm 1.3) \times 10^{-4}$		DESIG=8
$\Gamma_7$ $\tau^+ \tau^-$	$(6.0^{+0.8}_{-0.7}) \%$		DESIG=5
$\Gamma_8$ $Z\gamma$	$(3.4 \pm 1.1) \times 10^{-3}$		DESIG=6
$\Gamma_9$ $Z\rho(770)$	$< 1.21 \%$	95%	DESIG=25
$\Gamma_{10}$ $Z\phi(1020)$	$< 3.6 \times 10^{-3}$	95%	DESIG=26
$\Gamma_{11}$ $Z\eta_c$			DESIG=27
$\Gamma_{12}$ $ZJ/\psi$	$< 1.9 \times 10^{-3}$	95%	DESIG=28
$\Gamma_{13}$ $Z\psi(2S)$	$< 6.6 \times 10^{-3}$	95%	DESIG=29
$\Gamma_{14}$ $J/\psi\gamma$	$< 2.0 \times 10^{-4}$	95%	DESIG=11
$\Gamma_{15}$ $J/\psi J/\psi$	$< 3.8 \times 10^{-4}$	95%	DESIG=22
$\Gamma_{16}$ $\psi(2S)\gamma$	$< 9.9 \times 10^{-4}$	95%	DESIG=20
$\Gamma_{17}$ $\psi(2S)J/\psi$	$< 2.1 \times 10^{-3}$	95%	DESIG=30
$\Gamma_{18}$ $\psi(2S)\psi(2S)$	$< 3.0 \times 10^{-3}$	95%	DESIG=31
$\Gamma_{19}$ $\Upsilon(1S)\gamma$	$< 2.5 \times 10^{-4}$	95%	DESIG=12
$\Gamma_{20}$ $\Upsilon(1S)\Upsilon(1S)$	$< 1.7 \times 10^{-3}$	95%	DESIG=32
$\Gamma_{21}$ $\Upsilon(2S)\gamma$	$< 4.2 \times 10^{-4}$	95%	DESIG=13
$\Gamma_{22}$ $\Upsilon(3S)\gamma$	$< 3.4 \times 10^{-4}$	95%	DESIG=14
$\Gamma_{23}$ $\Upsilon(\text{nS})\Upsilon(\text{mS})$	$< 3.5 \times 10^{-4}$	95%	DESIG=23
$\Gamma_{24}$ $D^*\gamma$	$< 1.0 \times 10^{-3}$	95%	DESIG=35
$\Gamma_{25}$ $\rho(770)\gamma$	$< 3.7 \times 10^{-4}$	95%	DESIG=19
$\Gamma_{26}$ $\omega(782)\gamma$	$< 5.5 \times 10^{-4}$	95%	DESIG=33
$\Gamma_{27}$ $K^*(892)\gamma$	$< 2.2 \times 10^{-4}$	95%	DESIG=34
$\Gamma_{28}$ $\phi(1020)\gamma$	$< 3.0 \times 10^{-4}$	95%	DESIG=15
$\Gamma_{29}$ $e\mu$	LF $< 4.4 \times 10^{-5}$	95%	DESIG=17
$\Gamma_{30}$ $e\tau$	LF $< 2.0 \times 10^{-3}$	95%	DESIG=18
$\Gamma_{31}$ $\mu\tau$	LF $< 1.5 \times 10^{-3}$	95%	DESIG=9
$\Gamma_{32}$ invisible	$< 10.7 \%$	95%	DESIG=7
$\Gamma_{33}$ $\gamma$ invisible	$< 1.3 \%$	95%	DESIG=24



**H BRANCHING RATIOS** **$\Gamma(WW^*)/\Gamma_{\text{total}}$**  **$\Gamma_1/\Gamma$** 

VALUE	DOCUMENT ID	TECN	COMMENT
<b><math>0.257^{+0.026}_{-0.024}</math></b>	<sup>1</sup> ATLAS	22 ATLS	<i>pp</i> , 13 TeV

<sup>1</sup> ATLAS 22 report combined results (see their Extended Data Table 1) using up to 139 fb<sup>-1</sup> of data at  $E_{\text{cm}} = 13$  TeV, assuming  $m_H = 125.09$  GeV. SM values for the production cross-sections are assumed. See their Fig. 2b.

NODE=S126225

NODE=S126R20  
NODE=S126R20

NODE=S126R20;LINKAGE=A

 **$\Gamma(ZZ^*)/\Gamma_{\text{total}}$**  **$\Gamma_2/\Gamma$** 

VALUE	DOCUMENT ID	TECN	COMMENT
<b><math>0.028 \pm 0.003</math></b>	<sup>1</sup> ATLAS	22 ATLS	<i>pp</i> , 13 TeV

<sup>1</sup> ATLAS 22 report combined results (see their Extended Data Table 1) using up to 139 fb<sup>-1</sup> of data at  $E_{\text{cm}} = 13$  TeV, assuming  $m_H = 125.09$  GeV. SM values for the production cross-sections are assumed. See their Fig. 2b.

NODE=S126R21  
NODE=S126R21

NODE=S126R21;LINKAGE=A

 **$\Gamma(\gamma\gamma)/\Gamma_{\text{total}}$**  **$\Gamma_3/\Gamma$** 

VALUE	DOCUMENT ID	TECN	COMMENT
<b><math>0.0025 \pm 0.0002</math></b>	<sup>1</sup> ATLAS	22 ATLS	<i>pp</i> , 13 TeV

<sup>1</sup> ATLAS 22 report combined results (see their Extended Data Table 1) using up to 139 fb<sup>-1</sup> of data at  $E_{\text{cm}} = 13$  TeV, assuming  $m_H = 125.09$  GeV. SM values for the production cross-sections are assumed. See their Fig. 2b.

NODE=S126R22  
NODE=S126R22

NODE=S126R22;LINKAGE=A

 **$\Gamma(b\bar{b})/\Gamma_{\text{total}}$**  **$\Gamma_4/\Gamma$** 

VALUE	DOCUMENT ID	TECN	COMMENT
<b><math>0.53 \pm 0.08</math></b>	<sup>1</sup> ATLAS	22 ATLS	<i>pp</i> , 13 TeV

<sup>1</sup> ATLAS 22 report combined results (see their Extended Data Table 1) using up to 139 fb<sup>-1</sup> of data at  $E_{\text{cm}} = 13$  TeV, assuming  $m_H = 125.09$  GeV. SM values for the production cross-sections are assumed. See their Fig. 2b.

NODE=S126R23  
NODE=S126R23

NODE=S126R23;LINKAGE=A

 **$\Gamma(e^+e^-)/\Gamma_{\text{total}}$**  **$\Gamma_5/\Gamma$** 

VALUE	CL%	DOCUMENT ID	TECN	COMMENT
<b><math>&lt;3.0 \times 10^{-4}</math></b>	95	<sup>1</sup> TUMASYAN	23AU CMS	<i>pp</i> , 13 TeV
• • • We do not use the following data for averages, fits, limits, etc. • • •				
$<3.6 \times 10^{-4}$	95	<sup>2</sup> AAD	20F ATLS	<i>pp</i> , 13 TeV
$<1.9 \times 10^{-3}$	95	<sup>3</sup> KHACHATRYAN	15H CMS	<i>pp</i> , 7, 8 TeV

<sup>1</sup> TUMASYAN 23AU use 138 fb<sup>-1</sup> of *pp* collisions at  $E_{\text{cm}} = 13$  TeV.

<sup>2</sup> AAD 20F use 139 fb<sup>-1</sup> of *pp* collisions at  $E_{\text{cm}} = 13$  TeV. The best-fit value of the  $H \rightarrow ee$  branching fraction is  $(0.0 \pm 1.7 \pm 0.6) \times 10^{-4}$  for  $m_H = 125$  GeV.

<sup>3</sup> KHACHATRYAN 15H use 5.0 fb<sup>-1</sup> of *pp* collisions at  $E_{\text{cm}} = 7$  TeV and 19.7 fb<sup>-1</sup> at 8 TeV.

NODE=S126R03  
NODE=S126R03NODE=S126R03;LINKAGE=C  
NODE=S126R03;LINKAGE=B

NODE=S126R03;LINKAGE=A

 **$\Gamma(\mu^+\mu^-)/\Gamma_{\text{total}}$**  **$\Gamma_6/\Gamma$** 

VALUE (units 10 <sup>-4</sup> )	DOCUMENT ID	TECN	COMMENT
<b><math>2.6 \pm 1.3</math></b>	<sup>1</sup> ATLAS	22 ATLS	<i>pp</i> , 13 TeV

<sup>1</sup> ATLAS 22 report combined results (see their Extended Data Table 1) using up to 139 fb<sup>-1</sup> of data at  $E_{\text{cm}} = 13$  TeV, assuming  $m_H = 125.09$  GeV. SM values for the production cross-sections are assumed. See their Fig. 2b.

NODE=S126R24  
NODE=S126R24

NODE=S126R24;LINKAGE=A

 **$\Gamma(\tau^+\tau^-)/\Gamma_{\text{total}}$**  **$\Gamma_7/\Gamma$** 

VALUE	DOCUMENT ID	TECN	COMMENT
<b><math>0.060^{+0.008}_{-0.007}</math></b>	<sup>1</sup> ATLAS	22 ATLS	<i>pp</i> , 13 TeV

<sup>1</sup> ATLAS 22 report combined results (see their Extended Data Table 1) using up to 139 fb<sup>-1</sup> of data at  $E_{\text{cm}} = 13$  TeV, assuming  $m_H = 125.09$  GeV. SM values for the production cross-sections are assumed. See their Fig. 2b.

NODE=S126R25  
NODE=S126R25

NODE=S126R25;LINKAGE=A

 **$\Gamma(Z\gamma)/\Gamma_{\text{total}}$**  **$\Gamma_8/\Gamma$** 

VALUE (units 10 <sup>-3</sup> )	DOCUMENT ID	TECN	COMMENT
<b><math>3.4 \pm 1.1</math></b>	<sup>1</sup> AAD	24D LHC	<i>pp</i> , 13 TeV
• • • We do not use the following data for averages, fits, limits, etc. • • •			
$3.2 \pm 1.5$	<sup>2</sup> ATLAS	22 ATLS	<i>pp</i> , 13 TeV

<sup>1</sup> AAD 24D report combined results of ATLAS (AAD 20AG) and CMS (TUMASYAN 23F). SM values for the production cross-sections are assumed.

<sup>2</sup> ATLAS 22 report combined results (see their Extended Data Table 1) using up to 139 fb<sup>-1</sup> of data at  $E_{\text{cm}} = 13$  TeV, assuming  $m_H = 125.09$  GeV. SM values for the production cross-sections are assumed. See their Fig. 2b.

NODE=S126R26  
NODE=S126R26

NODE=S126R26;LINKAGE=B

NODE=S126R26;LINKAGE=A

$\Gamma(Z\rho(770))/\Gamma_{\text{total}}$  $\Gamma_9/\Gamma$ 

VALUE	CL%	DOCUMENT ID	TECN	COMMENT
$<1.21 \times 10^{-2}$	95	<sup>1</sup> SIRUNYAN	20BK CMS	$pp$ , 13 TeV

<sup>1</sup> SIRUNYAN 20BK search for  $H \rightarrow Z\rho$ ,  $Z \rightarrow e^+e^-/\mu^+\mu^-$ ,  $\rho \rightarrow \pi^+\pi^-$  with  $137 \text{ fb}^{-1}$  of  $pp$  collision data at  $E_{\text{cm}} = 13 \text{ TeV}$ . The quoted branching fraction is for the unpolarized decay. See their Table 3 for different polarizations.

NODE=S126R16  
NODE=S126R16

NODE=S126R16;LINKAGE=A

 $\Gamma(Z\phi(1020))/\Gamma_{\text{total}}$  $\Gamma_{10}/\Gamma$ 

VALUE	CL%	DOCUMENT ID	TECN	COMMENT
$<3.6 \times 10^{-3}$	95	<sup>1</sup> SIRUNYAN	20BK CMS	$pp$ , 13 TeV

<sup>1</sup> SIRUNYAN 20BK search for  $H \rightarrow Z\phi$ ,  $Z \rightarrow e^+e^-/\mu^+\mu^-$ ,  $\phi \rightarrow K^+K^-$  with  $137 \text{ fb}^{-1}$  of  $pp$  collision data at  $E_{\text{cm}} = 13 \text{ TeV}$ . The quoted branching fraction is for the unpolarized decay. See their Table 4 for different polarizations.

NODE=S126R17  
NODE=S126R17

NODE=S126R17;LINKAGE=A

 $\Gamma(Z\eta_c)/\Gamma_{\text{total}}$  $\Gamma_{11}/\Gamma$ 

VALUE	CL%	DOCUMENT ID	TECN	COMMENT
-------	-----	-------------	------	---------

• • • We do not use the following data for averages, fits, limits, etc. • • •

<sup>1</sup> AAD 20AE ATLS  $pp$ , 13 TeV

<sup>1</sup> AAD 20AE search for  $H \rightarrow Z\eta_c$  with two-leptons ( $e^+e^-/\mu^+\mu^-$ ) plus jet events using  $139 \text{ fb}^{-1}$  of  $pp$  collision data at  $E_{\text{cm}} = 13 \text{ TeV}$ . The upper limit of  $\sigma(pp \rightarrow H) \cdot \mathcal{B}(H \rightarrow Z\eta_c)$  is 110 pb at 95% CL.

NODE=S126R18  
NODE=S126R18

NODE=S126R18;LINKAGE=A

 $\Gamma(ZJ/\psi)/\Gamma_{\text{total}}$  $\Gamma_{12}/\Gamma$ 

VALUE	CL%	DOCUMENT ID	TECN	COMMENT
$<1.9 \times 10^{-3}$	95	<sup>1</sup> TUMASYAN	23C CMS	$pp$ , 13 TeV

• • • We do not use the following data for averages, fits, limits, etc. • • •

<sup>2</sup> AAD 20AE ATLS  $pp$ , 13 TeV

<sup>1</sup> TUMASYAN 23C search for  $H \rightarrow ZJ/\psi$ ,  $Z \rightarrow e^+e^-$  or  $\mu^+\mu^-$ ,  $J/\psi \rightarrow \mu^+\mu^-$  with  $138 \text{ fb}^{-1}$  of  $pp$  collision data at  $E_{\text{cm}} = 13 \text{ TeV}$ . The quoted value is for the Higgs decays for longitudinally polarized mesons. See their Table 1 for other cases.

<sup>2</sup> AAD 20AE search for  $H \rightarrow ZJ/\psi$  with two-leptons ( $e^+e^-/\mu^+\mu^-$ ) plus jet events using  $139 \text{ fb}^{-1}$  of  $pp$  collision data at  $E_{\text{cm}} = 13 \text{ TeV}$ . The upper limit of  $\sigma(pp \rightarrow H) \cdot \mathcal{B}(H \rightarrow ZJ/\psi)$  is 100 pb at 95% CL.

NODE=S126R19  
NODE=S126R19

NODE=S126R19;LINKAGE=B

NODE=S126R19;LINKAGE=A

 $\Gamma(Z\psi(2S))/\Gamma_{\text{total}}$  $\Gamma_{13}/\Gamma$ 

VALUE	CL%	DOCUMENT ID	TECN	COMMENT
$<6.6 \times 10^{-3}$	95	<sup>1</sup> TUMASYAN	23C CMS	$pp$ , 13 TeV

<sup>1</sup> TUMASYAN 23C search for  $H \rightarrow Z\psi(2S)$ ,  $Z \rightarrow e^+e^-$  or  $\mu^+\mu^-$ ,  $\psi(2S) \rightarrow \mu^+\mu^-$  with  $138 \text{ fb}^{-1}$  of  $pp$  collision data at  $E_{\text{cm}} = 13 \text{ TeV}$ . The quoted value is for the Higgs decays for longitudinally polarized mesons. See their Table 1 for other cases.

NODE=S126R27  
NODE=S126R27

NODE=S126R27;LINKAGE=A

 $\Gamma(J/\psi\gamma)/\Gamma_{\text{total}}$  $\Gamma_{14}/\Gamma$ 

VALUE	CL%	DOCUMENT ID	TECN	COMMENT
$<2.0 \times 10^{-4}$	95	<sup>1</sup> AAD	23CD ATLS	13 TeV, $138 \text{ fb}^{-1}$

• • • We do not use the following data for averages, fits, limits, etc. • • •

$<2.6 \times 10^{-4}$	95	<sup>2</sup> HAYRAPETY...25H	CMS	13 TeV, $123 \text{ fb}^{-1}$
$<7.6 \times 10^{-4}$	95	<sup>3</sup> SIRUNYAN	19AJ CMS	13 TeV, $35.9 \text{ fb}^{-1}$
$<3.5 \times 10^{-4}$	95	<sup>4</sup> AABOUD	18BL ATLS	13 TeV, $36.1 \text{ fb}^{-1}$
$<1.5 \times 10^{-3}$	95	<sup>5</sup> KHACHATRY...16B	CMS	8 TeV
$<1.5 \times 10^{-3}$	95	<sup>6</sup> AAD	15I ATLS	8 TeV

<sup>1</sup> AAD 23CD search for  $H \rightarrow J/\psi\gamma$ ,  $J/\psi \rightarrow \mu^+\mu^-$  with  $138 \text{ fb}^{-1}$  of  $pp$  collision data at  $E_{\text{cm}} = 13 \text{ TeV}$ . SM values for the production cross-sections are assumed.

<sup>2</sup> HAYRAPETYAN 25H search for  $H \rightarrow J/\psi\gamma$ ,  $J/\psi \rightarrow \mu^+\mu^-$  with  $123 \text{ fb}^{-1}$  of  $pp$  collision data at  $E_{\text{cm}} = 13 \text{ TeV}$ . SM values for the production cross-sections are assumed. See their Table 4 and Fig. 5.

<sup>3</sup> SIRUNYAN 19AJ search for  $H \rightarrow J/\psi\gamma$ ,  $J/\psi \rightarrow \mu^+\mu^-$  with  $35.9 \text{ fb}^{-1}$  of  $pp$  collision data at  $E_{\text{cm}} = 13 \text{ TeV}$ . The upper limit corresponds to 260 times the SM prediction and by combining the KHACHATRYAN 16B, it is 220 times the SM prediction.

<sup>4</sup> AABOUD 18BL search for  $H \rightarrow J/\psi\gamma$ ,  $J/\psi \rightarrow \mu^+\mu^-$  with  $36.1 \text{ fb}^{-1}$  of  $pp$  collision data at  $E_{\text{cm}} = 13 \text{ TeV}$ .

<sup>5</sup> KHACHATRYAN 16B use  $19.7 \text{ fb}^{-1}$  of  $pp$  collision data at 8 TeV.

<sup>6</sup> AAD 15I use  $19.7 \text{ fb}^{-1}$  of  $pp$  collision data at 8 TeV.

NODE=S126R04  
NODE=S126R04

NODE=S126R04;LINKAGE=E

NODE=S126R04;LINKAGE=F

NODE=S126R04;LINKAGE=D

NODE=S126R04;LINKAGE=C

NODE=S126R04;LINKAGE=B  
NODE=S126R04;LINKAGE=A

$\Gamma(J/\psi J/\psi)/\Gamma_{\text{total}}$ 

VALUE	CL%	DOCUMENT ID	TECN	COMMENT
$<3.8 \times 10^{-4}$	95	<sup>1</sup> TUMASYAN 23C	CMS	$pp$ , 13 TeV

• • • We do not use the following data for averages, fits, limits, etc. • • •

$<1.8 \times 10^{-3}$	95	<sup>2</sup> SIRUNYAN 19BR	CMS	$pp$ at 13 TeV
-----------------------	----	----------------------------	-----	----------------

<sup>1</sup> TUMASYAN 23C search for  $H \rightarrow J/\psi J/\psi$ ,  $J/\psi \rightarrow \mu^+ \mu^-$  with  $138 \text{ fb}^{-1}$  of  $pp$  collision data at  $E_{\text{cm}} = 13 \text{ TeV}$ . The quoted value is for the Higgs decays for longitudinally polarized mesons. See their Table 1 for other cases.

<sup>2</sup> SIRUNYAN 19BR search for  $H \rightarrow J/\psi J/\psi$ ,  $J/\psi \rightarrow \mu^+ \mu^-$  with  $37.5 \text{ fb}^{-1}$  of  $pp$  collision data at  $E_{\text{cm}} = 13 \text{ TeV}$ .  $J/\psi$ s from the Higgs decay are assumed to be unpolarized. For fully longitudinal (transverse) polarized  $J/\psi$ s, limits change by  $-22\%$  ( $+10\%$ ).

NODE=S126R13  
NODE=S126R13

NODE=S126R13;LINKAGE=B

NODE=S126R13;LINKAGE=A

 $\Gamma(\psi(2S)\gamma)/\Gamma_{\text{total}}$ 

VALUE	CL%	DOCUMENT ID	TECN	COMMENT
$<9.9 \times 10^{-4}$ (CL = 95%)		[ $<1.05 \times 10^{-3}$ (CL = 95%) OUR 2025 BEST LIMIT]		

$<9.9 \times 10^{-4}$	95	<sup>1</sup> HAYRAPETY...25H	CMS	13 TeV, $123 \text{ fb}^{-1}$
-----------------------	----	------------------------------	-----	-------------------------------

• • • We do not use the following data for averages, fits, limits, etc. • • •

$<1.05 \times 10^{-3}$	95	<sup>2</sup> AAD	23CD ATLS	13 TeV, $138 \text{ fb}^{-1}$
------------------------	----	------------------	-----------	-------------------------------

$<2.0 \times 10^{-3}$	95	<sup>3</sup> AABOUD	18BL ATLS	13 TeV, $36.1 \text{ fb}^{-1}$
-----------------------	----	---------------------	-----------	--------------------------------

<sup>1</sup> HAYRAPETYAN 25H search for  $H \rightarrow \psi(2S)\gamma$ ,  $\psi(2S) \rightarrow \mu^+ \mu^-$  with  $123 \text{ fb}^{-1}$  of  $pp$  collision data at  $E_{\text{cm}} = 13 \text{ TeV}$ . SM values for the production cross-sections are assumed. See their Table 4 and Fig. 5.

<sup>2</sup> AAD 23CD search for  $H \rightarrow \psi(2S)\gamma$ ,  $\psi(2S) \rightarrow \mu^+ \mu^-$  with  $138 \text{ fb}^{-1}$  of  $pp$  collision data at  $E_{\text{cm}} = 13 \text{ TeV}$ . SM values for the production cross-sections are assumed.

<sup>3</sup> AABOUD 18BL search for  $H \rightarrow \psi(2S)\gamma$ ,  $\psi(2S) \rightarrow \mu^+ \mu^-$  with  $36.1 \text{ fb}^{-1}$  of  $pp$  collision data at  $E_{\text{cm}} = 13 \text{ TeV}$ .

NODE=S126R12  
NODE=S126R12

NODE=S126R12;LINKAGE=C

NODE=S126R12;LINKAGE=B

NODE=S126R12;LINKAGE=A

 $\Gamma(\psi(2S)J/\psi)/\Gamma_{\text{total}}$ 

VALUE	CL%	DOCUMENT ID	TECN	COMMENT
$<2.1 \times 10^{-3}$	95	<sup>1</sup> TUMASYAN 23C	CMS	$pp$ , 13 TeV

<sup>1</sup> TUMASYAN 23C search for  $H \rightarrow \psi(2S)J/\psi$ ,  $\psi(2S) \rightarrow \mu^+ \mu^-$ ,  $J/\psi \rightarrow \mu^+ \mu^-$  with  $138 \text{ fb}^{-1}$  of  $pp$  collision data at  $E_{\text{cm}} = 13 \text{ TeV}$ . The quoted value is for the Higgs decays for longitudinally polarized mesons. See their Table 1 for other cases.

NODE=S126R28  
NODE=S126R28

NODE=S126R28;LINKAGE=A

 $\Gamma(\psi(2S)\psi(2S))/\Gamma_{\text{total}}$ 

VALUE	CL%	DOCUMENT ID	TECN	COMMENT
$<3.0 \times 10^{-3}$	95	<sup>1</sup> TUMASYAN 23C	CMS	$pp$ , 13 TeV

<sup>1</sup> TUMASYAN 23C search for  $H \rightarrow \psi(2S)\psi(2S)$ ,  $\psi(2S) \rightarrow \mu^+ \mu^-$  with  $138 \text{ fb}^{-1}$  of  $pp$  collision data at  $E_{\text{cm}} = 13 \text{ TeV}$ . The quoted value is for the Higgs decays for longitudinally polarized mesons. See their Table 1 for other cases.

NODE=S126R29  
NODE=S126R29

NODE=S126R29;LINKAGE=A

 $\Gamma(\Upsilon(1S)\gamma)/\Gamma_{\text{total}}$ 

VALUE	CL%	DOCUMENT ID	TECN	COMMENT
$<2.5 \times 10^{-4}$	95	<sup>1</sup> AAD	23CD ATLS	13 TeV, $138 \text{ fb}^{-1}$

• • • We do not use the following data for averages, fits, limits, etc. • • •

$<4.9 \times 10^{-4}$	95	<sup>2</sup> AABOUD	18BL ATLS	13 TeV, $36.1 \text{ fb}^{-1}$
-----------------------	----	---------------------	-----------	--------------------------------

$<1.3 \times 10^{-3}$	95	<sup>3</sup> AAD	15I ATLS	8 TeV
-----------------------	----	------------------	----------	-------

<sup>1</sup> AAD 23CD search for  $H \rightarrow \Upsilon(1S)\gamma$ ,  $\Upsilon(1S) \rightarrow \mu^+ \mu^-$  with  $138 \text{ fb}^{-1}$  of  $pp$  collision data at  $E_{\text{cm}} = 13 \text{ TeV}$ . SM values for the production cross-sections are assumed.

<sup>2</sup> AABOUD 18BL search for  $H \rightarrow \Upsilon(1S)\gamma$ ,  $\Upsilon(1S) \rightarrow \mu^+ \mu^-$  with  $36.1 \text{ fb}^{-1}$  of  $pp$  collision data at  $E_{\text{cm}} = 13 \text{ TeV}$ .

<sup>3</sup> AAD 15I use  $19.7 \text{ fb}^{-1}$  of  $pp$  collision data at 8 TeV.

NODE=S126R05  
NODE=S126R05

NODE=S126R05;LINKAGE=C

NODE=S126R05;LINKAGE=B

NODE=S126R05;LINKAGE=A

 $\Gamma(\Upsilon(1S)\Upsilon(1S))/\Gamma_{\text{total}}$ 

VALUE	CL%	DOCUMENT ID	TECN	COMMENT
$<1.7 \times 10^{-3}$	95	<sup>1</sup> TUMASYAN 23C	CMS	$pp$ , 13 TeV

<sup>1</sup> TUMASYAN 23C search for  $H \rightarrow \Upsilon(1S)\Upsilon(1S)$ ,  $\Upsilon(1S) \rightarrow \mu^+ \mu^-$  with  $138 \text{ fb}^{-1}$  of  $pp$  collision data at  $E_{\text{cm}} = 13 \text{ TeV}$ . The quoted value is for the Higgs decays for longitudinally polarized mesons. See their Table 1 for other cases.

NODE=S126R30  
NODE=S126R30

NODE=S126R30;LINKAGE=A

$\Gamma(\Upsilon(2S)\gamma)/\Gamma_{\text{total}}$ 

VALUE	CL%	DOCUMENT ID	TECN	COMMENT
$<4.2 \times 10^{-4}$	95	<sup>1</sup> AAD	23CD ATLS	13 TeV, 138 fb <sup>-1</sup>
• • • We do not use the following data for averages, fits, limits, etc. • • •				
$<5.9 \times 10^{-4}$	95	<sup>2</sup> AABOUD	18BL ATLS	13 TeV, 36.1 fb <sup>-1</sup>
$<1.9 \times 10^{-3}$	95	<sup>3</sup> AAD	15I ATLS	8 TeV

<sup>1</sup> AAD 23CD search for  $H \rightarrow \Upsilon(2S)\gamma$ ,  $\Upsilon(2S) \rightarrow \mu^+\mu^-$  with 138 fb<sup>-1</sup> of  $pp$  collision data at  $E_{\text{cm}} = 13$  TeV. SM values for the production cross-sections are assumed.

<sup>2</sup> AABOUD 18BL search for  $H \rightarrow \Upsilon(2S)\gamma$ ,  $\Upsilon(2S) \rightarrow \mu^+\mu^-$  with 36.1 fb<sup>-1</sup> of  $pp$  collision data at  $E_{\text{cm}} = 13$  TeV.

<sup>3</sup> AAD 15I use 19.7 fb<sup>-1</sup> of  $pp$  collision data at 8 TeV.

NODE=S126R06  
NODE=S126R06

NODE=S126R06;LINKAGE=C

NODE=S126R06;LINKAGE=B

NODE=S126R06;LINKAGE=A

 $\Gamma(\Upsilon(3S)\gamma)/\Gamma_{\text{total}}$ 

VALUE	CL%	DOCUMENT ID	TECN	COMMENT
$<3.4 \times 10^{-4}$	95	<sup>1</sup> AAD	23CD ATLS	13 TeV, 138 fb <sup>-1</sup>
• • • We do not use the following data for averages, fits, limits, etc. • • •				
$<5.7 \times 10^{-4}$	95	<sup>2</sup> AABOUD	18BL ATLS	13 TeV, 36.1 fb <sup>-1</sup>
$<1.3 \times 10^{-3}$	95	<sup>3</sup> AAD	15I ATLS	8 TeV

<sup>1</sup> AAD 23CD search for  $H \rightarrow \Upsilon(3S)\gamma$ ,  $\Upsilon(3S) \rightarrow \mu^+\mu^-$  with 138 fb<sup>-1</sup> of  $pp$  collision data at  $E_{\text{cm}} = 13$  TeV. SM values for the production cross-sections are assumed.

<sup>2</sup> AABOUD 18BL search for  $H \rightarrow \Upsilon(3S)\gamma$ ,  $\Upsilon(3S) \rightarrow \mu^+\mu^-$  with 36.1 fb<sup>-1</sup> of  $pp$  collision data at  $E_{\text{cm}} = 13$  TeV.

<sup>3</sup> AAD 15I use 19.7 fb<sup>-1</sup> of  $pp$  collision data at 8 TeV.

NODE=S126R07  
NODE=S126R07

NODE=S126R07;LINKAGE=C

NODE=S126R07;LINKAGE=B

NODE=S126R07;LINKAGE=A

 $\Gamma(\Upsilon(nS) \Upsilon(mS))/\Gamma_{\text{total}}$ 

VALUE	CL%	DOCUMENT ID	TECN	COMMENT
$<3.5 \times 10^{-4}$	95	<sup>1</sup> TUMASYAN	23C CMS	$pp$ , 13 TeV
• • • We do not use the following data for averages, fits, limits, etc. • • •				
$<1.4 \times 10^{-3}$	95	<sup>2</sup> SIRUNYAN	19BR CMS	$pp$ , 13 TeV

<sup>1</sup> TUMASYAN 23C search for  $H \rightarrow \Upsilon(nS) \Upsilon(mS)$  with  $\Upsilon(nS)$ ,  $\Upsilon(mS) \rightarrow \mu^+\mu^-$  ( $n, m = 1, 2, 3$ ) with 138 fb<sup>-1</sup> of  $pp$  collision data at  $E_{\text{cm}} = 13$  TeV. The quoted value is for the Higgs decays for longitudinally polarized mesons. See their Table 1 for other cases.

<sup>2</sup> SIRUNYAN 19BR search for  $H \rightarrow \Upsilon(nS) \Upsilon(mS)$  with  $\Upsilon(nS), \Upsilon(mS) \rightarrow \mu^+\mu^-$  ( $n, m = 1, 2, 3$ ) for 37.5 fb<sup>-1</sup> of  $pp$  collision data at  $E_{\text{cm}} = 13$  TeV.  $\Upsilon$ s from the Higgs decay are assumed to be unpolarized. For fully longitudinal (transverse) polarized  $\Upsilon$ s, limits change by  $-22\%$  ( $+10\%$ ). The three  $\Upsilon$  states selected in a mass range of 8.5–11 GeV are not distinguished.

NODE=S126R14  
NODE=S126R14

NODE=S126R14;LINKAGE=B

NODE=S126R14;LINKAGE=A

 $\Gamma(D^*\gamma)/\Gamma_{\text{total}}$ 

VALUE	CL%	DOCUMENT ID	TECN	COMMENT
$<1.0 \times 10^{-3}$	95	<sup>1</sup> AAD	24R ATLS	$pp$ , 13 TeV

<sup>1</sup> AAD 24R use 136.3 fb<sup>-1</sup> of  $pp$  collision data at 13 TeV. The 95% CL upper limit on the cross section times the branching ratio is 58 fb. The SM Higgs production cross section of  $m_H = 125.09$  GeV is assumed. See their Table 3.

NODE=S126R33  
NODE=S126R33

NODE=S126R33;LINKAGE=A

 $\Gamma(\rho(770)\gamma)/\Gamma_{\text{total}}$ 

VALUE	CL%	DOCUMENT ID	TECN	COMMENT
$< 3.7 \times 10^{-4}$ (CL = 95%)		[ $<10.4 \times 10^{-4}$ (CL = 95%) OUR 2025 BEST LIMIT]		
$< 3.7 \times 10^{-4}$	95	<sup>1</sup> HAYRAPETY...25G	CMS	$pp$ , 13 TeV
• • • We do not use the following data for averages, fits, limits, etc. • • •				
$<10.4 \times 10^{-4}$	95	<sup>2</sup> AABOUD	18AU ATLS	$pp$ , 13 TeV

<sup>1</sup> HAYRAPETYAN 25G search for  $H \rightarrow \rho^0\gamma$ ,  $\rho^0 \rightarrow \pi^+\pi^-$  with up to 138 fb<sup>-1</sup> of  $pp$  collision data at  $E_{\text{cm}} = 13$  TeV.

<sup>2</sup> AABOUD 18AU use 35.6 fb<sup>-1</sup> of  $pp$  collision data at 13 TeV. See their erratum AABOUD 23A.

NODE=S126R11  
NODE=S126R11

NODE=S126R11;LINKAGE=B

NODE=S126R11;LINKAGE=A

 $\Gamma(\omega(782)\gamma)/\Gamma_{\text{total}}$ 

VALUE	CL%	DOCUMENT ID	TECN	COMMENT
$<5.5 \times 10^{-4}$	95	<sup>1</sup> AAD	23BS ATLS	$pp$ , 13 TeV

<sup>1</sup> AAD 23BS use 89.5 fb<sup>-1</sup> of  $pp$  collision data at 13 TeV.

NODE=S126R31  
NODE=S126R31

NODE=S126R31;LINKAGE=A

$\Gamma(K^*(892)\gamma)/\Gamma_{\text{total}}$ 

VALUE	CL%	DOCUMENT ID	TECN	COMMENT
$<2.2 \times 10^{-4}$	95	<sup>1</sup> AAD	23BS ATLS	$pp$ , 13 TeV
• • • We do not use the following data for averages, fits, limits, etc. • • •				
$<3.0 \times 10^{-4}$	95	<sup>2</sup> HAYRAPETY...25G	CMS	$pp$ , 13 TeV
<sup>1</sup> AAD 23BS use 134 fb <sup>-1</sup> of $pp$ collision data at 13 TeV.				
<sup>2</sup> HAYRAPETYAN 25G search for $H \rightarrow K^{*0}\gamma$ , $K^{*0} \rightarrow K^{\pm}\pi^{\mp}$ with up to 138 fb <sup>-1</sup> of $pp$ collision data at $E_{\text{cm}} = 13$ TeV.				

 $\Gamma_{27}/\Gamma$ 

NODE=S126R32  
 NODE=S126R32

 $\Gamma(\phi(1020)\gamma)/\Gamma_{\text{total}}$ 

VALUE	CL%	DOCUMENT ID	TECN	COMMENT
$<3.0 \times 10^{-4}$ (CL = 95%)		[ $<5 \times 10^{-4}$ (CL = 95%) OUR 2025 BEST LIMIT]		
$<3.0 \times 10^{-4}$	95	<sup>1</sup> HAYRAPETY...25G	CMS	$pp$ , 13 TeV
• • • We do not use the following data for averages, fits, limits, etc. • • •				
$<5.0 \times 10^{-4}$	95	<sup>2</sup> AABOUD	18AU ATLS	$pp$ , 13 TeV
$<1.4 \times 10^{-3}$	95	<sup>3</sup> AABOUD	16K ATLS	$pp$ , 13 TeV
<sup>1</sup> HAYRAPETYAN 25G search for $H \rightarrow \phi\gamma$ , $\phi \rightarrow K^+K^-$ with up to 138 fb <sup>-1</sup> of $pp$ collision data at $E_{\text{cm}} = 13$ TeV.				
<sup>2</sup> AABOUD 18AU use 35.6 fb <sup>-1</sup> of $pp$ collision data at 13 TeV. See their erratum AABOUD 23A.				
<sup>3</sup> AABOUD 16K use 2.7 fb <sup>-1</sup> of $pp$ collision data at 13 TeV.				

 $\Gamma_{28}/\Gamma$ 

NODE=S126R00  
 NODE=S126R00

 $\Gamma(e\mu)/\Gamma_{\text{total}}$ 

VALUE	CL%	DOCUMENT ID	TECN	COMMENT
$<4.4 \times 10^{-5}$	95	<sup>1</sup> HAYRAPETY...23C	CMS	$pp$ , 13 TeV
• • • We do not use the following data for averages, fits, limits, etc. • • •				
$<6.1 \times 10^{-5}$	95	<sup>2</sup> AAD	20F ATLS	$pp$ , 13 TeV
$<3.5 \times 10^{-4}$	95	<sup>3</sup> KHACHATRY...16CD	CMS	$pp$ , 8 TeV
<sup>1</sup> HAYRAPETYAN 23C use 138 fb <sup>-1</sup> of $pp$ collisions at $E_{\text{cm}} = 13$ TeV. The limit constrains the $Y_{e\mu}$ Yukawa coupling to $\sqrt{ Y_{e\mu} ^2 +  Y_{\mu e} ^2} < 1.9 \times 10^{-4}$ at 95% CL (see their Fig. 6).				
<sup>2</sup> AAD 20F use 139 fb <sup>-1</sup> of $pp$ collisions at $E_{\text{cm}} = 13$ TeV. The best-fit value of the $H \rightarrow e\mu$ branching fraction is $(0.4 \pm 2.9 \pm 0.3) \times 10^{-5}$ for $m_H = 125$ GeV.				
<sup>3</sup> KHACHATRYAN 16CD search for $H \rightarrow e\mu$ in 19.7 fb <sup>-1</sup> of $pp$ collisions at $E_{\text{cm}} = 8$ TeV. The limit constrains the $Y_{e\mu}$ Yukawa coupling to $\sqrt{ Y_{e\mu} ^2 +  Y_{\mu e} ^2} < 5.4 \times 10^{-4}$ at 95% CL (see their Fig. 6).				

 $\Gamma_{29}/\Gamma$ 

NODE=S126R09  
 NODE=S126R09

 $\Gamma(e\tau)/\Gamma_{\text{total}}$ 

VALUE	CL%	DOCUMENT ID	TECN	COMMENT
$<2.0 \times 10^{-3}$	95	<sup>1</sup> AAD	23Q ATLS	$pp$ , 13 TeV
• • • We do not use the following data for averages, fits, limits, etc. • • •				
$<2.3 \times 10^{-3}$	95	<sup>2</sup> AAD	23Q ATLS	$pp$ , 13 TeV
$<2.2 \times 10^{-3}$	95	<sup>3</sup> SIRUNYAN	21Z CMS	$pp$ , 13 TeV
$<4.7 \times 10^{-3}$	95	<sup>4</sup> AAD	20A ATLS	$pp$ , 13 TeV
$<6.1 \times 10^{-3}$	95	<sup>5</sup> SIRUNYAN	18BH CMS	$pp$ , 13 TeV
$<10.4 \times 10^{-3}$	95	<sup>6</sup> AAD	17 ATLS	$pp$ , 8 TeV
$<6.9 \times 10^{-3}$	95	<sup>7</sup> KHACHATRY...16CD	CMS	$pp$ , 8 TeV
<sup>1</sup> AAD 23Q search for $H \rightarrow e\tau$ in 138 fb <sup>-1</sup> of $pp$ collisions at $E_{\text{cm}} = 13$ TeV. The result is obtained from a simultaneous fit of possible $H \rightarrow e\tau$ and $H \rightarrow \mu\tau$ signals (see their Figs. 13 and 14). The limit constrains the $Y_{e\tau}$ Yukawa coupling to $\sqrt{ Y_{e\tau} ^2 +  Y_{\tau e} ^2} < 1.3 \times 10^{-3}$ at 95% CL (see their Fig. 15).				
<sup>2</sup> AAD 23Q search for $H \rightarrow e\tau$ in 138 fb <sup>-1</sup> of $pp$ collisions at $E_{\text{cm}} = 13$ TeV. The limit constrains the $Y_{e\tau}$ Yukawa coupling to $\sqrt{ Y_{e\tau} ^2 +  Y_{\tau e} ^2} < 1.4 \times 10^{-3}$ at 95% CL (see their Fig. 12).				
<sup>3</sup> SIRUNYAN 21Z search for $H \rightarrow e\tau$ in 137 fb <sup>-1</sup> of $pp$ collisions at $E_{\text{cm}} = 13$ TeV. The limit constrains the $Y_{e\tau}$ Yukawa coupling to $\sqrt{ Y_{e\tau} ^2 +  Y_{\tau e} ^2} < 1.35 \times 10^{-3}$ at 95% CL (see their Fig. 8).				
<sup>4</sup> AAD 20A search for $H \rightarrow e\tau$ in 36.1 fb <sup>-1</sup> of $pp$ collisions at $E_{\text{cm}} = 13$ TeV. The limit constrains the $Y_{e\tau}$ Yukawa coupling to $\sqrt{ Y_{e\tau} ^2 +  Y_{\tau e} ^2} < 2.0 \times 10^{-3}$ at 95% CL (see their Fig. 5).				
<sup>5</sup> SIRUNYAN 18BH search for $H \rightarrow e\tau$ in 35.9 fb <sup>-1</sup> of $pp$ collisions at $E_{\text{cm}} = 13$ TeV. The limit constrains the $Y_{e\tau}$ Yukawa coupling to $\sqrt{ Y_{e\tau} ^2 +  Y_{\tau e} ^2} < 2.26 \times 10^{-3}$ at 95% CL (see their Fig. 10).				

 $\Gamma_{30}/\Gamma$ 

NODE=S126R10  
 NODE=S126R10

OCCUR=2

NODE=S126R10;LINKAGE=F

NODE=S126R10;LINKAGE=G

NODE=S126R10;LINKAGE=E

NODE=S126R10;LINKAGE=D

NODE=S126R10;LINKAGE=C

<sup>6</sup> AAD 17 search for  $H \rightarrow e\tau$  in  $20.3 \text{ fb}^{-1}$  of  $pp$  collisions at  $E_{\text{cm}} = 8 \text{ TeV}$ .

<sup>7</sup> KHACHATRYAN 16CD search for  $H \rightarrow e\tau$  in  $19.7 \text{ fb}^{-1}$  of  $pp$  collisions at  $E_{\text{cm}} = 8 \text{ TeV}$ .

The limit constrains the  $Y_{e\tau}$  Yukawa coupling to  $\sqrt{|Y_{e\tau}|^2 + |Y_{\tau e}|^2} < 2.4 \times 10^{-3}$  at 95% CL (see their Fig. 6).

NODE=S126R10;LINKAGE=B

NODE=S126R10;LINKAGE=A

### $\Gamma(\mu\tau)/\Gamma_{\text{total}}$

VALUE	CL%	DOCUMENT ID	TECN	COMMENT
<b>&lt; 1.5 × 10<sup>-3</sup></b>	95	<sup>1</sup> SIRUNYAN	21Z CMS	$pp$ , 13 TeV
• • • We do not use the following data for averages, fits, limits, etc. • • •				
< 1.8 × 10 <sup>-3</sup>	95	<sup>2</sup> AAD	23Q ATLS	$pp$ , 13 TeV
< 1.7 × 10 <sup>-3</sup>	95	<sup>3</sup> AAD	23Q ATLS	$pp$ , 13 TeV
< 2.8 × 10 <sup>-3</sup>	95	<sup>4</sup> AAD	20A ATLS	$pp$ , 13 TeV
< 26 × 10 <sup>-2</sup>	95	<sup>5</sup> AAIJ	18AMLHCB	$pp$ , 8 TeV
< 2.5 × 10 <sup>-3</sup>	95	<sup>6</sup> SIRUNYAN	18BH CMS	$pp$ , 13 TeV
< 1.43 × 10 <sup>-2</sup>	95	<sup>7</sup> AAD	17 ATLS	$pp$ , 8 TeV
< 1.51 × 10 <sup>-2</sup>	95	<sup>8</sup> KHACHATRY...15Q	CMS	$pp$ , 8 TeV

### $\Gamma_{31}/\Gamma$

NODE=S126R02  
NODE=S126R02

<sup>1</sup> SIRUNYAN 21Z search for  $H \rightarrow \mu\tau$  in  $137 \text{ fb}^{-1}$  of  $pp$  collisions at  $E_{\text{cm}} = 13 \text{ TeV}$ .

The limit constrains the  $Y_{\mu\tau}$  Yukawa coupling to  $\sqrt{|Y_{\mu\tau}|^2 + |Y_{\tau\mu}|^2} < 1.11 \times 10^{-3}$  at 95% CL (see their Fig. 8).

NODE=S126R02;LINKAGE=F

<sup>2</sup> AAD 23Q search for  $H \rightarrow \mu\tau$  in  $138 \text{ fb}^{-1}$  of  $pp$  collisions at  $E_{\text{cm}} = 13 \text{ TeV}$ . The result is obtained from a simultaneous fit of possible  $H \rightarrow e\tau$  and  $H \rightarrow \mu\tau$  signals (see their Figs. 13 and 14). The limit constrains the  $Y_{\mu\tau}$  Yukawa coupling to  $\sqrt{|Y_{\mu\tau}|^2 + |Y_{\tau\mu}|^2} < 1.2 \times 10^{-3}$  at 95% CL (see their Fig. 15).

NODE=S126R02;LINKAGE=G

<sup>3</sup> AAD 23Q search for  $H \rightarrow \mu\tau$  in  $138 \text{ fb}^{-1}$  of  $pp$  collisions at  $E_{\text{cm}} = 13 \text{ TeV}$ . The limit constrains the  $Y_{\mu\tau}$  Yukawa coupling to  $\sqrt{|Y_{\mu\tau}|^2 + |Y_{\tau\mu}|^2} < 1.2 \times 10^{-3}$  at 95% CL (see their Fig. 12).

NODE=S126R02;LINKAGE=H

<sup>4</sup> AAD 20A search for  $H \rightarrow \mu\tau$  in  $36.1 \text{ fb}^{-1}$  of  $pp$  collisions at  $E_{\text{cm}} = 13 \text{ TeV}$ . The limit constrains the  $Y_{\mu\tau}$  Yukawa coupling to  $\sqrt{|Y_{\mu\tau}|^2 + |Y_{\tau\mu}|^2} < 1.5 \times 10^{-3}$  at 95% CL (see their Fig. 5).

NODE=S126R02;LINKAGE=E

<sup>5</sup> AAIJ 18AM search for  $H \rightarrow \mu\tau$  in  $2.0 \text{ fb}^{-1}$  of  $pp$  collisions at  $E_{\text{cm}} = 8 \text{ TeV}$ . The limit constrains the  $Y_{\mu\tau}$  Yukawa coupling to  $\sqrt{|Y_{\mu\tau}|^2 + |Y_{\tau\mu}|^2} < 1.7 \times 10^{-2}$  at 95% CL assuming SM production cross sections.

NODE=S126R02;LINKAGE=D

<sup>6</sup> SIRUNYAN 18BH search for  $H \rightarrow \mu\tau$  in  $35.9 \text{ fb}^{-1}$  of  $pp$  collisions at  $E_{\text{cm}} = 13 \text{ TeV}$ . The limit constrains the  $Y_{\mu\tau}$  Yukawa coupling to  $\sqrt{|Y_{\mu\tau}|^2 + |Y_{\tau\mu}|^2} < 1.43 \times 10^{-3}$  at 95% CL (see their Fig. 10).

NODE=S126R02;LINKAGE=C

<sup>7</sup> AAD 17 search for  $H \rightarrow \mu\tau$  in  $20.3 \text{ fb}^{-1}$  of  $pp$  collisions at  $E_{\text{cm}} = 8 \text{ TeV}$ .

NODE=S126R02;LINKAGE=B

<sup>8</sup> KHACHATRYAN 15Q search for  $H \rightarrow \mu\tau$  with  $\tau$  decaying electronically or hadronically in  $19.7 \text{ fb}^{-1}$  of  $pp$  collisions at  $E_{\text{cm}} = 8 \text{ TeV}$ . The fit gives  $B(H \rightarrow \mu\tau) = (0.84^{+0.39}_{-0.37})\%$  with a significance of  $2.4 \sigma$ .

NODE=S126R02;LINKAGE=A

### $\Gamma(\text{invisible})/\Gamma_{\text{total}}$

Invisible final states.		DOCUMENT ID	TECN	COMMENT
VALUE	CL%			
<b>&lt; 0.107</b>	95	<sup>1</sup> AAD	23A ATLS	$pp$ , 7, 8, 13 TeV
• • • We do not use the following data for averages, fits, limits, etc. • • •				
< 0.113	95	<sup>2</sup> AAD	23A ATLS	$pp$ , 13 TeV
< 0.38	95	<sup>3</sup> AAD	23AF ATLS	$pp \rightarrow t\bar{t}H$ , 13 TeV
< 0.54	95	<sup>4</sup> TUMASYAN	23BA CMS	$pp \rightarrow t\bar{t}H$ , $V(\rightarrow q\bar{q})$ $H$ , 13 TeV
< 0.15	95	<sup>5</sup> TUMASYAN	23BA CMS	$pp$ , 7, 8, 13 TeV
< 0.19	95	<sup>6</sup> AAD	22D ATLS	$pp \rightarrow ZH$ , 13 TeV
< 0.145	95	<sup>7</sup> AAD	22P ATLS	$pp \rightarrow qqH$ , 13 TeV
< 0.37	95	<sup>8</sup> AAD	22S ATLS	$pp \rightarrow qqH\gamma$ , 13 TeV
< 0.13	95	<sup>9</sup> ATLAS	22 ATLS	$pp$ , 13 TeV
< 0.16	95	<sup>10</sup> CMS	22 CMS	$pp$ , 13 TeV
< 0.18	95	<sup>11</sup> TUMASYAN	22G CMS	$pp \rightarrow qqH$ , 8, 13 TeV
< 0.18	95	<sup>12</sup> TUMASYAN	22G CMS	$pp \rightarrow qqH$ , 13 TeV
< 0.34	95	<sup>13</sup> AAD	21F ATLS	$pp$ , 13 TeV
< 0.29	95	<sup>14</sup> SIRUNYAN	21A CMS	$pp \rightarrow ZH$ , 13 TeV
< 0.278	95	<sup>15</sup> TUMASYAN	21D CMS	$pp$ , 13 TeV, jet or $V(\rightarrow q\bar{q})$
< 0.37	95	<sup>16</sup> AABOUD	19AI ATLS	$pp \rightarrow qqH$ , 13 TeV
< 0.38	95	<sup>17</sup> AABOUD	19AL ATLS	$pp$ , 13 TeV

### $\Gamma_{32}/\Gamma$

NODE=S126R01  
NODE=S126R01  
NODE=S126R01

OCCUR=2

OCCUR=2

OCCUR=2



- 14 SIRUNYAN 21A search for  $H$  decaying to invisible final states associated with a  $Z$  decaying  $ee/\mu\mu$  using  $137 \text{ fb}^{-1}$  at 13 TeV. The limit is obtained for  $m_H = 125 \text{ GeV}$  and assuming the SM  $ZH$  production cross section. NODE=S126R01;LINKAGE=U
- 15 TUMASYAN 21D search for  $H$  decaying to invisible final states associated with an energetic jet or a  $V$ ,  $V \rightarrow q\bar{q}$  using  $101 \text{ fb}^{-1}$  at 13 TeV and the result is combined with SIRUNYAN 18S. NODE=S126R01;LINKAGE=W
- 16 AABOUD 19AI search for  $pp \rightarrow qqHX$  (VBF) with  $H$  decaying to invisible final states using  $36.1 \text{ fb}^{-1}$  of data. The quoted limit on the branching ratio is given for  $m_H = 125 \text{ GeV}$  and assumes the Standard Model rates for VBF and gluon-fusion production. NODE=S126R01;LINKAGE=K
- 17 AABOUD 19AL combine results of  $H$  decaying to invisible final states with VBF(AABOUD 19AI),  $ZH$ , and  $WH$  productions (AABOUD 18, AABOUD 18CA), which use  $36.1 \text{ fb}^{-1}$  of data at 13 TeV. The quoted limit is given for  $m_H = 125 \text{ GeV}$  and assumes the Standard Model rates for gluon fusion, VBF,  $ZH$ , and  $WH$  productions. NODE=S126R01;LINKAGE=M
- 18 AABOUD 19AL combine results of 7, 8 (AAD 15CX), and 13 TeV for  $H$  decaying to invisible final states. NODE=S126R01;LINKAGE=N
- 19 SIRUNYAN 19AT perform a combined fit with visible decay using  $35.9 \text{ fb}^{-1}$  of data at 13 TeV. NODE=S126R01;LINKAGE=O
- 20 SIRUNYAN 19BO search for  $pp \rightarrow qqHX$  (VBF) with  $H$  decaying to invisible final states using  $35.9 \text{ fb}^{-1}$  of data. The quoted limit on the branching ratio is given for  $m_H = 125.09 \text{ GeV}$  and assumes the Standard Model production rates. NODE=S126R01;LINKAGE=P
- 21 SIRUNYAN 19BO combine the VBF channel with results of other 13 TeV analyses: SIRUNYAN 18BV and SIRUNYAN 18S. The quoted limit on the branching ratio is given for  $m_H = 125.09 \text{ GeV}$  and assumes the Standard Model production rates. NODE=S126R01;LINKAGE=S
- 22 SIRUNYAN 19BO combine 13 TeV  $35.9 \text{ fb}^{-1}$  results with 7, 8, 13 TeV (KHACHATRYAN 17F) for  $H$  decaying to invisible final states. The quoted limit on the branching ratio is given for  $m_H = 125.09 \text{ GeV}$  and assumes the Standard Model production rates. The branching ratio is obtained to be  $0.05 \pm 0.03 \text{ (stat)} \pm 0.07 \text{ (syst)}$ . NODE=S126R01;LINKAGE=T
- 23 AABOUD 18 search for  $pp \rightarrow HZX$ ,  $Z \rightarrow ee, \mu\mu$  with  $H$  decaying to invisible final states in  $36.1 \text{ fb}^{-1}$  at  $E_{\text{cm}} = 13 \text{ TeV}$ . The quoted limit on the branching ratio is given for  $m_H = 125 \text{ GeV}$  and assumes the Standard Model rate for  $HZ$  production. NODE=S126R01;LINKAGE=H
- 24 AABOUD 18CA search for  $H$  decaying to invisible final states using  $WH$ , and  $ZH$  productions, where  $W$  and  $Z$  hadronically decay. The data of  $36.1 \text{ fb}^{-1}$  at  $E_{\text{cm}} = 13 \text{ TeV}$  is used. The quoted limit assumes SM production cross sections with combining the contributions from  $WH$ ,  $ZH$ , ggF and VBF production modes. NODE=S126R01;LINKAGE=J
- 25 SIRUNYAN 18BV search for  $H$  decaying to invisible final states associated with a  $Z$ ,  $Z \rightarrow \ell\ell$  using  $35.9 \text{ fb}^{-1}$  at 13 TeV. The limit is obtained for  $m_H = 125 \text{ GeV}$  and assuming the SM  $ZH$  production cross section. NODE=S126R01;LINKAGE=R
- 26 SIRUNYAN 18S search for  $H$  decaying to invisible final states associated with an energetic jet or a  $V$ ,  $V \rightarrow q\bar{q}$  using  $35.9 \text{ fb}^{-1}$  at 13 TeV. NODE=S126R01;LINKAGE=Q
- 27 AABOUD 17BD search for  $H$  decaying to invisible final states with  $\geq 1$  jet and VBF events using  $3.2 \text{ fb}^{-1}$  of  $pp$  collisions at  $E_{\text{cm}} = 13 \text{ TeV}$ . A cross-section ratio  $R^{\text{miss}}$  is used in the measurement. The quoted limit is given for  $m_H = 125 \text{ GeV}$ . NODE=S126R01;LINKAGE=I
- 28 KHACHATRYAN 17F search for  $H$  decaying to invisible final states with gluon fusion, VBF,  $ZH$ , and  $WH$  productions using  $2.3 \text{ fb}^{-1}$  of  $pp$  collisions at  $E_{\text{cm}} = 13 \text{ TeV}$ ,  $19.7 \text{ fb}^{-1}$  at 8 TeV, and  $5.1 \text{ fb}^{-1}$  at 7 TeV. The quoted limit is given for  $m_H = 125 \text{ GeV}$  and assumes the Standard Model rates for gluon fusion, VBF,  $ZH$ , and  $WH$  productions. NODE=S126R01;LINKAGE=G
- 29 AAD 16AF search for  $pp \rightarrow qqHX$  (VBF) with  $H$  decaying to invisible final states in  $20.3 \text{ fb}^{-1}$  at  $E_{\text{cm}} = 8 \text{ TeV}$ . The quoted limit on the branching ratio is given for  $m_H = 125 \text{ GeV}$  and assumes the Standard Model rates for VBF and gluon-fusion production. NODE=S126R01;LINKAGE=E
- 30 AAD 16AN perform fits to the ATLAS and CMS data at  $E_{\text{cm}} = 7$  and 8 TeV. The branching fraction of decays into BSM particles that are invisible or into undetected decay modes is measured for  $m_0 = 125.09 \text{ GeV}$ . NODE=S126R01;LINKAGE=F
- 31 AAD 15BD search for  $pp \rightarrow HWX$  and  $pp \rightarrow HZX$  with  $W$  or  $Z$  decaying hadronically and  $H$  decaying to invisible final states using data at  $E_{\text{cm}} = 8 \text{ TeV}$ . The quoted limit is given for  $m_H = 125 \text{ GeV}$ , assumes the Standard Model rates for the production processes and is based on a combination of the contributions from  $HW$ ,  $HZ$  and the gluon-fusion process. NODE=S126R01;LINKAGE=D
- 32 AAD 15CX search for  $H$  decaying to invisible final states with VBF,  $ZH$ , and  $WH$  productions using  $20.3 \text{ fb}^{-1}$  at 8 TeV, and  $4.7 \text{ fb}^{-1}$  at 7 TeV. The quoted limit is given for  $m_H = 125.36 \text{ GeV}$  and assumes the Standard Model rates for gluon fusion, VBF,  $ZH$ , and  $WH$  productions. The upper limit is improved to 0.23 by adding the measured visible decay rates. NODE=S126R01;LINKAGE=L
- 33 AAD 14O search for  $pp \rightarrow HZX$ ,  $Z \rightarrow \ell\ell$ , with  $H$  decaying to invisible final states in  $4.5 \text{ fb}^{-1}$  at  $E_{\text{cm}} = 7 \text{ TeV}$  and  $20.3 \text{ fb}^{-1}$  at  $E_{\text{cm}} = 8 \text{ TeV}$ . The quoted limit on the branching ratio is given for  $m_H = 125.5 \text{ GeV}$  and assumes the Standard Model rate for  $HZ$  production. NODE=S126R01;LINKAGE=A
- 34 CHATRCHYAN 14B search for  $pp \rightarrow HZX$ ,  $Z \rightarrow \ell\ell$  and  $Z \rightarrow b\bar{b}$ , and also  $pp \rightarrow qqHX$  with  $H$  decaying to invisible final states using data at  $E_{\text{cm}} = 7$  and 8 TeV. The quoted limit on the branching ratio is obtained from a combination of the limits from  $HZ$  and  $qqH$ . It is given for  $m_H = 125 \text{ GeV}$  and assumes the Standard Model rates for the two production processes. NODE=S126R01;LINKAGE=B
- 35 CHATRCHYAN 14B search for  $pp \rightarrow HZX$  with  $H$  decaying to invisible final states and  $Z \rightarrow \ell\ell$  in  $4.9 \text{ fb}^{-1}$  at  $E_{\text{cm}} = 7 \text{ TeV}$  and  $19.7 \text{ fb}^{-1}$  at  $E_{\text{cm}} = 8 \text{ TeV}$ , and also NODE=S126R01;LINKAGE=CH



with  $Z \rightarrow b\bar{b}$  in  $18.9 \text{ fb}^{-1}$  at  $E_{\text{cm}} = 8 \text{ TeV}$ . The quoted limit on the branching ratio is given for  $m_H = 125 \text{ GeV}$  and assumes the Standard Model rate for  $HZ$  production.

- 36 CHATRCHYAN 14B search for  $pp \rightarrow qqHX$  (vector boson fusion) with  $H$  decaying to invisible final states in  $19.5 \text{ fb}^{-1}$  at  $E_{\text{cm}} = 8 \text{ TeV}$ . The quoted limit on the branching ratio is given for  $m_H = 125 \text{ GeV}$  and assumes the Standard Model rate for  $qqH$  production.

NODE=S126R01;LINKAGE=C

$\Gamma(\gamma \text{ invisible})/\Gamma_{\text{total}}$

$\Gamma_{33}/\Gamma$

VALUE	CL%	DOCUMENT ID	TECN	COMMENT
<0.013	95	<sup>1</sup> AAD	24BH ATLS	VBF, $HZ$ , $H \rightarrow \gamma + \text{invisible}$ , 13 TeV

NODE=S126R15  
NODE=S126R15

• • • We do not use the following data for averages, fits, limits, etc. • • •

<0.035	95	<sup>2</sup> SIRUNYAN	21L CMS	VBF, $H \rightarrow \gamma + \text{invisible}$ , 13 TeV
<0.029	95	<sup>2,3</sup> SIRUNYAN	21L CMS	VBF, $HZ$ , $H \rightarrow \gamma + \text{invisible}$ , 13 TeV
<0.046	95	<sup>4</sup> SIRUNYAN	19CG CMS	$pp \rightarrow HZ$ , $H \rightarrow \gamma + \text{invisible}$ , $Z \rightarrow \ell\ell$ , 13 TeV

OCCUR=2

- <sup>1</sup> AAD 24BH search for  $H$  decaying to an invisible final state plus a  $\gamma$  in the VBF and  $HZ$  production using  $139 \text{ fb}^{-1}$  data at  $E_{\text{cm}} = 13 \text{ TeV}$ . The invisible state is called a dark photon. The quoted limit on the branching ratio is given for  $m_H = 125 \text{ GeV}$  assuming the Standard Model rates. The 95% CL upper limits on the branching ratio for the VBF and  $HZ$  production are 1.8% and 2.3%, respectively. See their Fig. 3(a).

NODE=S126R15;LINKAGE=D

- <sup>2</sup> SIRUNYAN 21L search for  $H$  decaying to an invisible final state plus a  $\gamma$  in the VBF production using  $130 \text{ fb}^{-1}$  data at  $E_{\text{cm}} = 13 \text{ TeV}$ . The invisible state is called a dark photon. The quoted limit on the branching ratio is given for  $m_H = 125 \text{ GeV}$  assuming the Standard Model rates.

NODE=S126R15;LINKAGE=B

- <sup>3</sup> The result of the VBF production is combined with the  $pp \rightarrow HZ$  result (SIRUNYAN 19CG).

NODE=S126R15;LINKAGE=C

- <sup>4</sup> SIRUNYAN 19CG search for  $pp \rightarrow HZ$ ,  $Z \rightarrow ee, \mu\mu$  with  $H$  decaying to invisible final states plus a  $\gamma$  in  $137 \text{ fb}^{-1}$  at  $E_{\text{cm}} = 13 \text{ TeV}$ . The quoted limit on the branching ratio is given for  $m_H = 125 \text{ GeV}$  assuming the Standard Model rate for  $HZ$  production and is obtained in the context of a theoretical model, where the undetected (invisible) particle is massless.

NODE=S126R15;LINKAGE=A

## H SIGNAL STRENGTHS IN DIFFERENT CHANNELS

NODE=S126230

The  $H$  signal strength in a particular final state  $xx$  is given by the cross section times branching ratio in this channel normalized to the Standard Model (SM) value,  $\sigma \cdot B(H \rightarrow xx) / (\sigma \cdot B(H \rightarrow xx))_{\text{SM}}$ , for the specified mass value of  $H$ . For the SM predictions, see DITTMAYER 11, DITTMAYER 12, and HEINEMEYER 13A. Results for fiducial and differential cross sections are also listed below.

NODE=S126230

### Combined final state

VALUE	DOCUMENT ID	TECN	COMMENT
<b>1.03 ±0.04 OUR AVERAGE</b>			
1.05 ±0.06	<sup>1</sup> ATLAS	22 ATLS	$pp$ , 13 TeV
1.002±0.057	<sup>2</sup> CMS	22 CMS	$pp$ , 13 TeV
1.09 ±0.07 ±0.04 <sup>+0.08</sup> <sub>-0.07</sub>	<sup>3,4</sup> AAD	16AN LHC	$pp$ , 7, 8 TeV
1.44 <sup>+0.59</sup> <sub>-0.56</sub>	<sup>5</sup> AALTONEN	13M TEVA	$p\bar{p} \rightarrow HX$ , 1.96 TeV
• • • We do not use the following data for averages, fits, limits, etc. • • •			
1.11 <sup>+0.09</sup> <sub>-0.08</sub>	<sup>6</sup> AAD	20 ATLS	$pp$ , 13 TeV
1.17 ±0.10	<sup>7</sup> SIRUNYAN	19AT CMS	$pp$ , 13 TeV
	<sup>8</sup> SIRUNYAN	19BA CMS	$pp$ , 13 TeV, differential cross sections
1.20 ±0.10 ±0.06 <sup>+0.09</sup> <sub>-0.08</sub>	<sup>4</sup> AAD	16AN ATLS	$pp$ , 7, 8 TeV
0.97 ±0.09 ±0.05 <sup>+0.08</sup> <sub>-0.07</sub>	<sup>4</sup> AAD	16AN CMS	$pp$ , 7, 8 TeV
1.18 ±0.10 ±0.07 <sup>+0.08</sup> <sub>-0.07</sub>	<sup>9</sup> AAD	16K ATLS	$pp$ , 7, 8 TeV
0.75 <sup>+0.28</sup> <sub>-0.26</sub> ±0.13 <sup>+0.08</sup> <sub>-0.05</sub>	<sup>9</sup> AAD	16K ATLS	$pp$ , 7 TeV
1.28 ±0.11 ±0.08 <sup>+0.10</sup> <sub>-0.07</sub>	<sup>9</sup> AAD	16K ATLS	$pp$ , 8 TeV
	<sup>10</sup> AAD	15P ATLS	$pp$ , 8 TeV, cross section
1.00 ±0.09 ±0.07 <sup>+0.08</sup> <sub>-0.07</sub>	<sup>11</sup> KHACHATRY...15AM	CMS	$pp$ , 7, 8 TeV

NODE=S126SA  
NODE=S126SA

OCCUR=2

OCCUR=3

OCCUR=2

OCCUR=3

1.33 $^{+0.14}_{-0.10}$ $\pm 0.15$	12 AAD	13AK ATLS	$pp$ , 7 and 8 TeV	
1.54 $^{+0.77}_{-0.73}$	13 AALTONEN	13L CDF	$p\bar{p} \rightarrow HX$ , 1.96 TeV	
1.40 $^{+0.92}_{-0.88}$	14 ABAZOV	13L D0	$p\bar{p} \rightarrow HX$ , 1.96 TeV	
1.4 $\pm 0.3$	15 AAD	12AI ATLS	$pp \rightarrow HX$ , 7, 8 TeV	
1.2 $\pm 0.4$	15 AAD	12AI ATLS	$pp \rightarrow HX$ , 7 TeV	OCCUR=2
1.5 $\pm 0.4$	15 AAD	12AI ATLS	$pp \rightarrow HX$ , 8 TeV	OCCUR=3
0.87 $\pm 0.23$	16 CHATRCHYAN	12N CMS	$pp \rightarrow HX$ , 7, 8 TeV	
<sup>1</sup> ATLAS 22 report combined results (see their Extended Data Table 1) using up to 139 fb <sup>-1</sup> of data at $E_{\text{cm}} = 13$ TeV, assuming $m_H = 125.09$ GeV. The Higgs production cross-sections, branching fractions and several ratios are found in their Figs. 2 and 3.				NODE=S126SA;LINKAGE=J
<sup>2</sup> CMS 22 report combined results (see their Extended Data Table 2) using 138 fb <sup>-1</sup> of data at $E_{\text{cm}} = 13$ TeV, assuming $m_H = 125.38$ GeV. Signal strengths for production modes and decay channels are found in their Fig. 2.				NODE=S126SA;LINKAGE=I
<sup>3</sup> AAD 16AN perform fits to the ATLAS and CMS data at $E_{\text{cm}} = 7$ and 8 TeV. The signal strengths for individual production processes are $1.03^{+0.16}_{-0.14}$ for gluon fusion, $1.18^{+0.25}_{-0.23}$ for vector boson fusion, $0.89^{+0.40}_{-0.38}$ for $WH$ production, $0.79^{+0.38}_{-0.36}$ for $ZH$ production, and $2.3^{+0.7}_{-0.6}$ for $t\bar{t}H$ production.				NODE=S126SA;LINKAGE=F
<sup>4</sup> AAD 16AN: The uncertainties represent statistics, experimental systematics, and added in quadrature theory systematics on the background and on the signal. The quoted signal strengths are given for $m_H = 125.09$ GeV. In the fit, relative branching ratios and relative production cross sections are fixed to those in the Standard Model.				NODE=S126SA;LINKAGE=G
<sup>5</sup> AALTONEN 13M combine all Tevatron data from the CDF and D0 Collaborations with up to 10.0 fb <sup>-1</sup> and 9.7 fb <sup>-1</sup> , respectively, of $p\bar{p}$ collisions at $E_{\text{cm}} = 1.96$ TeV. The quoted signal strength is given for $m_H = 125$ GeV.				NODE=S126SA;LINKAGE=AT
<sup>6</sup> AAD 20 combine results of up to 79.8 fb <sup>-1</sup> of data at $E_{\text{cm}} = 13$ TeV, assuming $m_H = 125.09$ GeV: $\gamma\gamma$ , $ZZ^*$ , $WW^*$ , $\tau\tau$ , $b\bar{b}$ , $\mu\mu$ , invisible, and off-shell analyses (see their Table I). The signal strengths for individual production processes are $1.04 \pm 0.09$ for gluon fusion, $1.21^{+0.24}_{-0.22}$ for vector boson fusion, $1.30^{+0.40}_{-0.38}$ for $WH$ production, $1.05^{+0.31}_{-0.29}$ for $ZH$ production, and $1.21^{+0.26}_{-0.24}$ for $t\bar{t}H+tH$ production (see their Fig. 2 and Table IV). Several results with the simplified template cross section and $\kappa$ -frameworks are presented: see their Figs. 9–11, Figs 20, 21 and Table VIII for stage-1 simplified template cross sections, their Figs. 12–17 and Tables X–XII for the $\kappa$ -framework.				NODE=S126SA;LINKAGE=H
<sup>7</sup> SIRUNYAN 19AT combine results of 35.9 fb <sup>-1</sup> of data at $E_{\text{cm}} = 13$ TeV, assuming $m_H = 125.09$ GeV. The signal strengths for individual production processes are $1.22^{+0.14}_{-0.12}$ for gluon fusion, $0.73^{+0.30}_{-0.27}$ for vector boson fusion, $2.18^{+0.58}_{-0.55}$ for $WH$ production, $0.87^{+0.44}_{-0.42}$ for $ZH$ production, and $1.18^{+0.30}_{-0.27}$ for $t\bar{t}H$ production. Several results with the simplified template cross section and $\kappa$ -frameworks are presented: see their Fig. 8 and Table 5 for stage-0 simplified template cross sections, their Figs. 9–18 and Tables 7–11 for the $\kappa$ -framework.				NODE=S126SA;LINKAGE=D
<sup>8</sup> SIRUNYAN 19BA measure differential cross sections for the Higgs boson transverse momentum, the number of jets, the rapidity of the Higgs boson and the transverse momentum of the leading jet using 35.9 fb <sup>-1</sup> of data at $E_{\text{cm}} = 13$ TeV with $H \rightarrow \gamma\gamma$ , $H \rightarrow ZZ^*$ , and $H \rightarrow b\bar{b}$ . The total cross section for Higgs boson production is measured to be $61.1 \pm 6.0 \pm 3.7$ pb using $H \rightarrow \gamma\gamma$ and $H \rightarrow ZZ^*$ channels. Several coupling measurements in the $\kappa$ -framework are performed.				NODE=S126SA;LINKAGE=E
<sup>9</sup> AAD 16K use up to 4.7 fb <sup>-1</sup> of $pp$ collisions at $E_{\text{cm}} = 7$ TeV and up to 20.3 fb <sup>-1</sup> at $E_{\text{cm}} = 8$ TeV. The third uncertainty in the measurement is theory systematics. The signal strengths for individual production modes are $1.23 \pm 0.14^{+0.09+0.16}_{-0.08-0.12}$ for gluon fusion, $1.23^{+0.28+0.13+0.11}_{-0.27-0.12-0.09}$ for vector boson fusion, $0.80^{+0.31}_{-0.30} \pm 0.17^{+0.10}_{-0.05}$ for $W/ZH$ production, and $1.81^{+0.52+0.58+0.31}_{-0.50-0.55-0.12}$ for $t\bar{t}H$ production. The quoted signal strengths are given for $m_H = 125.36$ GeV.				NODE=S126SA;LINKAGE=B
<sup>10</sup> AAD 15P measure total and differential cross sections of the process $pp \rightarrow HX$ at $E_{\text{cm}} = 8$ TeV with 20.3 fb <sup>-1</sup> . $\gamma\gamma$ and $4\ell$ final states are used. $\sigma(pp \rightarrow HX) = 33.0 \pm 5.3 \pm 1.6$ pb is given. See their Figs. 2 and 3 for data on differential cross sections.				NODE=S126SA;LINKAGE=C
<sup>11</sup> KHACHATRYAN 15AM use up to 5.1 fb <sup>-1</sup> of $pp$ collisions at $E_{\text{cm}} = 7$ TeV and up to 19.7 fb <sup>-1</sup> at $E_{\text{cm}} = 8$ TeV. The third uncertainty in the measurement is theory systematics. Fits to each production mode give the value of $0.85^{+0.19}_{-0.16}$ for gluon fusion, $1.16^{+0.37}_{-0.34}$ for vector boson fusion, $0.92^{+0.38}_{-0.36}$ for $WH$ , $ZH$ production, and $2.90^{+1.08}_{-0.94}$ for $t\bar{t}H$ production.				NODE=S126SA;LINKAGE=A
<sup>12</sup> AAD 13AK use 4.7 fb <sup>-1</sup> of $pp$ collisions at $E_{\text{cm}} = 7$ TeV and 20.7 fb <sup>-1</sup> at $E_{\text{cm}} = 8$ TeV. The combined signal strength is based on the $\gamma\gamma$ , $ZZ^* \rightarrow 4\ell$ , and $WW^* \rightarrow \ell\nu\ell\nu$ channels. The quoted signal strength is given for $m_H = 125.5$ GeV. Reported statistical error value modified following private communication with the experiment.				NODE=S126SA;LINKAGE=LH

- <sup>13</sup> AALTONEN 13L combine all CDF results with 9.45–10.0 fb<sup>-1</sup> of  $p\bar{p}$  collisions at  $E_{\text{cm}} = 1.96$  TeV. The quoted signal strength is given for  $m_H = 125$  GeV.
- <sup>14</sup> ABAZOV 13L combine all D0 results with up to 9.7 fb<sup>-1</sup> of  $p\bar{p}$  collisions at  $E_{\text{cm}} = 1.96$  TeV. The quoted signal strength is given for  $m_H = 125$  GeV.
- <sup>15</sup> AAD 12AI obtain results based on 4.6–4.8 fb<sup>-1</sup> of  $pp$  collisions at  $E_{\text{cm}} = 7$  TeV and 5.8–5.9 fb<sup>-1</sup> at  $E_{\text{cm}} = 8$  TeV. An excess of events over background with a local significance of  $5.9\sigma$  is observed at  $m_H = 126$  GeV. The quoted signal strengths are given for  $m_H = 126$  GeV. See also AAD 12DA.
- <sup>16</sup> CHATRCHYAN 12N obtain results based on 4.9–5.1 fb<sup>-1</sup> of  $pp$  collisions at  $E_{\text{cm}} = 7$  TeV and 5.1–5.3 fb<sup>-1</sup> at  $E_{\text{cm}} = 8$  TeV. An excess of events over background with a local significance of  $5.0\sigma$  is observed at about  $m_H = 125$  GeV. The combined signal strength is based on the  $\gamma\gamma$ ,  $ZZ^*$ ,  $WW^*$ ,  $\tau^+\tau^-$ , and  $b\bar{b}$  channels. The quoted signal strength is given for  $m_H = 125.5$  GeV. See also CHATRCHYAN 13Y.

NODE=S126SA;LINKAGE=LL

NODE=S126SA;LINKAGE=AB

NODE=S126SA;LINKAGE=AA

NODE=S126SA;LINKAGE=CA

**W W\* final state**

VALUE

DOCUMENT ID

TECN

COMMENT

**1.00±0.08 OUR AVERAGE**

0.97±0.09

<sup>1</sup> CMS

22

CMS

 $pp$ , 13 TeV1.09<sup>+0.18</sup><sub>-0.16</sub><sup>2,3</sup> AAD

16AN

LHC

 $pp$ , 7, 8 TeV0.94<sup>+0.85</sup><sub>-0.83</sub><sup>4</sup> AALTONEN

13M

TEVA

 $p\bar{p} \rightarrow HX$ , 1.96 TeV

● ● ● We do not use the following data for averages, fits, limits, etc. ● ● ●

0.92<sup>+0.25</sup><sub>-0.23</sub><sup>5</sup> AAD

25AG

CMS

 $pp \rightarrow WH/ZH$ , 13 TeV

1.20±0.50±0.11

<sup>6</sup> HAYRAPETY...

25AC

CMS

 $pp \rightarrow ZH$ , 13 TeV<sup>7</sup> HAYRAPETY...

24AG

CMS

 $pp, H \rightarrow WW^* (\rightarrow e\nu\mu\nu)$ , 13 TeV<sup>8</sup> AAD

23AP

ATLS

 $pp$ , 13 TeV, cross sections<sup>9</sup> AAD

23BV

ATLS

 $pp$ , 13 TeV, cross sections0.95<sup>+0.10</sup><sub>-0.09</sub><sup>10,11</sup> TUMASYAN

23W

CMS

 $pp$ , 13 TeV0.92<sup>+0.11</sup><sub>-0.10</sub><sup>10,12,13</sup> TUMASYAN

23W

CMS

 $pp$ , 13 TeV

OCCUR=2

0.71<sup>+0.28</sup><sub>-0.25</sub><sup>10,12,14</sup> TUMASYAN

23W

CMS

 $pp$ , 13 TeV

OCCUR=3

2.2 ±0.6

<sup>10,12,15</sup> TUMASYAN

23W

CMS

 $pp$ , 13 TeV

OCCUR=4

2.0 ±0.7

<sup>10,12,16</sup> TUMASYAN

23W

CMS

 $pp$ , 13 TeV

OCCUR=5

<sup>10,17</sup> TUMASYAN

23W

CMS

 $pp$ , 13 TeV

OCCUR=6

0.5 ±0.4<sup>+0.7</sup><sub>-0.6</sub><sup>18</sup> AAD

22V

ATLS

 $pp, WW^* (\rightarrow e\nu\mu\nu) + 2j$ , 13 TeV<sup>19</sup> AAD

22V

ATLS

 $pp, WW^* (\rightarrow e\nu\mu\nu) + 2j$ , 13 TeV

OCCUR=2

<sup>20</sup> AABOUD

19F

ATLS

 $pp$ , 13 TeV, cross sections2.5<sup>+0.9</sup><sub>-0.8</sub><sup>21</sup> AAD

19A

ATLS

 $pp \rightarrow HW/HZ, H \rightarrow WW^*$ , 13 TeV1.28<sup>+0.17</sup><sub>-0.16</sub><sup>22</sup> SIRUNYAN

19AT

CMS

 $pp$ , 13 TeV1.28<sup>+0.18</sup><sub>-0.17</sub><sup>23</sup> SIRUNYAN

19AX

CMS

 $pp$ , 13 TeV1.22<sup>+0.23</sup><sub>-0.21</sub><sup>3</sup> AAD

16AN

ATLS

 $pp$ , 7, 8 TeV

OCCUR=2

0.90<sup>+0.23</sup><sub>-0.21</sub><sup>3</sup> AAD

16AN

CMS

 $pp$ , 7, 8 TeV

OCCUR=3

<sup>24</sup> AAD

16AO

ATLS

 $pp$ , 8 TeV, cross sections1.18±0.16<sup>+0.17</sup><sub>-0.14</sub><sup>25</sup> AAD

16K

ATLS

 $pp$ , 7, 8 TeV1.09<sup>+0.16</sup><sub>-0.15</sub><sup>+0.17</sup><sub>-0.14</sub><sup>26</sup> AAD

15AA

ATLS

 $pp$ , 7, 8 TeV3.0<sup>+1.3</sup><sub>-1.1</sub><sup>+1.0</sup><sub>-0.7</sub><sup>27</sup> AAD

15AQ

ATLS

 $pp \rightarrow HW/ZX$ , 7, 8 TeV1.16<sup>+0.16</sup><sub>-0.15</sub><sup>+0.18</sup><sub>-0.15</sub><sup>28</sup> AAD

15AQ

ATLS

 $pp$ , 7, 8 TeV

OCCUR=2

0.72±0.12±0.10<sup>+0.12</sup><sub>-0.10</sub><sup>29</sup> CHATRCHYAN 14G

CMS

 $pp$ , 7, 8 TeV0.99<sup>+0.31</sup><sub>-0.28</sub><sup>30</sup> AAD

13AK

ATLS

 $pp$ , 7 and 8 TeV0.00<sup>+1.78</sup><sub>-0.00</sub><sup>31</sup> AALTONEN

13L

CDF

 $p\bar{p} \rightarrow HX$ , 1.96 TeV1.90<sup>+1.63</sup><sub>-1.52</sub><sup>32</sup> ABAZOV

13L

D0

 $p\bar{p} \rightarrow HX$ , 1.96 TeV

1.3 ±0.5

<sup>33</sup> AAD

12AI

ATLS

 $pp \rightarrow HX$ , 7, 8 TeV

0.5 ±0.6

<sup>33</sup> AAD

12AI

ATLS

 $pp \rightarrow HX$ , 7 TeV

OCCUR=2

1.9 ±0.7

<sup>33</sup> AAD

12AI

ATLS

 $pp \rightarrow HX$ , 8 TeV

OCCUR=3

0.60<sup>+0.42</sup><sub>-0.37</sub><sup>34</sup> CHATRCHYAN 12N

CMS

 $pp \rightarrow HX$ , 7, 8 TeV

- <sup>1</sup> CMS 22 report combined results (see their Extended Data Table 2) using up to  $138 \text{ fb}^{-1}$  of data at  $E_{\text{cm}} = 13 \text{ TeV}$ , assuming  $m_H = 125.38 \text{ GeV}$ . See their Fig. 2 right. NODE=S126SWW;LINKAGE=O
- <sup>2</sup> AAD 16AN perform fits to the ATLAS and CMS data at  $E_{\text{cm}} = 7$  and  $8 \text{ TeV}$ . The signal strengths for individual production processes are  $0.84 \pm 0.17$  for gluon fusion,  $1.2 \pm 0.4$  for vector boson fusion,  $1.6^{+1.2}_{-1.0}$  for  $WH$  production,  $5.9^{+2.6}_{-2.2}$  for  $ZH$  production, and  $5.0^{+1.8}_{-1.7}$  for  $t\bar{t}H$  production. NODE=S126SWW;LINKAGE=I
- <sup>3</sup> AAD 16AN: In the fit, relative production cross sections are fixed to those in the Standard Model. The quoted signal strength is given for  $m_H = 125.09 \text{ GeV}$ . NODE=S126SWW;LINKAGE=J
- <sup>4</sup> AALTONEN 13M combine all Tevatron data from the CDF and D0 Collaborations with up to  $10.0 \text{ fb}^{-1}$  and  $9.7 \text{ fb}^{-1}$ , respectively, of  $p\bar{p}$  collisions at  $E_{\text{cm}} = 1.96 \text{ TeV}$ . The quoted signal strength is given for  $m_H = 125 \text{ GeV}$ . NODE=S126SWW;LINKAGE=AT
- <sup>5</sup> AAD 25AG measure the signal strengths using  $H \rightarrow WW^* \rightarrow \ell\nu\ell\nu$  and  $H \rightarrow WW^* \rightarrow \ell\nu jj$  ( $\ell = e, \mu$ ) with  $140 \text{ fb}^{-1}$  data at  $E_{\text{cm}} = 13 \text{ TeV}$ . The signal strengths are summarized in their Table 9 and Fig. 12. The sum of  $WH$  and  $ZH$  cross sections times the  $H \rightarrow WW^*$  branching ratio is measured to be  $0.44^{+0.10+0.06}_{-0.09-0.05} \text{ pb}$  and these two-dimensional likelihood scans are shown in their Fig. 14. Cross sections times the  $H \rightarrow WW^*$  branching ratio and ratios to the SM values are given in their Tables 12, 13, 14 and Figs. 15 and 16, which are based on the simplified template cross section framework (reduced stage-1.2). NODE=S126SWW;LINKAGE=DA
- <sup>6</sup> HAYRAPETYAN 25AC measure the  $ZH$  production cross section to the SM prediction using  $H \rightarrow WW^*$  decay channel with  $138 \text{ fb}^{-1}$  and  $62 \text{ fb}^{-1}$  of  $pp$  collision data at  $E_{\text{cm}} = 13 \text{ TeV}$  and  $13.6 \text{ TeV}$ , respectively. Events with  $4\ell$  ( $\ell = e, \mu$ ) are used. The cross section times the  $H \rightarrow WW^*$  branching fraction and the signal strength for each center of mass energy are shown in their Table I. The corresponding significances are given in their Table II. NODE=S126SWW;LINKAGE=EA
- <sup>7</sup> HAYRAPETYAN 24AG search for the anomalous couplings of the Higgs boson to vector bosons, including  $CP$  violation effects using  $H \rightarrow WW^* \rightarrow e\nu\mu\nu$  decay channel ( $\ell = e, \mu$ ) with  $138 \text{ fb}^{-1}$  at  $E_{\text{cm}} = 13 \text{ TeV}$ . The anomalous HVV and Hgg coupling parameters are given in their Table 7. The data constrain the SMEFT Higgs and Warsaw bases coupling parameters as shown in their Tables 8, 9 and Fig. 12. NODE=S126SWW;LINKAGE=BA
- <sup>8</sup> AAD 23AP measure cross-sections times the  $H \rightarrow WW^*$  branching fraction in the  $H \rightarrow WW^* \rightarrow e\nu\mu\nu$  channel using  $139 \text{ fb}^{-1}$  of  $pp$  collisions at  $E_{\text{cm}} = 13 \text{ TeV}$ :  $\sigma_{ggF} \times B(H \rightarrow WW^*) = 12.0 \pm 1.4 \text{ pb}$ ,  $\sigma_{VBF} \times B(H \rightarrow WW^*) = 0.75^{+0.19}_{-0.16} \text{ pb}$ , and  $\sigma_{ggF+VBF} \times B(H \rightarrow WW^*) = 12.3 \pm 1.3 \text{ pb}$ . The results are given for  $m_H = 125.09 \text{ GeV}$ . Measured cross sections and ratios to the SM predictions in the reduced stage-1.2 (see their Fig. 5) simplified template cross section framework are shown in their Table VII and Fig. 15. NODE=S126SWW;LINKAGE=P
- <sup>9</sup> AAD 23BV measure fiducial total and differential cross sections of VBF process at  $E_{\text{cm}} = 13 \text{ TeV}$  with  $139 \text{ fb}^{-1}$  using  $H \rightarrow WW^* \rightarrow e\nu\mu\nu$ . The measured total fiducial cross section is  $1.68 \pm 0.33(\text{stat}) \pm 0.23(\text{syst}) \text{ fb}$  in their fiducial region (Table II and Section V). See their Fig. 9 for the comparison with theory predictions. The fiducial differential cross sections are shown in their Figs. 11, 12, and 13. Wilson coefficients in the Warsaw basis at 95% confidence interval are measured; see their Table V and Fig. 16. NODE=S126SWW;LINKAGE=Z
- <sup>10</sup> TUMASYAN 23W measure Higgs production rates with  $H \rightarrow WW^*$  at  $E_{\text{cm}} = 13 \text{ TeV}$  with  $138 \text{ fb}^{-1}$  data. The quoted results are given for  $m_H = 125.38 \text{ GeV}$ . NODE=S126SWW;LINKAGE=Q
- <sup>11</sup> The quoted global signal strength is obtained assuming the relative ratios of different Higgs production modes fixed to the SM values. NODE=S126SWW;LINKAGE=R
- <sup>12</sup> The 4 signal strengths for gluon-fusion (ggF), VBF,  $WH$  and  $ZH$  modes are fit assuming  $t\bar{t}H$  and  $b\bar{b}H$  fixed to the SM values. NODE=S126SWW;LINKAGE=T
- <sup>13</sup> The quoted result is for ggF production mode. NODE=S126SWW;LINKAGE=V
- <sup>14</sup> The quoted result is for VBF production mode. NODE=S126SWW;LINKAGE=U
- <sup>15</sup> The quoted result is for  $WH$  production mode. NODE=S126SWW;LINKAGE=W
- <sup>16</sup> The quoted result is for  $ZH$  production mode. NODE=S126SWW;LINKAGE=X
- <sup>17</sup> Measured cross sections and ratios to the SM predictions in the reduced stage-1.2 (see their Fig. 17) simplified template cross section framework (6 ggF, 4 VBF, and 4  $VH$ ) are shown in their Table 18 and Fig. 26. NODE=S126SWW;LINKAGE=Y
- <sup>18</sup> AAD 22V measure the signal strength for  $ggF+2\text{jets}$  with  $36.1 \text{ fb}^{-1}$  data at  $13 \text{ TeV}$ . NODE=S126SWW;LINKAGE=M
- <sup>19</sup> AAD 22v probe the Higgs couplings to longitudinally and transversely polarized  $W$  and  $Z$  using VBF ( $H \rightarrow WW^* \rightarrow e\nu\mu\nu$  plus two jets) with  $36.1 \text{ fb}^{-1}$  of data at  $E_{\text{cm}} = 13 \text{ TeV}$ . The ratios of the polarization-dependent couplings  $g_{HV_L V_L}$  and  $g_{HV_T V_T}$  to the Higgs- $V$  coupling predicted by the SM,  $a_L = g_{HV_L V_L}/g_{HVV}^{\text{SM}}$  and  $a_T = g_{HV_T V_T}/g_{HVV}^{\text{SM}}$  are measured to be  $0.91^{+0.10+0.09}_{-0.18-0.17}$  and  $1.2 \pm 0.4^{+0.2}_{-0.3}$ , respectively, assuming the standard  $Hgg$  coupling. These measurements are translated into pseudo-observables of  $\kappa_{VV}$  and  $\epsilon_{VV}$ :  $\kappa_{VV} = 0.91^{+0.10+0.09}_{-0.18-0.17}$  and  $\epsilon_{VV} = 0.13^{+0.28+0.08}_{-0.20-0.10}$ , where  $\kappa_{VV} = 1$  and  $\epsilon_{VV} = 0$  for the SM. See their Tables 9 and 10. NODE=S126SWW;LINKAGE=N
- <sup>20</sup> AABOUD 19F measure cross-sections times the  $H \rightarrow WW^*$  branching fraction in the  $H \rightarrow WW^* \rightarrow e\nu\mu\nu$  channel using  $36.1 \text{ fb}^{-1}$  of  $pp$  collisions at  $E_{\text{cm}} = 13$  NODE=S126SWW;LINKAGE=F

TeV:  $\sigma_{ggF} \times B(H \rightarrow WW^*) = 11.4^{+1.2+1.8}_{-1.1-1.7}$  pb and  $\sigma_{VBF} \times B(H \rightarrow WW^*) = 0.50^{+0.24}_{-0.22} \pm 0.17$  pb.

- 21 AAD 19A use  $36.1 \text{ fb}^{-1}$  data at 13 TeV. The cross section times branching fraction values are measured to be  $0.67^{+0.31+0.18}_{-0.27-0.14}$  pb for  $WH$ ,  $H \rightarrow WW^*$  and  $0.54^{+0.31+0.15}_{-0.24-0.07}$  pb for  $ZH$ ,  $H \rightarrow WW^*$ .

NODE=S126SWW;LINKAGE=L

- 22 SIRUNYAN 19AT perform a combine fit to  $35.9 \text{ fb}^{-1}$  of data at  $E_{\text{cm}} = 13$  TeV.

NODE=S126SWW;LINKAGE=G  
NODE=S126SWW;LINKAGE=K

- 23 SIRUNYAN 19AX measure the signal strengths, cross sections and so on using gluon fusion, VBF and  $VH$  production processes with  $35.9 \text{ fb}^{-1}$  of data. The quoted signal strength is given for  $m_H = 125.09$  GeV. Signal strengths for each production process is found in their Fig. 9. Measured cross sections and ratios to the SM predictions in the stage-0 simplified template cross section framework are shown in their Fig. 10.  $\kappa_F = 1.52^{+0.48}_{-0.41}$  and  $\kappa_V = 1.10 \pm 0.08$  are obtained (see their Fig. 11 (right)).

NODE=S126SWW;LINKAGE=H

- 24 AAD 16AO measure fiducial total and differential cross sections of gluon fusion process at  $E_{\text{cm}} = 8$  TeV with  $20.3 \text{ fb}^{-1}$  using  $H \rightarrow WW^* \rightarrow e\nu\mu\nu$ . The measured fiducial total cross section is  $36.0 \pm 9.7$  fb in their fiducial region (Table 7). See their Fig. 6 for fiducial differential cross sections. The results are given for  $m_H = 125$  GeV.

NODE=S126SWW;LINKAGE=E

- 25 AAD 16K use up to  $4.7 \text{ fb}^{-1}$  of  $pp$  collisions at  $E_{\text{cm}} = 7$  TeV and up to  $20.3 \text{ fb}^{-1}$  at  $E_{\text{cm}} = 8$  TeV. The quoted signal strength is given for  $m_H = 125.36$  GeV.

NODE=S126SWW;LINKAGE=B

- 26 AAD 15AA use  $4.5 \text{ fb}^{-1}$  of  $pp$  collisions at  $E_{\text{cm}} = 7$  TeV and  $20.3 \text{ fb}^{-1}$  at  $E_{\text{cm}} = 8$  TeV. The signal strength for the gluon fusion and vector boson fusion mode is  $1.02 \pm 0.19^{+0.22}_{-0.18}$  and  $1.27^{+0.44+0.30}_{-0.40-0.21}$ , respectively. The quoted signal strengths are given for  $m_H = 125.36$  GeV.

NODE=S126SWW;LINKAGE=C

- 27 AAD 15AQ use  $4.5 \text{ fb}^{-1}$  of  $pp$  collisions at  $E_{\text{cm}} = 7$  TeV and  $20.3 \text{ fb}^{-1}$  at  $E_{\text{cm}} = 8$  TeV. The quoted signal strength is given for  $m_H = 125.36$  GeV.

NODE=S126SWW;LINKAGE=D

- 28 AAD 15AQ combine their result on  $W/ZH$  production with the results of AAD 15AA (gluon fusion and vector boson fusion, slightly updated). The quoted signal strength is given for  $m_H = 125.36$  GeV.

NODE=S126SWW;LINKAGE=A

- 29 CHATRCHYAN 14G use  $4.9 \text{ fb}^{-1}$  of  $pp$  collisions at  $E_{\text{cm}} = 7$  TeV and  $19.4 \text{ fb}^{-1}$  at  $E_{\text{cm}} = 8$  TeV. The last uncertainty in the measurement is theory systematics. The quoted signal strength is given for  $m_H = 125.6$  GeV.

NODE=S126SWW;LINKAGE=LH

- 30 AAD 13AK use  $4.7 \text{ fb}^{-1}$  of  $pp$  collisions at  $E_{\text{cm}} = 7$  TeV and  $20.7 \text{ fb}^{-1}$  at  $E_{\text{cm}} = 8$  TeV. The quoted signal strength is given for  $m_H = 125.5$  GeV. Superseded by AAD 15AA.

NODE=S126SWW;LINKAGE=LL

- 31 AALTONEN 13L combine all CDF results with  $9.45\text{--}10.0 \text{ fb}^{-1}$  of  $p\bar{p}$  collisions at  $E_{\text{cm}} = 1.96$  TeV. The quoted signal strength is given for  $m_H = 125$  GeV.

NODE=S126SWW;LINKAGE=AB

- 32 ABAZOV 13L combine all D0 results with up to  $9.7 \text{ fb}^{-1}$  of  $p\bar{p}$  collisions at  $E_{\text{cm}} = 1.96$  TeV. The quoted signal strength is given for  $m_H = 125$  GeV.

NODE=S126SWW;LINKAGE=AA

- 33 AAD 12AI obtain results based on  $4.7 \text{ fb}^{-1}$  of  $pp$  collisions at  $E_{\text{cm}} = 7$  TeV and  $5.8 \text{ fb}^{-1}$  at  $E_{\text{cm}} = 8$  TeV. The quoted signal strengths are given for  $m_H = 126$  GeV. See also AAD 12DA.

NODE=S126SWW;LINKAGE=CA

- 34 CHATRCHYAN 12N obtain results based on  $4.9 \text{ fb}^{-1}$  of  $pp$  collisions at  $E_{\text{cm}} = 7$  TeV and  $5.1 \text{ fb}^{-1}$  at  $E_{\text{cm}} = 8$  TeV. The quoted signal strength is given for  $m_H = 125.5$  GeV. See also CHATRCHYAN 13Y.

## ZZ\* final state

VALUE	CL%	DOCUMENT ID	TECN	COMMENT
-------	-----	-------------	------	---------

### 1.02±0.08 OUR AVERAGE

$0.97^{+0.12}_{-0.11}$	1	CMS	22	CMS	$pp$ , 13 TeV
$1.01 \pm 0.11$	2,3	AAD	20AQ	ATLS	$pp$ , 13 TeV
$1.29^{+0.26}_{-0.23}$	4,5	AAD	16AN	LHC	$pp$ , 7, 8 TeV

NODE=S126SZZ  
NODE=S126SZZ

OCCUR=3

• • • We do not use the following data for averages, fits, limits, etc. • • •

$1.06^{+0.61}_{-0.45}$		6	AAD	25AQ ATLS	$pp$ , 13 TeV, off-shell		
		7	CHEKHOVSKY25B	CMS	$pp$ , 13.6 TeV, cross sections		
		8	AAD	24AQ ATLS	$pp$ , 13.6 TeV, cross sections		
		9	HAYRAPETY...23	CMS	$pp$ , 13 TeV cross sections		
		10	SIRUNYAN	21AE CMS	$pp$ , 13 TeV, couplings		
		11	SIRUNYAN	21S CMS	$pp$ , 13 TeV		
		2,12	AAD	20AQ ATLS	$pp$ , 13 TeV		
		13	AAD	20BA ATLS	$pp$ , 13 TeV cross sections		
		<6.5	95	14	AABOUD	19N ATLS	$pp$ , 13 TeV, off-shell
		$1.06^{+0.19}_{-0.17}$		15	SIRUNYAN	19AT CMS	$pp$ , 13 TeV
$1.28^{+0.21}_{-0.19}$		16	AABOUD	18AJ ATLS	$pp$ , 13 TeV		
		<3.8	95	17	AABOUD	18BP ATLS	$pp$ , 13 TeV, off-shell
		$1.05^{+0.15+0.11}_{-0.14-0.09}$		18	SIRUNYAN	17AV CMS	$pp$ , 13 TeV

OCCUR=2

$1.52^{+0.40}_{-0.34}$	<sup>5</sup> AAD	16AN ATLS	$pp$ , 7, 8 TeV	OCCUR=2
$1.04^{+0.32}_{-0.26}$	<sup>5</sup> AAD	16AN CMS	$pp$ , 7, 8 TeV	OCCUR=3
$1.46^{+0.35+0.19}_{-0.31-0.13}$	<sup>19</sup> AAD	16K ATLS	$pp$ , 7, 8 TeV	
	<sup>20</sup> KHACHATRY...	16AR CMS	$pp$ , 7, 8 TeV cross sections	
$1.44^{+0.34+0.21}_{-0.31-0.11}$	<sup>21</sup> AAD	15F ATLS	$pp \rightarrow HX$ , 7, 8 TeV	
	<sup>22</sup> AAD	14AR ATLS	$pp$ , 8 TeV, cross sections	
$0.93^{+0.26+0.13}_{-0.23-0.09}$	<sup>23</sup> CHATRCHYAN	14AA CMS	$pp$ , 7, 8 TeV	
$1.43^{+0.40}_{-0.35}$	<sup>24</sup> AAD	13AK ATLS	$pp$ , 7 and 8 TeV	
$0.80^{+0.35}_{-0.28}$	<sup>25</sup> CHATRCHYAN	13J CMS	$pp \rightarrow HX$ , 7, 8 TeV	
$1.2 \pm 0.6$	<sup>26</sup> AAD	12AI ATLS	$pp \rightarrow HX$ , 7, 8 TeV	
$1.4 \pm 1.1$	<sup>26</sup> AAD	12AI ATLS	$pp \rightarrow HX$ , 7 TeV	OCCUR=2
$1.1 \pm 0.8$	<sup>26</sup> AAD	12AI ATLS	$pp \rightarrow HX$ , 8 TeV	OCCUR=3
$0.73^{+0.45}_{-0.33}$	<sup>27</sup> CHATRCHYAN	12N CMS	$pp \rightarrow HX$ , 7, 8 TeV	
<sup>1</sup> CMS 22 report combined results (see their Extended Data Table 2) using up to $138 \text{ fb}^{-1}$ of data at $E_{\text{cm}} = 13 \text{ TeV}$ , assuming $m_H = 125.38 \text{ GeV}$ . See their Fig. 2 right.				NODE=S126SZZ;LINKAGE=S
<sup>2</sup> AAD 20AQ perform analyses using $H \rightarrow ZZ^* \rightarrow 4\ell$ ( $\ell = e, \mu$ ) with data of $139 \text{ fb}^{-1}$ at $E_{\text{cm}} = 13 \text{ TeV}$ . Results are given for $m_H = 125 \text{ GeV}$ .				NODE=S126SZZ;LINKAGE=P
<sup>3</sup> AAD 20AQ measured the inclusive cross section times branching ratio for $H \rightarrow ZZ^*$ decay ( $ y(H)  < 2.5$ ) to be $1.34 \pm 0.12 \text{ pb}$ (with $1.33 \pm 0.08 \text{ pb}$ expected in the SM).				NODE=S126SZZ;LINKAGE=Q
<sup>4</sup> AAD 16AN perform fits to the ATLAS and CMS data at $E_{\text{cm}} = 7$ and $8 \text{ TeV}$ . The signal strengths for individual production processes are $1.13^{+0.34}_{-0.31}$ for gluon fusion and $0.1^{+1.1}_{-0.6}$ for vector boson fusion.				NODE=S126SZZ;LINKAGE=G
<sup>5</sup> AAD 16AN: In the fit, relative production cross sections are fixed to those in the Standard Model. The quoted signal strength is given for $m_H = 125.09 \text{ GeV}$ .				NODE=S126SZZ;LINKAGE=H
<sup>6</sup> AAD 25AQ measure the off-shell Higgs signal strength to be $0.87^{+0.75}_{-0.54}$ using $H^* \rightarrow ZZ \rightarrow 4\ell$ ( $\ell = e, \mu$ ) with data of $140 \text{ fb}^{-1}$ at $E_{\text{cm}} = 13 \text{ TeV}$ . This result is combined with $ZZ \rightarrow 2\ell 2\nu$ decay channel (AAD 23BR), which corresponds to a significance of $3.7 \sigma$ . The quoted errors are values at 68%CL.				NODE=S126SZZ;LINKAGE=W
<sup>7</sup> CHEKHOVSKY 25B measure the fiducial cross section using $H \rightarrow ZZ^* \rightarrow 4\ell$ ( $\ell = e, \mu$ ) with data of $34.7 \text{ fb}^{-1}$ at $E_{\text{cm}} = 13.6 \text{ TeV}$ . The inclusive fiducial cross section is $2.89^{+0.53+0.29}_{-0.49-0.21} \text{ fb}$ with their defined fiducial region (see their Table 1), where $3.09^{+0.27}_{-0.24} \text{ fb}$ is expected in the SM. Differential fiducial cross sections are shown in their Fig. 5. The quoted results are given for $m_H = 125.38 \text{ GeV}$ .				NODE=S126SZZ;LINKAGE=V
<sup>8</sup> AAD 24AQ measure fiducial and total cross sections at $E_{\text{cm}} = 13.6 \text{ TeV}$ with $29.0 \text{ fb}^{-1}$ data. The quoted results are given for $m_H = 125.09 \text{ GeV}$ . The inclusive fiducial cross section is $2.80 \pm 0.74 \text{ fb}$ with their defined fiducial region (see their Table 5), where $3.67 \pm 0.19 \text{ fb}$ is expected in the SM. Assuming SM values for the acceptance and the branching fraction, the total cross section is $46 \pm 12 \text{ pb}$ , where $59.9 \pm 2.6 \text{ pb}$ is expected in the SM.				NODE=S126SZZ;LINKAGE=U
<sup>9</sup> HAYRAPETYAN 23 measure the cross sections for $pp \rightarrow H \rightarrow ZZ^* \rightarrow 4\ell$ ( $\ell = e, \mu$ ) using $138 \text{ fb}^{-1}$ at $E_{\text{cm}} = 13 \text{ TeV}$ . They give $\sigma = 2.73 \pm 0.22(\text{stat}) \pm 0.15(\text{syst}) \text{ fb}$ in their fiducial region (see their Section 5 and Table 2), where $2.86 \pm 0.15 \text{ fb}$ is expected in the Standard Model for $m_H = 125.38 \text{ GeV}$ . 26 differential and 6 double-differential cross sections are given; see their Figs. 6-23 and 24-25.				NODE=S126SZZ;LINKAGE=T
<sup>10</sup> SIRUNYAN 21AE obtains constraints on anomalous couplings to vector bosons ( $W$ , $Z$ , and gluon) and top quark using $H \rightarrow ZZ^* \rightarrow 4\ell$ ( $\ell = e, \mu$ ) with data of $137 \text{ fb}^{-1}$ at $E_{\text{cm}} = 13 \text{ TeV}$ . Their Table 5 and Figs 14-17 show (effective) couplings to gluon and top with combining gluon fusion, $t\bar{t}H$ and $tH$ production channels and the result of $t\bar{t}H$ , $H \rightarrow \gamma\gamma$ (SIRUNYAN 20AS). Their Tables 6-9 and Figs 18-22 show couplings to $W$ and $Z$ for different assumptions and bases (Higgs and Warsaw).				NODE=S126SZZ;LINKAGE=N
<sup>11</sup> SIRUNYAN 21S measure cross sections with the $H \rightarrow ZZ^* \rightarrow 4\ell$ ( $\ell = e, \mu$ ) channel using $137 \text{ fb}^{-1}$ data at $E_{\text{cm}} = 13 \text{ TeV}$ . Results are given for $m_H = 125.38 \text{ GeV}$ . The signal strengths for individual production processes in their Table 4. Cross sections are given in their Table 6 and Fig. 14, which are based on the simplified template cross section framework (reduced stage-1.2).				NODE=S126SZZ;LINKAGE=R
<sup>12</sup> AAD 20AQ present several results for the channel $H \rightarrow ZZ^* \rightarrow 4\ell$ ( $\ell = e, \mu$ ) with the simplified template cross section with $\kappa$ -frameworks and the effective field theory (EFT) approach; see their Table 8 and Fig. 10 for simplified template cross sections. $\kappa_V = 1.02 \pm 0.06$ and $\kappa_F = 0.88 \pm 0.16$ are obtained, see their Fig. 12 for the $\kappa$ -framework. See their Tables 9 and 10 and Figs. 16-18 for the EFT-framework.				NODE=S126SZZ;LINKAGE=O
<sup>13</sup> AAD 20BA measure the cross section for $pp \rightarrow H \rightarrow ZZ^* \rightarrow 4\ell$ ( $\ell = e, \mu$ ) using $139 \text{ fb}^{-1}$ at $E_{\text{cm}} = 13 \text{ TeV}$ . They give $\sigma \cdot B = 3.28 \pm 0.30 \pm 0.11 \text{ fb}$ in their fiducial				NODE=S126SZZ;LINKAGE=M

region, where  $3.41 \pm 0.18$  fb is expected in the Standard Model for  $m_H = 125$  GeV. Various differential cross sections are also given; see their Figs. 19-39. Constraints on Yukawa couplings for bottom and charm quarks are given in their Table 9 and Fig. 41.

- 14 AABOUD 19N measure the spectrum of the four-lepton invariant mass  $m_{4\ell}$  ( $\ell = e$  or  $\mu$ ) using  $36.1 \text{ fb}^{-1}$  of data at  $E_{\text{cm}} = 13$  TeV. The quoted signal strength upper limit is obtained from  $180 \text{ GeV} < m_{4\ell} < 1200 \text{ GeV}$ .
- 15 SIRUNYAN 19AT perform a combine fit to  $35.9 \text{ fb}^{-1}$  of data at  $E_{\text{cm}} = 13$  TeV.
- 16 AABOUD 18AJ perform analyses using  $H \rightarrow ZZ^* \rightarrow 4\ell$  ( $\ell = e, \mu$ ) with data of  $36.1 \text{ fb}^{-1}$  at  $E_{\text{cm}} = 13$  TeV. Results are given for  $m_H = 125.09$  GeV. The inclusive cross section times branching ratio for  $H \rightarrow ZZ^*$  decay ( $|\eta(H)| < 2.5$ ) is measured to be  $1.73^{+0.26}_{-0.24}$  pb (with  $1.34^{+0.09}_{-0.09}$  pb expected in the SM).
- 17 AABOUD 18BP measure an off-shell Higgs boson production using  $ZZ \rightarrow 4\ell$  and  $ZZ \rightarrow 2\ell 2\nu$  ( $\ell = e, \mu$ ) decay channels with  $36.1 \text{ fb}^{-1}$  of data at  $E_{\text{cm}} = 13$  TeV. The quoted signal strength upper limit is obtained from a combination of these two channels, where  $220 \text{ GeV} < m_{4\ell} < 2000 \text{ GeV}$  for  $ZZ \rightarrow 4\ell$  and  $250 \text{ GeV} < m_T^{ZZ} < 2000 \text{ GeV}$  for  $ZZ \rightarrow 2\ell 2\nu$  ( $m_T^{ZZ}$  is defined in their Section 5). See their Table 2 for each measurement.
- 18 SIRUNYAN 17AV use  $35.9 \text{ fb}^{-1}$  of  $pp$  collisions at  $E_{\text{cm}} = 13$  TeV. The quoted signal strength, obtained from the analysis of  $H \rightarrow ZZ^* \rightarrow 4\ell$  ( $\ell = e, \mu$ ) decays, is given for  $m_H = 125.09$  GeV. The signal strengths for different production modes are given in their Table 3. The fiducial and differential cross sections are shown in their Fig. 10.
- 19 AAD 16K use up to  $4.7 \text{ fb}^{-1}$  of  $pp$  collisions at  $E_{\text{cm}} = 7$  TeV and up to  $20.3 \text{ fb}^{-1}$  at  $E_{\text{cm}} = 8$  TeV. The quoted signal strength is given for  $m_H = 125.36$  GeV.
- 20 KHACHATRYAN 16AR use data of  $5.1 \text{ fb}^{-1}$  at  $E_{\text{cm}} = 7$  TeV and  $19.7 \text{ fb}^{-1}$  at 8 TeV. The fiducial cross sections for the production of 4 leptons via  $H \rightarrow 4\ell$  decays are measured to be  $0.56^{+0.67+0.21}_{-0.44-0.06}$  fb at 7 TeV and  $1.11^{+0.41+0.14}_{-0.35-0.10}$  fb at 8 TeV in their fiducial region (Table 2). The differential cross sections at  $E_{\text{cm}} = 8$  TeV are also shown in Figs. 4 and 5. The results are given for  $m_H = 125$  GeV.
- 21 AAD 15F use  $4.5 \text{ fb}^{-1}$  of  $pp$  collisions at  $E_{\text{cm}} = 7$  TeV and  $20.3 \text{ fb}^{-1}$  at  $E_{\text{cm}} = 8$  TeV. The quoted signal strength is given for  $m_H = 125.36$  GeV. The signal strength for the gluon fusion production mode is  $1.66^{+0.45+0.25}_{-0.41-0.15}$ , while the signal strength for the vector boson fusion production mode is  $0.26^{+1.60+0.36}_{-0.91-0.23}$ .
- 22 AAD 14AR measure the cross section for  $pp \rightarrow H \rightarrow ZZ^* \rightarrow 4\ell$  ( $\ell = e, \mu$ ) using  $20.3 \text{ fb}^{-1}$  at  $E_{\text{cm}} = 8$  TeV. They give  $\sigma \cdot B = 2.11^{+0.53}_{-0.47} \pm 0.08$  fb in their fiducial region, where  $1.30 \pm 0.13$  fb is expected in the Standard Model for  $m_H = 125.4$  GeV. Various differential cross sections are also given; see their Fig. 2.
- 23 CHATRCHYAN 14AA use  $5.1 \text{ fb}^{-1}$  of  $pp$  collisions at  $E_{\text{cm}} = 7$  TeV and  $19.7 \text{ fb}^{-1}$  at  $E_{\text{cm}} = 8$  TeV. The quoted signal strength is given for  $m_H = 125.6$  GeV. The signal strength for the gluon fusion and  $t\bar{t}H$  production mode is  $0.80^{+0.46}_{-0.36}$ , while the signal strength for the vector boson fusion and  $WH, ZH$  production mode is  $1.7^{+2.2}_{-2.1}$ .
- 24 AAD 13AK use  $4.7 \text{ fb}^{-1}$  of  $pp$  collisions at  $E_{\text{cm}} = 7$  TeV and  $20.7 \text{ fb}^{-1}$  at  $E_{\text{cm}} = 8$  TeV. The quoted signal strength is given for  $m_H = 125.5$  GeV.
- 25 CHATRCHYAN 13J obtain results based on  $ZZ \rightarrow 4\ell$  final states in  $5.1 \text{ fb}^{-1}$  of  $pp$  collisions at  $E_{\text{cm}} = 7$  TeV and  $12.2 \text{ fb}^{-1}$  at  $E_{\text{cm}} = 8$  TeV. The quoted signal strength is given for  $m_H = 125.8$  GeV. Superseded by CHATRCHYAN 14AA.
- 26 AAD 12AI obtain results based on  $4.7\text{--}4.8 \text{ fb}^{-1}$  of  $pp$  collisions at  $E_{\text{cm}} = 7$  TeV and  $5.8 \text{ fb}^{-1}$  at  $E_{\text{cm}} = 8$  TeV. The quoted signal strengths are given for  $m_H = 126$  GeV. See also AAD 12DA.
- 27 CHATRCHYAN 12N obtain results based on  $4.9\text{--}5.1 \text{ fb}^{-1}$  of  $pp$  collisions at  $E_{\text{cm}} = 7$  TeV and  $5.1\text{--}5.3 \text{ fb}^{-1}$  at  $E_{\text{cm}} = 8$  TeV. An excess of events over background with a local significance of  $5.0 \sigma$  is observed at about  $m_H = 125$  GeV. The quoted signal strengths are given for  $m_H = 125.5$  GeV. See also CHATRCHYAN 12BY and CHATRCHYAN 13Y.

NODE=S126SZZ;LINKAGE=K

NODE=S126SZZ;LINKAGE=J  
NODE=S126SZZ;LINKAGE=F

NODE=S126SZZ;LINKAGE=L

NODE=S126SZZ;LINKAGE=E

NODE=S126SZZ;LINKAGE=D

NODE=S126SZZ;LINKAGE=I

NODE=S126SZZ;LINKAGE=B

NODE=S126SZZ;LINKAGE=C

NODE=S126SZZ;LINKAGE=A

NODE=S126SZZ;LINKAGE=LH

NODE=S126SZZ;LINKAGE=CA

NODE=S126SZZ;LINKAGE=AA

NODE=S126SZZ;LINKAGE=CH

## $\gamma\gamma$ final state

VALUE	DOCUMENT ID	TECN	COMMENT
<b>1.10±0.06 OUR AVERAGE</b>			
$1.04^{+0.10}_{-0.09}$	1 AAD	23Y ATLS	$pp$ , 13 TeV
$1.13 \pm 0.09$	2 CMS	22 CMS	$pp$ , 13 TeV
$1.14^{+0.19}_{-0.18}$	3,4 AAD	16AN LHC	$pp$ , 7, 8 TeV
$5.97^{+3.39}_{-3.12}$	5 AALTONEN	13M TEVA	$p\bar{p} \rightarrow HX$ , 1.96 TeV

NODE=S126SGG  
NODE=S126SGG

• • • We do not use the following data for averages, fits, limits, etc. • • •

	<sup>6</sup> AAD	24AQ ATLS	$pp$ , 13.6 TeV, cross sections	
	<sup>7</sup> TUMASYAN	23Q CMS	$pp$ , 13 TeV, cross sections	
	<sup>8</sup> AAD	22N ATLS	$pp$ , 13 TeV, diff. $x$ -sections	
$1.12 \pm 0.09$	<sup>9</sup> SIRUNYAN	21O CMS	$pp$ , 13 TeV	
$1.20^{+0.18}_{-0.14}$	<sup>10</sup> SIRUNYAN	19AT CMS	$pp$ , 13 TeV	
	<sup>11</sup> SIRUNYAN	19L CMS	$pp$ , 13 TeV, diff. $x$ -section	
$0.99^{+0.15}_{-0.14}$	<sup>12</sup> AABOUD	18BO ATLS	$pp$ , 13 TeV	
$1.18^{+0.17}_{-0.14}$	<sup>13</sup> SIRUNYAN	18DS CMS	$pp$ , $H \rightarrow \gamma\gamma$ , 13 TeV, floated $m_H$	
$1.14^{+0.27}_{-0.25}$	<sup>4</sup> AAD	16AN ATLS	$pp$ , 7, 8 TeV	OCCUR=2
$1.11^{+0.25}_{-0.23}$	<sup>4</sup> AAD	16AN CMS	$pp$ , 7, 8 TeV	OCCUR=3
	<sup>14</sup> KHACHATRY...	16G CMS	$pp$ , 8 TeV, diff. $x$ -section	
$1.17 \pm 0.23^{+0.10+0.12}_{-0.08-0.08}$	<sup>15</sup> AAD	14BC ATLS	$pp \rightarrow HX$ , 7, 8 TeV	
	<sup>16</sup> AAD	14BJ ATLS	$pp$ , 8 TeV, diff. $x$ -section	
$1.14 \pm 0.21^{+0.09+0.13}_{-0.05-0.09}$	<sup>17</sup> KHACHATRY...	14P CMS	$pp$ , 7, 8 TeV	
$1.55^{+0.33}_{-0.28}$	<sup>18</sup> AAD	13AK ATLS	$pp$ , 7 and 8 TeV	
$7.81^{+4.61}_{-4.42}$	<sup>19</sup> AALTONEN	13L CDF	$p\bar{p} \rightarrow HX$ , 1.96 TeV	
$4.20^{+4.60}_{-4.20}$	<sup>20</sup> ABAZOV	13L D0	$p\bar{p} \rightarrow HX$ , 1.96 TeV	
$1.8 \pm 0.5$	<sup>21</sup> AAD	12AI ATLS	$pp \rightarrow HX$ , 7, 8 TeV	
$2.2 \pm 0.7$	<sup>21</sup> AAD	12AI ATLS	$pp \rightarrow HX$ , 7 TeV	OCCUR=2
$1.5 \pm 0.6$	<sup>21</sup> AAD	12AI ATLS	$pp \rightarrow HX$ , 8 TeV	OCCUR=3
$1.54^{+0.46}_{-0.42}$	<sup>22</sup> CHATRCHYAN	12N CMS	$pp \rightarrow HX$ , 7, 8 TeV	
<sup>1</sup> AAD 23Y use $139 \text{ fb}^{-1}$ of $pp$ collisions at $E_{\text{cm}} = 13 \text{ TeV}$ . The quoted results are given for $m_H = 125.09 \text{ GeV}$ and $\Gamma_H = 4.07 \text{ MeV}$ . Measured $\sigma \cdot B$ and ratios to the SM predictions for the different production modes are shown in their Table 9 and Fig. 9. Measured cross sections and ratios to the SM predictions in the reduced stage-1.2 (see their Fig. 11) simplified template cross section framework are shown in their Table 10 and Fig. 12. Wilson coefficients in the Warsaw basis (see their Table 11) at 95% CL are measured; see their Table 16 and Fig. 17.				NODE=S126SGG;LINKAGE=P
<sup>2</sup> CMS 22 report combined results (see their Extended Data Table 2) using up to $138 \text{ fb}^{-1}$ of data at $E_{\text{cm}} = 13 \text{ TeV}$ , assuming $m_H = 125.38 \text{ GeV}$ . See their Fig. 2 right.				NODE=S126SGG;LINKAGE=N
<sup>3</sup> AAD 16AN perform fits to the ATLAS and CMS data at $E_{\text{cm}} = 7$ and 8 TeV. The signal strengths for individual production processes are $1.10^{+0.23}_{-0.22}$ for gluon fusion, $1.3 \pm 0.5$ for vector boson fusion, $0.5^{+1.3}_{-1.2}$ for $WH$ production, $0.5^{+3.0}_{-2.5}$ for $ZH$ production, and $2.2^{+1.6}_{-1.3}$ for $t\bar{t}H$ production.				NODE=S126SGG;LINKAGE=H
<sup>4</sup> AAD 16AN: In the fit, relative production cross sections are fixed to those in the Standard Model. The quoted signal strength is given for $m_H = 125.09 \text{ GeV}$ .				NODE=S126SGG;LINKAGE=I
<sup>5</sup> AALTONEN 13M combine all Tevatron data from the CDF and D0 Collaborations with up to $10.0 \text{ fb}^{-1}$ and $9.7 \text{ fb}^{-1}$ , respectively, of $p\bar{p}$ collisions at $E_{\text{cm}} = 1.96 \text{ TeV}$ . The quoted signal strength is given for $m_H = 125 \text{ GeV}$ .				NODE=S126SGG;LINKAGE=AT
<sup>6</sup> AAD 24AQ measure fiducial and total cross sections at $E_{\text{cm}} = 13.6 \text{ TeV}$ with $31.4 \text{ fb}^{-1}$ data. The quoted results are given for $m_H = 125.09 \text{ GeV}$ . The inclusive fiducial cross section is $76^{+14}_{-13} \text{ fb}$ with their defined fiducial region (see their Table 2), where $67.6 \pm 3.7 \text{ fb}$ is expected in the SM. Assuming SM values for the acceptance and the branching fraction, the total cross section is $67^{+12}_{-11} \text{ pb}$ , where $59.9 \pm 2.6 \text{ pb}$ is expected in the SM.				NODE=S126SGG;LINKAGE=Q
<sup>7</sup> TUMASYAN 23Q measure fiducial and differential cross sections at $E_{\text{cm}} = 13 \text{ TeV}$ with $137 \text{ fb}^{-1}$ data. The quoted results are given for $m_H = 125.38 \text{ GeV}$ . The inclusive fiducial $\sigma \cdot B$ is $73.4^{+5.4}_{-5.3}(\text{stat})^{+2.4}_{-2.2}(\text{syst}) \text{ fb}$ with their defined fiducial region (see their Section 7 and Table 2), where $75.4 \pm 4.1 \text{ fb}$ is expected in the Standard Model. See their Fig. 8 including other fiducial $\sigma \cdot B$ defined in their Table 3. Differential $\sigma \cdot B$ are shown in their Figs. 10–15. Double-differential $\sigma \cdot B$ are in their Figs. 16 and 17.				NODE=S126SGG;LINKAGE=O
<sup>8</sup> AAD 22N measure fiducial and differential cross sections of $pp \rightarrow H \rightarrow \gamma\gamma$ at $E_{\text{cm}} = 13 \text{ TeV}$ with $139 \text{ fb}^{-1}$ data. The quoted results are given for $m_H = 125.09 \text{ GeV}$ . The inclusive fiducial $\sigma \cdot B$ is $67 \pm 5 \pm 4 \text{ fb}$ with their defined fiducial region. Other fiducial $\sigma \cdot B$ are in their Table 3. Differential $\sigma \cdot B$ are shown in their Figs. 8–13, 15, 25–32, 35, 36. Double-differential $\sigma \cdot B$ are in their Figs. 14, 33, 34. Modifications of the $b$ - and $c$ -quark Yukawa couplings to $H$ , $\kappa_b$ and $\kappa_c$ at 95% CL are in their Table 6 and Fig. 18. Wilson coefficients at 95% CL are in their Table 7 and Fig. 21.				NODE=S126SGG;LINKAGE=M



- <sup>9</sup> SIRUNYAN 21O measures cross sections and couplings with the  $H \rightarrow \gamma\gamma$  channel using  $137 \text{ fb}^{-1}$  data at  $E_{\text{cm}} = 13 \text{ TeV}$ . Results are given for  $m_H = 125.38 \text{ GeV}$ . The signal strengths for individual production processes are given in their Fig. 16. Cross sections are given in their Tables 12 and 13 and Figs. 18 and 20, which are based on the simplified template cross section framework (reduced stage-1.2). Results in the  $\kappa$ -framework are given in their Fig. 22.
- <sup>10</sup> SIRUNYAN 19AT perform a combine fit to  $35.9 \text{ fb}^{-1}$  of data at  $E_{\text{cm}} = 13 \text{ TeV}$ .
- <sup>11</sup> SIRUNYAN 19L measure fiducial and differential cross sections of the process  $pp \rightarrow H \rightarrow \gamma\gamma$  at  $E_{\text{cm}} = 13 \text{ TeV}$  with  $35.9 \text{ fb}^{-1}$ . See their Figs. 4–11.
- <sup>12</sup> AABOUD 18BO use  $36.1 \text{ fb}^{-1}$  of  $pp$  collisions at  $E_{\text{cm}} = 13 \text{ TeV}$ . The signal strengths for the individual production modes are:  $0.81^{+0.19}_{-0.18}$  for gluon fusion,  $2.0^{+0.6}_{-0.5}$  for vector boson fusion,  $0.7^{+0.9}_{-0.8}$  for  $VH$  production ( $V = W, Z$ ), and  $0.5 \pm 0.6$  for  $t\bar{t}H$  and  $tH$  production. Other measurements of cross sections and couplings are summarized in their Section 10. The quoted values are given for  $m_H = 125.09 \text{ GeV}$ .
- <sup>13</sup> SIRUNYAN 18DS use  $35.9 \text{ fb}^{-1}$  of  $pp \rightarrow H$  collisions with  $H \rightarrow \gamma\gamma$  at  $E_{\text{cm}} = 13 \text{ TeV}$ . The Higgs mass is floated in the measurement of a signal strength. The result is  $1.18^{+0.12}_{-0.11}(\text{stat.})^{+0.09}_{-0.07}(\text{syst.})^{+0.07}_{-0.06}(\text{theory})$ , which is largely insensitive to the Higgs mass around  $125 \text{ GeV}$ .
- <sup>14</sup> KHACHATRYAN 16G measure fiducial and differential cross sections of the process  $pp \rightarrow HX$ ,  $H \rightarrow \gamma\gamma$  at  $E_{\text{cm}} = 8 \text{ TeV}$  with  $19.7 \text{ fb}^{-1}$ . See their Figs. 4–6 and Table 1 for data.
- <sup>15</sup> AAD 14BC use  $4.5 \text{ fb}^{-1}$  of  $pp$  collisions at  $E_{\text{cm}} = 7 \text{ TeV}$  and  $20.3 \text{ fb}^{-1}$  at  $E_{\text{cm}} = 8 \text{ TeV}$ . The last uncertainty in the measurement is theory systematics. The quoted signal strength is given for  $m_H = 125.4 \text{ GeV}$ . The signal strengths for the individual production modes are:  $1.32 \pm 0.38$  for gluon fusion,  $0.8 \pm 0.7$  for vector boson fusion,  $1.0 \pm 1.6$  for  $WH$  production,  $0.1^{+3.7}_{-0.1}$  for  $ZH$  production, and  $1.6^{+2.7}_{-1.8}$  for  $t\bar{t}H$  production.
- <sup>16</sup> AAD 14BJ measure fiducial and differential cross sections of the process  $pp \rightarrow HX$ ,  $H \rightarrow \gamma\gamma$  at  $E_{\text{cm}} = 8 \text{ TeV}$  with  $20.3 \text{ fb}^{-1}$ . See their Table 3 and Figs. 3–12 for data.
- <sup>17</sup> KHACHATRYAN 14P use  $5.1 \text{ fb}^{-1}$  of  $pp$  collisions at  $E_{\text{cm}} = 7 \text{ TeV}$  and  $19.7 \text{ fb}^{-1}$  at  $E_{\text{cm}} = 8 \text{ TeV}$ . The last uncertainty in the measurement is theory systematics. The quoted signal strength is given for  $m_H = 124.7 \text{ GeV}$ . The signal strength for the gluon fusion and  $t\bar{t}H$  production mode is  $1.13^{+0.37}_{-0.31}$ , while the signal strength for the vector boson fusion and  $WH, ZH$  production mode is  $1.16^{+0.63}_{-0.58}$ .
- <sup>18</sup> AAD 13AK use  $4.7 \text{ fb}^{-1}$  of  $pp$  collisions at  $E_{\text{cm}} = 7 \text{ TeV}$  and  $20.7 \text{ fb}^{-1}$  at  $E_{\text{cm}} = 8 \text{ TeV}$ . The quoted signal strength is given for  $m_H = 125.5 \text{ GeV}$ .
- <sup>19</sup> AALTONEN 13L combine all CDF results with  $9.45\text{--}10.0 \text{ fb}^{-1}$  of  $p\bar{p}$  collisions at  $E_{\text{cm}} = 1.96 \text{ TeV}$ . The quoted signal strength is given for  $m_H = 125 \text{ GeV}$ .
- <sup>20</sup> ABAZOV 13L combine all D0 results with up to  $9.7 \text{ fb}^{-1}$  of  $p\bar{p}$  collisions at  $E_{\text{cm}} = 1.96 \text{ TeV}$ . The quoted signal strength is given for  $m_H = 125 \text{ GeV}$ .
- <sup>21</sup> AAD 12AI obtain results based on  $4.8 \text{ fb}^{-1}$  of  $pp$  collisions at  $E_{\text{cm}} = 7 \text{ TeV}$  and  $5.9 \text{ fb}^{-1}$  at  $E_{\text{cm}} = 8 \text{ TeV}$ . The quoted signal strengths are given for  $m_H = 126 \text{ GeV}$ . See also AAD 12DA.
- <sup>22</sup> CHATRCHYAN 12N obtain results based on  $5.1 \text{ fb}^{-1}$  of  $pp$  collisions at  $E_{\text{cm}} = 7 \text{ TeV}$  and  $5.3 \text{ fb}^{-1}$  at  $E_{\text{cm}} = 8 \text{ TeV}$ . The quoted signal strength is given for  $m_H = 125.5 \text{ GeV}$ . See also CHATRCHYAN 13Y.

NODE=S126SGG;LINKAGE=L

NODE=S126SGG;LINKAGE=K  
NODE=S126SGG;LINKAGE=J

NODE=S126SGG;LINKAGE=F

NODE=S126SGG;LINKAGE=G

NODE=S126SGG;LINKAGE=E

NODE=S126SGG;LINKAGE=B

NODE=S126SGG;LINKAGE=D

NODE=S126SGG;LINKAGE=A

NODE=S126SGG;LINKAGE=LH

NODE=S126SGG;LINKAGE=LL

NODE=S126SGG;LINKAGE=AB

NODE=S126SGG;LINKAGE=AA

NODE=S126SGG;LINKAGE=CA

### $c\bar{c}$ final state

VALUE	CL%	DOCUMENT ID	TECN	COMMENT
< <b>11.5 (CL = 95%)</b>	[<14 (CL = 95%) OUR 2025 BEST LIMIT]			
< <b>11.5</b>	95	<sup>1</sup> AAD	25Y ATLS	$pp \rightarrow WH/ZH$ , 13 TeV
● ● ● We do not use the following data for averages, fits, limits, etc. ● ● ●				
$1.0^{+5.4}_{-5.2}$		<sup>1</sup> AAD	25Y ATLS	$pp \rightarrow WH/ZH$ , 13 TeV
$9.4^{+20.3}_{-19.9}$		<sup>2</sup> TUMASYAN	23AD CMS	$pp \rightarrow WH/ZH$ (boosted), 13 TeV
< 47	95	<sup>2</sup> TUMASYAN	23AD CMS	$pp \rightarrow WH/ZH$ (boosted), 13 TeV
< 14	95	<sup>3</sup> TUMASYAN	23AH CMS	$pp \rightarrow WH/ZH$ , 13 TeV
– 9 $\pm 10$ $\pm 11$		<sup>4,5</sup> AAD	22W ATLS	$pp \rightarrow WH/ZH$ , 13 TeV
– 9 $\pm 10$ $\pm 12$		<sup>4,6</sup> AAD	22W ATLS	$pp \rightarrow WH/ZH$ , 13 TeV
< 26	95	<sup>4</sup> AAD	22W ATLS	$pp \rightarrow WH/ZH$ , 13 TeV
37 $\pm 17$ $^{+11}_{-9}$		<sup>7</sup> SIRUNYAN	20AE CMS	$pp$ , 13 TeV
< 110	95	<sup>8</sup> AABOUD	18M ATLS	$pp$ , 13 TeV

NODE=S126SCC  
NODE=S126SCC

OCCUR=2

OCCUR=3

OCCUR=2

OCCUR=3

OCCUR=2

- <sup>1</sup> AAD 25Y present measurements of  $VH, H \rightarrow b\bar{b}$  and  $H \rightarrow c\bar{c}$  ( $V = W, Z$ ) using  $140 \text{ fb}^{-1}$  of  $pp$  collision data at  $E_{\text{cm}} = 13 \text{ TeV}$ . Two-dimensional likelihood scan of  $(\mu_{VH}^{bb}, \mu_{VH}^{cc})$  is shown in their Fig. 11.
- <sup>2</sup> TUMASYAN 23AD search for Higgs produced with transverse momenta greater than 450 GeV and decaying to  $c\bar{c}$  using  $138 \text{ fb}^{-1}$  of  $pp$  collision data at  $E_{\text{cm}} = 13 \text{ TeV}$ .
- <sup>3</sup> TUMASYAN 23AH search for  $VH, H \rightarrow c\bar{c}$  ( $V = W, Z$ ) using  $138 \text{ fb}^{-1}$  of  $pp$  collision data at  $E_{\text{cm}} = 13 \text{ TeV}$ . The upper limit on  $\sigma(pp \rightarrow VH) \cdot \mathcal{B}(H \rightarrow c\bar{c})$  is 0.94 pb at 95% CL. See their Fig. 4. The quoted values are given for  $m_H = 125.38 \text{ GeV}$ .
- <sup>4</sup> AAD 22W search for  $VH, H \rightarrow c\bar{c}$  ( $V = W, Z$ ) using  $139 \text{ fb}^{-1}$  of  $pp$  collision data at  $E_{\text{cm}} = 13 \text{ TeV}$ . The results are given for  $m_H = 125 \text{ GeV}$ .
- <sup>5</sup> The analysis of  $VH, H \rightarrow c\bar{c}$  is combined with  $VH, H \rightarrow b\bar{b}$  (AAD 21AB). The ratio  $|\kappa_c/\kappa_b|$  is constrained to be less than 4.5 at 95% CL. See their Fig. 7.
- <sup>6</sup> The constraint on the charm Yukawa coupling modifier  $\kappa_c$  is measured to be  $|\kappa_c| < 8.5$  at 95% CL. See their Fig. 4.
- <sup>7</sup> SIRUNYAN 20AE use  $35.9 \text{ fb}^{-1}$  at of  $pp$  collisions at  $E_{\text{cm}} = 13 \text{ TeV}$ . The measured best fit value of  $\sigma(pp \rightarrow VH) \cdot \mathcal{B}(H \rightarrow c\bar{c})$  is  $2.40^{+1.12+0.65}_{-1.11-0.61}$  pb (equivalent to  $< 4.5$  pb at 95% CL upper limit, i.e. 70 times the standard model), where  $V$  is  $W \rightarrow \ell\nu$ ,  $Z \rightarrow \ell\ell$ , or  $Z \rightarrow \nu\nu$  ( $\ell = e, \mu$ ). The quoted values are given for  $m_H = 125 \text{ GeV}$ .
- <sup>8</sup> AABOUD 18M use  $36.1 \text{ fb}^{-1}$  at of  $pp$  collisions at  $E_{\text{cm}} = 13 \text{ TeV}$ . The upper limit on  $\sigma(pp \rightarrow ZH) \cdot \mathcal{B}(H \rightarrow c\bar{c})$  is 2.7 pb at 95% CL. This corresponds to 110 times the standard model. The quoted values are given for  $m_H = 125 \text{ GeV}$ .

NODE=S126SCC;LINKAGE=I

NODE=S126SCC;LINKAGE=G

NODE=S126SCC;LINKAGE=H

NODE=S126SCC;LINKAGE=D

NODE=S126SCC;LINKAGE=E

NODE=S126SCC;LINKAGE=F

NODE=S126SCC;LINKAGE=C

NODE=S126SCC;LINKAGE=A

 **$b\bar{b}$  final state**

VALUE	DOCUMENT ID	TECN	COMMENT
-------	-------------	------	---------

**0.94±0.11 OUR AVERAGE**

[0.99 ± 0.12 OUR 2025 AVERAGE]

$0.92^{+0.16}_{-0.15}$	<sup>1</sup> AAD	25Y	ATLS	$pp \rightarrow VH, H \rightarrow b\bar{b}$ , 13 TeV
$1.05^{+0.22}_{-0.21}$	<sup>2</sup> CMS	22	CMS	$pp$ , 13 TeV
$0.95 \pm 0.32^{+0.20}_{-0.17}$	<sup>3</sup> AAD	21AJ	ATLS	VBF, $H \rightarrow b\bar{b}$ , $pp$ , 13 TeV, 126 $\text{fb}^{-1}$
$0.70^{+0.29}_{-0.27}$	<sup>4,5</sup> AAD	16AN	LHC	$pp$ , 7, 8 TeV
$1.59^{+0.69}_{-0.72}$	<sup>6</sup> AALTONEN	13M	TEVA	$p\bar{p} \rightarrow HX$ , 1.96 TeV
• • • We do not use the following data for averages, fits, limits, etc. • • •				
	<sup>7</sup> CHEKHOVSKY25A	CMS		$VH, H \rightarrow b\bar{b}$ , $pp$ , 13 TeV
$1.4^{+1.0}_{-0.9}$	<sup>8</sup> AAD	24F	ATLS	$VH$ , boosted $H \rightarrow b\bar{b}$ , $pp$ , 13 TeV
$2.2^{+0.9}_{-0.8}$	<sup>9</sup> HAYRAPETY...24AM	CMS		$pp \rightarrow ZH, Z/H \rightarrow b\bar{b}$ , 13 TeV
$4.9^{+1.9}_{-1.6}$	<sup>10</sup> HAYRAPETY...24AY	CMS		ggF, VBF, boosted $H \rightarrow b\bar{b}$ , $pp$ , 13 TeV
$1.6^{+1.7}_{-1.5}$	<sup>11</sup> HAYRAPETY...24AY	CMS		ggF, VBF, boosted $H \rightarrow b\bar{b}$ , $pp$ , 13 TeV
$1.01^{+0.55}_{-0.46}$	<sup>12</sup> HAYRAPETY...24U	CMS		VBF, $H \rightarrow b\bar{b}$ , $pp$ , 13 TeV, 90.8 $\text{fb}^{-1}$
$0.99^{+0.48}_{-0.41}$	<sup>13</sup> HAYRAPETY...24U	CMS		ggF, VBF, $H \rightarrow b\bar{b}$ , $pp$ , 13 TeV, 90.8 $\text{fb}^{-1}$
$-2.7^{+5.6}_{-2.1} \pm 3.5$	<sup>14</sup> HAYRAPETY...24U	CMS		ggF, $H \rightarrow b\bar{b}$ , $pp$ , 13 TeV, 90.8 $\text{fb}^{-1}$
$1.59^{+0.63}_{-0.72} \pm 0.54$	<sup>14</sup> HAYRAPETY...24U	CMS		VBF, $H \rightarrow b\bar{b}$ , $pp$ , 13 TeV, 90.8 $\text{fb}^{-1}$
$1.15^{+0.22}_{-0.20}$	<sup>15</sup> TUMASYAN	24	CMS	$pp \rightarrow WH/ZH, H \rightarrow b\bar{b}$ , 13 TeV, 138 $\text{fb}^{-1}$
$0.8 \pm 3.2$	<sup>16</sup> AAD	22X	ATLS	boosted $H \rightarrow b\bar{b}$ , $pp$ , 13 TeV
$1.02^{+0.12+0.14}_{-0.11-0.13}$	<sup>17</sup> AAD	21AB	ATLS	$pp \rightarrow VH, H \rightarrow b\bar{b}$ , 13 TeV
$0.95 \pm 0.18^{+0.19}_{-0.18}$	<sup>17</sup> AAD	21AB	ATLS	$pp \rightarrow HW, H \rightarrow b\bar{b}$ , 13 TeV, 139 $\text{fb}^{-1}$
$1.08 \pm 0.17^{+0.18}_{-0.15}$	<sup>17</sup> AAD	21AB	ATLS	$pp \rightarrow HZ, H \rightarrow b\bar{b}$ , 13 TeV, 139 $\text{fb}^{-1}$
$0.72^{+0.29+0.26}_{-0.28-0.22}$	<sup>18</sup> AAD	21H	ATLS	$pp \rightarrow HW/HZ, H \rightarrow b\bar{b}$ , boosted $W/Z$ , 13 TeV, 139 $\text{fb}^{-1}$
$1.3 \pm 1.0$	<sup>19</sup> AAD	21M	ATLS	VBF+ $\gamma$ , $H \rightarrow b\bar{b}$ , $pp$ , 13 TeV, 132 $\text{fb}^{-1}$
$3.7 \pm 1.2^{+0.11}_{-0.9}$	<sup>20</sup> SIRUNYAN	20BL	CMS	boosted $H \rightarrow b\bar{b}$ , $pp$ , 13 TeV
	<sup>21</sup> AABOUD	19U	ATLS	$pp \rightarrow VH, H \rightarrow b\bar{b}$ , 13 TeV, cross sections

NODE=S126SBB  
 NODE=S126SBB  
 NEW

OCCUR=2

OCCUR=2

OCCUR=3

OCCUR=4

OCCUR=2

OCCUR=3

1.12±0.29	22	SIRUNYAN	19AT CMS	$pp$ , 13 TeV	
1.16 <sup>+0.27</sup> <sub>-0.25</sub>	23	AABOUD	18BN ATLS	$pp \rightarrow HW/HZ, H \rightarrow b\bar{b}$ , 13 TeV, 79.8 fb <sup>-1</sup>	
0.98 <sup>+0.22</sup> <sub>-0.21</sub>	24	AABOUD	18BN ATLS	$pp \rightarrow HW/HZ, H \rightarrow b\bar{b}$ , 7, 8, 13 TeV	OCCUR=2
1.01±0.20	25	AABOUD	18BN ATLS	$pp \rightarrow HX, ggF, VBF, VH, t\bar{t}H$ 7, 8, 13 TeV	OCCUR=3
2.5 <sup>+1.4</sup> <sub>-1.3</sub>	26,27	AABOUD	18BQ ATLS	$pp \rightarrow HX, VBF, ggF, VH, t\bar{t}H$ , 13 TeV	
3.0 <sup>+1.7</sup> <sub>-1.6</sub>	26,28	AABOUD	18BQ ATLS	$pp \rightarrow HX, VBF$ , 13 TeV	OCCUR=2
	29	AALTONEN	18C CDF	$p\bar{p} \rightarrow HX$ , 1.96 TeV	
1.19 <sup>+0.40</sup> <sub>-0.38</sub>	30	SIRUNYAN	18AE CMS	$pp \rightarrow HW/HZ, H \rightarrow b\bar{b}$ , 13 TeV	
1.06 <sup>+0.31</sup> <sub>-0.29</sub>	31	SIRUNYAN	18AE CMS	$pp \rightarrow HW/HZ, H \rightarrow b\bar{b}$ , 7, 8, 13 TeV	OCCUR=2
1.06±0.26	32	SIRUNYAN	18DB CMS	$pp \rightarrow HW/HZ, H \rightarrow b\bar{b}$ , 13 TeV, 77.2 fb <sup>-1</sup>	
1.01±0.22	33	SIRUNYAN	18DB CMS	$pp \rightarrow HW/HZ, H \rightarrow b\bar{b}$ , 7, 8, 13 TeV	OCCUR=2
1.04±0.20	34	SIRUNYAN	18DB CMS	$pp \rightarrow HX, ggF, VBF, VH, t\bar{t}H$ 7, 8, 13 TeV	OCCUR=3
2.3 <sup>+1.8</sup> <sub>-1.6</sub>	35	SIRUNYAN	18E CMS	$pp \rightarrow HX$ , boosted, 13 TeV	
1.20 <sup>+0.24+0.34</sup> <sub>-0.23-0.28</sub>	36	AABOUD	17BA ATLS	$pp \rightarrow HW/ZX, H \rightarrow b\bar{b}$ , 13 TeV, 36.1 fb <sup>-1</sup>	
0.90±0.18 <sup>+0.21</sup> <sub>-0.19</sub>	37	AABOUD	17BA ATLS	$pp \rightarrow HW/ZX, H \rightarrow b\bar{b}$ , 7, 8, 13 TeV	OCCUR=2
-0.8 ±1.3 <sup>+1.8</sup> <sub>-1.9</sub>	38	AABOUD	16X ATLS	$pp \rightarrow HX, VBF$ , 8 TeV	
0.62±0.37	5	AAD	16AN ATLS	$pp$ , 7, 8 TeV	OCCUR=2
0.81 <sup>+0.45</sup> <sub>-0.43</sub>	5	AAD	16AN CMS	$pp$ , 7, 8 TeV	OCCUR=3
0.63 <sup>+0.31+0.24</sup> <sub>-0.30-0.23</sub>	39	AAD	16K ATLS	$pp$ , 7, 8 TeV	
0.52±0.32±0.24	40	AAD	15G ATLS	$pp \rightarrow HW/ZX$ , 7, 8 TeV	
2.8 <sup>+1.6</sup> <sub>-1.4</sub>	41	KHACHATRY...15Z	CMS	$pp \rightarrow HX, VBF$ , 8 TeV	
1.03 <sup>+0.44</sup> <sub>-0.42</sub>	42	KHACHATRY...15Z	CMS	$pp$ , 8 TeV, combined	OCCUR=2
1.0 ±0.5	43	CHATRCHYAN14AI	CMS	$pp \rightarrow HW/ZX$ , 7, 8 TeV	
1.72 <sup>+0.92</sup> <sub>-0.87</sub>	44	AALTONEN	13L CDF	$p\bar{p} \rightarrow HX$ , 1.96 TeV	
1.23 <sup>+1.24</sup> <sub>-1.17</sub>	45	ABAZOV	13L D0	$p\bar{p} \rightarrow HX$ , 1.96 TeV	
0.5 ±2.2	46	AAD	12AI ATLS	$pp \rightarrow HW/ZX$ , 7 TeV	
	47	AALTONEN	12T TEVA	$p\bar{p} \rightarrow HW/ZX$ , 1.96 TeV	
0.48 <sup>+0.81</sup> <sub>-0.70</sub>	48	CHATRCHYAN12N	CMS	$pp \rightarrow HW/ZX$ , 7, 8 TeV	

<sup>1</sup> AAD 25Y present measurements of  $VH, H \rightarrow b\bar{b}$  ( $V = W, Z$ ) using 140 fb<sup>-1</sup> of  $pp$  collision data at  $E_{\text{cm}} = 13$  TeV. The observed significance for  $WH$  and  $ZH$  are 5.3 and 4.9  $\sigma$ , respectively. See their Fig. 12. Cross sections are given in their Table 8 and Figs. 15 and 16, which are based on the simplified template cross section framework (extended stage-1.2).

NODE=S126SBB;LINKAGE=RA

<sup>2</sup> CMS 22 report combined results (see their Extended Data Table 2) using up to 138 fb<sup>-1</sup> of data at  $E_{\text{cm}} = 13$  TeV, assuming  $m_H = 125.38$  GeV. See their Fig. 2 right.

NODE=S126SBB;LINKAGE=HA

<sup>3</sup> AAD 21AJ present measurements of  $H \rightarrow b\bar{b}$  in the VBF production mode. The inclusive VBF cross sections with and without the branching ratio of  $H \rightarrow b\bar{b}$  are  $2.07 \pm 0.70^{+0.46}_{-0.37}$  fb and  $3.56 \pm 1.21^{+0.80}_{-0.64}$  fb, respectively. The latter is obtained assuming the SM value of  $B(H \rightarrow b\bar{b}) = 0.5809$  and  $m_H = 125$  GeV.

NODE=S126SBB;LINKAGE=DA

<sup>4</sup> AAD 16AN perform fits to the ATLAS and CMS data at  $E_{\text{cm}} = 7$  and 8 TeV. The signal strengths for individual production processes are  $1.0 \pm 0.5$  for  $WH$  production,  $0.4 \pm 0.4$  for  $ZH$  production, and  $1.1 \pm 1.0$  for  $t\bar{t}H$  production.

NODE=S126SBB;LINKAGE=H

<sup>5</sup> AAD 16AN: In the fit, relative production cross sections are fixed to those in the Standard Model. The quoted signal strength is given for  $m_H = 125.09$  GeV.

NODE=S126SBB;LINKAGE=I

<sup>6</sup> AALTONEN 13M combine all Tevatron data from the CDF and D0 Collaborations with up to 10.0 fb<sup>-1</sup> and 9.7 fb<sup>-1</sup>, respectively, of  $p\bar{p}$  collisions at  $E_{\text{cm}} = 1.96$  TeV. The quoted signal strength is given for  $m_H = 125$  GeV.

NODE=S126SBB;LINKAGE=AT

<sup>7</sup> CHEKHOVSKY 25A constrain six Wilson coefficients in the Warsaw basis using 138 fb<sup>-1</sup> of  $pp$  collision data at  $E_{\text{cm}} = 13$  TeV. The results are shown in their Figs. 7 (for linear and quadratic), 9–13 (two-dimensional likelihood scan). The limits on the energy scale for three different assumptions for each Wilson coefficient are shown in their Fig. 8.

NODE=S126SBB;LINKAGE=QA

<sup>8</sup> AAD 24F present studies of the  $VH$  production mode in the boosted  $V \rightarrow q\bar{q}$  and  $H \rightarrow b\bar{b}$  ( $p_T(H) > 250$  GeV) using 137 fb<sup>-1</sup> of  $pp$  collision data at  $E_{\text{cm}} = 13$  TeV. The

NODE=S126SBB;LINKAGE=LA

- quoted signal strength is given for  $m_H = 125.09$  GeV and corresponds to a significance of 1.7 standard deviations. The corresponding inclusive cross section is  $3.1 \pm 1.3^{+1.8}_{-1.4}$  pb. The signal strengths and cross sections are given in their Table I for three  $p_T(H)$  regions:  $250 < p_T(H) < 450$  GeV,  $450 < p_T(H) < 650$  GeV,  $650 \text{ GeV} < p_T(H)$  with  $|y(H)| < 2$ .
- 9 HAYRAPETYAN 24AM search for  $ZH$ ,  $H \rightarrow b\bar{b}$ ,  $Z \rightarrow b\bar{b}$  using  $133 \text{ fb}^{-1}$  of  $pp$  collision data at  $E_{\text{cm}} = 13$  TeV. The upper limit at 95% CL on the  $ZH$  production is 5.0 times the SM prediction. NODE=S126SBB;LINKAGE=MA
- 10 HAYRAPETYAN 24AY present measurements of boosted  $H \rightarrow b\bar{b}$  ( $p_T > 450$  GeV) via VBF or gluon fusion productions using  $138 \text{ fb}^{-1}$  of  $pp$  collision data at  $E_{\text{cm}} = 13$  TeV. The result is given for the VBF production. See their Table 3. The  $VH$  and  $t\bar{t}H$  production rates are fixed to the SM values. The VBF signal strengths and the fiducial cross sections for two different  $m_{jj}$  regions and STXS stage 1.2 bins are shown in their Figs. 9 and 10, respectively. NODE=S126SBB;LINKAGE=OA
- 11 HAYRAPETYAN 24AY present measurements of boosted  $H \rightarrow b\bar{b}$  ( $p_T > 450$  GeV) via VBF or gluon fusion productions using  $138 \text{ fb}^{-1}$  of  $pp$  collision data at  $E_{\text{cm}} = 13$  TeV. The result is given for the gluon fusion production. See their Table 3. The  $VH$  and  $t\bar{t}H$  production rates are fixed to the SM values. The gluon fusion signal strengths and the fiducial cross sections for 6 different  $p_T$  regions and STXS stage 1.2 bins are shown in their Figs. 9 and 10, respectively. NODE=S126SBB;LINKAGE=PA
- 12 HAYRAPETYAN 24U present measurements of  $H \rightarrow b\bar{b}$  in the VBF production mode using  $90.8 \text{ fb}^{-1}$  of data at  $E_{\text{cm}} = 13$  TeV constraining the ggF production to be the SM expectation. The quoted signal strength corresponds to a significance of 2.4 standard deviations. NODE=S126SBB;LINKAGE=IA
- 13 HAYRAPETYAN 24U present measurements of  $H \rightarrow b\bar{b}$  in the inclusive (ggF+VBF) production mode using  $90.8 \text{ fb}^{-1}$  of data at  $E_{\text{cm}} = 13$  TeV. The quoted signal strength corresponds to a significance of 2.6 standard deviations. NODE=S126SBB;LINKAGE=JA
- 14 HAYRAPETYAN 24U present measurements of  $H \rightarrow b\bar{b}$  in the ggF and VBF production modes using  $90.8 \text{ fb}^{-1}$  of data at  $E_{\text{cm}} = 13$  TeV. The signal strengths for the ggF and VBF production modes are independently obtained. See their Fig. 11. NODE=S126SBB;LINKAGE=KA
- 15 TUMASYAN 24 report the measurement of  $VH$ ,  $H \rightarrow b\bar{b}$  ( $V = W, Z$ ) using  $138 \text{ fb}^{-1}$  of  $pp$  collision data at  $E_{\text{cm}} = 13$  TeV. The quoted signal strength corresponds to a significance of 6.3 standard deviations. Signal strengths for  $WH$  and  $ZH$  are given in their Fig. 7. Signal strengths and  $\sigma \cdot B$  for 8 different bins defined based on the the simplified template cross section framework are given in their Figs. 8 and 9 and Table VII. NODE=S126SBB;LINKAGE=NA
- 16 AAD 22X measure cross sections using a boosted  $H \rightarrow b\bar{b}$  with large-radius jets. The data is  $136 \text{ fb}^{-1}$  of  $pp$  collisions at  $E_{\text{cm}} = 13$  TeV. All the results are given for  $m_H = 125$  GeV. The inclusive signal strength is given using data with a  $H$  candidate jet  $p_T > 250$  GeV. The fiducial  $H$  production cross section ( $p_T(H) > 450$  GeV and  $|y(H)| < 2$ ) is  $< 115 \text{ fb}$  (95% CL) and the upper limits for other four different  $p_T$  regions are shown in their Fig 12. The measured fiducial  $H$  production cross section ( $p_T(H) > 1 \text{ TeV}$ ) is  $2.3 \pm 3.9(\text{stat}) \pm 1.3(\text{syst}) \pm 0.5(\text{theory}) \text{ fb}$ . NODE=S126SBB;LINKAGE=GA
- 17 AAD 21AB search for  $VH$ ,  $H \rightarrow b\bar{b}$  ( $V = W, Z$ ) using  $139 \text{ fb}^{-1}$  of  $pp$  collision data at  $E_{\text{cm}} = 13$  TeV. The results are given for  $m_H = 125$  GeV. Cross sections are given in their Table 13 and Fig. 7, which are based on the simplified template cross section framework (reduced stage-1.2). Wilson coefficients of the Warsaw-basis operators are given in their Fig. 9. NODE=S126SBB;LINKAGE=BA
- 18 AAD 21H present measurements of  $H \rightarrow b\bar{b}$  with a boosted vector boson ( $p_T > 250$  GeV) using  $139 \text{ fb}^{-1}$  of  $pp$  collision data at  $E_{\text{cm}} = 13$  TeV. Cross sections are given in their Table 6 and Fig. 4, which are based on the simplified template cross section framework (reduced stage-1.2). Wilson coefficients of the Warsaw-basis operators are given in their Fig. 5. NODE=S126SBB;LINKAGE=EA
- 19 AAD 21M search for VBF+ $\gamma$ ,  $H \rightarrow b\bar{b}$  using  $132 \text{ fb}^{-1}$  of  $pp$  collision data at  $E_{\text{cm}} = 13$  TeV. NODE=S126SBB;LINKAGE=FA
- 20 SIRUNYAN 20BL search for boosted  $H \rightarrow b\bar{b}$  (a  $H$  candidate jet  $p_T > 450$  GeV) using  $137 \text{ fb}^{-1}$  of  $pp$  collision data at  $E_{\text{cm}} = 13$  TeV. The quoted signal strength corresponds to a significance of 2.5 standard deviations and is given for  $m_H = 125$  GeV. A differential fiducial cross section as a function of Higgs boson  $p_T$  for ggF is shown in their Fig. 7, assuming the other production modes occur at the expected SM rates. The reported value is  $3.7 \pm 1.2^{+0.8+0.8}_{-0.7-0.5}$  where the last uncertainty comes from theoretical modeling. We have combined the systematic uncertainties in quadrature. NODE=S126SBB;LINKAGE=Z
- 21 AABOUD 19U measure cross sections of  $pp \rightarrow VH$ ,  $H \rightarrow b\bar{b}$  production as a function of the gauge boson transverse momentum using data of  $79.8 \text{ fb}^{-1}$ . The kinematic fiducial volumes used is based on the simplified template cross section framework (reduced stage-1). See their Table 3 and Fig. 3. NODE=S126SBB;LINKAGE=Y
- 22 SIRUNYAN 19AT perform a combine fit to  $35.9 \text{ fb}^{-1}$  of data at  $E_{\text{cm}} = 13$  TeV. NODE=S126SBB;LINKAGE=X
- 23 AABOUD 18BN search for  $VH$ ,  $H \rightarrow b\bar{b}$  ( $V = W, Z$ ) using  $79.8 \text{ fb}^{-1}$  of  $pp$  collision data at  $E_{\text{cm}} = 13$  TeV. The quoted signal strength corresponds to a significance of 4.9 standard deviations and is given for  $m_H = 125$  GeV. NODE=S126SBB;LINKAGE=N
- 24 AABOUD 18BN combine results of  $79.8 \text{ fb}^{-1}$  at  $E_{\text{cm}} = 13$  TeV with results of  $VH$  at  $E_{\text{cm}} = 7$  and  $8$  TeV. NODE=S126SBB;LINKAGE=O

- 25 AABOUD 18BN combine results of  $VH$  at  $E_{\text{cm}} = 7, 8$  and  $13$  TeV with results of VBF (+gluon fusion) and  $t\bar{t}H$  at  $E_{\text{cm}} = 7, 8$ , and  $13$  TeV to perform a search for the  $H \rightarrow b\bar{b}$  decay. The quoted signal strength assumes a SM production strength and corresponds to a significance of 5.4 standard deviations. NODE=S126SBB;LINKAGE=P
- 26 AABOUD 18BQ search for  $H \rightarrow b\bar{b}$  produced through vector-boson fusion (VBF) and VBF+ $\gamma$  with  $30.6 \text{ fb}^{-1}$   $pp$  collision data at  $E_{\text{cm}} = 13$  TeV. The quoted signal strength is given for  $m_H = 125$  GeV. NODE=S126SBB;LINKAGE=Q
- 27 The signal strength is measured including all production modes (VBF, ggF,  $VH$ ,  $t\bar{t}H$ ). NODE=S126SBB;LINKAGE=U
- 28 The signal strength is measured for VBF-only and others (ggF,  $VH$ ,  $t\bar{t}H$ ) are constrained to Standard Model expectations with uncertainties described in their Section VIII B. NODE=S126SBB;LINKAGE=V
- 29 AALTONEN 18C use  $5.4 \text{ fb}^{-1}$  of  $p\bar{p}$  collisions at  $E_{\text{cm}} = 1.96$  TeV. The upper limit at 95% CL on  $p\bar{p} \rightarrow H \rightarrow b\bar{b}$  is 33 times the SM prediction, which corresponds to a cross section of  $40.6 \text{ pb}$ . NODE=S126SBB;LINKAGE=W
- 30 SIRUNYAN 18AE use  $35.9 \text{ fb}^{-1}$  of  $pp$  collision data at  $E_{\text{cm}} = 13$  TeV. The quoted signal strength corresponds to 3.3 standard deviations and is given for  $m_H = 125.09$  GeV. NODE=S126SBB;LINKAGE=L
- 31 SIRUNYAN 18AE combine the result of  $35.9 \text{ fb}^{-1}$  at  $E_{\text{cm}} = 13$  TeV with the results obtained from data of up to  $5.1 \text{ fb}^{-1}$  at  $E_{\text{cm}} = 7$  TeV and up to  $18.9 \text{ fb}^{-1}$  at  $E_{\text{cm}} = 8$  TeV (CHATRCHYAN 14AI and KHACHATRYAN 15Z). The quoted signal strength corresponds to 3.8 standard deviations and is given for  $m_H = 125.09$  GeV. NODE=S126SBB;LINKAGE=M
- 32 SIRUNYAN 18DB search for  $VH$ ,  $H \rightarrow b\bar{b}$  ( $V = W, Z$ ) using  $77.2 \text{ fb}^{-1}$  of  $pp$  collision data at  $E_{\text{cm}} = 13$  TeV. The quoted signal strength corresponds to a significance of 4.4 standard deviations and is given for  $m_H = 125.09$  GeV. NODE=S126SBB;LINKAGE=R
- 33 SIRUNYAN 18DB combine the result of  $77.2 \text{ fb}^{-1}$  at  $E_{\text{cm}} = 13$  TeV with the results obtained from data of up to  $5.1 \text{ fb}^{-1}$  at  $E_{\text{cm}} = 7$  TeV and up to  $18.9 \text{ fb}^{-1}$  at  $E_{\text{cm}} = 8$  TeV. The quoted signal strength corresponds to a significance of 4.8 standard deviations and is given for  $m_H = 125.09$  GeV. NODE=S126SBB;LINKAGE=S
- 34 SIRUNYAN 18DB combine results of  $77.2 \text{ fb}^{-1}$  at  $E_{\text{cm}} = 13$  TeV with results of gluon fusion (ggF), VBF and  $t\bar{t}H$  at  $E_{\text{cm}} = 7$  TeV,  $8$  TeV and  $13$  TeV to perform a search for the  $H \rightarrow b\bar{b}$  decay. The quoted signal strength assumes a SM production strength and corresponds to a significance of 5.6 standard deviations and is given for  $m_H = 125.09$  GeV. NODE=S126SBB;LINKAGE=T
- 35 SIRUNYAN 18E use  $35.9 \text{ fb}^{-1}$  at  $E_{\text{cm}} = 13$  TeV. The quoted signal strength is given for  $m_H = 125$  GeV. They measure  $\sigma \cdot B$  for gluon fusion production of  $H \rightarrow b\bar{b}$  with  $p_T > 450$  GeV,  $|\eta| < 2.5$  to be  $74 \pm 48^{+17}_{-10} \text{ fb}$ . NODE=S126SBB;LINKAGE=K
- 36 AABOUD 17BA use  $36.1 \text{ fb}^{-1}$  at  $E_{\text{cm}} = 13$  TeV. The quoted signal strength is given for  $m_H = 125$  GeV. They give  $\sigma(WH) \cdot B(H \rightarrow b\bar{b}) = 1.08^{+0.54}_{-0.47} \text{ pb}$  and  $\sigma(ZH) \cdot B(H \rightarrow b\bar{b}) = 0.57^{+0.26}_{-0.23} \text{ pb}$ . NODE=S126SBB;LINKAGE=F
- 37 AABOUD 17BA combine 7, 8 and 13 TeV analyses. The quoted signal strength is given for  $m_H = 125$  GeV. NODE=S126SBB;LINKAGE=G
- 38 AABOUD 16X search for vector-boson fusion production of  $H$  decaying to  $b\bar{b}$  in  $20.2 \text{ fb}^{-1}$  of  $pp$  collisions at  $E_{\text{cm}} = 8$  TeV. The quoted signal strength is given for  $m_H = 125$  GeV. NODE=S126SBB;LINKAGE=J
- 39 AAD 16K use up to  $4.7 \text{ fb}^{-1}$  of  $pp$  collisions at  $E_{\text{cm}} = 7$  TeV and up to  $20.3 \text{ fb}^{-1}$  at  $E_{\text{cm}} = 8$  TeV. The quoted signal strength is given for  $m_H = 125.36$  GeV. NODE=S126SBB;LINKAGE=E
- 40 AAD 15G use  $4.7 \text{ fb}^{-1}$  of  $pp$  collisions at  $E_{\text{cm}} = 7$  TeV and  $20.3 \text{ fb}^{-1}$  at  $E_{\text{cm}} = 8$  TeV. The quoted signal strength is given for  $m_H = 125.36$  GeV. NODE=S126SBB;LINKAGE=B
- 41 KHACHATRYAN 15Z search for vector-boson fusion production of  $H$  decaying to  $b\bar{b}$  in up to  $19.8 \text{ fb}^{-1}$  of  $pp$  collisions at  $E_{\text{cm}} = 8$  TeV. The quoted signal strength is given for  $m_H = 125$  GeV. NODE=S126SBB;LINKAGE=C
- 42 KHACHATRYAN 15Z combined vector boson fusion,  $WH$ ,  $ZH$  production, and  $t\bar{t}H$  production results. The quoted signal strength is given for  $m_H = 125$  GeV. NODE=S126SBB;LINKAGE=D
- 43 CHATRCHYAN 14AI use up to  $5.1 \text{ fb}^{-1}$  of  $pp$  collisions at  $E_{\text{cm}} = 7$  TeV and up to  $18.9 \text{ fb}^{-1}$  at  $E_{\text{cm}} = 8$  TeV. The quoted signal strength is given for  $m_H = 125$  GeV. See also CHATRCHYAN 14AJ. NODE=S126SBB;LINKAGE=A
- 44 AALTONEN 13L combine all CDF results with  $9.45\text{--}10.0 \text{ fb}^{-1}$  of  $p\bar{p}$  collisions at  $E_{\text{cm}} = 1.96$  TeV. The quoted signal strength is given for  $m_H = 125$  GeV. NODE=S126SBB;LINKAGE=LL
- 45 ABAZOV 13L combine all D0 results with up to  $9.7 \text{ fb}^{-1}$  of  $p\bar{p}$  collisions at  $E_{\text{cm}} = 1.96$  TeV. The quoted signal strength is given for  $m_H = 125$  GeV. NODE=S126SBB;LINKAGE=AB
- 46 AAD 12AI obtain results based on  $4.6\text{--}4.8 \text{ fb}^{-1}$  of  $pp$  collisions at  $E_{\text{cm}} = 7$  TeV. The quoted signal strengths are given in their Fig. 10 for  $m_H = 126$  GeV. See also Fig. 13 of AAD 12DA. NODE=S126SBB;LINKAGE=AA
- 47 AALTONEN 12T combine AALTONEN 12Q, AALTONEN 12R, AALTONEN 12S, ABAZOV 12O, ABAZOV 12P, and ABAZOV 12K. An excess of events over background is observed which is most significant in the region  $m_H = 120\text{--}135$  GeV, with a local significance of up to  $3.3 \sigma$ . The local significance at  $m_H = 125$  GeV is  $2.8 \sigma$ , which corresponds to  $(\sigma(HW) + \sigma(HZ)) \cdot B(H \rightarrow b\bar{b}) = (0.23^{+0.09}_{-0.08}) \text{ pb}$ , compared to the Standard Model expectation at  $m_H = 125$  GeV of  $0.12 \pm 0.01 \text{ pb}$ . Superseded by AALTONEN 13M. NODE=S126SBB;LINKAGE=AL
- 48 CHATRCHYAN 12N obtain results based on  $5.0 \text{ fb}^{-1}$  of  $pp$  collisions at  $E_{\text{cm}} = 7$  TeV and  $5.1 \text{ fb}^{-1}$  at  $E_{\text{cm}} = 8$  TeV. The quoted signal strength is given for  $m_H = 125.5$  GeV. See also CHATRCHYAN 13Y. NODE=S126SBB;LINKAGE=CA

$\mu^+\mu^-$  final state

VALUE	CL%	DOCUMENT ID	TECN	COMMENT
<b>1.21±0.35 OUR AVERAGE</b>				
$1.21^{+0.45}_{-0.42}$		<sup>1</sup> CMS	22 CMS	$pp$ , 13 TeV
$1.2 \pm 0.6$		<sup>2</sup> AAD	21 ATLS	$pp$ , 13 TeV
• • • We do not use the following data for averages, fits, limits, etc. • • •				
$1.19^{+0.40+0.15}_{-0.39-0.14}$		<sup>3</sup> SIRUNYAN	21C CMS	$pp$ , 13 TeV
$0.68^{+1.25}_{-1.24}$		<sup>4</sup> SIRUNYAN	19AT CMS	$pp$ , 13 TeV
$0.7 \pm 1.0^{+0.2}_{-0.1}$		<sup>5</sup> SIRUNYAN	19E CMS	$pp$ , 13 TeV, 35.9 fb <sup>-1</sup>
$1.0 \pm 1.0 \pm 0.1$		<sup>5</sup> SIRUNYAN	19E CMS	$pp$ , 7, 8, 13 TeV
$-0.1 \pm 1.4$		<sup>6</sup> AABOUD	17Y ATLS	$pp$ , 7, 8, 13 TeV
$-0.1 \pm 1.5$		<sup>6</sup> AABOUD	17Y ATLS	$pp$ , 13 TeV
$0.1 \pm 2.5$		<sup>7</sup> AAD	16AN LHC	$pp$ , 7, 8 TeV
$-0.6 \pm 3.6$		<sup>7</sup> AAD	16AN ATLS	$pp$ , 7, 8 TeV
$0.9^{+3.6}_{-3.5}$		<sup>7</sup> AAD	16AN CMS	$pp$ , 7, 8 TeV
$< 7.4$	95	<sup>8</sup> KHACHATRY...15H	CMS	$pp \rightarrow HX$ , 7, 8 TeV
$< 7.0$	95	<sup>9</sup> AAD	14AS ATLS	$pp \rightarrow HX$ , 7, 8 TeV

NODE=S126SMU  
NODE=S126SMU

<sup>1</sup> CMS 22 report combined results (see their Extended Data Table 2) using up to 138 fb<sup>-1</sup> of data at  $E_{cm} = 13$  TeV, assuming  $m_H = 125.38$  GeV. See their Fig. 2 right.

<sup>2</sup> AAD 21 search for  $H \rightarrow \mu^+\mu^-$  using 139 fb<sup>-1</sup> of  $pp$  collision data at  $E_{cm} = 13$  TeV. The quoted signal strength corresponds to a significance of 2.0 standard deviations and is given for  $m_H = 125.09$  GeV. The upper limit on the cross section times branching fraction is 2.2 times the SM prediction at 95% CL, which corresponds to the branching fraction upper limit of  $4.7 \times 10^{-4}$  (assuming SM production cross sections).

<sup>3</sup> SIRUNYAN 21 search for  $H \rightarrow \mu^+\mu^-$  using 137 fb<sup>-1</sup> of  $pp$  collision data at  $E_{cm} = 13$  TeV. The quoted signal strength corresponds to a significance of 3.0 standard deviations and is given for  $m_H = 125.38$  GeV.

<sup>4</sup> SIRUNYAN 19AT perform a combine fit to 35.9 fb<sup>-1</sup> of data at  $E_{cm} = 13$  TeV.

<sup>5</sup> SIRUNYAN 19E search for  $H \rightarrow \mu^+\mu^-$  using 35.9 fb<sup>-1</sup> of  $pp$  collisions at  $E_{cm} = 13$  TeV and combine with results of 7 TeV (5.0 fb<sup>-1</sup>) and 8 TeV (19.7 fb<sup>-1</sup>). The upper limit at 95% CL on the signal strength is 2.9, which corresponds to the SM Higgs boson branching fraction to a muon pair of  $6.4 \times 10^{-4}$ .

<sup>6</sup> AABOUD 17Y use 36.1 fb<sup>-1</sup> of  $pp$  collisions at  $E_{cm} = 13$  TeV, 20.3 fb<sup>-1</sup> at 8 TeV and 4.5 fb<sup>-1</sup> at 7 TeV. The quoted signal strength is given for  $m_H = 125$  GeV.

<sup>7</sup> AAD 16AN: In the fit, relative production cross sections are fixed to those in the Standard Model. The quoted signal strength is given for  $m_H = 125.09$  GeV.

<sup>8</sup> KHACHATRYAN 15H use 5.0 fb<sup>-1</sup> of  $pp$  collisions at  $E_{cm} = 7$  TeV and 19.7 fb<sup>-1</sup> at 8 TeV. The quoted signal strength is given for  $m_H = 125$  GeV.

<sup>9</sup> AAD 14AS search for  $H \rightarrow \mu^+\mu^-$  in 4.5 fb<sup>-1</sup> of  $pp$  collisions at  $E_{cm} = 7$  TeV and 20.3 fb<sup>-1</sup> at  $E_{cm} = 8$  TeV. The quoted signal strength is given for  $m_H = 125.5$  GeV.

NODE=S126SMU;LINKAGE=K

NODE=S126SMU;LINKAGE=I

NODE=S126SMU;LINKAGE=J

NODE=S126SMU;LINKAGE=H

NODE=S126SMU;LINKAGE=F

NODE=S126SMU;LINKAGE=E

NODE=S126SMU;LINKAGE=D

NODE=S126SMU;LINKAGE=B

NODE=S126SMU;LINKAGE=A

 $\tau^+\tau^-$  final state

VALUE	DOCUMENT ID	TECN	COMMENT
<b>0.91±0.09 OUR AVERAGE</b>			
$0.85 \pm 0.10$	<sup>1</sup> CMS	22 CMS	$pp$ , 13 TeV
$1.09^{+0.18+0.26+0.16}_{-0.17-0.22-0.11}$	<sup>2</sup> AABOUD	19AQ ATLS	$pp$ , 13 TeV
$1.11^{+0.24}_{-0.22}$	<sup>3,4</sup> AAD	16AN LHC	$pp$ , 7, 8 TeV
$1.68^{+2.28}_{-1.68}$	<sup>5</sup> AALTONEN	13M TEVA	$p\bar{p} \rightarrow HX$ , 1.96 TeV
• • • We do not use the following data for averages, fits, limits, etc. • • •			
	<sup>6</sup> AAD	25W ATLS	$pp$ , 13 TeV
$1.28^{+0.30+0.25}_{-0.29-0.21}$	<sup>7</sup> AAD	24BE ATLS	$pp \rightarrow WH/ZH, H \rightarrow \tau\tau$ , 13 TeV
$1.64^{+0.68}_{-0.54}$	<sup>8</sup> HAYRAPETY...24AT	CMS	$pp$ , 13 TeV, boosted $H \rightarrow \tau\tau$
$0.82^{+0.11}_{-0.10}$	<sup>9,10</sup> TUMASYAN	23Y CMS	$pp$ , 13 TeV
$0.67^{+0.20}_{-0.18}$	<sup>9,11</sup> TUMASYAN	23Y CMS	$pp$ , 13 TeV
$0.81^{+0.17}_{-0.16}$	<sup>9,12</sup> TUMASYAN	23Y CMS	$pp$ , 13 TeV
$1.79^{+0.47}_{-0.42}$	<sup>9,13</sup> TUMASYAN	23Y CMS	$pp$ , 13 TeV
	<sup>14</sup> AAD	22Q ATLS	$pp$ , 13 TeV
	<sup>15</sup> TUMASYAN	22AJ CMS	$pp$ , 13 TeV
$2.5^{+1.4}_{-1.3}$	<sup>16</sup> SIRUNYAN	19AF CMS	$pp \rightarrow HW/HZ, H \rightarrow \tau\tau$ , 13 TeV

NODE=S126STT  
NODE=S126STT

OCCUR=2

OCCUR=3

OCCUR=4

$1.24^{+0.29}_{-0.27}$	17	SIRUNYAN	19AF CMS	$pp$ , 13 TeV	OCCUR=2
$1.02^{+0.26}_{-0.24}$	18	SIRUNYAN	19AT CMS	$pp$ , 13 TeV	
$1.09^{+0.27}_{-0.26}$	19	SIRUNYAN	18Y CMS	$pp$ , 13 TeV	
$0.98 \pm 0.18$	20	SIRUNYAN	18Y CMS	$pp$ , 7, 8, 13 TeV	OCCUR=2
$2.3 \pm 1.6$	21	AAD	16AC ATLS	$pp \rightarrow HW/ZX$ , 8 TeV	
$1.41^{+0.40}_{-0.36}$	4	AAD	16AN ATLS	$pp$ , 7, 8 TeV	OCCUR=2
$0.88^{+0.30}_{-0.28}$	4	AAD	16AN CMS	$pp$ , 7, 8 TeV	OCCUR=3
$1.44^{+0.30+0.29}_{-0.29-0.23}$	22	AAD	16K ATLS	$pp$ , 7, 8 TeV	
$1.43^{+0.27+0.32}_{-0.26-0.25} \pm 0.09$	23	AAD	15AH ATLS	$pp \rightarrow HX$ , 7, 8 TeV	
$0.78 \pm 0.27$	24	CHATRCHYAN	14K CMS	$pp \rightarrow HX$ , 7, 8 TeV	
$0.00^{+8.44}_{-0.00}$	25	AALTONEN	13L CDF	$p\bar{p} \rightarrow HX$ , 1.96 TeV	
$3.96^{+4.11}_{-3.38}$	26	ABAZOV	13L D0	$p\bar{p} \rightarrow HX$ , 1.96 TeV	
$0.4^{+1.6}_{-2.0}$	27	AAD	12AI ATLS	$pp \rightarrow HX$ , 7 TeV	
$0.09^{+0.76}_{-0.74}$	28	CHATRCHYAN	12N CMS	$pp \rightarrow HX$ , 7, 8 TeV	
<p><sup>1</sup> CMS 22 report combined results (see their Extended Data Table 2) using up to <math>138 \text{ fb}^{-1}</math> of data at <math>E_{\text{cm}} = 13 \text{ TeV}</math>, assuming <math>m_H = 125.38 \text{ GeV}</math>. See their Fig. 2 right.</p>					NODE=S126STT;LINKAGE=N
<p><sup>2</sup> AABOUD 19AQ use <math>36.1 \text{ fb}^{-1}</math> of data. The first, second and third quoted errors are statistical, experimental systematic and theory systematic uncertainties, respectively. The quoted signal strength is given for <math>m_H = 125 \text{ GeV}</math> and corresponds to 4.4 standard deviations. Combining with 7 TeV and 8 TeV results (AAD 15AH), the observed significance is 6.4 standard deviations. The cross sections in the <math>H \rightarrow \tau\tau</math> decay channel (<math>m_H = 125 \text{ GeV}</math>) are measured to <math>3.77^{+0.60}_{-0.59}</math> (stat) <math>^{+0.87}_{-0.74}</math> (syst) pb for the inclusive, <math>0.28 \pm 0.09^{+0.11}_{-0.09}</math> pb for VBF, and <math>3.1 \pm 1.0^{+1.6}_{-1.3}</math> pb for gluon-fusion production. See their Table XI for the cross sections in the framework of simplified template cross sections.</p>					NODE=S126STT;LINKAGE=K
<p><sup>3</sup> AAD 16AN perform fits to the ATLAS and CMS data at <math>E_{\text{cm}} = 7</math> and 8 TeV. The signal strengths for individual production processes are <math>1.0 \pm 0.6</math> for gluon fusion, <math>1.3 \pm 0.4</math> for vector boson fusion, <math>-1.4 \pm 1.4</math> for <math>WH</math> production, <math>2.2^{+2.2}_{-1.8}</math> for <math>ZH</math> production, and <math>-1.9^{+3.7}_{-3.3}</math> for <math>t\bar{t}H</math> production.</p>					NODE=S126STT;LINKAGE=G
<p><sup>4</sup> AAD 16AN: In the fit, relative production cross sections are fixed to those in the Standard Model. The quoted signal strength is given for <math>m_H = 125.09 \text{ GeV}</math>.</p>					NODE=S126STT;LINKAGE=H
<p><sup>5</sup> AALTONEN 13M combine all Tevatron data from the CDF and D0 Collaborations with up to <math>10.0 \text{ fb}^{-1}</math> and <math>9.7 \text{ fb}^{-1}</math>, respectively, of <math>p\bar{p}</math> collisions at <math>E_{\text{cm}} = 1.96 \text{ TeV}</math>. The quoted signal strength is given for <math>m_H = 125 \text{ GeV}</math>.</p>					NODE=S126STT;LINKAGE=AT
<p><sup>6</sup> AAD 25W measure different types of cross sections with <math>pp \rightarrow H \rightarrow \tau\tau</math> at <math>E_{\text{cm}} = 13 \text{ TeV}</math> with <math>140 \text{ fb}^{-1}</math> data. Their Fig. 5 show <math>\sigma \cdot B</math> relative to the SM expectations for the total and per-production-mode, and their Figs. 6 and 8 show those in the simplified template cross section framework. Their Table 7 show the measurements of <math>\sigma \cdot B</math> for per-production-mode. The differential fiducial cross sections defined in their Table 8 are given in their Fig. 10. Six Wilson coefficients in the Warsaw basis are in their Figs. 12 and 13 at 95% CL. The constraints on the Wilson coefficients <math>c_{HW}</math> and <math>c_{H\widetilde{W}}</math> are obtained to be <math>[-1.90, +0.51]</math> and <math>[-0.31, +0.88]</math> at 95% CL, respectively, for the interference term alone (the linear term) assuming only one of the Wilson coefficients is non-zero.</p>					NODE=S126STT;LINKAGE=X
<p><sup>7</sup> AAD 24BE measure the <math>VH</math> Higgs production (<math>V = W, Z</math>) with <math>H \rightarrow \tau\tau</math> at <math>E_{\text{cm}} = 13 \text{ TeV}</math> with <math>140 \text{ fb}^{-1}</math> data. The quoted signal strength corresponds to 4.2 standard deviations. The signal strengths for individual <math>WH</math> and <math>ZH</math> productions are <math>1.48^{+0.56}_{-0.50}</math> and <math>1.09^{+0.51}_{-0.44}</math>, respectively. The results are given for <math>m_H = 125 \text{ GeV}</math>. See their Fig. 4.</p>					NODE=S126STT;LINKAGE=V
<p><sup>8</sup> HAYRAPETYAN 24AT present measurements of the boosted <math>H \rightarrow \tau\tau</math> (<math>p_T &gt; 250 \text{ GeV}</math>) using <math>138 \text{ fb}^{-1}</math> of <math>pp</math> collision data at <math>E_{\text{cm}} = 13 \text{ TeV}</math>. The quoted signal strength corresponds to a significance of 3.5 standard deviations. The fiducial inclusive production cross section is measured to be <math>3.88^{+1.69}_{-1.35} \text{ fb}</math>. The differential fiducial cross sections as a function of Higgs boson and leading jet <math>p_T</math> are given in their Fig. 3.</p>					NODE=S126STT;LINKAGE=W
<p><sup>9</sup> TUMASYAN 23Y measure Higgs production with <math>pp \rightarrow H \rightarrow \tau\tau</math> at <math>E_{\text{cm}} = 13 \text{ TeV}</math> with <math>138 \text{ fb}^{-1}</math> data. The quoted results are given for <math>m_H = 125.38 \text{ GeV}</math>.</p>					NODE=S126STT;LINKAGE=P
<p><sup>10</sup> The inclusive <math>\sigma \cdot B</math> is <math>2800^{+356}_{-335} \text{ fb}</math> (see their Figs. 10 and 14). See their Fig. 15 for the 68 % and 95 % CL contours in the <math>\kappa_V - \kappa_F</math> plane.</p>					NODE=S126STT;LINKAGE=Q
<p><sup>11</sup> The quoted result is for the stage-0 simplified template cross section (STXS) and the <math>\sigma_{ggF} \cdot B</math> is <math>2030^{+598}_{-555} \text{ fb}</math> (see their Figs. 10 and 14). Measured cross sections and</p>					NODE=S126STT;LINKAGE=R

ratios to the SM predictions in the reduced stage-1.2 STXS (see their Fig. 1) are shown in their Table 9 and Figs. 12 and 14.

- 12 The quoted result is for the stage-0 STXS and the  $\sigma_{VBF} \cdot B$  is  $267^{+53.9}_{-52.6}$  fb (see their Figs. 10 and 14). Measured cross sections and ratios to the SM predictions in the reduced stage-1.2 STXS (see their Fig. 2) are shown in their Table 9 and Figs. 12, 14.
- 13 The quoted result is for the stage-0 STXS and the  $\sigma_{VH} \cdot B$  is  $79.0^{+20.5}_{-18.6}$  fb (see their Figs. 10 and 14). Measured cross sections and ratios to the SM predictions in the reduced stage-1.2 STXS (see their Fig. 3) are shown in their Table 9 and Figs. 12, 14.
- 14 AAD 22Q measure cross sections of  $pp \rightarrow H \rightarrow \tau\tau$  at  $E_{cm} = 13$  TeV with  $139 \text{ fb}^{-1}$  data. The quoted results are given for  $m_H = 125.09$  GeV and  $|\gamma(H)| < 2.5$  is required. The inclusive fiducial  $\sigma \cdot B$  is  $2.94 \pm 0.21^{+0.37}_{-0.32}$  pb. The fiducial  $\sigma \cdot B$  for the four dominant production modes are  $2.65 \pm 0.41^{+0.91}_{-0.67}$  pb for ggF,  $0.197 \pm 0.028^{+0.032}_{-0.026}$  pb for VBF,  $0.115 \pm 0.058^{+0.042}_{-0.040}$  pb for  $VH$ ,  $0.033 \pm 0.031^{+0.022}_{-0.017}$  pb for  $t\bar{t}H$ . The cross sections using simplified template cross section framework (STXS) are given in their Fig. 14(a) and Table 15. The STXS bins (a reduced stage 1.2) are defined in their Fig. 1.
- 15 TUMASYAN 22AJ measure cross sections with  $pp \rightarrow H \rightarrow \tau\tau$  at  $E_{cm} = 13$  TeV with  $138 \text{ fb}^{-1}$  data. The fiducial inclusive  $\sigma \cdot B$  is  $426 \pm 102$  fb while  $408 \pm 27$  fb is expected in the Standard Mode for  $m_H = 125.38$  GeV. Three differential cross sections are given; see their Fig. 1.
- 16 SIRUNYAN 19AF use  $35.9 \text{ fb}^{-1}$  of data. The quoted signal strength is given for  $m_H = 125$  GeV and corresponds to 2.3 standard deviations.
- 17 SIRUNYAN 19AF use  $35.9 \text{ fb}^{-1}$  of data.  $HW/Z$  channels are added with a few updates on gluon fusion and vector boson fusion with respect to SIRUNYAN 18Y. The quoted signal strength is given for  $m_H = 125$  GeV and corresponds to 5.5 standard deviations. The signal strengths for the individual production modes are:  $1.12^{+0.53}_{-0.50}$  for gluon fusion,  $1.13^{+0.45}_{-0.42}$  for vector boson fusion,  $3.39^{+1.68}_{-1.54}$  for  $WH$  and  $1.23^{+1.62}_{-1.35}$  for  $ZH$ . See their Fig. 7 for other couplings ( $\kappa_V, \kappa_F$ ).
- 18 SIRUNYAN 19AT perform a combine fit to  $35.9 \text{ fb}^{-1}$  of data at  $E_{cm} = 13$  TeV. This combination is based on SIRUNYAN 18Y.
- 19 SIRUNYAN 18Y use  $35.9 \text{ fb}^{-1}$  of  $pp$  collisions at  $E_{cm} = 13$  TeV. The quoted signal strength is given for  $m_H = 125.09$  GeV and corresponds to 4.9 standard deviations.
- 20 SIRUNYAN 18Y combine the result of  $35.9 \text{ fb}^{-1}$  at  $E_{cm} = 13$  TeV with the results obtained from data of  $4.9 \text{ fb}^{-1}$  at  $E_{cm} = 7$  TeV and  $19.7 \text{ fb}^{-1}$  at  $E_{cm} = 8$  TeV (KHACHATRYAN 15AM). The quoted signal strength is given for  $m_H = 125.09$  GeV and corresponds to 5.9 standard deviations.
- 21 AAD 16AC measure the signal strength with  $pp \rightarrow HW/ZX$  processes using  $20.3 \text{ fb}^{-1}$  of  $E_{cm} = 8$  TeV. The quoted signal strength is given for  $m_H = 125$  GeV.
- 22 AAD 16K use up to  $4.7 \text{ fb}^{-1}$  of  $pp$  collisions at  $E_{cm} = 7$  TeV and up to  $20.3 \text{ fb}^{-1}$  at  $E_{cm} = 8$  TeV. The quoted signal strength is given for  $m_H = 125.36$  GeV.
- 23 AAD 15AH use  $4.5 \text{ fb}^{-1}$  of  $pp$  collisions at  $E_{cm} = 7$  TeV and  $20.3 \text{ fb}^{-1}$  at  $E_{cm} = 8$  TeV. The third uncertainty in the measurement is theory systematics. The signal strength for the gluon fusion mode is  $2.0 \pm 0.8^{+1.2}_{-0.8} \pm 0.3$  and that for vector boson fusion and  $W/ZH$  production modes is  $1.24^{+0.49+0.31}_{-0.45-0.29} \pm 0.08$ . The quoted signal strength is given for  $m_H = 125.36$  GeV.
- 24 CHATRCHYAN 14K use  $4.9 \text{ fb}^{-1}$  of  $pp$  collisions at  $E_{cm} = 7$  TeV and  $19.7 \text{ fb}^{-1}$  at  $E_{cm} = 8$  TeV. The quoted signal strength is given for  $m_H = 125$  GeV. See also CHATRCHYAN 14AJ.
- 25 AALTONEN 13L combine all CDF results with  $9.45\text{--}10.0 \text{ fb}^{-1}$  of  $p\bar{p}$  collisions at  $E_{cm} = 1.96$  TeV. The quoted signal strength is given for  $m_H = 125$  GeV.
- 26 ABAZOV 13L combine all D0 results with up to  $9.7 \text{ fb}^{-1}$  of  $p\bar{p}$  collisions at  $E_{cm} = 1.96$  TeV. The quoted signal strength is given for  $m_H = 125$  GeV.
- 27 AAD 12AI obtain results based on  $4.7 \text{ fb}^{-1}$  of  $pp$  collisions at  $E_{cm} = 7$  TeV. The quoted signal strengths are given in their Fig. 10 for  $m_H = 126$  GeV. See also Fig. 13 of AAD 12DA.
- 28 CHATRCHYAN 12N obtain results based on  $4.9 \text{ fb}^{-1}$  of  $pp$  collisions at  $E_{cm}=7$  TeV and  $5.1 \text{ fb}^{-1}$  at  $E_{cm}=8$  TeV. The quoted signal strength is given for  $m_H=125.5$  GeV. See also CHATRCHYAN 13Y.

NODE=S126STT;LINKAGE=S

NODE=S126STT;LINKAGE=T

NODE=S126STT;LINKAGE=M

NODE=S126STT;LINKAGE=U

NODE=S126STT;LINKAGE=I

NODE=S126STT;LINKAGE=J

NODE=S126STT;LINKAGE=L

NODE=S126STT;LINKAGE=D

NODE=S126STT;LINKAGE=E

NODE=S126STT;LINKAGE=F

NODE=S126STT;LINKAGE=C

NODE=S126STT;LINKAGE=B

NODE=S126STT;LINKAGE=A

NODE=S126STT;LINKAGE=LL

NODE=S126STT;LINKAGE=AB

NODE=S126STT;LINKAGE=AA

NODE=S126STT;LINKAGE=CA

## Z $\gamma$ final state

VALUE	CL%	DOCUMENT ID	TECN	COMMENT
<b>2.2 <math>\pm</math> 0.7</b>		1 AAD	24D LHC	$pp$ , 13 TeV
• • • We do not use the following data for averages, fits, limits, etc. • • •				
2.4 $\pm$ 0.9		2 TUMASYAN	23F CMS	$pp$ , 13 TeV
2.59 <sup>+1.07</sup> <sub>-0.96</sub>		3 CMS	22 CMS	$pp$ , 13 TeV
< 3.6	95	4 AAD	20AG ATLS	$pp$ , 13 TeV
< 7.4	95	5 SIRUNYAN	18DQ CMS	$pp$ , 13 TeV
< 6.6	95	6 AABOUD	17AW ATLS	$pp$ , 13 TeV
< 11	95	7 AAD	14J ATLS	$pp$ , 7, 8 TeV
< 9.5	95	8 CHATRCHYAN	13BK CMS	$pp$ , 7, 8 TeV

NODE=S126SZG  
NODE=S126SZG



- <sup>1</sup> AAD 24D report combined results of ATLAS (AAD 20AG) and CMS (TUMASYAN 23F). The reported signal strength corresponds to a significance of  $3.4\sigma$ .
- <sup>2</sup> TUMASYAN 23F search for  $H \rightarrow Z\gamma$ ,  $Z \rightarrow ee$ ,  $\mu\mu$  in  $138\text{ fb}^{-1}$  of  $pp$  collisions at  $E_{\text{cm}} = 13\text{ TeV}$ , assuming  $m_H = 125.38\text{ GeV}$ .  $\sigma(pp \rightarrow H) \cdot B(H \rightarrow Z\gamma)$  is measured to be  $0.21 \pm 0.08\text{ pb}$ . The ratio of branching fractions  $B(H \rightarrow Z\gamma)/B(H \rightarrow \gamma\gamma)$  is measured to be  $1.5^{+0.7}_{-0.6}$ .
- <sup>3</sup> CMS 22 report combined results (see their Extended Data Table 2) using up to  $138\text{ fb}^{-1}$  of data at  $E_{\text{cm}} = 13\text{ TeV}$ , assuming  $m_H = 125.38\text{ GeV}$ . See their Fig. 2 right.
- <sup>4</sup> AAD 20AG search for  $H \rightarrow Z\gamma$ ,  $Z \rightarrow ee$ ,  $\mu\mu$  in  $139\text{ fb}^{-1}$  of  $pp$  collisions at  $E_{\text{cm}} = 13\text{ TeV}$ . The signal strength is  $2.0 \pm 0.9^{+0.4}_{-0.3}$  at  $m_H = 125.09\text{ GeV}$ , which corresponds to a significance of  $2.2\sigma$ . The upper limit of  $\sigma(pp \rightarrow H) \cdot B(H \rightarrow Z\gamma)$  is  $305\text{ fb}$  at 95% CL.
- <sup>5</sup> SIRUNYAN 18DQ search for  $H \rightarrow Z\gamma$ ,  $Z \rightarrow ee$ ,  $\mu\mu$  in  $35.9\text{ fb}^{-1}$  of  $pp$  collisions at  $E_{\text{cm}} = 13\text{ TeV}$ . The quoted signal strength (see their Figs. 6 and 7) is given for  $m_H = 125\text{ GeV}$ .
- <sup>6</sup> AABOUD 17AW search for  $H \rightarrow Z\gamma$ ,  $Z \rightarrow ee$ ,  $\mu\mu$  in  $36.1\text{ fb}^{-1}$  of  $pp$  collisions at  $E_{\text{cm}} = 13\text{ TeV}$ . The quoted signal strength is given for  $m_H = 125.09\text{ GeV}$ . The upper limit on the branching ratio of  $H \rightarrow Z\gamma$  is 1.0% at 95% CL assuming the SM Higgs boson production.
- <sup>7</sup> AAD 14J search for  $H \rightarrow Z\gamma \rightarrow \ell\ell\gamma$  in  $4.5\text{ fb}^{-1}$  of  $pp$  collisions at  $E_{\text{cm}} = 7\text{ TeV}$  and  $20.3\text{ fb}^{-1}$  at  $E_{\text{cm}} = 8\text{ TeV}$ . The quoted signal strength is given for  $m_H = 125.5\text{ GeV}$ .
- <sup>8</sup> CHATRCHYAN 13BK search for  $H \rightarrow Z\gamma \rightarrow \ell\ell\gamma$  in  $5.0\text{ fb}^{-1}$  of  $pp$  collisions at  $E_{\text{cm}} = 7\text{ TeV}$  and  $19.6\text{ fb}^{-1}$  at  $E_{\text{cm}} = 8\text{ TeV}$ . A limit on cross section times branching ratio which corresponds to (4–25) times the expected Standard Model cross section is given in the range  $m_H = 120\text{--}160\text{ GeV}$  at 95% CL. The quoted limit is given for  $m_H = 125\text{ GeV}$ , where 10 is expected for no signal.

NODE=S126SZG;LINKAGE=G

NODE=S126SZG;LINKAGE=F

NODE=S126SZG;LINKAGE=E

NODE=S126SZG;LINKAGE=D

NODE=S126SZG;LINKAGE=C

NODE=S126SZG;LINKAGE=B

NODE=S126SZG;LINKAGE=A

NODE=S126SZG;LINKAGE=TH

 **$\gamma^*\gamma$  final state**

VALUE	CL%	DOCUMENT ID	TECN	COMMENT
<b><math>1.5 \pm 0.5^{+0.2}_{-0.1}</math></b>		<sup>1</sup> AAD	21I ATLS	$pp$ , 13 TeV, $H \rightarrow \ell\ell\gamma$ , 139 fb <sup>-1</sup>
• • • We do not use the following data for averages, fits, limits, etc. • • •				
<4.0	95	<sup>2</sup> SIRUNYAN	18DQ CMS	$pp \rightarrow HX$ , 13 TeV, $H \rightarrow \gamma^*\gamma$
<6.7	95	<sup>3</sup> KHACHATRYAN	16B CMS	$pp$ , 8 TeV, $ee\gamma$ , $\mu\mu\gamma$
<sup>1</sup> AAD 21I search for $H \rightarrow \ell\ell\gamma$ ( $\ell = e, \mu$ ) in $139\text{ fb}^{-1}$ of $pp$ collisions at $E_{\text{cm}} = 13\text{ TeV}$ . The mass of dilepton $m_{\ell\ell}$ is smaller than 30 GeV. This region is dominated by the decay through $\gamma^*$ . The quoted signal strength corresponds to a significance of 3.2 standard deviations and is given for $m_H = 125.09\text{ GeV}$ . The cross section times the branching ratio of $H \rightarrow \ell\ell\gamma$ for $m_{\ell\ell} < 30\text{ GeV}$ is measured to be $8.7 \pm 2.7^{+0.7}_{-0.6}\text{ fb}$ .				
<sup>2</sup> SIRUNYAN 18DQ search for $H \rightarrow \gamma^*\gamma$ , $\gamma^* \rightarrow \mu\mu$ in $35.9\text{ fb}^{-1}$ of $pp$ collisions at $E_{\text{cm}} = 13\text{ TeV}$ . The mass of $\gamma^*$ is smaller than 50 GeV except in $J/\psi$ and $\Upsilon$ mass regions. The quoted signal strength (see their Figs. 6 and 7) is given for $m_H = 125\text{ GeV}$ .				
<sup>3</sup> KHACHATRYAN 16B search for $H \rightarrow \gamma^*\gamma \rightarrow e^+e^-\gamma$ and $\mu^+\mu^-\gamma$ (with $m(e^+e^-) < 3.5\text{ GeV}$ and $m(\mu^+\mu^-) < 20\text{ GeV}$ ) in $19.7\text{ fb}^{-1}$ of $pp$ collisions at $E_{\text{cm}} = 8\text{ TeV}$ . See their Fig. 6 for limits on individual channels.				

NODE=S126A01  
NODE=S126A01

NODE=S126A01;LINKAGE=C

NODE=S126A01;LINKAGE=A

NODE=S126A01;LINKAGE=B

**HIGGS COUPLINGS****Fermion coupling ( $\kappa_F$ )**

VALUE	DOCUMENT ID	TECN	COMMENT
<b><math>0.94 \pm 0.05</math> OUR AVERAGE</b>			
0.86 $^{+0.14}_{-0.11}$	<sup>1</sup> TUMASYAN	23W CMS	$pp$ , 13 TeV, $H \rightarrow WW^*$
0.95 $\pm 0.05$	<sup>2</sup> ATLAS	22 ATLS	$pp$ , 13 TeV
• • • We do not use the following data for averages, fits, limits, etc. • • •			
1.00 $^{+0.16}_{-0.13}$	<sup>3</sup> AAD	23Y ATLS	$pp$ , 13 TeV, $H \rightarrow \gamma\gamma$
0.906	<sup>4</sup> CMS	22 CMS	$pp$ , 13 TeV
<sup>1</sup> TUMASYAN 23W measure Higgs production rates with $H \rightarrow WW^*$ at $E_{\text{cm}} = 13\text{ TeV}$ with $138\text{ fb}^{-1}$ data, assuming $m_H = 125.38\text{ GeV}$ . See their Fig. 25 for the 68% and 95% CL contours in the $\kappa_V - \kappa_F$ plane.			
<sup>2</sup> ATLAS 22 report combined results (see their Extended Data Table 1) using up to $139\text{ fb}^{-1}$ of data at $E_{\text{cm}} = 13\text{ TeV}$ , assuming $m_H = 125.09\text{ GeV}$ , $\kappa_V \geq 0$ , and $\kappa_F \geq 0$ ( $B_{\text{inv}} = B_{\text{undetected}} = 0$ ). See their Fig. 4.			
<sup>3</sup> AAD 23Y measure Higgs production rates with $H \rightarrow \gamma\gamma$ at $E_{\text{cm}} = 13\text{ TeV}$ with $139\text{ fb}^{-1}$ data, assuming $m_H = 125.09\text{ GeV}$ . See their Fig. 23 for the 68% and 95% CL contours in the $\kappa_V - \kappa_F$ plane, where $\kappa_F > 0$ is assumed.			
<sup>4</sup> CMS 22 report combined results (see their Extended Data Table 2) using up to $138\text{ fb}^{-1}$ of data at $E_{\text{cm}} = 13\text{ TeV}$ , assuming $m_H = 125.38\text{ GeV}$ . No uncertainty is given while their Fig. 3 left shows 68% and 95% CL contours.			

NODE=S126250

NODE=S126KFC  
NODE=S126KFC

NODE=S126KFC;LINKAGE=C

NODE=S126KFC;LINKAGE=A

NODE=S126KFC;LINKAGE=D

NODE=S126KFC;LINKAGE=B

**Gauge boson coupling ( $\kappa_V$ )**

VALUE	CL%	DOCUMENT ID	TECN	COMMENT
<b>1.023±0.026 OUR AVERAGE</b>				
0.99 ±0.05		<sup>1</sup> TUMASYAN	23W CMS	13 TeV, $H \rightarrow WW^*$
1.035±0.031		<sup>2</sup> ATLAS	22 ATLS	$pp$ , 13 TeV
• • • We do not use the following data for averages, fits, limits, etc. • • •				
−3.7 to 3.8	95	<sup>3</sup> HAYRAPETYAN...24AW	CMS	13 TeV, $VHH, HH \rightarrow b\bar{b}b\bar{b}$
1.02 $^{+0.06}_{-0.05}$		<sup>4</sup> AAD	23Y ATLS	13 TeV, $H \rightarrow \gamma\gamma$
1.014		<sup>5</sup> CMS	22 CMS	$pp$ , 13 TeV
<sup>1</sup> TUMASYAN 23W measure Higgs production rates with $H \rightarrow WW^*$ at $E_{cm} = 13$ TeV with 138 fb <sup>−1</sup> data, assuming $m_H = 125.38$ GeV. See their Fig. 25 for the 68% and 95% CL contours in the $\kappa_V - \kappa_F$ plane.				
<sup>2</sup> ATLAS 22 report combined results (see their Extended Data Table 1) using up to 139 fb <sup>−1</sup> of data at $E_{cm} = 13$ TeV, assuming $m_H = 125.09$ GeV, $\kappa_V \geq 0$ , and $\kappa_F \geq 0$ ( $B_{inv} = B_{undetected} = 0$ ). See their Fig. 4.				
<sup>3</sup> HAYRAPETYAN 24AW search for non-resonant $HH$ production in association with a vector boson using $HH \rightarrow b\bar{b}b\bar{b}$ with data of 138 fb <sup>−1</sup> at $E_{cm} = 13$ TeV. The vector boson decays both leptonically ( $W \rightarrow \ell\nu$ , $Z \rightarrow \ell\ell$ , $\nu\nu$ , $\ell = e, \mu$ ) and hadronically. See their Fig. 19. All other Higgs couplings are fixed to the SM values.				
<sup>4</sup> AAD 23Y measure Higgs production rates with $H \rightarrow \gamma\gamma$ at $E_{cm} = 13$ TeV with 139 fb <sup>−1</sup> data, assuming $m_H = 125.09$ GeV. See their Fig. 23 for the 68% and 95% CL contours in the $\kappa_V - \kappa_F$ plane, where $\kappa_F > 0$ is assumed.				
<sup>5</sup> CMS 22 report combined results (see their Extended Data Table 2) using up to 138 fb <sup>−1</sup> of data at $E_{cm} = 13$ TeV, assuming $m_H = 125.38$ GeV. See their Fig. 3 left.				

NODE=S126KVC  
 NODE=S126KVC

NODE=S126KVC;LINKAGE=C

NODE=S126KVC;LINKAGE=A

NODE=S126KVC;LINKAGE=E

NODE=S126KVC;LINKAGE=D

NODE=S126KVC;LINKAGE=B

**W boson coupling ( $\kappa_W$ )**

VALUE	DOCUMENT ID	TECN	COMMENT
• • • We do not use the following data for averages, fits, limits, etc. • • •			
	<sup>1</sup> HAYRAPETYAN...25B	CMS	$pp$ , 13 TeV, VBF $WH$ , coupling sign
	<sup>2</sup> AAD	24BMATLS	$pp$ , 13 TeV, VBF $WH$ , coupling sign
1.02±0.05	<sup>3,4</sup> ATLAS	22 ATLS	$pp$ , 13 TeV
1.05±0.06	<sup>3,5</sup> ATLAS	22 ATLS	$pp$ , 13 TeV
1.00 $^{+0.00}_{-0.02}$	<sup>3,6</sup> ATLAS	22 ATLS	$pp$ , 13 TeV
1.06±0.07	<sup>7,8</sup> CMS	22 CMS	$pp$ , 13 TeV
1.02±0.08	<sup>7,9</sup> CMS	22 CMS	$pp$ , 13 TeV
<sup>1</sup> HAYRAPETYAN 25B present the determination of the relative sign of $\kappa_W$ and $\kappa_Z$ with VBF $WH$ , $H \rightarrow b\bar{b}$ using 138 fb <sup>−1</sup> of data at $E_{cm} = 13$ TeV. The opposite-sign coupling hypothesis is excluded with a significance beyond 5 $\sigma$ .			
<sup>2</sup> AAD 24BM present the determination of the relative sign of $\kappa_W$ and $\kappa_Z$ with VBF $WH$ , $H \rightarrow b\bar{b}$ using 140 fb <sup>−1</sup> of data at $E_{cm} = 13$ TeV. The opposite-sign coupling hypothesis is excluded with a significance beyond 5 $\sigma$ .			
<sup>3</sup> ATLAS 22 report combined results (see their Extended Data Table 1) using up to 139 fb <sup>−1</sup> of data at $E_{cm} = 13$ TeV, assuming $m_H = 125.09$ GeV.			
<sup>4</sup> All modifiers( $\kappa$ ) > 0, and $\kappa_c = \kappa_t$ ( $B_{inv} = B_{undetected} = 0$ ) are assumed. Only SM particles assume to contribute to the loop-induced processes. See their Fig. 5, which shows both $\kappa_c = \kappa_t$ and $\kappa_c$ floating.			
<sup>5</sup> $B_{inv} = B_{undetected} = 0$ is assumed. Coupling strength modifiers including effective photon, $Z\gamma$ and gluon are measured. See their Fig. 6.			
<sup>6</sup> $B_{inv}$ floating, $B_{undetected} \geq 0$ , and $\kappa_V \leq 1$ are assumed. Coupling strength modifiers including effective photon, $Z\gamma$ and gluon are measured. See their Fig. 6.			
<sup>7</sup> CMS 22 report combined results (see their Extended Data Table 2) using up to 138 fb <sup>−1</sup> of data at $E_{cm} = 13$ TeV, assuming $m_H = 125.38$ GeV.			
<sup>8</sup> Only SM particles assume to contribute to the loop-induced processes. See their Fig. 3 right.			
<sup>9</sup> Coupling strength modifiers including effective photon, $Z\gamma$ and gluon are measured. See their Fig. 4 left.			

NODE=S126KWC  
 NODE=S126KWC

OCCUR=2

OCCUR=3

OCCUR=2

NODE=S126KWC;LINKAGE=I

NODE=S126KWC;LINKAGE=H

NODE=S126KWC;LINKAGE=A

NODE=S126KWC;LINKAGE=F

NODE=S126KWC;LINKAGE=B

NODE=S126KWC;LINKAGE=E

NODE=S126KWC;LINKAGE=C

NODE=S126KWC;LINKAGE=G

NODE=S126KWC;LINKAGE=D

**Z boson coupling ( $\kappa_Z$ )**

VALUE	DOCUMENT ID	TECN	COMMENT
• • • We do not use the following data for averages, fits, limits, etc. • • •			
	<sup>1</sup> HAYRAPETYAN...25B	CMS	$pp$ , 13 TeV, VBF $WH$ , coupling sign
	<sup>2</sup> AAD	24BMATLS	$pp$ , 13 TeV, VBF $WH$ , coupling sign
0.99 $^{+0.06}_{-0.05}$	<sup>3,4</sup> ATLAS	22 ATLS	$pp$ , 13 TeV
0.99±0.06	<sup>3,5</sup> ATLAS	22 ATLS	$pp$ , 13 TeV
0.98 $^{+0.02}_{-0.05}$	<sup>3,6</sup> ATLAS	22 ATLS	$pp$ , 13 TeV
1.04±0.07	<sup>7,8</sup> CMS	22 CMS	$pp$ , 13 TeV
1.04±0.07	<sup>7,9</sup> CMS	22 CMS	$pp$ , 13 TeV

NODE=S126KZC  
 NODE=S126KZC

OCCUR=2

OCCUR=3

OCCUR=2

- <sup>1</sup> HAYRAPETYAN 25B present the determination of the relative sign of  $\kappa_W$  and  $\kappa_Z$  with VBF  $WH, H \rightarrow b\bar{b}$  using  $138 \text{ fb}^{-1}$  of data at  $E_{\text{cm}} = 13 \text{ TeV}$ . The opposite-sign coupling hypothesis is excluded with a significance beyond  $5\sigma$ .
- <sup>2</sup> AAD 24BM present the determination of the relative sign of  $\kappa_W$  and  $\kappa_Z$  with VBF  $WH, H \rightarrow b\bar{b}$  using  $140 \text{ fb}^{-1}$  of data at  $E_{\text{cm}} = 13 \text{ TeV}$ . The opposite-sign coupling hypothesis is excluded with a significance beyond  $5\sigma$ .
- <sup>3</sup> ATLAS 22 report combined results (see their Extended Data Table 1) using up to  $139 \text{ fb}^{-1}$  of data at  $E_{\text{cm}} = 13 \text{ TeV}$ , assuming  $m_H = 125.09 \text{ GeV}$ .
- <sup>4</sup> All modifiers( $\kappa$ )  $> 0$ , and  $\kappa_C = \kappa_t$  ( $B_{\text{inv}} = B_{\text{undetected}} = 0$ ) are assumed. Only SM particles assume to contribute to the loop-induced processes. See their Fig. 5, which shows both  $\kappa_C = \kappa_t$  and  $\kappa_C$  floating.
- <sup>5</sup>  $B_{\text{inv}} = B_{\text{undetected}} = 0$  is assumed. Coupling strength modifiers including effective photon,  $Z\gamma$  and gluon are measured. See their Fig. 6.
- <sup>6</sup>  $B_{\text{inv}}$  floating,  $B_{\text{undetected}} \geq 0$ , and  $\kappa_V \leq 1$  are assumed. Coupling strength modifiers including effective photon,  $Z\gamma$  and gluon are measured. See their Fig. 6.
- <sup>7</sup> CMS 22 report combined results (see their Extended Data Table 2) using up to  $138 \text{ fb}^{-1}$  of data at  $E_{\text{cm}} = 13 \text{ TeV}$ , assuming  $m_H = 125.38 \text{ GeV}$ .
- <sup>8</sup> Only SM particles assume to contribute to the loop-induced processes. See their Fig. 3 right.
- <sup>9</sup> Coupling strength modifiers including effective photon,  $Z\gamma$  and gluon are measured. See their Fig. 4 left.

NODE=S126KZC;LINKAGE=I

NODE=S126KZC;LINKAGE=H

NODE=S126KZC;LINKAGE=A

NODE=S126KZC;LINKAGE=F

NODE=S126KZC;LINKAGE=B

NODE=S126KZC;LINKAGE=E

NODE=S126KZC;LINKAGE=C

NODE=S126KZC;LINKAGE=G

NODE=S126KZC;LINKAGE=D

### top Yukawa coupling ( $\kappa_t$ )

VALUE	CL%	DOCUMENT ID	TECN	COMMENT
-------	-----	-------------	------	---------

NODE=S126YTC  
NODE=S126YTC

• • • We do not use the following data for averages, fits, limits, etc. • • •

		<sup>1</sup> HAYRAPETY...25R	CMS	$t\bar{t}H, tH, H \rightarrow b\bar{b}$ , 13 TeV
$0.84^{+0.30}_{-0.46}$		<sup>2</sup> AAD	24J ATLS	$t\bar{t}H, tH, H \rightarrow b\bar{b}$ , 13 TeV
$<1.9$	95	<sup>3</sup> AAD	23BC ATLS	$pp$ , 13 TeV
$0.87-1.20$	95	<sup>4</sup> AAD	23Y ATLS	$pp$ , 13 TeV
$0.65-1.25$	95	<sup>5</sup> AAD	23Y ATLS	$pp$ , 13 TeV
$-1.09- -0.74$ or $0.77-1.3$	95	<sup>6</sup> TUMASYAN	23P CMS	$pp$ , 13 TeV
$0.86-1.26$		<sup>6,7</sup> TUMASYAN	23P CMS	$pp$ , 13 TeV
$0.95 \pm 0.07$		<sup>8,9</sup> ATLAS	22 ATLS	$pp$ , 13 TeV
$0.94 \pm 0.11$		<sup>8,10</sup> ATLAS	22 ATLS	$pp$ , 13 TeV
$0.94 \pm 0.11$		<sup>8,11</sup> ATLAS	22 ATLS	$pp$ , 13 TeV
$0.95^{+0.07}_{-0.08}$		<sup>12,13</sup> CMS	22 CMS	$pp$ , 13 TeV
$1.01^{+0.11}_{-0.10}$		<sup>12,14</sup> CMS	22 CMS	$pp$ , 13 TeV
$-0.9- -0.7$ or $0.7-1.1$	95	<sup>15</sup> SIRUNYAN	21R CMS	$pp$ , 13 TeV
$<1.7$	95	<sup>16</sup> SIRUNYAN	20C CMS	$pp$ , 13 TeV
$<1.67$	95	<sup>17</sup> SIRUNYAN	19BY CMS	$pp$ , 13 TeV
$<2.1$	95	<sup>18</sup> SIRUNYAN	18BU CMS	$pp$ , 13 TeV

OCCUR=2

OCCUR=2

OCCUR=2

OCCUR=3

OCCUR=2

- <sup>1</sup> HAYRAPETYAN 25R measure the  $t\bar{t}H$  and  $tH$  productions with  $H \rightarrow b\bar{b}$  decay channel using  $138 \text{ fb}^{-1}$  of data at  $E_{\text{cm}} = 13 \text{ TeV}$ . Two-dimensional likelihood scan of  $(\kappa_t, \kappa_V)$  is shown in their Fig. 15. Assuming  $\kappa_V = 1$ ,  $\kappa_t$  is measured to be  $[-0.55, -0.24]$  and  $[0.20, 0.72]$  at 68% CL.

NODE=S126YTC;LINKAGE=R

- <sup>2</sup> AAD 24J measure the  $CP$  structure of the top Yukawa coupling using  $139 \text{ fb}^{-1}$  of data at  $E_{\text{cm}} = 13 \text{ TeV}$ . The top Yukawa coupling strength modifier  $\kappa_t$  is measured with the  $CP$ -mixing angle  $\alpha$ . See their Fig. 3.

NODE=S126YTC;LINKAGE=S

- <sup>3</sup> AAD 23BC measure the production of four top quarks with same-sign and multilepton final states with  $140 \text{ fb}^{-1}$   $pp$  collision data at  $E_{\text{cm}} = 13 \text{ TeV}$ . The results constrain the ratio of the top quark Yukawa coupling  $y_t$  to its Standard Model value, yielding  $|y_t/y_t^{\text{SM}}| < 1.9$  (see their erratum) at 95% CL. See their Fig. 8 as a function of  $\kappa_t$  and  $CP$ -mixing angle.

NODE=S126YTC;LINKAGE=Q

- <sup>4</sup> AAD 23Y constrain  $\kappa_t$  from Higgs production rates with  $H \rightarrow \gamma\gamma$  with  $139 \text{ fb}^{-1}$   $pp$  collision data at  $E_{\text{cm}} = 13 \text{ TeV}$ . The quoted result is obtained assuming the SM loop structure in  $gg \rightarrow H$  and  $H \rightarrow \gamma\gamma$ . See their Fig. 14.

NODE=S126YTC;LINKAGE=O

- <sup>5</sup> AAD 23Y constrain  $\kappa_t$  from Higgs production rates with  $H \rightarrow \gamma\gamma$  with  $139 \text{ fb}^{-1}$   $pp$  collision data at  $E_{\text{cm}} = 13 \text{ TeV}$ . The quoted result is obtained assuming effective couplings  $\kappa_{\text{gluon}}$  and  $\kappa_\gamma$  for  $gg \rightarrow H$  and  $H \rightarrow \gamma\gamma$ , respectively. See their Fig. 14.

NODE=S126YTC;LINKAGE=P

- <sup>6</sup> TUMASYAN 23P constrain  $\kappa_t$  from  $t\bar{t}H$  and  $tH$  decaying  $H \rightarrow WW^*$  and  $H \rightarrow \tau\tau$  (multilepton decay mode) with  $138 \text{ fb}^{-1}$   $pp$  collision data at  $E_{\text{cm}} = 13 \text{ TeV}$ . The  $\kappa_t$  is obtained by fixing  $\tilde{\kappa}_t = 0$  and other couplings ( $\kappa_V$  etc.) to the SM values. See their Fig. 9 for 2-dim contours and Table 6.

NODE=S126YTC;LINKAGE=M

- <sup>7</sup> The quoted result is obtained by combining with other  $t\bar{t}H$  decaying  $H \rightarrow \gamma\gamma$  (SIRUNYAN 20AS) and  $H \rightarrow 4\ell$  (SIRUNYAN 21AE) and  $\tilde{\kappa}_t = 0$ . See their Fig. 12 for 2-dim contours and Table 7.

NODE=S126YTC;LINKAGE=N

- <sup>8</sup> ATLAS 22 report combined results (see their Extended Data Table 1) using up to  $139 \text{ fb}^{-1}$  of data at  $E_{\text{cm}} = 13 \text{ TeV}$ , assuming  $m_H = 125.09 \text{ GeV}$ .

NODE=S126YTC;LINKAGE=E

- <sup>9</sup> All modifiers( $\kappa$ ) > 0, and  $\kappa_C = \kappa_t$  ( $B_{inv} = B_{undetected} = 0$ ) are assumed. Only SM particles assume to contribute to the loop-induced processes. See their Fig. 5, which shows both  $\kappa_C = \kappa_t$  and  $\kappa_C$  floating.
- <sup>10</sup>  $B_{inv} = B_{undetected} = 0$  is assumed. Coupling strength modifiers including effective photon,  $Z\gamma$  and gluon are measured. See their Fig. 6.
- <sup>11</sup>  $B_{inv}$  floating,  $B_{undetected} \geq 0$ , and  $\kappa_V \leq 1$  are assumed. Coupling strength modifiers including effective photon,  $Z\gamma$  and gluon are measured. See their Fig. 6.
- <sup>12</sup> CMS 22 report combined results (see their Extended Data Table 2) using up to 138 fb<sup>-1</sup> of data at  $E_{cm} = 13$  TeV, assuming  $m_H = 125.38$  GeV.
- <sup>13</sup> Only SM particles assume to contribute to the loop-induced processes. See their Fig. 3 right.
- <sup>14</sup> Coupling strength modifiers including effective photon,  $Z\gamma$  and gluon are measured. See their Fig. 4 left.
- <sup>15</sup> SIRUNYAN 21R constrain the ratio of the top quark Yukawa coupling  $y_t$  to its Standard Model value from  $t\bar{t}H$  and  $tH$  production rates using 137 fb<sup>-1</sup>  $pp$  collision data at  $E_{cm} = 13$  TeV. Assuming a SM Higgs couplings to  $\tau$ 's, the joint interval  $-0.9 < \kappa_t (=y_t/y_t^{SM}) < -0.7$  and  $0.7 < \kappa_t < 1.1$  is obtained at 95% CL (see their Fig. 17).
- <sup>16</sup> SIRUNYAN 20C search for the production of four top quarks with same-sign and multi-lepton final states with 137 fb<sup>-1</sup>  $pp$  collision data at  $E_{cm} = 13$  TeV. The results constraint the ratio of the top quark Yukawa coupling  $y_t$  to its Standard Model value by comparing to the central value of a theoretical prediction (see their Refs. [1-2]), yielding  $|y_t/y_t^{SM}| < 1.7$  at 95% CL. See their Fig. 5.
- <sup>17</sup> SIRUNYAN 19BY measure the top quark Yukawa coupling from  $t\bar{t}$  kinematic distributions, the invariant mass of the top quark pair and the rapidity difference between  $t$  and  $\bar{t}$ , in the  $\ell$ +jets final state with 35.8 fb<sup>-1</sup>  $pp$  collision data at  $E_{cm} = 13$  TeV. The results constraint the ratio of the top quark Yukawa coupling to its the Standard Model to be  $1.07^{+0.34}_{-0.43}$  with an upper limit of 1.67 at 95% CL (see their Table III).
- <sup>18</sup> SIRUNYAN 18BU search for the production of four top quarks with same-sign and multi-lepton final states with 35.9 fb<sup>-1</sup>  $pp$  collision data at  $E_{cm} = 13$  TeV. The results constraint the ratio of the top quark Yukawa coupling  $y_t$  to its the Standard Model by comparing to the central value of a theoretical prediction (see their Ref. [16]), yielding  $|y_t/y_t^{SM}| < 2.1$  at 95% CL.

### bottom quark Yukawa coupling ( $\kappa_b$ )

VALUE	CL%	DOCUMENT ID	TECN	COMMENT
● ● ● We do not use the following data for averages, fits, limits, etc. ● ● ●				
$0.65 <  \kappa_b  < 1.37$	95	<sup>1</sup> AAD	25Y ATLS	$pp \rightarrow VH, H \rightarrow b\bar{b}, 13$ TeV
$-1.09$ to $-0.86$ OR $0.81$ to $1.09$	95	<sup>2</sup> AAD	23C ATLS	$pp, 13$ TeV, $\gamma\gamma, ZZ^* \rightarrow 4\ell$ cross sections
		<sup>3</sup> AAD	23CD ATLS	$pp, 13$ TeV, $H \rightarrow \Upsilon(nS)\gamma$
$-1.1$ to $1.1$	95	<sup>4</sup> HAYRAPETYAN...23	CMS	$pp, 13$ TeV, $ZZ^* \rightarrow 4\ell$ cross sections
$0.90 \pm 0.11$		<sup>5,6</sup> ATLAS	22 ATLS	$pp, 13$ TeV
$0.89 \pm 0.11$		<sup>5,7</sup> ATLAS	22 ATLS	$pp, 13$ TeV
$0.82^{+0.09}_{-0.08}$		<sup>5,8</sup> ATLAS	22 ATLS	$pp, 13$ TeV
$1.02^{+0.15}_{-0.17}$		<sup>9,10</sup> CMS	22 CMS	$pp, 13$ TeV
$0.99^{+0.17}_{-0.16}$		<sup>9,11</sup> CMS	22 CMS	$pp, 13$ TeV
<sup>1</sup> AAD 25Y present measurements of $VH, H \rightarrow b\bar{b}$ and $H \rightarrow c\bar{c}$ ( $V = W, Z$ ) using 140 fb <sup>-1</sup> of $pp$ collision data at $E_{cm} = 13$ TeV. The quoted value is obtained assuming $\kappa_C = 1$ , all other couplings to their SM predictions, and only SM decays.				
<sup>2</sup> AAD 23C combine results of $H \rightarrow \gamma\gamma$ and $H \rightarrow ZZ^* \rightarrow 4\ell$ ( $\ell = e, \mu$ ) using 139 fb <sup>-1</sup> at $E_{cm} = 13$ TeV. The Higgs boson transverse momentum ( $p_T^H$ ) distribution constrains $\kappa_b$ and $\kappa_C$ , assuming other couplings fixed to the SM values. The $\kappa_b$ is obtained using the $p_T^H$ shape and normalisation. Other cases are given in their Tables 6 and 7.				
<sup>3</sup> AAD 23CD search for $H \rightarrow \Upsilon(nS)\gamma, \Upsilon(nS) \rightarrow \mu^+\mu^-$ ( $n=1,2,3$ ) with 138 fb <sup>-1</sup> of $pp$ collision data at $E_{cm} = 13$ TeV. They interpret the $H \rightarrow \Upsilon(nS)\gamma$ search to constraint the bottom Yukawa coupling by comparing to $H \rightarrow \gamma\gamma$ . An observed 95% CL interval of $(-37, 40)$ is obtained for $\kappa_b/\kappa_\gamma$ .				
<sup>4</sup> HAYRAPETYAN 23 measure the cross sections for $pp \rightarrow H \rightarrow ZZ^* \rightarrow 4\ell$ ( $\ell = e, \mu$ ) using 138 fb <sup>-1</sup> at $E_{cm} = 13$ TeV. The $\kappa_b$ is obtained from the $p_T$ differential cross section of the ggF production employing the dependence of the branching fraction on $\kappa_b$ and $\kappa_C$ .				
<sup>5</sup> ATLAS 22 report combined results (see their Extended Data Table 1) using up to 139fb <sup>-1</sup> of data at $E_{cm} = 13$ TeV, assuming $m_H = 125.09$ GeV.				
<sup>6</sup> All modifiers ( $\kappa$ ) > 0, and $\kappa_C = \kappa_t$ ( $B_{inv} = B_{undetected} = 0$ ) are assumed. Only SM particles assume to contribute to the loop-induced processes. See their Fig. 5, which shows both $\kappa_C = \kappa_t$ and $\kappa_C$ floating.				

NODE=S126YTC;LINKAGE=J

NODE=S126YTC;LINKAGE=F

NODE=S126YTC;LINKAGE=I

NODE=S126YTC;LINKAGE=G

NODE=S126YTC;LINKAGE=K

NODE=S126YTC;LINKAGE=H

NODE=S126YTC;LINKAGE=D

NODE=S126YTC;LINKAGE=A

NODE=S126YTC;LINKAGE=B

NODE=S126YTC;LINKAGE=C

NODE=S126KBC

NODE=S126KBC

OCCUR=2

OCCUR=3

OCCUR=2

NODE=S126KBC;LINKAGE=K

NODE=S126KBC;LINKAGE=I

NODE=S126KBC;LINKAGE=J

NODE=S126KBC;LINKAGE=H

NODE=S126KBC;LINKAGE=A

NODE=S126KBC;LINKAGE=G

- <sup>7</sup>  $B_{inv} = B_{undetected} = 0$  is assumed. Coupling strength modifiers including effective photon,  $Z\gamma$  and gluon are measured. See their Fig. 6.
- <sup>8</sup>  $B_{inv}$  floating,  $B_{undetected} \geq 0$ , and  $\kappa_V \leq 1$  are assumed. Coupling strength modifiers including effective photon,  $Z\gamma$  and gluon are measured. See their Fig. 6.
- <sup>9</sup> CMS 22 report combined results (see their Extended Data Table 2) using up to  $138 \text{ fb}^{-1}$  of data at  $E_{\text{cm}} = 13 \text{ TeV}$ , assuming  $m_H = 125.38 \text{ GeV}$ .
- <sup>10</sup> Only SM particles assume to contribute to the loop-induced processes. See their Fig. 3 right.
- <sup>11</sup> Coupling strength modifiers including effective photon,  $Z\gamma$  and gluon are measured. See their Fig. 4 left.

NODE=S126KBC;LINKAGE=B

NODE=S126KBC;LINKAGE=E

NODE=S126KBC;LINKAGE=C

NODE=S126KBC;LINKAGE=F

NODE=S126KBC;LINKAGE=D

### charm quark Yukawa coupling ( $\kappa_c$ )

VALUE	CL%	DOCUMENT ID	TECN	COMMENT
• • • We do not use the following data for averages, fits, limits, etc. • • •				
$ \kappa_c  < 4.2$	95	<sup>1</sup> AAD 25Y ATLS		$pp \rightarrow VH, 13 \text{ TeV}$
$-166 \text{ to } 208$	95	<sup>2</sup> HAYRAPETY...25H CMS		$pp, 13 \text{ TeV}, H \rightarrow J/\psi\gamma$
$ \kappa_c  < 190$	95	<sup>3</sup> HAYRAPETY...24D CMS		$pp, 13 \text{ TeV}, H\gamma, H \rightarrow WW^* \rightarrow e\nu\mu\nu$
$ \kappa_c  < 2.27$	95	<sup>4</sup> AAD 23C ATLS		$pp, 13 \text{ TeV}, \gamma\gamma, ZZ^* \rightarrow 4\ell \text{ cross sections}$
		<sup>5</sup> AAD 23CD ATLS		$pp, 13 \text{ TeV}, H \rightarrow J/\psi\gamma$
$-5.3 \text{ to } 5.2$	95	<sup>6</sup> HAYRAPETY...23 CMS		$pp, 13 \text{ TeV}, ZZ^* \rightarrow 4\ell \text{ cross sections}$
$1.1 <  \kappa_c  < 5.5$	95	<sup>7</sup> TUMASYAN 23AH CMS		$pp \rightarrow WH/ZH, 13 \text{ TeV}$
$0.03^{+3.02}_{-0.03}$		<sup>8</sup> ATLAS 22 ATLS		$pp, 13 \text{ TeV}$

NODE=S126KCC  
NODE=S126KCC

- <sup>1</sup> AAD 25Y present measurements of  $VH, H \rightarrow b\bar{b}$  and  $H \rightarrow c\bar{c}$  ( $V = W, Z$ ) using  $140 \text{ fb}^{-1}$  of  $pp$  collision data at  $E_{\text{cm}} = 13 \text{ TeV}$ . The quoted value is obtained assuming  $\kappa_b = 1$ , all other couplings to their SM predictions, and only SM decays. The ratio of  $\kappa_b$  and  $\kappa_c$  is measured to be  $|\kappa_c/\kappa_b| < 3.6$  at 95% CL.
- <sup>2</sup> HAYRAPETYAN 25H search for  $H \rightarrow J/\psi\gamma, J/\psi \rightarrow \mu^+\mu^-$  with  $123 \text{ fb}^{-1}$  of  $pp$  collision data at  $E_{\text{cm}} = 13 \text{ TeV}$ . They interpret the  $H \rightarrow J/\psi\gamma$  search to constrain the charm Yukawa coupling by comparing to  $H \rightarrow \gamma\gamma$ . An observed 95% CL interval of  $(-157, 199)$  is obtained for  $\kappa_c/\kappa_\gamma$ . The quoted value is obtained assuming  $\kappa_\gamma = 1$ .
- <sup>3</sup> HAYRAPETYAN 24D search for the  $H\gamma$  production using  $H \rightarrow WW^* \rightarrow e\nu\mu\nu$  with  $138 \text{ fb}^{-1}$  of  $pp$  collision data at  $E_{\text{cm}} = 13 \text{ TeV}$ . They interpret the  $H\gamma$  search to constrain the charm Yukawa coupling assuming that the charm quark and the Higgs interaction vertex shown in their Fig. 1 is the only parameter. See their Table II.
- <sup>4</sup> AAD 23C combine results of  $H \rightarrow \gamma\gamma$  and  $H \rightarrow ZZ^* \rightarrow 4\ell$  ( $\ell = e, \mu$ ) using  $139 \text{ fb}^{-1}$  at  $E_{\text{cm}} = 13 \text{ TeV}$ . The Higgs boson transverse momentum ( $p_T^H$ ) distribution constrains  $\kappa_b$  and  $\kappa_c$ , assuming other couplings fixed to the SM values. The  $\kappa_c$  is obtained using the  $p_T^H$  shape and normalisation. Other cases are given in their Tables 6 and 7. See their Table 8 for results combined with  $VH, H \rightarrow b\bar{b}$  and  $c\bar{c}$ .
- <sup>5</sup> AAD 23CD search for  $H \rightarrow J/\psi\gamma, J/\psi \rightarrow \mu^+\mu^-$  with  $138 \text{ fb}^{-1}$  of  $pp$  collision data at  $E_{\text{cm}} = 13 \text{ TeV}$ . They interpret the  $H \rightarrow J/\psi\gamma$  search to constrain the charm Yukawa coupling by comparing to  $H \rightarrow \gamma\gamma$ . An observed 95% CL interval of  $(-133, 175)$  is obtained for  $\kappa_c/\kappa_\gamma$ .
- <sup>6</sup> HAYRAPETYAN 23 measure the cross sections for  $pp \rightarrow H \rightarrow ZZ^* \rightarrow 4\ell$  ( $\ell = e, \mu$ ) using  $138 \text{ fb}^{-1}$  at  $E_{\text{cm}} = 13 \text{ TeV}$ . The  $\kappa_c$  is obtained from the  $p_T$  differential cross section of the ggF production employing the dependence of the branching fraction of  $\kappa_b$  and  $\kappa_c$ .
- <sup>7</sup> TUMASYAN 23AH search for  $VH, H \rightarrow c\bar{c}$  ( $V = W, Z$ ) using  $138 \text{ fb}^{-1}$  of  $pp$  collision data at  $E_{\text{cm}} = 13 \text{ TeV}$ . The quoted values are obtained from the measured signal strength in the  $\kappa$ -framework, where only the Higgs decay width for  $H \rightarrow c\bar{c}$  is changed while assuming all the other decay widths and the production cross section to be SM ones. The quoted values are given for  $m_H = 125.38 \text{ GeV}$ .
- <sup>8</sup> ATLAS 22 report combined results (see their Extended Data Table 1) using up to  $139 \text{ fb}^{-1}$  of data at  $E_{\text{cm}} = 13 \text{ TeV}$ , assuming  $m_H = 125.09 \text{ GeV}$ , and all modifiers ( $\kappa$ )  $> 0$  ( $B_{inv} = B_{undetected} = 0$ ). Only SM particles assume to contribute to the loop-induced processes. See their Fig. 5, which shows both  $\kappa_c = \kappa_t$  and  $\kappa_c$  floating.

NODE=S126KCC;LINKAGE=H

NODE=S126KCC;LINKAGE=G

NODE=S126KCC;LINKAGE=F

NODE=S126KCC;LINKAGE=D

NODE=S126KCC;LINKAGE=E

NODE=S126KCC;LINKAGE=C

NODE=S126KCC;LINKAGE=B

NODE=S126KCC;LINKAGE=A

### strange quark Yukawa coupling ( $\kappa_s$ )

VALUE	CL%	DOCUMENT ID	TECN	COMMENT
• • • We do not use the following data for averages, fits, limits, etc. • • •				
$ \kappa_s  < 1700$	95	<sup>1</sup> HAYRAPETY...24D CMS		$pp, 13 \text{ TeV}, H\gamma, H \rightarrow WW^* \rightarrow e\nu\mu\nu$

NODE=S126KSC  
NODE=S126KSC

- <sup>1</sup> HAYRAPETYAN 24D search for the  $H\gamma$  production using  $H \rightarrow WW^* \rightarrow e\nu\mu\nu$  with  $138 \text{ fb}^{-1}$  of  $pp$  collision data at  $E_{\text{cm}} = 13 \text{ TeV}$ . They interpret the  $H\gamma$  search to constrain the strange quark Yukawa coupling assuming that the strange quark and the Higgs interaction vertex shown in their Fig. 1 is the only parameter. See their Table II.

NODE=S126KSC;LINKAGE=A

**down quark Yukawa coupling ( $\kappa_d$ )**

VALUE	CL%	DOCUMENT ID	TECN	COMMENT
● ● ● We do not use the following data for averages, fits, limits, etc. ● ● ●				
$ \kappa_d  < 17000$	95	<sup>1</sup> HAYRAPETY...24D	CMS	$pp, 13 \text{ TeV}, H\gamma, H \rightarrow WW^* \rightarrow e\nu\mu\nu$

<sup>1</sup> HAYRAPETYAN 24D search for the  $H\gamma$  production using  $H \rightarrow WW^* \rightarrow e\nu\mu\nu$  with  $138 \text{ fb}^{-1}$  of  $pp$  collision data at  $E_{\text{cm}} = 13 \text{ TeV}$ . They interpret the  $H\gamma$  search to constraint the down quark Yukawa coupling assuming that the down quark and the Higgs interaction vertex shown in their Fig. 1 is the only parameter. See their Table II.

NODE=S126KDC  
NODE=S126KDC

NODE=S126KDC;LINKAGE=A

**up quark Yukawa coupling ( $\kappa_u$ )**

VALUE	CL%	DOCUMENT ID	TECN	COMMENT
● ● ● We do not use the following data for averages, fits, limits, etc. ● ● ●				
$ \kappa_u  < 16000$	95	<sup>1</sup> HAYRAPETY...24D	CMS	$pp, 13 \text{ TeV}, H\gamma, H \rightarrow WW^* \rightarrow e\nu\mu\nu$

<sup>1</sup> HAYRAPETYAN 24D search for the  $H\gamma$  production using  $H \rightarrow WW^* \rightarrow e\nu\mu\nu$  with  $138 \text{ fb}^{-1}$  of  $pp$  collision data at  $E_{\text{cm}} = 13 \text{ TeV}$ . They interpret the  $H\gamma$  search to constraint the up quark Yukawa coupling assuming that the up quark and the Higgs interaction vertex shown in their Fig. 1 is the only parameter. See their Table II.

NODE=S126KUC  
NODE=S126KUC

NODE=S126KUC;LINKAGE=A

**tau Yukawa coupling ( $\kappa_\tau$ )**

VALUE	DOCUMENT ID	TECN	COMMENT
● ● ● We do not use the following data for averages, fits, limits, etc. ● ● ●			
$0.94 \pm 0.07$	<sup>1,2</sup> ATLAS	22	ATLS $pp, 13 \text{ TeV}$
$0.93 \pm 0.07$	<sup>1,3</sup> ATLAS	22	ATLS $pp, 13 \text{ TeV}$
$0.91^{+0.07}_{-0.06}$	<sup>1,4</sup> ATLAS	22	ATLS $pp, 13 \text{ TeV}$
$0.93 \pm 0.08$	<sup>5,6</sup> CMS	22	CMS $pp, 13 \text{ TeV}$
$0.92 \pm 0.08$	<sup>5,7</sup> CMS	22	CMS $pp, 13 \text{ TeV}$

<sup>1</sup> ATLAS 22 report combined results (see their Extended Data Table 1) using up to  $139 \text{ fb}^{-1}$  of data at  $E_{\text{cm}} = 13 \text{ TeV}$ , assuming  $m_H = 125.09 \text{ GeV}$ .

<sup>2</sup> All modifiers( $\kappa$ )  $> 0$ , and  $\kappa_c = \kappa_t$  ( $B_{\text{inv}} = B_{\text{undetected}} = 0$ ) are assumed. Only SM particles assume to contribute to the loop-induced processes. See their Fig. 5, which shows both  $\kappa_c = \kappa_t$  and  $\kappa_c$  floating.

<sup>3</sup>  $B_{\text{inv}} = B_{\text{undetected}} = 0$  is assumed. Coupling strength modifiers including effective photon,  $Z\gamma$  and gluon are measured. See their Fig. 6.

<sup>4</sup>  $B_{\text{inv}}$  floating,  $B_{\text{undetected}} \geq 0$ , and  $\kappa_V \leq 1$  are assumed. Coupling strength modifiers including effective photon,  $Z\gamma$  and gluon are measured. See their Fig. 6.

<sup>5</sup> CMS 22 report combined results (see their Extended Data Table 2) using up to  $138 \text{ fb}^{-1}$  of data at  $E_{\text{cm}} = 13 \text{ TeV}$ , assuming  $m_H = 125.38 \text{ GeV}$ .

<sup>6</sup> Only SM particles assume to contribute to the loop-induced processes. See their Fig. 3 right.

<sup>7</sup> Coupling strength modifiers including effective photon,  $Z\gamma$  and gluon are measured. See their Fig. 4 left.

NODE=S126KTA  
NODE=S126KTA

OCCUR=2

OCCUR=3

OCCUR=2

NODE=S126KTA;LINKAGE=A

NODE=S126KTA;LINKAGE=F

NODE=S126KTA;LINKAGE=B

NODE=S126KTA;LINKAGE=E

NODE=S126KTA;LINKAGE=C

NODE=S126KTA;LINKAGE=G

NODE=S126KTA;LINKAGE=D

**muon Yukawa coupling ( $\kappa_\mu$ )**

VALUE	DOCUMENT ID	TECN	COMMENT
● ● ● We do not use the following data for averages, fits, limits, etc. ● ● ●			
$1.07^{+0.25}_{-0.31}$	<sup>1,2</sup> ATLAS	22	ATLS $pp, 13 \text{ TeV}$
$1.06^{+0.25}_{-0.30}$	<sup>1,3</sup> ATLAS	22	ATLS $pp, 13 \text{ TeV}$
$1.04^{+0.23}_{-0.30}$	<sup>1,4</sup> ATLAS	22	ATLS $pp, 13 \text{ TeV}$
$1.12 \pm 0.20$	<sup>5,6</sup> CMS	22	CMS $pp, 13 \text{ TeV}$
$1.12^{+0.21}_{-0.22}$	<sup>5,7</sup> CMS	22	CMS $pp, 13 \text{ TeV}$

<sup>1</sup> ATLAS 22 report combined results (see their Extended Data Table 1) using up to  $139 \text{ fb}^{-1}$  of data at  $E_{\text{cm}} = 13 \text{ TeV}$ , assuming  $m_H = 125.09 \text{ GeV}$ .

<sup>2</sup> All modifiers( $\kappa$ )  $> 0$ , and  $\kappa_c = \kappa_t$  ( $B_{\text{inv}} = B_{\text{undetected}} = 0$ ) are assumed. Only SM particles assume to contribute to the loop-induced processes. See their Fig. 5, which shows both  $\kappa_c = \kappa_t$  and  $\kappa_c$  floating.

<sup>3</sup>  $B_{\text{inv}} = B_{\text{undetected}} = 0$  is assumed. Coupling strength modifiers including effective photon,  $Z\gamma$  and gluon are measured. See their Fig. 6.

<sup>4</sup>  $B_{\text{inv}}$  floating,  $B_{\text{undetected}} \geq 0$ , and  $\kappa_V \leq 1$  are assumed. Coupling strength modifiers including effective photon,  $Z\gamma$  and gluon are measured. See their Fig. 6.

<sup>5</sup> CMS 22 report combined results (see their Extended Data Table 2) using up to  $138 \text{ fb}^{-1}$  of data at  $E_{\text{cm}} = 13 \text{ TeV}$ , assuming  $m_H = 125.38 \text{ GeV}$ .

<sup>6</sup> Only SM particles assume to contribute to the loop-induced processes. See their Fig. 3 right.

<sup>7</sup> Coupling strength modifiers including effective photon,  $Z\gamma$  and gluon are measured. See their Fig. 4 left.

NODE=S126KMU  
NODE=S126KMU

OCCUR=2

OCCUR=3

OCCUR=2

NODE=S126KMU;LINKAGE=A

NODE=S126KMU;LINKAGE=F

NODE=S126KMU;LINKAGE=B

NODE=S126KMU;LINKAGE=E

NODE=S126KMU;LINKAGE=C

NODE=S126KMU;LINKAGE=G

NODE=S126KMU;LINKAGE=D

**photon effective coupling ( $\kappa_\gamma$ )**

VALUE	DOCUMENT ID	TECN	COMMENT
-------	-------------	------	---------

• • • We do not use the following data for averages, fits, limits, etc. • • •

$1.02^{+0.08}_{-0.07}$	<sup>1</sup> AAD	23Y	ATLS	$pp$ , 13 TeV
$1.01 \pm 0.06$	<sup>2,3</sup> ATLAS	22	ATLS	$pp$ , 13 TeV
$0.98 \pm 0.05$	<sup>2,4</sup> ATLAS	22	ATLS	$pp$ , 13 TeV
$1.10 \pm 0.08$	<sup>5</sup> CMS	22	CMS	$pp$ , 13 TeV

NODE=S126KGC  
NODE=S126KGC

OCCUR=2

<sup>1</sup> AAD 23Y constrain  $\kappa_\gamma$  from Higgs production rates with  $H \rightarrow \gamma\gamma$  with 139 fb<sup>-1</sup>  $pp$  collision data at  $E_{\text{cm}} = 13$  TeV. The quoted result is obtained assuming effective couplings  $\kappa_{\text{gluon}}$  and  $\kappa_\gamma$  for  $gg \rightarrow H$  and  $H \rightarrow \gamma\gamma$ , respectively and other couplings fixed to the SM values. See their Fig. 15.

NODE=S126KGC;LINKAGE=E

<sup>2</sup> ATLAS 22 report combined results (see their Extended Data Table 1) using up to 139 fb<sup>-1</sup> of data at  $E_{\text{cm}} = 13$  TeV, assuming  $m_H = 125.09$  GeV. Coupling strength modifiers including effective photon,  $Z\gamma$  and gluon are measured. See their Fig. 6.

NODE=S126KGC;LINKAGE=A

<sup>3</sup>  $B_{\text{inv}} = B_{\text{undetected}} = 0$  is assumed.

NODE=S126KGC;LINKAGE=D

<sup>4</sup>  $B_{\text{inv}}$  floating,  $B_{\text{undetected}} \geq 0$ , and  $\kappa_V \leq 1$  are assumed.

NODE=S126KGC;LINKAGE=C

<sup>5</sup> CMS 22 report combined results (see their Extended Data Table 2) using up to 138 fb<sup>-1</sup> of data at  $E_{\text{cm}} = 13$  TeV, assuming  $m_H = 125.38$  GeV. Coupling strength modifiers including effective photon,  $Z\gamma$  and gluon are measured. See their Fig. 4 left.

NODE=S126KGC;LINKAGE=B

**gluon effective coupling ( $\kappa_{\text{gluon}}$ )**

VALUE	DOCUMENT ID	TECN	COMMENT
-------	-------------	------	---------

• • • We do not use the following data for averages, fits, limits, etc. • • •

$1.01^{+0.11}_{-0.09}$	<sup>1</sup> AAD	23Y	ATLS	$pp$ , 13 TeV
$0.95 \pm 0.07$	<sup>2,3</sup> ATLAS	22	ATLS	$pp$ , 13 TeV
$0.94^{+0.07}_{-0.06}$	<sup>2,4</sup> ATLAS	22	ATLS	$pp$ , 13 TeV
$0.92 \pm 0.08$	<sup>5</sup> CMS	22	CMS	$pp$ , 13 TeV

NODE=S126KGL  
NODE=S126KGL

OCCUR=2

<sup>1</sup> AAD 23Y constrain  $\kappa_{\text{gluon}}$  from Higgs production rates with  $H \rightarrow \gamma\gamma$  with 139 fb<sup>-1</sup>  $pp$  collision data at  $E_{\text{cm}} = 13$  TeV. The quoted result is obtained assuming effective couplings  $\kappa_{\text{gluon}}$  and  $\kappa_\gamma$  for  $gg \rightarrow H$  and  $H \rightarrow \gamma\gamma$ , respectively and other couplings fixed to the SM values. See their Fig. 15.

NODE=S126KGL;LINKAGE=D

<sup>2</sup> ATLAS 22 report combined results (see their Extended Data Table 1) using up to 139fb<sup>-1</sup> of data at  $E_{\text{cm}} = 13$  TeV, assuming  $m_H = 125.09$  GeV. Coupling strength modifiers including effective photon,  $Z\gamma$  and gluon are measured. See their Fig. 6.

NODE=S126KGL;LINKAGE=A

<sup>3</sup>  $B_{\text{inv}} = B_{\text{undetected}} = 0$  is assumed.

NODE=S126KGL;LINKAGE=E

<sup>4</sup>  $B_{\text{inv}}$  floating,  $B_{\text{undetected}} \geq 0$ , and  $\kappa_V \leq 1$  are assumed.

NODE=S126KGL;LINKAGE=C

<sup>5</sup> CMS 22 report combined results (see their Extended Data Table 2) using up to 138 fb<sup>-1</sup> of data at  $E_{\text{cm}} = 13$  TeV, assuming  $m_H = 125.38$  GeV. Coupling strength modifiers including effective photon,  $Z\gamma$  and gluon are measured. See their Fig. 4 left.

NODE=S126KGL;LINKAGE=B

 **$Z\gamma$  effective coupling ( $\kappa_{Z\gamma}$ )**

VALUE	DOCUMENT ID	TECN	COMMENT
-------	-------------	------	---------

• • • We do not use the following data for averages, fits, limits, etc. • • •

$1.38^{+0.31}_{-0.37}$	<sup>1,2</sup> ATLAS	22	ATLS	$pp$ , 13 TeV
$1.35^{+0.29}_{-0.36}$	<sup>1,3</sup> ATLAS	22	ATLS	$pp$ , 13 TeV
$1.65^{+0.34}_{-0.37}$	<sup>4</sup> CMS	22	CMS	$pp$ , 13 TeV

NODE=S126KZG  
NODE=S126KZG

OCCUR=2

<sup>1</sup> ATLAS 22 report combined results (see their Extended Data Table 1) using up to 139 fb<sup>-1</sup> of data at  $E_{\text{cm}} = 13$  TeV, assuming  $m_H = 125.09$  GeV. Coupling strength modifiers including effective photon,  $Z\gamma$  and gluon are measured. See their Fig. 6.

NODE=S126KZG;LINKAGE=A

<sup>2</sup>  $B_{\text{inv}} = B_{\text{undetected}} = 0$  is assumed.

NODE=S126KZG;LINKAGE=D

<sup>3</sup>  $B_{\text{inv}}$  floating,  $B_{\text{undetected}} \geq 0$ , and  $\kappa_V \leq 1$  are assumed.

NODE=S126KZG;LINKAGE=C

<sup>4</sup> CMS 22 report combined results (see their Extended Data Table 2) using up to 138 fb<sup>-1</sup> of data at  $E_{\text{cm}} = 13$  TeV, assuming  $m_H = 125.38$  GeV. Coupling strength modifiers including effective photon,  $Z\gamma$  and gluon are measured. See their Fig. 4 left.

NODE=S126KZG;LINKAGE=B

**OTHER  $H$  PRODUCTION PROPERTIES**

NODE=S126240

**$t\bar{t}H$  production**

Signal strength relative to the Standard Model cross section.

VALUE	DOCUMENT ID	TECN	COMMENT
-------	-------------	------	---------

**$0.91^{+0.20}_{-0.18}$  OUR AVERAGE** Error includes scale factor of 1.6. See the ideogram below.

[1.10  $\pm$  0.18 OUR 2025 AVERAGE]

$0.81^{+0.22}_{-0.19}$	<sup>1</sup> AAD	25AJ ATLS	$pp$ , 13 TeV, $H \rightarrow b\bar{b}$
$0.33 \pm 0.26$	<sup>2</sup> HAYRAPETYAN...25R	CMS	$pp$ , 13 TeV, $H \rightarrow b\bar{b}$
$0.92 \pm 0.19^{+0.17}_{-0.13}$	<sup>3</sup> SIRUNYAN	21R CMS	$pp$ , 13 TeV, $H \rightarrow \tau\tau$ , $WW^*$ , $ZZ^*$
$1.43^{+0.33+0.21}_{-0.31-0.15}$	<sup>4</sup> AAD	20Z ATLS	$pp$ , 13 TeV, $H \rightarrow \gamma\gamma$
$1.6^{+0.5}_{-0.4}$	<sup>5</sup> AABOUD	18AC ATLS	$pp$ , 13 TeV, $H \rightarrow \tau\tau$ , $WW^*$ , $ZZ^*$
$1.9^{+0.8}_{-0.7}$	<sup>6</sup> AAD	16AN ATLS	$pp$ , 7, 8 TeV

NEW

OCCUR=2

● ● ● We do not use the following data for averages, fits, limits, etc. ● ● ●

$-0.27^{+0.86}_{-0.83}$	<sup>7</sup> TUMASYAN	23AI ATLS	$pp$ , 13 TeV, boosted $H \rightarrow b\bar{b}$
$0.35^{+0.36}_{-0.34}$	<sup>8</sup> AAD	22M ATLS	$pp$ , 13 TeV, $H \rightarrow b\bar{b}$
$1.38^{+0.36}_{-0.29}$	<sup>9</sup> SIRUNYAN	20AS CMS	$pp$ , 13 TeV, $H \rightarrow \gamma\gamma$
$0.72 \pm 0.24 \pm 0.38$	<sup>10</sup> SIRUNYAN	19R CMS	$pp$ , 13 TeV, $H \rightarrow b\bar{b}$
$1.2 \pm 0.3$	<sup>11</sup> AABOUD	18AC ATLS	$pp$ , 13 TeV, $H \rightarrow b\bar{b} \tau\tau$ , $\gamma\gamma$ , $WW^*$ , $ZZ^*$
	<sup>12</sup> AABOUD	18BK ATLS	$pp$ , 13 TeV, $H \rightarrow b\bar{b} \tau\tau$ , $\gamma\gamma$ , $WW^*$ , $ZZ^*$
$0.84^{+0.64}_{-0.61}$	<sup>13</sup> AABOUD	18T ATLS	$pp$ , 13 TeV, $H \rightarrow b\bar{b}$
$0.9 \pm 1.5$	<sup>14</sup> SIRUNYAN	18BD CMS	$pp$ , 13 TeV, $H \rightarrow b\bar{b}$
$1.23^{+0.45}_{-0.43}$	<sup>15</sup> SIRUNYAN	18BQ CMS	$pp$ , 13 TeV, $H \rightarrow \tau\tau$ , $WW^*$ , $ZZ^*$
$1.26^{+0.31}_{-0.26}$	<sup>16</sup> SIRUNYAN	18L CMS	$pp$ , 7, 8, 13 TeV, $H \rightarrow b\bar{b}, \tau\tau, \gamma\gamma, WW^*, ZZ^*$
$1.7 \pm 0.8$	<sup>17</sup> AAD	16AL ATLS	$pp$ , 7, 8 TeV, $H \rightarrow b\bar{b}, \tau\tau, \gamma\gamma, WW^*$ , and $ZZ^*$
$2.3^{+0.7}_{-0.6}$	<sup>6,18</sup> AAD	16AN LHC	$pp$ , 7, 8 TeV
$2.9^{+1.0}_{-0.9}$	<sup>6</sup> AAD	16AN CMS	$pp$ , 7, 8 TeV
$1.81^{+0.52+0.58+0.31}_{-0.50-0.55-0.12}$	<sup>19</sup> AAD	16K ATLS	$pp$ , 7, 8 TeV
$1.4^{+2.1+0.6}_{-1.4-0.3}$	<sup>20</sup> AAD	15 ATLS	$pp$ , 7, 8 TeV
$1.5 \pm 1.1$	<sup>21</sup> AAD	15BC ATLS	$pp$ , 8 TeV
$2.1^{+1.4}_{-1.2}$	<sup>22</sup> AAD	15T ATLS	$pp$ , 8 TeV
$1.2^{+1.6}_{-1.5}$	<sup>23</sup> KHACHATRYAN...15AN	CMS	$pp$ , 8 TeV
$2.8^{+1.0}_{-0.9}$	<sup>24</sup> KHACHATRYAN...14H	CMS	$pp$ , 7, 8 TeV
$9.49^{+6.60}_{-6.28}$	<sup>25</sup> AALTONEN	13L CDF	$p\bar{p}$ , 1.96 TeV
$< 5.8$ at 95% CL	<sup>26</sup> CHATRCHYAN13X	CMS	$pp$ , 7, 8 TeV, $H \rightarrow b\bar{b}$

OCCUR=2

OCCUR=3

OCCUR=2

<sup>1</sup> AAD 25AJ measure the  $t\bar{t}H$  production with  $H \rightarrow b\bar{b}$  decay channel using 140 fb<sup>-1</sup> of data at  $E_{\text{cm}} = 13$  TeV. The  $t\bar{t}H$  cross section is measured to be  $411^{+101}_{-92}$  fb for a Higgs boson mass of 125.09 GeV. The signal strengths with simplified template cross section bins are given in their Fig. 3.

NODE=S126STH;LINKAGE=AA

<sup>2</sup> HAYRAPETYAN 25R measure the  $t\bar{t}H$  and  $tH$  productions with  $H \rightarrow b\bar{b}$  decay channel using 138 fb<sup>-1</sup> of data at  $E_{\text{cm}} = 13$  TeV. The quoted value is obtained assuming the  $tH$  contribution predicted in the SM. The signal strengths with simplified template cross section bins are given in their Fig. 12. Two-dimensional likelihood scan of  $(\mu_{tH}, \mu_{t\bar{t}H})$  is shown in their Fig. 14.

NODE=S126STH;LINKAGE=BA

<sup>3</sup> SIRUNYAN 21R search for  $t\bar{t}H$  in final states with electrons, muons and hadronically decaying  $\tau$  leptons ( $H \rightarrow WW^*, ZZ^*, \tau\tau$ ) with 137 fb<sup>-1</sup> of  $pp$  collision data at  $E_{\text{cm}} = 13$  TeV. The quoted signal strength corresponds to a significance of 4.7 standard deviations and is given for  $m_H = 125$  GeV.

NODE=S126STH;LINKAGE=W

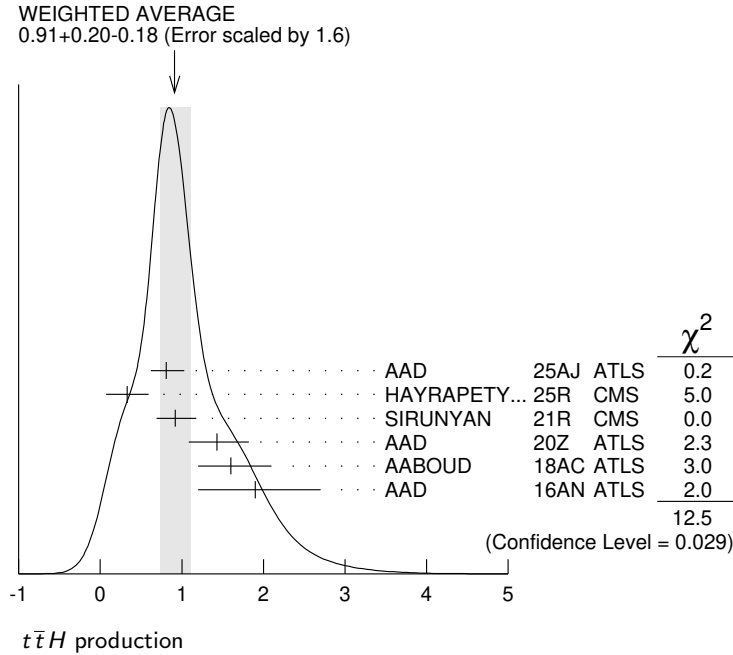
<sup>4</sup> AAD 20Z measure  $\sigma_{t\bar{t}H} \cdot \text{B}(H \rightarrow \gamma\gamma)$  to be  $1.64^{+0.38+0.17}_{-0.36-0.14}$  fb in 139 fb<sup>-1</sup> of data at  $E_{\text{cm}} = 13$  TeV.

NODE=S126STH;LINKAGE=V



- 5 AABOUD 18AC search for  $t\bar{t}H$  production with  $H$  decaying to  $\tau\tau$ ,  $WW^*(\rightarrow \ell\nu\ell\nu, \ell\nu q\bar{q})$ ,  $ZZ^*(\rightarrow \ell\ell\nu\nu, \ell\ell q\bar{q})$  in  $36.1 \text{ fb}^{-1}$  of  $pp$  collisions at  $E_{\text{cm}} = 13 \text{ TeV}$ . The quoted signal strength is given for  $m_H = 125 \text{ GeV}$ . See their Table 13 and Fig. 13. NODE=S126STH;LINKAGE=M
- 6 AAD 16AN: In the fit, relative branching ratios are fixed to those in the Standard Model. The quoted signal strength is given for  $m_H = 125.09 \text{ GeV}$ . NODE=S126STH;LINKAGE=K
- 7 TUMASYAN 23AI measure boosted  $H \rightarrow b\bar{b}$  ( $p_T > 200 \text{ GeV}$ ) in  $t\bar{t}H$  production using  $138 \text{ fb}^{-1}$  of data at  $E_{\text{cm}} = 13 \text{ TeV}$ . The differential cross section for the Higgs  $p_T$  is shown in their Fig. 8 and Table V. Limits on eight Wilson coefficients at 68% and 95% CL are shown in their Fig. 10 and Table VI. NODE=S126STH;LINKAGE=Z
- 8 AAD 22M measure  $H \rightarrow b\bar{b}$  in  $t\bar{t}H$  production using  $139 \text{ fb}^{-1}$  of data at  $E_{\text{cm}} = 13 \text{ TeV}$ . See their Fig. 14. The signal strengths and 95% CL cross section upper limits with simplified template cross section bins are given in their Figs. 18 and 19, respectively. NODE=S126STH;LINKAGE=Y
- 9 SIRUNYAN 20AS measure  $\sigma_{t\bar{t}H} \cdot \text{B}(H \rightarrow \gamma\gamma)$  to be  $1.56^{+0.34}_{-0.32} \text{ fb}$  in  $137 \text{ fb}^{-1}$  of data at  $E_{\text{cm}} = 13 \text{ TeV}$ . NODE=S126STH;LINKAGE=U
- 10 SIRUNYAN 19R search for  $t\bar{t}H$  production with  $H$  decaying to  $b\bar{b}$  in  $35.9 \text{ fb}^{-1}$  of data at  $E_{\text{cm}} = 13 \text{ TeV}$ . The quoted signal strength is given for  $m_H = 125 \text{ GeV}$ . NODE=S126STH;LINKAGE=S
- 11 AABOUD 18AC combine results of  $t\bar{t}H$ ,  $H \rightarrow \tau\tau$ ,  $WW^*(\rightarrow \ell\nu\ell\nu, \ell\nu q\bar{q})$ ,  $ZZ^*(\rightarrow \ell\ell\nu\nu, \ell\ell q\bar{q})$  with results of  $t\bar{t}H$ ,  $H \rightarrow b\bar{b}$  (AABOUD 18T),  $\gamma\gamma$  (AABOUD 18BO),  $ZZ^*(\rightarrow 4\ell)$  (AABOUD 18AJ) in  $36.1 \text{ fb}^{-1}$  of  $pp$  collisions at  $E_{\text{cm}} = 13 \text{ TeV}$ . The quoted signal strength is given for  $m_H = 125 \text{ GeV}$ . See their Table 14. NODE=S126STH;LINKAGE=N
- 12 AABOUD 18BK use  $79.8 \text{ fb}^{-1}$  data for  $t\bar{t}H$  production with  $H \rightarrow \gamma\gamma$  and  $ZZ^* \rightarrow 4\ell$  ( $\ell = e, \mu$ ) and  $36.1 \text{ fb}^{-1}$  for other decay channels at  $E_{\text{cm}} = 13 \text{ TeV}$ . A significance of 5.8 standard deviations is observed for  $m_H = 125.09 \text{ GeV}$  and its signal strength without the uncertainty of the  $t\bar{t}H$  cross section is  $1.32^{+0.28}_{-0.26}$ . Combining with results of 7 and 8 TeV (AAD 16K), the significance is 6.3 standard deviations. Assuming Standard Model branching fractions, the total  $t\bar{t}H$  production cross section at 13 TeV is measured to be  $670 \pm 90^{+110}_{-100} \text{ fb}$ . NODE=S126STH;LINKAGE=O
- 13 AABOUD 18T search for  $t\bar{t}H$  production with  $H$  decaying to  $b\bar{b}$  in  $36.1 \text{ fb}^{-1}$  of  $pp$  collisions at  $E_{\text{cm}} = 13 \text{ TeV}$ . The quoted signal strength is given for  $m_H = 125 \text{ GeV}$ . NODE=S126STH;LINKAGE=H
- 14 SIRUNYAN 18BD search for  $t\bar{t}H$ ,  $H \rightarrow b\bar{b}$  in the all-jet final state with  $35.9 \text{ fb}^{-1}$   $pp$  collision data at  $E_{\text{cm}} = 13 \text{ TeV}$ . The quoted signal strength is given for  $m_H = 125 \text{ GeV}$ . NODE=S126STH;LINKAGE=Q
- 15 SIRUNYAN 18BQ search for  $t\bar{t}H$  in final states with electrons, muons and hadronically decaying  $\tau$  leptons ( $H \rightarrow WW^*, ZZ^*, \tau\tau$ ) with  $35.9 \text{ fb}^{-1}$  of  $pp$  collision data at  $E_{\text{cm}} = 13 \text{ TeV}$ . The quoted signal strength corresponds to a significance of 3.2 standard deviations and is given for  $m_H = 125 \text{ GeV}$ . NODE=S126STH;LINKAGE=P
- 16 SIRUNYAN 18L use up to 5.1, 19.7 and  $35.9 \text{ fb}^{-1}$  of  $pp$  collisions at  $E_{\text{cm}} = 7, 8$ , and 13 TeV, respectively. The quoted signal strength corresponds to a significance of 5.2 standard deviations and is given for  $m_H = 125.09 \text{ GeV}$ .  $H$  decay channels of  $WW^*, ZZ^*, \gamma\gamma, \tau\tau$ , and  $b\bar{b}$  are used. See their Table 1 and Fig. 2 for results on individual channels. NODE=S126STH;LINKAGE=G
- 17 AAD 16AL search for  $t\bar{t}H$  production with  $H$  decaying to  $\gamma\gamma$  in  $4.5 \text{ fb}^{-1}$  of  $pp$  collisions at  $E_{\text{cm}} = 7 \text{ TeV}$  and  $b\bar{b}, \tau\tau, \gamma\gamma, WW^*$ , and  $ZZ^*$  in  $20.3 \text{ fb}^{-1}$  at  $E_{\text{cm}} = 8 \text{ TeV}$ . The quoted signal strength is given for  $m_H = 125 \text{ GeV}$ . This paper combines the results of previous papers, and the new result of this paper only is:  $\mu = 1.6 \pm 2.6$ . NODE=S126STH;LINKAGE=I
- 18 AAD 16AN perform fits to the ATLAS and CMS data at  $E_{\text{cm}} = 7$  and 8 TeV. NODE=S126STH;LINKAGE=J
- 19 AAD 16K use up to  $4.7 \text{ fb}^{-1}$  of  $pp$  collisions at  $E_{\text{cm}} = 7 \text{ TeV}$  and up to  $20.3 \text{ fb}^{-1}$  at  $E_{\text{cm}} = 8 \text{ TeV}$ . The third uncertainty in the measurement is theory systematics. The quoted signal strength is given for  $m_H = 125.36 \text{ GeV}$ . NODE=S126STH;LINKAGE=F
- 20 AAD 15 search for  $t\bar{t}H$  production with  $H$  decaying to  $\gamma\gamma$  in  $4.5 \text{ fb}^{-1}$  of  $pp$  collisions at  $E_{\text{cm}} = 7 \text{ TeV}$  and  $20.3 \text{ fb}^{-1}$  at  $E_{\text{cm}} = 8 \text{ TeV}$ . The quoted result on the signal strength is equivalent to an upper limit of 6.7 at 95% CL and is given for  $m_H = 125.4 \text{ GeV}$ . NODE=S126STH;LINKAGE=B
- 21 AAD 15BC search for  $t\bar{t}H$  production with  $H$  decaying to  $b\bar{b}$  in  $20.3 \text{ fb}^{-1}$  of  $pp$  collisions at  $E_{\text{cm}} = 8 \text{ TeV}$ . The corresponding upper limit is 3.4 at 95% CL. The quoted signal strength is given for  $m_H = 125 \text{ GeV}$ . NODE=S126STH;LINKAGE=C
- 22 AAD 15T search for  $t\bar{t}H$  production with  $H$  resulting in multilepton final states (mainly from  $WW^*, \tau\tau, ZZ^*$ ) in  $20.3 \text{ fb}^{-1}$  of  $pp$  collisions at  $E_{\text{cm}} = 8 \text{ TeV}$ . The quoted result on the signal strength is given for  $m_H = 125 \text{ GeV}$  and corresponds to an upper limit of 4.7 at 95% CL. The data sample is independent from AAD 15 and AAD 15BC. NODE=S126STH;LINKAGE=D
- 23 KHACHATRYAN 15AN search for  $t\bar{t}H$  production with  $H$  decaying to  $b\bar{b}$  in  $19.5 \text{ fb}^{-1}$  of  $pp$  collisions at  $E_{\text{cm}} = 8 \text{ TeV}$ . The quoted result on the signal strength is equivalent to an upper limit of 4.2 at 95% CL and is given for  $m_H = 125 \text{ GeV}$ . NODE=S126STH;LINKAGE=E
- 24 KHACHATRYAN 14H search for  $t\bar{t}H$  production with  $H$  decaying to  $b\bar{b}, \tau\tau, \gamma\gamma, WW^*$ , and  $ZZ^*$ , in  $5.1 \text{ fb}^{-1}$  of  $pp$  collisions at  $E_{\text{cm}} = 7 \text{ TeV}$  and  $19.7 \text{ fb}^{-1}$  at  $E_{\text{cm}} = 8 \text{ TeV}$ . The quoted signal strength is given for  $m_H = 125.6 \text{ GeV}$ . NODE=S126STH;LINKAGE=A
- 25 AALTONEN 13L combine all CDF results with  $9.45\text{--}10.0 \text{ fb}^{-1}$  of  $p\bar{p}$  collisions at  $E_{\text{cm}} = 1.96 \text{ TeV}$ . The quoted signal strength is given for  $m_H = 125 \text{ GeV}$ . NODE=S126STH;LINKAGE=LL
- 26 CHATRCHYAN 13X search for  $t\bar{t}H$  production followed by  $H \rightarrow b\bar{b}$ , one top decaying to  $\ell\nu$  and the other to either  $\ell\nu$  or  $q\bar{q}$  in  $5.0 \text{ fb}^{-1}$  and  $5.1 \text{ fb}^{-1}$  of  $pp$  collisions at  $E_{\text{cm}} = 7$  and 8 TeV. A limit on cross section times branching ratio which corresponds to (4.0–8.6) times the expected Standard Model cross section is given for  $m_H = 110\text{--}140$  NODE=S126STH;LINKAGE=TY

GeV at 95% CL. The quoted limit is given for  $m_H = 125$  GeV, where 5.2 is expected for no signal.



### $b\bar{b}H$ production

VALUE	CL%	DOCUMENT ID	TECN	COMMENT
<b>&lt;3.7</b>	95	<sup>1</sup> HAYRAPETYAN...25	CMS	$pp$ , 13 TeV, $H \rightarrow \tau\tau, WW^*$

<sup>1</sup> HAYRAPETYAN 25 search for  $b\bar{b}H$  and  $bH$  in final states with leptons using 138 fb<sup>-1</sup> of data at  $E_{cm} = 13$  TeV.  $H \rightarrow \tau\tau$  or  $H \rightarrow WW^* \rightarrow \ell\nu\ell\nu$  are considered. Upper limits at 95% CL on the signal strength for each final state are found in their Fig. 3. Combining with TUMASYAN 23Y, two-dimensional exclusion regions as a function of the  $\kappa_b$  and  $\kappa_t$  parameters are shown in their Fig. 4. The best fit value is  $(\kappa_t, \kappa_b) = (-0.73, 1.58)$ . All other Higgs couplings are fixed to the SM values.

NODE=S126SBH  
NODE=S126SBH

NODE=S126SBH;LINKAGE=A

### $tH$ production

VALUE	CL%	DOCUMENT ID	TECN	COMMENT
<b>5.7±2.7±3.0</b>		<sup>1</sup> SIRUNYAN	21R CMS	$pp$ , 13 TeV
• • • We do not use the following data for averages, fits, limits, etc. • • •				
<14.6	95	<sup>2</sup> HAYRAPETYAN...25R	CMS	$pp$ , 13 TeV
<12	95	<sup>3</sup> AAD	20Z ATLS	$pp$ , 13 TeV
		<sup>4</sup> SIRUNYAN	19BK CMS	$pp$ , 13 TeV
		<sup>5</sup> KHACHATRYAN...16AU	CMS	$pp$ , 8 TeV

<sup>1</sup> SIRUNYAN 21R search for  $tH$  in final states with electrons, muons and hadronically decaying  $\tau$  leptons ( $H \rightarrow WW^*, ZZ^*, \tau\tau$ ) with 137 fb<sup>-1</sup> of  $pp$  collision data at  $E_{cm} = 13$  TeV. The quoted signal strength corresponds to a significance of 1.4 standard deviations and is given for  $m_H = 125$  GeV.

<sup>2</sup> HAYRAPETYAN 25R measure the  $t\bar{t}H$  and  $tH$  productions with  $H \rightarrow b\bar{b}$  decay channel using 138 fb<sup>-1</sup> of data at  $E_{cm} = 13$  TeV. The quoted value is obtained assuming the  $t\bar{t}H$  contribution predicted in the SM. Two-dimensional likelihood scan of  $(\mu_{tH}, \mu_{t\bar{t}H})$  is shown in their Fig. 14.

<sup>3</sup> AAD 20Z search for the  $tH$  associated production using  $H \rightarrow \gamma\gamma$  in 139 fb<sup>-1</sup> of data at  $E_{cm} = 13$  TeV. An upper limit on its rate is set to be 12 times the Standard Model at 95% CL ( $m_H = 125.09$  GeV).

<sup>4</sup> SIRUNYAN 19BK search for the  $tH$  associated production using multilepton signatures ( $H \rightarrow WW^*, H \rightarrow \tau\tau, H \rightarrow ZZ^*$ ) and signatures with a single lepton and a  $b\bar{b}$  pair ( $H \rightarrow b\bar{b}$ ) using 35.9 fb<sup>-1</sup> at  $E_{cm} = 13$  TeV. Results are combined with  $H \rightarrow \gamma\gamma$  (SIRUNYAN 18DS). The observed 95% CL upper limit on the  $tH$  production cross section times  $H \rightarrow WW^* + \tau\tau + ZZ^* + b\bar{b} + \gamma\gamma$  branching fraction is 1.94 pb (assuming SM  $t\bar{t}H$  production cross section). See their Table X and Fig. 14. The values outside the ranges of  $[-0.9, -0.5]$  and  $[1.0, 2.1]$  times the standard model top quark Yukawa coupling are excluded at 95% CL.

<sup>5</sup> KHACHATRYAN 16AU search for the  $tH$  associated production in 19.7 fb<sup>-1</sup> at  $E_{cm} = 8$  TeV. The 95% CL upper limits on the  $tH$  associated production cross section is measured to be 600–1000 fb depending on the assumed  $\gamma\gamma$  branching ratios of the Higgs boson. The  $\gamma\gamma$  branching ratio is varied to be by a factor of 0.5–3.0 of the Standard Model Higgs boson ( $m_H = 125$  GeV). The results of the signal strengths for a negative Higgs-boson trilinear coupling are given. The results are given for  $m_H = 125$  GeV.

NODE=S126PTH  
NODE=S126PTH

NODE=S126PTH;LINKAGE=D

NODE=S126PTH;LINKAGE=E

NODE=S126PTH;LINKAGE=C

NODE=S126PTH;LINKAGE=B

NODE=S126PTH;LINKAGE=A

**$cH$  production**

VALUE	DOCUMENT ID	TECN	COMMENT
-------	-------------	------	---------

• • • We do not use the following data for averages, fits, limits, etc. • • •

<sup>1</sup> AAD 25R ATLS  $pp$ , 13 TeV

<sup>1</sup> AAD 25R search for the production of a Higgs boson and one or more charm quarks ( $H+c$ ) with  $H \rightarrow \gamma\gamma$  using  $140 \text{ fb}^{-1}$  of data at  $E_{\text{cm}} = 13 \text{ TeV}$ . The observed  $H+c$  cross section is  $5.3 \pm 3.2 \text{ pb}$ . The observed upper limit on the  $H+c$  cross section at 95% CL is  $10.6 \text{ pb}$ .

NODE=S126SCH  
NODE=S126SCH

NODE=S126SCH;LINKAGE=A

**VBS/VBF  $WH$  production**

$WH$  production through vector boson scattering (VBS) or vector boson fusion (VBF).

The VBS/VBF  $WH$  production cross section related to the SM prediction.

VALUE	CL%	DOCUMENT ID	TECN	COMMENT
-------	-----	-------------	------	---------

• • • We do not use the following data for averages, fits, limits, etc. • • •

<14.3 95 <sup>1</sup> HAYRAPETY...25B CMS  $pp$ , 13 TeV, VBF  $WH$ , coupling sign

< 9.0 95 <sup>2</sup> AAD 24BMATLS  $pp$ , 13 TeV, VBF  $WH$ , coupling sign

<sup>1</sup> HAYRAPETYAN 25B present the determination of the relative sign of  $\kappa_W$  and  $\kappa_Z$  with VBF  $WH$ ,  $H \rightarrow b\bar{b}$  using  $148 \text{ fb}^{-1}$  of data at  $E_{\text{cm}} = 13 \text{ TeV}$ . The upper limit at 95% CL on the cross section for VBF  $WH$  production is obtained. The signal strength is measured to be  $2.2^{+6.1}_{-5.8}$ .

<sup>2</sup> AAD 24BM present the determination of the relative sign of  $\kappa_W$  and  $\kappa_Z$  with VBF  $WH$ ,  $H \rightarrow b\bar{b}$  using  $140 \text{ fb}^{-1}$  of data at  $E_{\text{cm}} = 13 \text{ TeV}$ . The upper limit at 95% CL on the cross section for VBF  $WH$  production is obtained. The signal strength is measured to be  $0.9^{+4.0}_{-4.3}$ .

NODE=S126SVB

NODE=S126SVB

NODE=S126SVB

NODE=S126SVB;LINKAGE=B

NODE=S126SVB;LINKAGE=A

 **$HH$  production**

The  $HH$  production cross section relative to the SM prediction.

VALUE	CL%	DOCUMENT ID	TECN	COMMENT
-------	-----	-------------	------	---------

< 2.4 95 <sup>1</sup> AAD 23AT ATLS 13 TeV,  $b\bar{b}b\bar{b}$ ,  $b\bar{b}\tau\tau$ ,  $b\bar{b}\gamma\gamma$

• • • We do not use the following data for averages, fits, limits, etc. • • •

< 5.9 95 <sup>2</sup> AAD 24AZ ATLS 13 TeV,  $b\bar{b}\tau\tau$

< 17 95 <sup>3</sup> AAD 24BG ATLS 13 TeV,  $b\bar{b}ZZ^*$ ,  $VVVV$ ,  $VV\tau\tau$ ,  $\tau\tau\tau\tau$ ,  $\gamma\gamma VV$ ,  $\gamma\gamma\tau\tau$

< 2.9 95 <sup>4</sup> AAD 24BL ATLS 13 TeV,  $b\bar{b}b\bar{b}$ ,  $b\bar{b}\tau\tau$ ,  $b\bar{b}\gamma\gamma$ , multilepton,  $b\bar{b}\ell\ell$

< 4.0 95 <sup>5</sup> AAD 24X ATLS 13 TeV,  $b\bar{b}\gamma\gamma$

< 9.7 95 <sup>6</sup> AAD 24Y ATLS 13 TeV,  $b\bar{b}WW^*$ ,  $b\bar{b}ZZ^*$ ,  $b\bar{b}\tau\tau$ , multilepton

< 14 95 <sup>7</sup> HAYRAPETY...24AE CMS 13 TeV,  $b\bar{b}WW^*$

<294 95 <sup>8</sup> HAYRAPETY...24AW CMS 13 TeV,  $VHH$ ,  $HH \rightarrow b\bar{b}b\bar{b}$

<183 95 <sup>9</sup> AAD 23AD ATLS 13 TeV,  $VHH$ ,  $HH \rightarrow b\bar{b}b\bar{b}$

< 5.4 95 <sup>10</sup> AAD 23BK ATLS 13 TeV,  $b\bar{b}b\bar{b}$

< 4.7 95 <sup>11</sup> AAD 23Z ATLS 13 TeV,  $b\bar{b}\tau\tau$

< 9.9 95 <sup>12</sup> TUMASYAN 23AE CMS 13 TeV,  $b\bar{b}b\bar{b}$

< 3.3 95 <sup>13,14</sup> TUMASYAN 23D CMS 13 TeV,  $b\bar{b}\tau\tau$

<124 95 <sup>13,15</sup> TUMASYAN 23D CMS 13 TeV,  $b\bar{b}\tau\tau$

< 32.4 95 <sup>16</sup> TUMASYAN 23I CMS 13 TeV,  $b\bar{b}ZZ^*$  ( $ZZ^* \rightarrow 4\ell$ )

< 21.3 95 <sup>17</sup> TUMASYAN 23O CMS 13 TeV,  $WW^*WW^*$ ,  $WW^*\tau\tau$ ,  $\tau\tau\tau\tau$

< 4.2 95 <sup>18</sup> AAD 22Y ATLS 13 TeV,  $\gamma\gamma b\bar{b}$

< 3.4 95 <sup>19</sup> CMS 22 CMS 13 TeV,  $b\bar{b}ZZ^*$ ,  $b\bar{b}\gamma\gamma$ ,  $b\bar{b}\tau\tau$ ,  $b\bar{b}b\bar{b}$ , multilepton

< 3.9 95 <sup>20</sup> TUMASYAN 22AN CMS 13 TeV,  $b\bar{b}b\bar{b}$

< 7.7 95 <sup>21</sup> SIRUNYAN 21K CMS 13 TeV,  $\gamma\gamma b\bar{b}$

< 6.9 95 <sup>22</sup> AAD 20C ATLS 13 TeV,  $b\bar{b}\gamma\gamma$ ,  $b\bar{b}\tau\tau$ ,  $b\bar{b}b\bar{b}$ ,  $b\bar{b}WW^*$ ,  $WW^*\gamma\gamma$ ,  $WW^*WW^*$

< 40 95 <sup>23</sup> AAD 20E ATLS 13 TeV,  $HH \rightarrow b\bar{b}\ell\nu\ell\nu$

<840 95 <sup>24</sup> AAD 20X ATLS 13 TeV, VBF,  $b\bar{b}b\bar{b}$

< 12.9 95 <sup>25</sup> AABOUD 19A ATLS 13 TeV,  $b\bar{b}b\bar{b}$

<300 95 <sup>26</sup> AABOUD 19O ATLS 13 TeV,  $b\bar{b}WW^*$

<160 95 <sup>27</sup> AABOUD 19T ATLS 13 TeV,  $WW^*WW^*$

< 24 95 <sup>28</sup> SIRUNYAN 19 CMS 13 TeV,  $\gamma\gamma b\bar{b}$

< 75 95 <sup>29</sup> SIRUNYAN 19AB CMS 13 TeV,  $b\bar{b}b\bar{b}$

< 22.2 95 <sup>30</sup> SIRUNYAN 19BE CMS 13 TeV,  $b\bar{b}\gamma\gamma$ ,  $b\bar{b}\tau\tau$ ,  $b\bar{b}b\bar{b}$ ,  $b\bar{b}WW^*$ ,  $b\bar{b}ZZ^*$

<179 95 <sup>31</sup> SIRUNYAN 19H CMS 13 TeV,  $b\bar{b}b\bar{b}$

NODE=S126SHH

NODE=S126SHH

NODE=S126SHH

OCCUR=2

<230	95	32	AABOUD	18BU ATLS	13 TeV, $\gamma\gamma WW^*$
< 12.7	95	33	AABOUD	18CQ ATLS	13 TeV, $b\bar{b}\tau\tau$
< 22	95	34	AABOUD	18CW ATLS	13 TeV, $\gamma\gamma b\bar{b}$
< 30	95	35	SIRUNYAN	18A CMS	13 TeV, $b\bar{b}\tau\tau$
< 79	95	36	SIRUNYAN	18F CMS	13 TeV, $b\bar{b}\ell\nu\ell\nu$
< 43	95	37	SIRUNYAN	17CN CMS	8 TeV, $b\bar{b}\tau\tau, \gamma\gamma b\bar{b}, b\bar{b}b\bar{b}$
<108	95	38	AABOUD	16I ATLS	13 TeV, $b\bar{b}b\bar{b}$
< 74	95	39	KHACHATRY...	16BQ CMS	8 TeV, $\gamma\gamma b\bar{b}$
< 70	95	40	AAD	15CE ATLS	8 TeV, $b\bar{b}b\bar{b}, b\bar{b}\tau\tau, \gamma\gamma b\bar{b}, \gamma\gamma WW$

- <sup>1</sup> AAD 23AT combine results from 126–139 fb<sup>-1</sup> of data at  $E_{\text{cm}} = 13$  TeV for  $pp \rightarrow HH \rightarrow b\bar{b}b\bar{b}$  (AAD 23BK),  $b\bar{b}\tau\tau$  (AAD 23Z), and  $b\bar{b}\gamma\gamma$  (AAD 22Y).  
NODE=S126SHH;LINKAGE=GA
- <sup>2</sup> AAD 24AZ search for non-resonant  $HH$  production using  $HH \rightarrow b\bar{b}\tau\tau$  with data of 140 fb<sup>-1</sup> at  $E_{\text{cm}} = 13$  TeV. The result is interpreted: limits on Wilson coefficients of the Higgs effective field theory (HEFT) and the SM effective field theory (SMEFT) are shown in their Table IV and Figs. 11 and 12; the ggF  $HH$  production cross sections (7 benchmark points) of HEFT are shown in their Fig. 10. In those interpretations the VBF  $HH$  production is neglected.  
NODE=S126SHH;LINKAGE=KA
- <sup>3</sup> AAD 24BG search for non-resonant  $HH$  production targeting the  $b\bar{b}ZZ^*, VVVV, VV\tau\tau, \tau\tau\tau\tau, \gamma\gamma VV, \gamma\gamma\tau\tau$  decay channels with data of 140 fb<sup>-1</sup> at  $E_{\text{cm}} = 13$  TeV. Signal strengths for the 11 different signal regions are given in their Fig. 8.  
NODE=S126SHH;LINKAGE=IA
- <sup>4</sup> AAD 24BL combine results from 126–140 fb<sup>-1</sup> of data at  $E_{\text{cm}} = 13$  TeV for  $pp \rightarrow HH \rightarrow b\bar{b}b\bar{b}$  (AAD 23BK, AAD 24BV),  $b\bar{b}\tau\tau$  (AAD 24AZ),  $b\bar{b}\gamma\gamma$  (AAD 24X), multilepton (AAD 24BG), and  $b\bar{b}\ell\ell$  (AAD 24Y). See their Fig. 2. The signal strength is measured to be  $0.5^{+1.2}_{-1.0}$ . Constraints for three interaction parameters ( $c_{tthh}, c_{gghh}, c_{hhhh}$ ) in the Higgs effective field theory are set. See their Fig. 4.  
NODE=S126SHH;LINKAGE=NA
- <sup>5</sup> AAD 24X search for non-resonant  $HH$  production using  $HH \rightarrow b\bar{b}\gamma\gamma$  with data of 140 fb<sup>-1</sup> at  $E_{\text{cm}} = 13$  TeV. The result is interpreted: limits on three Wilson coefficients and the ggF  $HH$  production cross sections (7 benchmark points shown in their Table 5) of the Higgs effective field theory are shown in their Table 4 and Fig. 8, respectively; limits on two Wilson coefficients of the SM effective field theory are shown in their Table 6 and Fig. 9. In those interpretations only the ggF  $HH$  production is considered instead of both ggF and VBF.  
NODE=S126SHH;LINKAGE=JA
- <sup>6</sup> AAD 24Y search for non-resonant  $HH$  production in  $2b + 2\ell + \nu s$  final state ( $\ell = e, \mu$ ) targeting  $b\bar{b}WW^*, b\bar{b}ZZ^*,$  and  $b\bar{b}\tau\tau$  decay channels with data of 140 fb<sup>-1</sup> at  $E_{\text{cm}} = 13$  TeV. The signal strength is measured to be  $-8.5^{+7.7}_{-8.4}$ . See their Fig. 6.  
NODE=S126SHH;LINKAGE=HA
- <sup>7</sup> HAYRAPETYAN 24AE search for non-resonant  $HH$  production using  $HH \rightarrow b\bar{b}WW^*$  with data of 138 fb<sup>-1</sup> at  $E_{\text{cm}} = 13$  TeV. The result is interpreted: the ggF  $HH$  production cross sections (20 benchmark points) of the Higgs effective field theory are shown in their Fig. 16; the coupling between two top quarks and two Higgs bosons is constrained between [-0.8, 1.3] at 95%CL (see their Fig. 17) with all other Higgs couplings fixed to the SM values.  
NODE=S126SHH;LINKAGE=LA
- <sup>8</sup> HAYRAPETYAN 24AW search for non-resonant  $HH$  production in association with a vector boson using  $HH \rightarrow b\bar{b}b\bar{b}$  with data of 138 fb<sup>-1</sup> at  $E_{\text{cm}} = 13$  TeV. The vector boson decays both leptonically ( $W \rightarrow \ell\nu, Z \rightarrow \ell\ell, \nu\nu, \ell = e, \mu$ ) and hadronically. The quoted value is the upper limit of the  $VHH$  cross section. See their Figs. 13 and 16 (left) for the best fit and the upper limit of the  $VHH$  cross section, respectively. In addition, upper limits at 95% CL on  $VHH$  and  $HH$  cross sections are shown as a function of  $\kappa_\lambda, \kappa_{2V},$  and  $\kappa_V$  in their Figs. 17, 18, and 19.  
NODE=S126SHH;LINKAGE=MA
- <sup>9</sup> AAD 23AD search for non-resonant  $HH$  production in association with a vector boson using  $HH \rightarrow b\bar{b}b\bar{b}$  with data of 139 fb<sup>-1</sup> at  $E_{\text{cm}} = 13$  TeV. The vector boson decays leptonically ( $W \rightarrow \ell\nu, Z \rightarrow \ell\ell, \nu\nu, \ell = e, \mu$ ).  
NODE=S126SHH;LINKAGE=Z
- <sup>10</sup> AAD 23BK search for non-resonant  $HH$  production using  $HH \rightarrow b\bar{b}b\bar{b}$  with data of 126 fb<sup>-1</sup> at  $E_{\text{cm}} = 13$  TeV.  
NODE=S126SHH;LINKAGE=FA
- <sup>11</sup> AAD 23Z search for non-resonant  $HH$  production using  $HH \rightarrow b\bar{b}\tau\tau$  with data of 139 fb<sup>-1</sup> at  $E_{\text{cm}} = 13$  TeV. The upper limit on the  $pp \rightarrow HH$  production cross section at 95% CL is measured to be 140 fb, which corresponds to 4.7 times the SM prediction (see their Table 6).  
NODE=S126SHH;LINKAGE=X
- <sup>12</sup> TUMASYAN 23AE search for  $HH$  production using  $HH \rightarrow b\bar{b}b\bar{b}$ , where both  $b\bar{b}$  pairs are highly boosted, with data of 138 fb<sup>-1</sup> at  $E_{\text{cm}} = 13$  TeV.  
NODE=S126SHH;LINKAGE=AA
- <sup>13</sup> TUMASYAN 23D search for non-resonant  $HH$  production using  $HH \rightarrow b\bar{b}\tau\tau$  with data of 138 fb<sup>-1</sup> at  $E_{\text{cm}} = 13$  TeV.  
NODE=S126SHH;LINKAGE=BA
- <sup>14</sup> The upper limit on the  $pp \rightarrow HH$  production cross section (gluon fusion and VBF) at 95% CL is measured to be 102 fb, which corresponds to 3.3 times the SM prediction (see their Table 2).  
NODE=S126SHH;LINKAGE=DA
- <sup>15</sup> The upper limit on the VBF  $pp \rightarrow HH$  production cross section at 95% CL is measured to be 212 fb, which corresponds to 124 times the SM prediction (see their Table 3).  
NODE=S126SHH;LINKAGE=CA
- <sup>16</sup> TUMASYAN 23I search for non-resonant  $HH$  production using  $HH \rightarrow b\bar{b}ZZ^* (ZZ^* \rightarrow 4\ell, \ell = e, \mu)$  with data of 138 fb<sup>-1</sup> at  $E_{\text{cm}} = 13$  TeV.  
NODE=S126SHH;LINKAGE=Y

- 17 TUMASYAN 230 search for non-resonant  $HH$  production using  $HH \rightarrow WW^*WW^*, WW^*\tau\tau$ , and  $\tau\tau\tau\tau$  (multilepton) with data of  $138 \text{ fb}^{-1}$  at  $E_{\text{cm}} = 13 \text{ TeV}$ . See their Fig. 9 for different final states and these combination. NODE=S126SHH;LINKAGE=EA
- 18 AAD 22Y search for non-resonant  $HH$  production using  $HH \rightarrow \gamma\gamma b\bar{b}$  with data of  $139 \text{ fb}^{-1}$  at  $E_{\text{cm}} = 13 \text{ TeV}$ . The upper limit on the  $pp \rightarrow HH$  production cross section at 95% CL is measured to be 130 fb, which corresponds to 4.2 times the SM prediction. NODE=S126SHH;LINKAGE=V
- 19 CMS 22 report combined results (see their Extended Data Table 2) using  $138 \text{ fb}^{-1}$  of data at  $E_{\text{cm}} = 13 \text{ TeV}$ . See their Fig. 5 (left) for different final states and these combination. NODE=S126SHH;LINKAGE=U
- 20 TUMASYAN 22AN search for non-resonant  $HH$  production using  $HH \rightarrow b\bar{b}b\bar{b}$  with data of  $138 \text{ fb}^{-1}$  at  $E_{\text{cm}} = 13 \text{ TeV}$ . The upper limit on the  $pp \rightarrow HH$  production cross section at 95% CL is measured to be 120 fb, which corresponds to 3.9 times the SM prediction. NODE=S126SHH;LINKAGE=W
- 21 SIRUNYAN 21K search for non-resonant  $HH$  production using  $HH \rightarrow \gamma\gamma b\bar{b}$  with data of  $137 \text{ fb}^{-1}$  at  $E_{\text{cm}} = 13 \text{ TeV}$ . The upper limit on the  $pp \rightarrow HH \rightarrow \gamma\gamma b\bar{b}$  production cross section at 95% CL is measured to be 0.67 fb, which corresponds to about 7.7 times the SM prediction. NODE=S126SHH;LINKAGE=T
- 22 AAD 20C combine results of up to  $36.1 \text{ fb}^{-1}$  data at  $E_{\text{cm}} = 13 \text{ TeV}$  for  $pp \rightarrow HH \rightarrow b\bar{b}\gamma\gamma, b\bar{b}\tau\tau, b\bar{b}b\bar{b}, b\bar{b}WW^*, WW^*\gamma\gamma, WW^*WW^*$  (AABOUD 18CW, AABOUD 18CQ, AABOUD 19A, AABOUD 190, AABOUD 18BU, and AABOUD 19T). NODE=S126SHH;LINKAGE=Q
- 23 AAD 20E search non-resonant for  $HH$  production using  $HH \rightarrow b\bar{b}\ell\nu\ell\nu$ , where one of the Higgs bosons decays to  $b\bar{b}$  and the other decays to either  $WW^*, ZZ^*$ , or  $\tau\tau$ , with data of  $139 \text{ fb}^{-1}$  at  $E_{\text{cm}} = 13 \text{ TeV}$ . The upper limit on the  $pp \rightarrow HH$  production cross section at 95% CL is measured to be 1.2 pb, which corresponds to about 40 times the SM prediction. NODE=S126SHH;LINKAGE=E
- 24 AAD 20X search for  $HH \rightarrow b\bar{b}b\bar{b}$  process via VBF with data of  $126 \text{ fb}^{-1}$  at  $E_{\text{cm}} = 13 \text{ TeV}$ . The upper limit on the SM non-resonant  $HH$  production cross section is 1460 fb at 95% CL, which corresponds to 840 times the SM prediction. NODE=S126SHH;LINKAGE=S
- 25 AABOUD 19A search for  $HH$  production using  $HH \rightarrow b\bar{b}b\bar{b}$  with data of  $36.1 \text{ fb}^{-1}$  at  $E_{\text{cm}} = 13 \text{ TeV}$ . The upper limit on the  $pp \rightarrow HH \rightarrow b\bar{b}b\bar{b}$  production cross section at 95% is measured to be 147 fb, which corresponds to about 12.9 times the SM prediction. NODE=S126SHH;LINKAGE=J
- 26 AABOUD 190 search for  $HH$  production using  $HH \rightarrow b\bar{b}WW^*$  with data of  $36.1 \text{ fb}^{-1}$  at  $E_{\text{cm}} = 13 \text{ TeV}$ . The upper limit on the  $pp \rightarrow HH$  production cross section at 95% CL is calculated to be 10 pb from the observed upper limit on the  $pp \rightarrow HH \rightarrow b\bar{b}WW^*$  production cross section of 2.5 pb assuming the SM branching fractions. The former corresponds to about 300 times the SM prediction. NODE=S126SHH;LINKAGE=N
- 27 AABOUD 19T search for  $HH$  production using  $HH \rightarrow WW^*WW^*$  with data of  $36.1 \text{ fb}^{-1}$  at  $E_{\text{cm}} = 13 \text{ TeV}$ . The upper limit on the  $pp \rightarrow HH$  production cross section at 95% is measured to be 5.3 pb, which corresponds to about 160 times the SM prediction. NODE=S126SHH;LINKAGE=O
- 28 SIRUNYAN 19 search for  $HH$  production using  $HH \rightarrow \gamma\gamma b\bar{b}$  with data of  $35.9 \text{ fb}^{-1}$  at  $E_{\text{cm}} = 13 \text{ TeV}$ . The upper limit on the  $pp \rightarrow HH \rightarrow \gamma\gamma b\bar{b}$  production cross section at 95% CL is measured to be 2.0 fb, which corresponds to about 24 times the SM prediction. NODE=S126SHH;LINKAGE=H
- 29 SIRUNYAN 19AB search for  $HH$  production using  $HH \rightarrow b\bar{b}b\bar{b}$ , where 4 heavy flavor jets from two Higgs bosons are resolved, with data of  $35.9 \text{ fb}^{-1}$  at  $E_{\text{cm}} = 13 \text{ TeV}$ . The upper limit on the  $pp \rightarrow HH \rightarrow b\bar{b}b\bar{b}$  production cross section at 95% is measured to be 847 fb, which corresponds to about 75 times the SM prediction. NODE=S126SHH;LINKAGE=M
- 30 SIRUNYAN 19BE combine results of 13 TeV  $35.9 \text{ fb}^{-1}$  data: SIRUNYAN 19, SIRUNYAN 18A, SIRUNYAN 19AB, SIRUNYAN 19H, and SIRUNYAN 18F. NODE=S126SHH;LINKAGE=P
- 31 SIRUNYAN 19H search for  $HH$  production using  $HH \rightarrow b\bar{b}b\bar{b}$ , where one of  $b\bar{b}$  pairs is highly boosted and the other one is resolved, with data of  $35.9 \text{ fb}^{-1}$  at  $E_{\text{cm}} = 13 \text{ TeV}$ . The upper limit on the  $pp \rightarrow HH \rightarrow b\bar{b}b\bar{b}$  production cross section at 95% is measured to be 1980 fb, which corresponds to about 179 times the SM prediction. NODE=S126SHH;LINKAGE=L
- 32 AABOUD 18BU search for  $HH$  production using  $\gamma\gamma WW^*$  with the final state of  $\gamma\gamma\ell\nu jj$  using data of  $36.1 \text{ fb}^{-1}$  at  $E_{\text{cm}} = 13 \text{ TeV}$ . The upper limit on the  $pp \rightarrow HH$  production cross section at 95% CL is measured to be 7.7 pb, which corresponds to about 230 times the SM prediction. The upper limit on the  $pp \rightarrow HH \rightarrow \gamma\gamma WW^*$  at 95% CL is measured to be 7.5 fb (see their Table 6). NODE=S126SHH;LINKAGE=G
- 33 AABOUD 18CQ search for  $HH$  production using  $HH \rightarrow b\bar{b}\tau\tau$  with data of  $36.1 \text{ fb}^{-1}$  at  $E_{\text{cm}} = 13 \text{ TeV}$ . The upper limit on the  $pp \rightarrow HH \rightarrow b\bar{b}\tau\tau$  production cross section at 95% is measured to be 30.9 fb, which corresponds to about 12.7 times the SM prediction. NODE=S126SHH;LINKAGE=K
- 34 AABOUD 18CW search for  $HH$  production using  $HH \rightarrow \gamma\gamma b\bar{b}$  with data of  $36.1 \text{ fb}^{-1}$  at  $E_{\text{cm}} = 13 \text{ TeV}$ . The upper limit on the  $pp \rightarrow HH$  production cross section at 95% is measured to be 0.73 pb, which corresponds to about 22 times the SM prediction. NODE=S126SHH;LINKAGE=I
- 35 SIRUNYAN 18A search for  $HH$  production using  $HH \rightarrow b\bar{b}\tau\tau$  with data of  $35.9 \text{ fb}^{-1}$  at  $E_{\text{cm}} = 13 \text{ TeV}$ . The upper limit on the  $gg \rightarrow HH \rightarrow b\bar{b}\tau\tau$  production cross section is measured to be 75.4 fb, which corresponds to about 30 times the SM prediction. NODE=S126SHH;LINKAGE=B
- 36 SIRUNYAN 18F search non-resonant for  $HH$  production using  $HH \rightarrow b\bar{b}\ell\nu\ell\nu$ , where  $\ell\nu\ell\nu$  is either  $WW \rightarrow \ell\nu\ell\nu$  or  $ZZ \rightarrow \ell\nu\ell\nu$  ( $\ell$  is  $e, \mu$  or a leptonically decaying  $\tau$ ), with data of  $35.9 \text{ fb}^{-1}$  at  $E_{\text{cm}} = 13 \text{ TeV}$ . The upper limit on the  $HH \rightarrow b\bar{b}\ell\nu\ell\nu$  NODE=S126SHH;LINKAGE=F

production cross section at 95% CL is measured to be 72 fb, which corresponds to about 79 times the SM prediction.

- 37 SIRUNYAN 17CN search for  $HH$  production using  $HH \rightarrow b\bar{b}\tau\tau$  with data of  $18.3 \text{ fb}^{-1}$  at  $E_{\text{cm}} = 8 \text{ TeV}$ . Results are then combined with the published results of the  $HH \rightarrow \gamma\gamma b\bar{b}$  and  $HH \rightarrow b\bar{b}b\bar{b}$ , which use data of up to  $19.7 \text{ fb}^{-1}$  at  $E_{\text{cm}} = 8 \text{ TeV}$ . The upper limit on the  $gg \rightarrow HH$  production cross section is measured to be  $0.59 \text{ pb}$  from  $b\bar{b}\tau\tau$ , which corresponds to about 59 times the SM prediction (gluon fusion). The combined upper limit is  $0.43 \text{ pb}$ , which is about 43 times the SM prediction. The quoted values are given for  $m_H = 125 \text{ GeV}$ .
- 38 AABOUD 16I search for  $HH$  production using  $HH \rightarrow b\bar{b}b\bar{b}$  with data of  $3.2 \text{ fb}^{-1}$  at  $E_{\text{cm}} = 13 \text{ TeV}$ . The upper limit on the  $pp \rightarrow HH \rightarrow b\bar{b}b\bar{b}$  production cross section is measured to be  $1.22 \text{ pb}$ . This result corresponds to about 108 times the SM prediction (gluon fusion), which is  $11.3^{+0.9}_{-1.0} \text{ fb}$  (NNLO+NNLL) including top quark mass effects. The quoted values are given for  $m_H = 125 \text{ GeV}$ .
- 39 KHACHATRYAN 16BQ search for  $HH$  production using  $HH \rightarrow \gamma\gamma b\bar{b}$  with data of  $19.7 \text{ fb}^{-1}$  at  $E_{\text{cm}} = 8 \text{ TeV}$ . The upper limit on the  $gg \rightarrow HH \rightarrow \gamma\gamma b\bar{b}$  production is measured to be  $1.85 \text{ fb}$ , which corresponds to about 74 times the SM prediction and is translated into  $0.71 \text{ pb}$  for  $gg \rightarrow HH$  production cross section.
- 40 AAD 15CE search for  $HH$  production using  $HH \rightarrow b\bar{b}\tau\tau$  and  $HH \rightarrow \gamma\gamma WW$  with data of  $20.3 \text{ fb}^{-1}$  at  $E_{\text{cm}} = 8 \text{ TeV}$ . These results are then combined with the published results of the  $HH \rightarrow \gamma\gamma b\bar{b}$  and  $HH \rightarrow b\bar{b}b\bar{b}$ , which use data of up to  $20.3 \text{ fb}^{-1}$  at  $E_{\text{cm}} = 8 \text{ TeV}$ . The upper limits on the  $gg \rightarrow HH$  production cross section are measured to be  $1.6 \text{ pb}$ ,  $11.4 \text{ pb}$ ,  $2.2 \text{ pb}$  and  $0.62 \text{ pb}$  from  $b\bar{b}\tau\tau$ ,  $\gamma\gamma WW$ ,  $\gamma\gamma b\bar{b}$  and  $b\bar{b}b\bar{b}$ , respectively. The combined upper limit is  $0.69 \text{ pb}$ , which corresponds to about 70 times the SM prediction. The quoted results are given for  $m_H = 125.4 \text{ GeV}$ . See their Table 4.

NODE=S126SHH;LINKAGE=E

NODE=S126SHH;LINKAGE=D

NODE=S126SHH;LINKAGE=A

NODE=S126SHH;LINKAGE=C

### HHH production

The  $HHH$  production cross section relative to the SM prediction.

VALUE	CL%	DOCUMENT ID	TECN	COMMENT
<b>&lt;760</b>	95	<sup>1</sup> AAD	25J ATLS	13 TeV, $b\bar{b}b\bar{b}b\bar{b}$

- <sup>1</sup> AAD 25J search for non-resonant  $HHH$  production using  $HHH \rightarrow b\bar{b}b\bar{b}b\bar{b}$  with data of  $126 \text{ fb}^{-1}$  at  $E_{\text{cm}} = 13 \text{ TeV}$ . The upper limit on the  $pp \rightarrow HHH$  production cross section at 95% CL is measured to be  $59 \text{ fb}$ .

NODE=S126HHH  
NODE=S126HHH  
NODE=S126HHH

NODE=S126HHH;LINKAGE=A

### Higgs trilinear self coupling modifier $\kappa_\lambda$

Signal strength relative to the SM prediction,  $\kappa_\lambda = \kappa_3 = \lambda_{HHH} / \lambda_{HHH}^{\text{SM}}$ .

VALUE	CL%	DOCUMENT ID	TECN	COMMENT
<b><math>3.8^{+2.1}_{-3.6}</math></b>		<sup>1</sup> AAD	24BL ATLS	13 TeV, $b\bar{b}b\bar{b}$ , $b\bar{b}\tau\tau$ , $b\bar{b}\gamma\gamma$ , multilepton, $b\bar{b}\ell\ell$

• • • We do not use the following data for averages, fits, limits, etc. • • •

– 11 to 17	95	<sup>2</sup> AAD	25J ATLS	13 TeV, $b\bar{b}b\bar{b}b\bar{b}$
– 1.2 to 7.5	95	<sup>3</sup> HAYRAPETY...25F	CMS	13 TeV, single and double Higgs production
– 3.1 to 9.0	95	<sup>4</sup> AAD	24AZ ATLS	13 TeV, $b\bar{b}\tau\tau$
– 6.2 to 11.6	95	<sup>5</sup> AAD	24BG ATLS	13 TeV, $b\bar{b}ZZ^*$ , $VVVV$ , $VV\tau\tau$ , $\tau\tau\tau\tau$ , $\gamma\gamma VV$ , $\gamma\gamma\tau\tau$
– 1.2 to 7.2	95	<sup>1</sup> AAD	24BL ATLS	13 TeV, $b\bar{b}b\bar{b}$ , $b\bar{b}\tau\tau$ , $b\bar{b}\gamma\gamma$ , multilepton, $b\bar{b}\ell\ell$
– 1.4 to 6.9	95	<sup>6</sup> AAD	24X ATLS	13 TeV, $b\bar{b}\gamma\gamma$
– 6.2 to 13.3	95	<sup>7</sup> AAD	24Y ATLS	13 TeV, $b\bar{b}WW^*$ , $b\bar{b}ZZ^*$ , $b\bar{b}\tau\tau$ , multilepton
– 7.2 to 13.8	95	<sup>8</sup> HAYRAPETY...24AE	CMS	13 TeV, $b\bar{b}WW^*$
– 37.7 to 37.2	95	<sup>9</sup> HAYRAPETY...24AW	CMS	13 TeV, $VHH$ , $HH \rightarrow b\bar{b}b\bar{b}$
– 34.4 to 33.3	95	<sup>10</sup> AAD	23AD ATLS	13 TeV, $VHH$ , $HH \rightarrow b\bar{b}b\bar{b}$
– 0.6 to 6.6	95	<sup>11</sup> AAD	23AT ATLS	13 TeV, $b\bar{b}b\bar{b}$ , $b\bar{b}\tau\tau$ , $b\bar{b}\gamma\gamma$
– 0.4 to 6.3	95	<sup>12</sup> AAD	23AT ATLS	13 TeV, $b\bar{b}b\bar{b}$ , $b\bar{b}\tau\tau$ , $b\bar{b}\gamma\gamma$
– 3.5 to 11.3	95	<sup>13</sup> AAD	23BK ATLS	13 TeV, $b\bar{b}b\bar{b}$
– 5.4 to 14.9	95	<sup>14</sup> HAYRAPETY...23	CMS	13 TeV, $ZZ^* \rightarrow 4\ell$ cross sections
– 9.9 to 16.9	95	<sup>15</sup> TUMASYAN	23AE CMS	13 TeV, $b\bar{b}b\bar{b}$
– 1.7 to 8.7	95	<sup>16</sup> TUMASYAN	23D CMS	13 TeV, $b\bar{b}\tau\tau$
– 8.8 to 13.4	95	<sup>17</sup> TUMASYAN	23I CMS	13 TeV, $b\bar{b}ZZ^*$ ( $ZZ^* \rightarrow 4\ell$ )
– 6.9 to 11.1	95	<sup>18</sup> TUMASYAN	23O CMS	13 TeV, $WW^*WW^*$ , $WW^*\tau\tau$ , $\tau\tau\tau\tau$
– 1.5 to 6.7	95	<sup>19</sup> AAD	22Y ATLS	13 TeV, $\gamma\gamma b\bar{b}$
– 1.24 to 6.49	95	<sup>20</sup> CMS	22 CMS	13 TeV, $b\bar{b}ZZ^*$ , $b\bar{b}\gamma\gamma$ , $b\bar{b}\tau\tau$ , $b\bar{b}b\bar{b}$ , multilepton

NODE=S126KLA  
NODE=S126KLA  
NODE=S126KLA  
OCCUR=2

OCCUR=2

– 2.3 to 9.4	95	21 TUMASYAN	22AN CMS	13 TeV, $b\bar{b}b\bar{b}$	
– 3.3 to 8.5	95	22 SIRUNYAN	21K CMS	13 TeV, $\gamma\gamma b\bar{b}$	
– 5.0 to 12.0	95	23 AAD	20C ATLS	13 TeV, $b\bar{b}\gamma\gamma, b\bar{b}\tau\tau, b\bar{b}b\bar{b}, b\bar{b}WW^*, WW^*\gamma\gamma, WW^*WW^*$	
–11 to 17	95	24 SIRUNYAN	19 CMS	13 TeV, $\gamma\gamma b\bar{b}$	
–11.8 to 18.8	95	25 SIRUNYAN	19BE CMS	13 TeV, $b\bar{b}\gamma\gamma b\bar{b}\tau\tau, b\bar{b}b\bar{b}, b\bar{b}WW^*, b\bar{b}ZZ^*$	
– 8.2 to 13.2	95	26 AABOUD	18CWATLS	13 TeV, $\gamma\gamma b\bar{b}$	
		27 SIRUNYAN	18A CMS	13 TeV, $b\bar{b}\tau\tau$	
–17 to 22.5	95	28 KHACHATRY...	16BQ CMS	8 TeV, $\gamma\gamma b\bar{b}$	
<sup>1</sup> AAD 24BL combine results from 126–140 fb <sup>−1</sup> of data at $E_{\text{cm}} = 13$ TeV for $pp \rightarrow HH \rightarrow b\bar{b}b\bar{b}$ (AAD 23BK, AAD 24BV), $b\bar{b}\tau\tau$ (AAD 24AZ), $b\bar{b}\gamma\gamma$ (AAD 24X), multi-lepton (AAD 24BG), and $b\bar{b}\ell\ell$ (AAD 24Y). See their Fig. 3. All other Higgs couplings are fixed to the SM values.					NODE=S126KLA;LINKAGE=BA
<sup>2</sup> AAD 25J search for non-resonant $HHH$ production using $HHH \rightarrow b\bar{b}b\bar{b}b\bar{b}$ with data of 126 fb <sup>−1</sup> at $E_{\text{cm}} = 13$ TeV. Two-dimensional likelihood scan of $(\kappa_3 (= \kappa_\lambda), \kappa_4)$ is shown in their Fig. 9. The quoted values are obtained by assuming $\kappa_4 = 1$ . Note that the quoted values are calculated using the kappa framework, which outside the unitarity bounds requires additional modification to preserve unitarity for their results.					NODE=S126KLA;LINKAGE=CA
<sup>3</sup> HAYRAPETYAN 25F constrain the Higgs trilinear self-coupling using single and double Higgs production with data at $E_{\text{cm}} = 13$ TeV. The production modes and decay channels used are listed in their Tables 1 and 2 for single- and double-Higgs, respectively. Only single- and double-Higgs channels give $-1.8 < \kappa_\lambda < 12.0$ and $-1.7 < \kappa_\lambda < 7.0$ , respectively. All the other Higgs boson couplings are fixed to their SM values. Their Table 3 shows results with some of the couplings are loosened. Two-dimensional likelihood scan of $(\kappa_\lambda, \kappa_t)$ is shown in their Fig. 5.					NODE=S126KLA;LINKAGE=DA
<sup>4</sup> AAD 24AZ search for non-resonant $HH$ production using $HH \rightarrow b\bar{b}\tau\tau$ with data of 140 fb <sup>−1</sup> at $E_{\text{cm}} = 13$ TeV. Two-dimensional exclusion regions as a function of the $\kappa_\lambda$ and $\kappa_{2V}$ couplings are shown in their Fig. 9. All other Higgs couplings are fixed to the SM values.					NODE=S126KLA;LINKAGE=Y
<sup>5</sup> AAD 24BG search for non-resonant $HH$ production targeting the $b\bar{b}ZZ^*, VVVV, VV\tau\tau, \tau\tau\tau\tau, \gamma\gamma VV, \gamma\gamma\tau\tau$ decay channels with data of 140 fb <sup>−1</sup> at $E_{\text{cm}} = 13$ TeV. The limits are obtained with the values of all other couplings fixed to their SM value.					NODE=S126KLA;LINKAGE=S
<sup>6</sup> AAD 24X search for non-resonant $HH$ production using $HH \rightarrow b\bar{b}\gamma\gamma$ with data of 140 fb <sup>−1</sup> at $E_{\text{cm}} = 13$ TeV. Two-dimensional exclusion regions as a function of the $\kappa_\lambda$ and $\kappa_{2V}$ couplings are shown in their Fig. 6. All other Higgs couplings are fixed to the SM values.					NODE=S126KLA;LINKAGE=X
<sup>7</sup> AAD 24Y search for non-resonant $HH$ production in $2b + 2\ell + \nu s$ final state ( $\ell = e, \mu$ ) targeting $b\bar{b}WW^*, b\bar{b}ZZ^*$ , and $b\bar{b}\tau\tau$ decay channels with data of 140 fb <sup>−1</sup> at $E_{\text{cm}} = 13$ TeV. All other coupling modifiers are set to their SM values.					NODE=S126KLA;LINKAGE=R
<sup>8</sup> HAYRAPETYAN 24AE search for non-resonant $HH$ production using $HH \rightarrow b\bar{b}WW^*$ with data of 138 fb <sup>−1</sup> at $E_{\text{cm}} = 13$ TeV. Two-dimensional exclusion regions as a function of the $(\kappa_\lambda, \kappa_{2V})$ and $(\kappa_\lambda, \kappa_t)$ are shown in their Figs. 13 and 15. All other Higgs couplings are fixed to the SM values.					NODE=S126KLA;LINKAGE=Z
<sup>9</sup> HAYRAPETYAN 24AW search for non-resonant $HH$ production in association with a vector boson using $HH \rightarrow b\bar{b}b\bar{b}$ with data of 138 fb <sup>−1</sup> at $E_{\text{cm}} = 13$ TeV. The vector boson decays both leptonically ( $W \rightarrow \ell\nu, Z \rightarrow \ell\ell, \nu\nu, \ell = e, \mu$ ) and hadronically. All other Higgs couplings are fixed to the SM values. Two-dimensional exclusion regions as a function of the $\kappa_{2V}$ and $\kappa_\lambda$ parameters are shown in their Fig. 14, with other couplings fixed to the SM values. The best fit value is $(\kappa_\lambda, \kappa_{2V}) = (-2.6, 10.1)$ .					NODE=S126KLA;LINKAGE=AA
<sup>10</sup> AAD 23AD search for non-resonant $HH$ production in association with a vector boson using $HH \rightarrow b\bar{b}b\bar{b}$ with data of 139 fb <sup>−1</sup> at $E_{\text{cm}} = 13$ TeV. The vector boson decays leptonically ( $W \rightarrow \ell\nu, Z \rightarrow \ell\ell, \nu\nu, \ell = e, \mu$ ). The quoted $\kappa_\lambda$ is measured assuming all other Higgs boson couplings are at their SM value.					NODE=S126KLA;LINKAGE=F
<sup>11</sup> AAD 23AT combine results from 126–139 fb <sup>−1</sup> of data at $E_{\text{cm}} = 13$ TeV for $pp \rightarrow HH \rightarrow b\bar{b}b\bar{b}$ (AAD 23BK), $b\bar{b}\tau\tau$ (AAD 23Z), and $b\bar{b}\gamma\gamma$ (AAD 22Y). The quoted values are obtained from the profile likelihood scan as a function of $\kappa_\lambda$ as shown in their Fig. 5(a). All other coupling modifiers are assumed to have their SM values.					NODE=S126KLA;LINKAGE=M
<sup>12</sup> AAD 23AT combine results from 126–139 fb <sup>−1</sup> of data at $E_{\text{cm}} = 13$ TeV for $pp \rightarrow HH \rightarrow b\bar{b}b\bar{b}$ (AAD 23BK), $b\bar{b}\tau\tau$ (AAD 23Z), and $b\bar{b}\gamma\gamma$ (AAD 22Y) with single-Higgs boson analyses ( $\gamma\gamma, ZZ^*, WW^*, \tau\tau, b\bar{b}$ , see their Table 1). The quoted values are obtained from the profile likelihood scan as a function of $\kappa_\lambda$ as shown in their Fig. 5(a), assuming that all other Higgs boson couplings are at their SM values. Results with other assumptions are shown in their Table 2.					NODE=S126KLA;LINKAGE=N
<sup>13</sup> AAD 23BK search for non-resonant $HH$ production using $HH \rightarrow b\bar{b}b\bar{b}$ with data of 126 fb <sup>−1</sup> at $E_{\text{cm}} = 13$ TeV. The quoted values are obtained from the one-dimensional profile likelihood scan as a function of $\kappa_\lambda$ . See their Fig. 12 (a). The $\mu_{ggF+VBF}$ measurement for different values of $\kappa_\lambda$ constrains $-3.9 < \kappa_\lambda < 11.1$ at 95% CL as shown in their Fig. 10 (a). $\kappa_{2V} = \kappa_V = 1$ is assumed in both cases.					NODE=S126KLA;LINKAGE=L
<sup>14</sup> HAYRAPETYAN 23 measure the cross sections for $pp \rightarrow H \rightarrow ZZ^* \rightarrow 4\ell$ ( $\ell = e, \mu$ ) using 138 fb <sup>−1</sup> at $E_{\text{cm}} = 13$ TeV.					NODE=S126KLA;LINKAGE=O

- 15 TUMASYAN 23AE search for  $HH$  production using  $HH \rightarrow b\bar{b}b\bar{b}$ , where both  $b\bar{b}$  pairs are highly boosted, with data of  $138 \text{ fb}^{-1}$  at  $E_{\text{cm}} = 13 \text{ TeV}$ . The quoted  $\kappa_\lambda$  is measured assuming all other Higgs boson couplings are at their SM values. NODE=S126KLA;LINKAGE=G
- 16 TUMASYAN 23D search for non-resonant  $HH$  production using  $HH \rightarrow b\bar{b}\tau\tau$  with data of  $138 \text{ fb}^{-1}$  at  $E_{\text{cm}} = 13 \text{ TeV}$ . The quoted values are obtained from the upper limit on the  $HH$  production cross section times the  $b\bar{b}\tau\tau$  branching fraction for different values of  $\kappa_\lambda$ . See their Fig. 8 (left). All other coupling modifiers are assumed to be 1. In addition, two-dimensional exclusion regions as a function of the  $\kappa_\lambda$  and  $\kappa_t$  couplings, with  $\kappa_{2V} = \kappa_V = 1$ , are shown in their Fig. 9 (left). The one-dimensional likelihood scan as a function of  $\kappa_\lambda$  is given in their Fig 10 (left), from which a 95% confidence interval of  $-1.77 < \kappa_\lambda < 8.73$  is extracted. NODE=S126KLA;LINKAGE=J
- 17 TUMASYAN 23AI search for non-resonant  $HH$  production using  $HH \rightarrow b\bar{b}ZZ^*$  ( $ZZ^* \rightarrow 4\ell, \ell=e,\mu$ ) with data of  $138 \text{ fb}^{-1}$  at  $E_{\text{cm}} = 13 \text{ TeV}$ . See their Fig. 4. NODE=S126KLA;LINKAGE=E
- 18 TUMASYAN 23O search for non-resonant  $HH$  production using  $HH \rightarrow WW^*WW^*, WW^*\tau\tau$ , and  $\tau\tau\tau\tau$  (multilepton) with data of  $138 \text{ fb}^{-1}$  at  $E_{\text{cm}} = 13 \text{ TeV}$ . See their Fig. 10 for different final states and these combination. Limits are set on a variety of new-physics models using an effective field theory approach. See their Figs. 11, 12, and 13. NODE=S126KLA;LINKAGE=K
- 19 AAD 22Y search for non-resonant  $HH$  production using  $HH \rightarrow \gamma\gamma b\bar{b}$  with data of  $139 \text{ fb}^{-1}$  at  $E_{\text{cm}} = 13 \text{ TeV}$ . The quoted  $\kappa_\lambda$  is obtained from their Fig. 12 where the theory uncertainties are not included while a negative log-likelihood scan vs.  $\kappa_\lambda$  is shown in their Fig. 13 with the theory uncertainties, which provides  $\kappa_\lambda = 2.8^{+2.0}_{-2.2}$  for the  $1\sigma$  confidence interval. NODE=S126KLA;LINKAGE=V
- 20 CMS 22 report combined results (see their Extended Data Table 2) using  $138 \text{ fb}^{-1}$  of data at  $E_{\text{cm}} = 13 \text{ TeV}$ . See their Fig. 6 (left). NODE=S126KLA;LINKAGE=U
- 21 TUMASYAN 22AN search for non-resonant  $HH$  production using  $HH \rightarrow b\bar{b}b\bar{b}$  with data of  $138 \text{ fb}^{-1}$  at  $E_{\text{cm}} = 13 \text{ TeV}$ . The upper limit on the  $pp \rightarrow HH$  production cross section at 95% CL is shown as a function of  $\kappa_\lambda$  in their Fig. 2 (top). NODE=S126KLA;LINKAGE=W
- 22 SIRUNYAN 21K search for non-resonant  $HH$  production using  $HH \rightarrow \gamma\gamma b\bar{b}$  with data of  $137 \text{ fb}^{-1}$  at  $E_{\text{cm}} = 13 \text{ TeV}$ . NODE=S126KLA;LINKAGE=T
- 23 AAD 20C combine results of up to  $36.1 \text{ fb}^{-1}$  data at  $E_{\text{cm}} = 13 \text{ TeV}$  for  $pp \rightarrow HH \rightarrow b\bar{b}\gamma\gamma, b\bar{b}\tau\tau, b\bar{b}b\bar{b}, b\bar{b}WW^*, WW^*\gamma\gamma, WW^*WW^*$  (AABOUD 18CW, AABOUD 18CQ, AABOUD 19A, AABOUD 190, AABOUD 18BU, and AABOUD 19T). NODE=S126KLA;LINKAGE=Q
- 24 SIRUNYAN 19 search for  $HH$  production using  $HH \rightarrow \gamma\gamma b\bar{b}$  with data of  $35.9 \text{ fb}^{-1}$  at  $E_{\text{cm}} = 13 \text{ TeV}$ . The quoted  $\kappa_\lambda$  is measured assuming all other Higgs boson couplings are at their SM value. NODE=S126KLA;LINKAGE=H
- 25 SIRUNYAN 19BE combine results of 13 TeV  $35.9 \text{ fb}^{-1}$  data: SIRUNYAN 19, SIRUNYAN 18A, SIRUNYAN 19AB, SIRUNYAN 19H, and SIRUNYAN 18F. NODE=S126KLA;LINKAGE=P
- 26 AABOUD 18CW search for  $HH$  production using  $HH \rightarrow \gamma\gamma b\bar{b}$  with data of  $36.1 \text{ fb}^{-1}$  at  $E_{\text{cm}} = 13 \text{ TeV}$ . The quoted  $\kappa_\lambda$  is measured assuming all other Higgs boson couplings are at their SM value. NODE=S126KLA;LINKAGE=I
- 27 SIRUNYAN 18A search for  $HH$  production using  $HH \rightarrow b\bar{b}\tau\tau$  with data of  $35.9 \text{ fb}^{-1}$  at  $E_{\text{cm}} = 13 \text{ TeV}$ . The upper limit on production cross section times branching fraction at 95% CL is shown as a function of  $\kappa_\lambda/\kappa_t$  in their Fig. 6 (top) where  $\kappa_t = y_t / y_t^{\text{SM}}$  (top Yukawa coupling  $y_t$ ). NODE=S126KLA;LINKAGE=C
- 28 KHACHATRYAN 16BQ search for  $HH$  production using  $HH \rightarrow \gamma\gamma b\bar{b}$  with data of  $19.7 \text{ fb}^{-1}$  at  $E_{\text{cm}} = 8 \text{ TeV}$ . NODE=S126KLA;LINKAGE=D

### Higgs quartic self coupling modifier $\kappa_4$

Signal strength relative to the SM prediction,  $\kappa_4 = \lambda_{HHHH}/\lambda_{HHHH}^{\text{SM}}$ .

VALUE	CL%	DOCUMENT ID	TECN	COMMENT
-------	-----	-------------	------	---------

• • • We do not use the following data for averages, fits, limits, etc. • • •

–230 to 240 95 1 AAD 25J ATLS 13 TeV,  $b\bar{b}b\bar{b}b\bar{b}$

1 AAD 25J search for non-resonant  $HHH$  production using  $HHH \rightarrow b\bar{b}b\bar{b}b\bar{b}$  with data of  $126 \text{ fb}^{-1}$  at  $E_{\text{cm}} = 13 \text{ TeV}$ . Two-dimensional likelihood scan of  $(\kappa_3 (= \kappa_\lambda), \kappa_4)$  is shown in their Fig. 9. The quoted values are obtained by assuming  $\kappa_3 = 1$ . Note that the quoted values are calculated using the kappa framework, which outside the unitarity bounds requires additional modification to preserve unitarity for their results.

### Higgs-gauge boson quartic coupling modifier $\kappa_{2V}$

Signal strength relative to the SM prediction,  $\kappa_{2V} = \lambda_{VVHH}/\lambda_{VVHH}^{\text{SM}}$ ,  $V = W, Z$ .

VALUE	CL%	DOCUMENT ID	TECN	COMMENT
-------	-----	-------------	------	---------

1.02<sup>+0.22</sup><sub>-0.23</sub> 1 AAD 24BL ATLS 13 TeV,  $b\bar{b}b\bar{b}, b\bar{b}\tau\tau, b\bar{b}\gamma\gamma$ , multilepton,  $b\bar{b}\ell\ell$

NODE=S126KH4

NODE=S126KH4

NODE=S126KH4

NODE=S126KH4;LINKAGE=A

NODE=S126K2V

NODE=S126K2V

NODE=S126K2V

OCCUR=2





- <sup>11</sup> AAD 23AD search for non-resonant  $HH$  production in association with a vector boson using  $HH \rightarrow b\bar{b}b\bar{b}$  with data of  $139 \text{ fb}^{-1}$  at  $E_{\text{cm}} = 13 \text{ TeV}$ . The vector boson decays leptonically ( $W \rightarrow \ell\nu$ ,  $Z \rightarrow \ell\ell$ ,  $\nu\nu$ ,  $\ell = e, \mu$ ). The constraints on  $\kappa_{2W}$  and  $\kappa_{2Z}$  are separately measured to be  $-12.3 < \kappa_{2W} < 13.5$  and  $-9.9 < \kappa_{2Z} < 11.3$  (95% CL). The quoted  $\kappa_{2V}$  ( $V = W, Z$ ) is measured assuming all other Higgs boson couplings are at their SM value.
- <sup>12</sup> AAD 23AT combine results from  $126\text{--}139 \text{ fb}^{-1}$  of data at  $E_{\text{cm}} = 13 \text{ TeV}$  for  $pp \rightarrow HH \rightarrow b\bar{b}b\bar{b}$  (AAD 23BK),  $b\bar{b}\tau\tau$  (AAD 23Z), and  $b\bar{b}\gamma\gamma$  (AAD 22Y). The quoted values are obtained from the 95% CL VBF  $HH$  cross-section upper limit as a function of  $\kappa_{2V}$  as shown in their Fig. 4(b). All other coupling modifiers are assumed to have their SM values.
- <sup>13</sup> AAD 23BK search for non-resonant  $HH$  production using  $HH \rightarrow b\bar{b}b\bar{b}$  with data of  $126 \text{ fb}^{-1}$  at  $E_{\text{cm}} = 13 \text{ TeV}$ . The quoted values are obtained from the one-dimensional profile likelihood scan as a function of  $\kappa_{2V}$ . See their Fig. 12 (b). The  $\mu_{VBF}$  measurement for different values of  $\kappa_{2V}$  constrains  $-0.03 < \kappa_{2V} < 2.11$  at 95% CL as shown in their Fig. 10 (b).  $\kappa_\lambda = \kappa_V = 1$  is assumed in both cases.
- <sup>14</sup> TUMASYAN 23AE search for  $HH$  production using  $HH \rightarrow b\bar{b}b\bar{b}$ , where both  $b\bar{b}$  pairs are highly boosted, with data of  $138 \text{ fb}^{-1}$  at  $E_{\text{cm}} = 13 \text{ TeV}$ . The  $\kappa_{2V} = 0$  is excluded at  $6.3 \sigma$  assuming all other Higgs boson couplings are at their SM values.
- <sup>15</sup> TUMASYAN 23D search for non-resonant  $HH$  production using  $HH \rightarrow b\bar{b}\tau\tau$  with data of  $138 \text{ fb}^{-1}$  at  $E_{\text{cm}} = 13 \text{ TeV}$ . The quoted values are obtained from the upper limits on the  $HH$  production cross section times the  $b\bar{b}\tau\tau$  branching fraction for different values of  $\kappa_{2V}$ . See their Fig. 8 (right). All other coupling modifiers are assumed to be 1. In addition, two-dimensional exclusion regions as a function of the  $\kappa_{2V}$  and  $\kappa_V$  couplings, with  $\kappa_\lambda = \kappa_t = 1$ , are shown in their Fig. 9 (right). The one-dimensional likelihood scan as a function of  $\kappa_{2V}$  is given in their Fig. 10 (right), from which a 95% confidence interval of  $-0.34 < \kappa_{2V} < 2.49$  is extracted.
- <sup>16</sup> CMS 22 report combined results (see their Extended Data Table 2) using  $138 \text{ fb}^{-1}$  of data at  $E_{\text{cm}} = 13 \text{ TeV}$ . See their Fig. 6 (right).
- <sup>17</sup> TUMASYAN 22AN search for non-resonant  $HH$  production using  $HH \rightarrow b\bar{b}b\bar{b}$  with data of  $138 \text{ fb}^{-1}$  at  $E_{\text{cm}} = 13 \text{ TeV}$ . The upper limit on the  $pp \rightarrow HH$  production cross section at 95% CL is shown as a function of  $\kappa_{2V}$  in their Fig. 2 (bottom).
- <sup>18</sup> SIRUNYAN 21K search for non-resonant  $HH$  production using  $HH \rightarrow \gamma\gamma b\bar{b}$  with data of  $137 \text{ fb}^{-1}$  at  $E_{\text{cm}} = 13 \text{ TeV}$ .
- <sup>19</sup> AAD 20X search for  $HH \rightarrow b\bar{b}b\bar{b}$  process via VBF with data of  $126 \text{ fb}^{-1}$  at  $E_{\text{cm}} = 13 \text{ TeV}$ .

NODE=S126K2V;LINKAGE=H

NODE=S126K2V;LINKAGE=L

NODE=S126K2V;LINKAGE=K

NODE=S126K2V;LINKAGE=I

NODE=S126K2V;LINKAGE=J

NODE=S126K2V;LINKAGE=G

NODE=S126K2V;LINKAGE=A

NODE=S126K2V;LINKAGE=E

NODE=S126K2V;LINKAGE=F

### $H$ production cross section in $pp$ collisions at $\sqrt{s} = 13 \text{ TeV}$

VALUE (pb)	DOCUMENT ID	TECN	COMMENT
<b><math>56.8 \pm 3.4</math> OUR AVERAGE</b>			
$55.5^{+4.0}_{-3.8}$	<sup>1</sup> AAD	23C ATLS	$pp$ , 13 TeV, $\gamma\gamma$ , $ZZ^* \rightarrow 4\ell$ ( $\ell = e, \mu$ )
$61.1 \pm 6.0 \pm 3.7$	<sup>2</sup> SIRUNYAN	19BA CMS	$pp$ , 13 TeV, $\gamma\gamma$ , $ZZ^* \rightarrow 4\ell$ ( $\ell = e, \mu$ )
• • • We do not use the following data for averages, fits, limits, etc. • • •			
$58 \pm 4 \pm 4$	<sup>3</sup> AAD	22N ATLS	$pp$ , 13 TeV, $\gamma\gamma$
$53.5 \pm 4.9 \pm 2.1$	<sup>4</sup> AAD	20BA ATLS	$pp$ , 13 TeV, $ZZ^* \rightarrow 4\ell$ ( $\ell = e, \mu$ )
$57.0^{+6.0+4.0}_{-5.9-3.3}$	<sup>5</sup> AABOUD	18CG ATLS	$pp$ , 13 TeV, $\gamma\gamma$ , $ZZ^* \rightarrow 4\ell$ ( $\ell = e, \mu$ )
$47.9^{+9.1}_{-8.6}$	<sup>5</sup> AABOUD	18CG ATLS	$pp$ , 13 TeV, $\gamma\gamma$
$68^{+11}_{-10}$	<sup>5</sup> AABOUD	18CG ATLS	$pp$ , 13 TeV, $ZZ^* \rightarrow 4\ell$ ( $\ell = e, \mu$ )
$69^{+10}_{-9} \pm 5$	<sup>6</sup> AABOUD	17CO ATLS	$pp$ , 13 TeV, $ZZ^* \rightarrow 4\ell$

NODE=S126A02  
NODE=S126A02

OCCUR=2

OCCUR=3

- <sup>1</sup> AAD 23C combine AAD 22N and AAD 20BA, where both use  $139 \text{ fb}^{-1}$  of  $pp$  collisions at  $E_{\text{cm}} = 13 \text{ TeV}$ . The Higgs production cross sections at  $E_{\text{cm}} = 7$  and  $8 \text{ TeV}$  are obtained to be  $34^{+11}_{-10} \text{ pb}$  and  $33.3^{+5.8}_{-5.4} \text{ pb}$ , respectively. The quoted value is given for  $m_H = 125.09 \text{ GeV}$ . The differential cross sections are given in their Figs. 3 and 4.
- <sup>2</sup> SIRUNYAN 19BA use  $35.9 \text{ fb}^{-1}$  of  $pp$  collisions at  $E_{\text{cm}} = 13 \text{ TeV}$ . The quoted value is given for  $m_H = 125.09 \text{ GeV}$ .
- <sup>3</sup> AAD 22N use  $139 \text{ fb}^{-1}$  of  $pp$  collisions at  $E_{\text{cm}} = 13 \text{ TeV}$ . The quoted value is given for  $m_H = 125.09 \text{ GeV}$ .
- <sup>4</sup> AAD 20BA use  $139 \text{ fb}^{-1}$  of  $pp$  collisions at  $E_{\text{cm}} = 13 \text{ TeV}$  with  $H \rightarrow ZZ^* \rightarrow 4\ell$  where  $\ell = e, \mu$ . The quoted value is given for  $m_H = 125 \text{ GeV}$  and assumes the Standard Model branching ratio.
- <sup>5</sup> AABOUD 18CG use  $36.1 \text{ fb}^{-1}$  of  $pp$  collisions at  $E_{\text{cm}} = 13 \text{ TeV}$ . All the quoted values are given for  $m_H = 125.09 \text{ GeV}$ .
- <sup>6</sup> AABOUD 17CO use  $36.1 \text{ fb}^{-1}$  of  $pp$  collisions at  $E_{\text{cm}} = 13 \text{ TeV}$  with  $H \rightarrow ZZ^* \rightarrow 4\ell$  where  $\ell = e, \mu$  for  $m_H = 125 \text{ GeV}$ . Differential cross sections for the Higgs boson transverse momentum, Higgs boson rapidity, and other related quantities are measured as shown in their Figs. 8 and 9.

NODE=S126A02;LINKAGE=F

NODE=S126A02;LINKAGE=C

NODE=S126A02;LINKAGE=E

NODE=S126A02;LINKAGE=D

NODE=S126A02;LINKAGE=A

NODE=S126A02;LINKAGE=B

**$H$  production cross section in  $pp$  collisions at  $\sqrt{s} = 13.6$  TeV**

VALUE (pb)	DOCUMENT ID	TECN	COMMENT
<b>58.2±8.7</b>	<sup>1</sup> AAD	24AQ ATLS	$pp$ , 13.6 TeV, $\gamma\gamma$ , $ZZ^* \rightarrow 4\ell$ ( $\ell = e, \mu$ )

<sup>1</sup> AAD 24AQ measure the total cross section to be  $67^{+12}_{-11}$  pb and  $46 \pm 12$  pb using  $H \rightarrow \gamma\gamma$  and  $H \rightarrow ZZ^* \rightarrow 4\ell$ , respectively, with data of  $31.4 \text{ fb}^{-1}$  and  $29.0 \text{ fb}^{-1}$  of  $pp$  collisions at  $E_{\text{cm}} = 13.6$  TeV. The SM expected value is  $59.9 \pm 2.6$  pb. All the values are given for  $m_H = 125.09$  GeV.

NODE=S126A03  
NODE=S126A03

NODE=S126A03;LINKAGE=A

 **$H$  REFERENCES**

AAD	25AG	JHEP 2508 034	G. Aad <i>et al.</i>	(ATLAS Collab.)	REFID=63492
AAD	25AJ	EPJ C85 210	G. Aad <i>et al.</i>	(ATLAS Collab.)	REFID=63502
AAD	25AP	PL B865 139449 (errat.)	G. Aad <i>et al.</i>	(ATLAS Collab.)	REFID=63558
AAD	25AQ	RPP 88 057803	G. Aad <i>et al.</i>	(ATLAS Collab.)	REFID=63599
AAD	25E	PL B861 139277	G. Aad <i>et al.</i>	(ATLAS Collab.)	REFID=63356
AAD	25J	PR D111 032006	G. Aad <i>et al.</i>	(ATLAS Collab.)	REFID=63374
AAD	25R	JHEP 2502 045	G. Aad <i>et al.</i>	(ATLAS Collab.)	REFID=63436
AAD	25W	JHEP 2503 010	G. Aad <i>et al.</i>	(ATLAS Collab.)	REFID=63449
AAD	25Y	JHEP 2504 075	G. Aad <i>et al.</i>	(ATLAS Collab.)	REFID=63458
CHEKHOVSKY	25A	JHEP 2503 114	V. Chekhovsky <i>et al.</i>	(CMS Collab.)	REFID=63452
CHEKHOVSKY	25B	JHEP 2505 079	V. Chekhovsky <i>et al.</i>	(CMS Collab.)	REFID=63468
HAYRAPETY...	25	PL B860 139173	A. Hayrapetyan <i>et al.</i>	(CMS Collab.)	REFID=63167
HAYRAPETY...	25AC	PRL 135 091802	A. Hayrapetyan <i>et al.</i>	(CMS Collab.)	REFID=63539
HAYRAPETY...	25B	PL B860 139202	A. Hayrapetyan <i>et al.</i>	(CMS Collab.)	REFID=63170
HAYRAPETY...	25F	PL B861 139210	A. Hayrapetyan <i>et al.</i>	(CMS Collab.)	REFID=63355
HAYRAPETY...	25G	PL B862 139296	A. Hayrapetyan <i>et al.</i>	(CMS Collab.)	REFID=63357
HAYRAPETY...	25H	PL B865 139462	A. Hayrapetyan <i>et al.</i>	(CMS Collab.)	REFID=63358
HAYRAPETY...	25L	PR D111 092014	A. Hayrapetyan <i>et al.</i>	(CMS Collab.)	REFID=63402
HAYRAPETY...	25R	JHEP 2502 097	A. Hayrapetyan <i>et al.</i>	(CMS Collab.)	REFID=63442
AAD	24AG	JHEP 2405 105	G. Aad <i>et al.</i>	(ATLAS Collab.)	REFID=62853
AAD	24AQ	EPJ C84 78	G. Aad <i>et al.</i>	(ATLAS Collab.)	REFID=62882
AAD	24AZ	PR D110 032012	G. Aad <i>et al.</i>	(ATLAS Collab.)	REFID=62935
AAD	24BE	PL B855 138817	G. Aad <i>et al.</i>	(ATLAS Collab.)	REFID=62960
AAD	24BG	JHEP 2408 164	G. Aad <i>et al.</i>	(ATLAS Collab.)	REFID=62989
AAD	24BH	JHEP 2408 153	G. Aad <i>et al.</i>	(ATLAS Collab.)	REFID=62990
AAD	24BL	PRL 133 101801	G. Aad <i>et al.</i>	(ATLAS Collab.)	REFID=63041
AAD	24BM	PRL 133 141801	G. Aad <i>et al.</i>	(ATLAS Collab.)	REFID=63052
AAD	24BV	PL B858 139007	G. Aad <i>et al.</i>	(ATLAS Collab.)	REFID=63118
AAD	24D	PRL 132 021803	G. Aad <i>et al.</i>	(ATLAS and CMS Collabs.)	REFID=62627
AAD	24F	PRL 132 131802	G. Aad <i>et al.</i>	(ATLAS Collab.)	REFID=62720
AAD	24J	PL B849 138469	G. Aad <i>et al.</i>	(ATLAS Collab.)	REFID=62745
AAD	24R	PL B855 138762	G. Aad <i>et al.</i>	(ATLAS Collab.)	REFID=62759
AAD	24X	JHEP 2401 066	G. Aad <i>et al.</i>	(ATLAS Collab.)	REFID=62828
AAD	24Y	JHEP 2402 037	G. Aad <i>et al.</i>	(ATLAS Collab.)	REFID=62832
HAYRAPETY...	24AE	JHEP 2407 293	A. Hayrapetyan <i>et al.</i>	(CMS Collab.)	REFID=62876
HAYRAPETY...	24AG	EPJ C84 779	A. Hayrapetyan <i>et al.</i>	(CMS Collab.)	REFID=62898
HAYRAPETY...	24AM	EPJ C84 712	A. Hayrapetyan <i>et al.</i>	(CMS Collab.)	REFID=62996
HAYRAPETY...	24AT	PL B857 138964	A. Hayrapetyan <i>et al.</i>	(CMS Collab.)	REFID=63115
HAYRAPETY...	24AW	JHEP 2410 061	A. Hayrapetyan <i>et al.</i>	(CMS Collab.)	REFID=63126
HAYRAPETY...	24AY	JHEP 2412 035	A. Hayrapetyan <i>et al.</i>	(CMS Collab.)	REFID=63141
HAYRAPETY...	24D	PRL 132 121901	A. Hayrapetyan <i>et al.</i>	(CMS Collab.)	REFID=62717
HAYRAPETY...	24U	JHEP 2401 173	A. Hayrapetyan <i>et al.</i>	(CMS Collab.)	REFID=62830
TUMASYAN	24	PR D109 092011	A. Tumasyan <i>et al.</i>	(CMS Collab.)	REFID=62798
AABOUD	23A	JHEP 2312 158 (errat.)	M. Aaboud <i>et al.</i>	(ATLAS Collab.)	REFID=62575
AAD	23A	PL B842 137963	G. Aad <i>et al.</i>	(ATLAS Collab.)	REFID=62107
AAD	23AD	EPJ C83 519	G. Aad <i>et al.</i>	(ATLAS Collab.)	REFID=62169
AAD	23AF	EPJ C83 503	G. Aad <i>et al.</i>	(ATLAS Collab.)	REFID=62171
AAD	23AK	EPJ C83 563	G. Aad <i>et al.</i>	(ATLAS Collab.)	REFID=62180
AAD	23AN	PRL 131 061802	G. Aad <i>et al.</i>	(ATLAS Collab.)	REFID=62321
AAD	23AP	PR D108 032005	G. Aad <i>et al.</i>	(ATLAS Collab.)	REFID=62344
AAD	23AT	PL B843 137745	G. Aad <i>et al.</i>	(ATLAS Collab.)	REFID=62361
AAD	23AU	PL B843 137880	G. Aad <i>et al.</i>	(ATLAS Collab.)	REFID=62363
AAD	23BC	EPJ C83 496	G. Aad <i>et al.</i>	(ATLAS Collab.)	REFID=62381
Also		EPJ C84 156 (errat.)	G. Aad <i>et al.</i>	(ATLAS Collab.)	REFID=62994
AAD	23BK	PR D108 052003	G. Aad <i>et al.</i>	(ATLAS Collab.)	REFID=62408
AAD	23BP	PRL 131 251802	G. Aad <i>et al.</i>	(ATLAS Collab.)	REFID=62471
AAD	23BR	PL B846 138223	G. Aad <i>et al.</i>	(ATLAS Collab.)	REFID=62477
Also		PL B854 138734 (errat.)	G. Aad <i>et al.</i>	(ATLAS Collab.)	REFID=62757
Also		PL B865 139449 (errat.)	G. Aad <i>et al.</i>	(ATLAS Collab.)	REFID=63558
AAD	23BS	PL B847 138292	G. Aad <i>et al.</i>	(ATLAS Collab.)	REFID=62479
AAD	23BU	PL B847 138315	G. Aad <i>et al.</i>	(ATLAS Collab.)	REFID=62481
AAD	23BV	PR D108 072003	G. Aad <i>et al.</i>	(ATLAS Collab.)	REFID=62488
AAD	23C	JHEP 2305 028	G. Aad <i>et al.</i>	(ATLAS Collab.)	REFID=62115
AAD	23CD	EPJ C83 781	G. Aad <i>et al.</i>	(ATLAS Collab.)	REFID=62546
AAD	23Q	JHEP 2307 166	G. Aad <i>et al.</i>	(ATLAS Collab.)	REFID=62138
AAD	23Y	JHEP 2307 088	G. Aad <i>et al.</i>	(ATLAS Collab.)	REFID=62154
AAD	23Z	JHEP 2307 040	G. Aad <i>et al.</i>	(ATLAS Collab.)	REFID=62161
HAYRAPETY...	23	JHEP 2308 040	A. Hayrapetyan <i>et al.</i>	(CMS Collab.)	REFID=62378
HAYRAPETY...	23C	PR D108 072004	A. Hayrapetyan <i>et al.</i>	(CMS Collab.)	REFID=62489
TUMASYAN	23AD	PRL 131 041801	A. Tumasyan <i>et al.</i>	(CMS Collab.)	REFID=62238
TUMASYAN	23AE	PRL 131 041803	A. Tumasyan <i>et al.</i>	(CMS Collab.)	REFID=62239
TUMASYAN	23AH	PRL 131 061801	A. Tumasyan <i>et al.</i>	(CMS Collab.)	REFID=62320
TUMASYAN	23AI	PR D108 032008	A. Tumasyan <i>et al.</i>	(CMS Collab.)	REFID=62347
TUMASYAN	23AJ	PR D108 032013	A. Tumasyan <i>et al.</i>	(CMS Collab.)	REFID=62351
TUMASYAN	23AU	PL B846 137783	A. Tumasyan <i>et al.</i>	(CMS Collab.)	REFID=62475
TUMASYAN	23BA	EPJ C83 933	A. Tumasyan <i>et al.</i>	(CMS Collab.)	REFID=62551
TUMASYAN	23C	PL B842 137534	A. Tumasyan <i>et al.</i>	(CMS Collab.)	REFID=62104
TUMASYAN	23D	PL B842 137531	A. Tumasyan <i>et al.</i>	(CMS Collab.)	REFID=62105
TUMASYAN	23F	JHEP 2305 233	A. Tumasyan <i>et al.</i>	(CMS Collab.)	REFID=62112
TUMASYAN	23I	JHEP 2306 130	A. Tumasyan <i>et al.</i>	(CMS Collab.)	REFID=62125
TUMASYAN	23O	JHEP 2307 095	A. Tumasyan <i>et al.</i>	(CMS Collab.)	REFID=62150
TUMASYAN	23P	JHEP 2307 092	A. Tumasyan <i>et al.</i>	(CMS Collab.)	REFID=62151
TUMASYAN	23Q	JHEP 2307 091	A. Tumasyan <i>et al.</i>	(CMS Collab.)	REFID=62152

NODE=S126

TUMASYAN	23W	EPJ C83 667	A. Tumasyan <i>et al.</i>	(CMS Collab.)	REFID=62174
TUMASYAN	23Y	EPJ C83 562	A. Tumasyan <i>et al.</i>	(CMS Collab.)	REFID=62181
AAD	22D	PL B829 137066	G. Aad <i>et al.</i>	(ATLAS Collab.)	REFID=61705
AAD	22M	JHEP 2206 097	G. Aad <i>et al.</i>	(ATLAS Collab.)	REFID=61806
AAD	22N	JHEP 2208 027	G. Aad <i>et al.</i>	(ATLAS Collab.)	REFID=61815
AAD	22P	JHEP 2208 104	G. Aad <i>et al.</i>	(ATLAS Collab.)	REFID=61818
AAD	22Q	JHEP 2208 175	G. Aad <i>et al.</i>	(ATLAS Collab.)	REFID=61819
AAD	22S	EPJ C82 105	G. Aad <i>et al.</i>	(ATLAS Collab.)	REFID=61823
AAD	22V	EPJ C82 622	G. Aad <i>et al.</i>	(ATLAS Collab.)	REFID=61835
AAD	22W	EPJ C82 717	G. Aad <i>et al.</i>	(ATLAS Collab.)	REFID=61837
AAD	22X	PR D105 092003	G. Aad <i>et al.</i>	(ATLAS Collab.)	REFID=61869
AAD	22Y	PR D106 052001	G. Aad <i>et al.</i>	(ATLAS Collab.)	REFID=61938
ATLAS	22	NAT 607 52	ATLAS Collaboration	(ATLAS Collab.)	REFID=61850;ERROR=1
Also		NAT 612 E24 (errat.)	ATLAS Collaboration	(ATLAS Collab.)	REFID=61997;ERROR=2
CMS	22	NAT 607 60	CMS Collaboration	(CMS Collab.)	REFID=61851;ERROR=3
TUMASYAN	22AJ	PRL 128 081805	A. Tumasyan <i>et al.</i>	(CMS Collab.)	REFID=61864
TUMASYAN	22AM	NATP 18 1329	A. Tumasyan <i>et al.</i>	(CMS Collab.)	REFID=61979
TUMASYAN	22AN	PRL 129 081802	A. Tumasyan <i>et al.</i>	(CMS Collab.)	REFID=61984
TUMASYAN	22G	PR D105 092007	A. Tumasyan <i>et al.</i>	(CMS Collab.)	REFID=61742
TUMASYAN	22Y	JHEP 2206 012	A. Tumasyan <i>et al.</i>	(CMS Collab.)	REFID=61803
AAD	21	PL B812 135980	G. Aad <i>et al.</i>	(ATLAS Collab.)	REFID=60710
AAD	21AB	EPJ C81 178	G. Aad <i>et al.</i>	(ATLAS Collab.)	REFID=61324
AAD	21AJ	EPJ C81 537	G. Aad <i>et al.</i>	(ATLAS Collab.)	REFID=61338
AAD	21F	PR D103 112006	G. Aad <i>et al.</i>	(ATLAS Collab.)	REFID=61247
AAD	21H	PL B816 136204	G. Aad <i>et al.</i>	(ATLAS Collab.)	REFID=61268
AAD	21I	PL B819 136412	G. Aad <i>et al.</i>	(ATLAS Collab.)	REFID=61272
AAD	21M	JHEP 2103 268	G. Aad <i>et al.</i>	(ATLAS Collab.)	REFID=61284
SIRUNYAN	21	PL B812 135992	A.M. Sirunyan <i>et al.</i>	(CMS Collab.)	REFID=60712
SIRUNYAN	21A	EPJ C81 13	A.M. Sirunyan <i>et al.</i>	(CMS Collab.)	REFID=60775
Also		EPJ C81 333 (errat.)	A.M. Sirunyan <i>et al.</i>	(CMS Collab.)	REFID=61322
SIRUNYAN	21AE	PR D104 052004	A.M. Sirunyan <i>et al.</i>	(CMS Collab.)	REFID=61514
SIRUNYAN	21B	EPJ C81 3	A.M. Sirunyan <i>et al.</i>	(CMS Collab.)	REFID=60776
SIRUNYAN	21C	JHEP 2101 148	A.M. Sirunyan <i>et al.</i>	(CMS Collab.)	REFID=61041
SIRUNYAN	21K	JHEP 2103 257	A.M. Sirunyan <i>et al.</i>	(CMS Collab.)	REFID=61285
SIRUNYAN	21L	JHEP 2103 011	A.M. Sirunyan <i>et al.</i>	(CMS Collab.)	REFID=61292
SIRUNYAN	21O	JHEP 2107 027	A.M. Sirunyan <i>et al.</i>	(CMS Collab.)	REFID=61320
SIRUNYAN	21R	EPJ C81 378	A.M. Sirunyan <i>et al.</i>	(CMS Collab.)	REFID=61331
SIRUNYAN	21S	EPJ C81 488	A.M. Sirunyan <i>et al.</i>	(CMS Collab.)	REFID=61339
SIRUNYAN	21Z	PR D104 032013	A.M. Sirunyan <i>et al.</i>	(CMS Collab.)	REFID=61390
TUMASYAN	21D	JHEP 2111 153	A. Tumasyan <i>et al.</i>	(CMS Collab.)	REFID=61559
AAD	20	PR D101 012002	G. Aad <i>et al.</i>	(ATLAS Collab.)	REFID=60046
AAD	20A	PL B800 135069	G. Aad <i>et al.</i>	(ATLAS Collab.)	REFID=60143
AAD	20AE	PRL 125 221802	G. Aad <i>et al.</i>	(ATLAS Collab.)	REFID=60697
AAD	20AG	PL B809 135754	G. Aad <i>et al.</i>	(ATLAS Collab.)	REFID=60706
AAD	20AQ	EPJ C80 957	G. Aad <i>et al.</i>	(ATLAS Collab.)	REFID=60770
Also		EPJ C81 29 (errat.)	G. Aad <i>et al.</i>	(ATLAS Collab.)	REFID=61321
Also		EPJ C81 398 (errat.)	G. Aad <i>et al.</i>	(ATLAS Collab.)	REFID=61336
AAD	20BA	EPJ C80 942	G. Aad <i>et al.</i>	(ATLAS Collab.)	REFID=60917
AAD	20C	PL B800 135103	G. Aad <i>et al.</i>	(ATLAS Collab.)	REFID=60147
AAD	20E	PL B801 135145	G. Aad <i>et al.</i>	(ATLAS Collab.)	REFID=60193
AAD	20F	PL B801 135148	G. Aad <i>et al.</i>	(ATLAS Collab.)	REFID=60194
AAD	20N	PL B805 135426	G. Aad <i>et al.</i>	(ATLAS Collab.)	REFID=60399
AAD	20X	JHEP 2007 108	G. Aad <i>et al.</i>	(ATLAS Collab.)	REFID=60511
Also		JHEP 2101 145 (errat.)	G. Aad <i>et al.</i>	(ATLAS Collab.)	REFID=61275
Also		JHEP 2105 207 (errat.)	G. Aad <i>et al.</i>	(ATLAS Collab.)	REFID=61301
AAD	20Z	PRL 125 061802	G. Aad <i>et al.</i>	(ATLAS Collab.)	REFID=60576
SIRUNYAN	20AE	JHEP 2003 131	A.M. Sirunyan <i>et al.</i>	(CMS Collab.)	REFID=60483
SIRUNYAN	20AH	JHEP 2005 032	A.M. Sirunyan <i>et al.</i>	(CMS Collab.)	REFID=60491
SIRUNYAN	20AS	PRL 125 061801	A.M. Sirunyan <i>et al.</i>	(CMS Collab.)	REFID=60575
SIRUNYAN	20BK	JHEP 2011 039	A.M. Sirunyan <i>et al.</i>	(CMS Collab.)	REFID=60763
SIRUNYAN	20BL	JHEP 2012 085	A.M. Sirunyan <i>et al.</i>	(CMS Collab.)	REFID=60766
SIRUNYAN	20C	EPJ C80 75	A.M. Sirunyan <i>et al.</i>	(CMS Collab.)	REFID=60222
SIRUNYAN	20L	PL B805 135425	A.M. Sirunyan <i>et al.</i>	(CMS Collab.)	REFID=60398
AABOUD	19A	JHEP 1901 030	M. Aaboud <i>et al.</i>	(ATLAS Collab.)	REFID=59370
AABOUD	19AI	PL B793 499	M. Aaboud <i>et al.</i>	(ATLAS Collab.)	REFID=59755
AABOUD	19AL	PRL 122 231801	M. Aaboud <i>et al.</i>	(ATLAS Collab.)	REFID=59792
AABOUD	19AQ	PR D99 072001	M. Aaboud <i>et al.</i>	(ATLAS Collab.)	REFID=59853
AABOUD	19F	PL B789 508	M. Aaboud <i>et al.</i>	(ATLAS Collab.)	REFID=59431
AABOUD	19N	JHEP 1904 048	M. Aaboud <i>et al.</i>	(ATLAS Collab.)	REFID=59669
AABOUD	19O	JHEP 1904 092	M. Aaboud <i>et al.</i>	(ATLAS Collab.)	REFID=59672
AABOUD	19T	JHEP 1905 124	M. Aaboud <i>et al.</i>	(ATLAS Collab.)	REFID=59684
AABOUD	19U	JHEP 1905 141	M. Aaboud <i>et al.</i>	(ATLAS Collab.)	REFID=59685
AAD	19A	PL B798 134949	G. Aad <i>et al.</i>	(ATLAS Collab.)	REFID=59981
SIRUNYAN	19	PL B788 7	A.M. Sirunyan <i>et al.</i>	(CMS Collab.)	REFID=59412
SIRUNYAN	19AB	JHEP 1904 112	A.M. Sirunyan <i>et al.</i>	(CMS Collab.)	REFID=59674
SIRUNYAN	19AF	JHEP 1906 093	A.M. Sirunyan <i>et al.</i>	(CMS Collab.)	REFID=59691
SIRUNYAN	19AJ	EPJ C79 94	A.M. Sirunyan <i>et al.</i>	(CMS Collab.)	REFID=59703
SIRUNYAN	19AT	EPJ C79 421	A.M. Sirunyan <i>et al.</i>	(CMS Collab.)	REFID=59725
SIRUNYAN	19AX	PL B791 96	A.M. Sirunyan <i>et al.</i>	(CMS Collab.)	REFID=59745
SIRUNYAN	19BA	PL B792 369	A.M. Sirunyan <i>et al.</i>	(CMS Collab.)	REFID=59752
SIRUNYAN	19BE	PRL 122 121803	A.M. Sirunyan <i>et al.</i>	(CMS Collab.)	REFID=59768
SIRUNYAN	19BK	PR D99 092005	A.M. Sirunyan <i>et al.</i>	(CMS Collab.)	REFID=59875
SIRUNYAN	19BL	PR D99 112003	A.M. Sirunyan <i>et al.</i>	(CMS Collab.)	REFID=59886
SIRUNYAN	19BO	PL B793 520	A.M. Sirunyan <i>et al.</i>	(CMS Collab.)	REFID=59927
SIRUNYAN	19BR	PL B797 134811	A.M. Sirunyan <i>et al.</i>	(CMS Collab.)	REFID=59934
SIRUNYAN	19BY	PR D100 072007	A.M. Sirunyan <i>et al.</i>	(CMS Collab.)	REFID=60014
SIRUNYAN	19BZ	PR D100 112002	A.M. Sirunyan <i>et al.</i>	(CMS Collab.)	REFID=60038
SIRUNYAN	19CG	JHEP 1910 139	A.M. Sirunyan <i>et al.</i>	(CMS Collab.)	REFID=60087
SIRUNYAN	19E	PRL 122 021801	A.M. Sirunyan <i>et al.</i>	(CMS Collab.)	REFID=59555
SIRUNYAN	19H	JHEP 1901 040	A.M. Sirunyan <i>et al.</i>	(CMS Collab.)	REFID=59630
SIRUNYAN	19L	JHEP 1901 183	A.M. Sirunyan <i>et al.</i>	(CMS Collab.)	REFID=59634
SIRUNYAN	19R	JHEP 1903 026	A.M. Sirunyan <i>et al.</i>	(CMS Collab.)	REFID=59655

AABOUD	18	PL B776 318	M. Aaboud <i>et al.</i>	(ATLAS Collab.)	REFID=58621
AABOUD	18AC	PR D97 072003	M. Aaboud <i>et al.</i>	(ATLAS Collab.)	REFID=58991
AABOUD	18AJ	JHEP 1803 095	M. Aaboud <i>et al.</i>	(ATLAS Collab.)	REFID=59087
AABOUD	18AU	JHEP 1807 127	M. Aaboud <i>et al.</i>	(ATLAS Collab.)	REFID=59128
Also		JHEP 2312 158 (errat.)	M. Aaboud <i>et al.</i>	(ATLAS Collab.)	REFID=62575
AABOUD	18BK	PL B784 173	M. Aaboud <i>et al.</i>	(ATLAS Collab.)	REFID=59293
AABOUD	18BL	PL B786 134	M. Aaboud <i>et al.</i>	(ATLAS Collab.)	REFID=59294
AABOUD	18BM	PL B784 345	M. Aaboud <i>et al.</i>	(ATLAS Collab.)	REFID=59295
AABOUD	18BN	PL B786 59	M. Aaboud <i>et al.</i>	(ATLAS Collab.)	REFID=59290
AABOUD	18BO	PR D98 052005	M. Aaboud <i>et al.</i>	(ATLAS Collab.)	REFID=59291
AABOUD	18BP	PL B786 223	M. Aaboud <i>et al.</i>	(ATLAS Collab.)	REFID=59297
AABOUD	18BQ	PR D98 052003	M. Aaboud <i>et al.</i>	(ATLAS Collab.)	REFID=59298
AABOUD	18BU	EPJ C78 1007	M. Aaboud <i>et al.</i>	(ATLAS Collab.)	REFID=59333
AABOUD	18CA	JHEP 1810 180	M. Aaboud <i>et al.</i>	(ATLAS Collab.)	REFID=59356
AABOUD	18CG	PL B786 114	M. Aaboud <i>et al.</i>	(ATLAS Collab.)	REFID=59405
AABOUD	18CQ	PRL 121 191801	M. Aaboud <i>et al.</i>	(ATLAS Collab.)	REFID=59529
AABOUD	18CW	JHEP 1811 040	M. Aaboud <i>et al.</i>	(ATLAS Collab.)	REFID=59567
AABOUD	18M	PRL 120 211802	M. Aaboud <i>et al.</i>	(ATLAS Collab.)	REFID=58831
AABOUD	18T	PR D97 072016	M. Aaboud <i>et al.</i>	(ATLAS Collab.)	REFID=58927
AAIJ	18AM	EPJ C78 1008	R. Aaij <i>et al.</i>	(LHCb Collab.)	REFID=59334
AALTONEN	18C	PR D98 072002	T. Aaltonen <i>et al.</i>	(CDF Collab.)	REFID=59454
SIRUNYAN	18A	PL B778 101	A.M. Sirunyan <i>et al.</i>	(CMS Collab.)	REFID=58627
SIRUNYAN	18AE	PL B780 501	A.M. Sirunyan <i>et al.</i>	(CMS Collab.)	REFID=59010
SIRUNYAN	18BD	JHEP 1806 101	A.M. Sirunyan <i>et al.</i>	(CMS Collab.)	REFID=59116
SIRUNYAN	18BH	JHEP 1806 001	A.M. Sirunyan <i>et al.</i>	(CMS Collab.)	REFID=59124
SIRUNYAN	18BQ	JHEP 1808 066	A.M. Sirunyan <i>et al.</i>	(CMS Collab.)	REFID=59144
SIRUNYAN	18BU	EPJ C78 140	A.M. Sirunyan <i>et al.</i>	(CMS Collab.)	REFID=59154
SIRUNYAN	18BV	EPJ C78 291	A.M. Sirunyan <i>et al.</i>	(CMS Collab.)	REFID=59173
SIRUNYAN	18DB	PRL 121 121801	A.M. Sirunyan <i>et al.</i>	(CMS Collab.)	REFID=59308
SIRUNYAN	18DQ	JHEP 1811 152	A.M. Sirunyan <i>et al.</i>	(CMS Collab.)	REFID=59366
SIRUNYAN	18DS	JHEP 1811 185	A.M. Sirunyan <i>et al.</i>	(CMS Collab.)	REFID=59368
SIRUNYAN	18E	PRL 120 071802	A.M. Sirunyan <i>et al.</i>	(CMS Collab.)	REFID=58729
SIRUNYAN	18F	JHEP 1801 054	A.M. Sirunyan <i>et al.</i>	(CMS Collab.)	REFID=58787
SIRUNYAN	18L	PRL 120 231801	A.M. Sirunyan <i>et al.</i>	(CMS Collab.)	REFID=58837
SIRUNYAN	18S	PR D97 092005	A.M. Sirunyan <i>et al.</i>	(CMS Collab.)	REFID=58938
SIRUNYAN	18Y	PL B779 283	A.M. Sirunyan <i>et al.</i>	(CMS Collab.)	REFID=59001
AABOUD	17AW	JHEP 1710 112	M. Aaboud <i>et al.</i>	(ATLAS Collab.)	REFID=58335
AABOUD	17BA	JHEP 1712 024	M. Aaboud <i>et al.</i>	(ATLAS Collab.)	REFID=58352
AABOUD	17BD	EPJ C77 765	M. Aaboud <i>et al.</i>	(ATLAS Collab.)	REFID=58360
AABOUD	17CO	JHEP 1710 132	M. Aaboud <i>et al.</i>	(ATLAS Collab.)	REFID=59637
AABOUD	17Y	PRL 119 051802	M. Aaboud <i>et al.</i>	(ATLAS Collab.)	REFID=57947
AAD	17	EPJ C77 70	G. Aad <i>et al.</i>	(ATLAS Collab.)	REFID=57780
KHACHATRY...	17F	JHEP 1702 135	V. Khachatryan <i>et al.</i>	(CMS Collab.)	REFID=57781
SIRUNYAN	17AM	PL B775 1	A.M. Sirunyan <i>et al.</i>	(CMS Collab.)	REFID=58295
SIRUNYAN	17AV	JHEP 1711 047	A.M. Sirunyan <i>et al.</i>	(CMS Collab.)	REFID=58345
SIRUNYAN	17CN	PR D96 072004	A.M. Sirunyan <i>et al.</i>	(CMS Collab.)	REFID=58658
AABOUD	16I	PR D94 052002	M. Aaboud <i>et al.</i>	(ATLAS Collab.)	REFID=57426
AABOUD	16K	PRL 117 111802	M. Aaboud <i>et al.</i>	(ATLAS Collab.)	REFID=57462
AABOUD	16X	JHEP 1611 112	M. Aaboud <i>et al.</i>	(ATLAS Collab.)	REFID=57661
AAD	16	PL B753 69	G. Aad <i>et al.</i>	(ATLAS Collab.)	REFID=57004
AAD	16AC	PR D93 092005	G. Aad <i>et al.</i>	(ATLAS Collab.)	REFID=57281
AAD	16AF	JHEP 1601 172	G. Aad <i>et al.</i>	(ATLAS Collab.)	REFID=57316
AAD	16AL	JHEP 1605 160	G. Aad <i>et al.</i>	(ATLAS Collab.)	REFID=57334
AAD	16AN	JHEP 1608 045	G. Aad <i>et al.</i>	(ATLAS and CMS Collabs.)	REFID=57343
AAD	16AO	JHEP 1608 104	G. Aad <i>et al.</i>	(ATLAS Collab.)	REFID=57346
AAD	16BL	EPJ C76 658	G. Aad <i>et al.</i>	(ATLAS Collab.)	REFID=57683
AAD	16K	EPJ C76 6	G. Aad <i>et al.</i>	(ATLAS Collab.)	REFID=57029
KHACHATRY...	16AB	PL B759 672	V. Khachatryan <i>et al.</i>	(CMS Collab.)	REFID=57240
KHACHATRY...	16AR	JHEP 1604 005	V. Khachatryan <i>et al.</i>	(CMS Collab.)	REFID=57325
KHACHATRY...	16AU	JHEP 1606 177	V. Khachatryan <i>et al.</i>	(CMS Collab.)	REFID=57339
KHACHATRY...	16B	PL B753 341	V. Khachatryan <i>et al.</i>	(CMS Collab.)	REFID=57005
KHACHATRY...	16BA	JHEP 1609 051	V. Khachatryan <i>et al.</i>	(CMS Collab.)	REFID=57356
KHACHATRY...	16BQ	PR D94 052012	V. Khachatryan <i>et al.</i>	(CMS Collab.)	REFID=57433
KHACHATRY...	16CD	PL B763 472	V. Khachatryan <i>et al.</i>	(CMS Collab.)	REFID=57698
KHACHATRY...	16G	EPJ C76 13	V. Khachatryan <i>et al.</i>	(CMS Collab.)	REFID=57026
AAD	15	PL B740 222	G. Aad <i>et al.</i>	(ATLAS Collab.)	REFID=56266
AAD	15AA	PR D92 012006	G. Aad <i>et al.</i>	(ATLAS Collab.)	REFID=56593
AAD	15AH	JHEP 1504 117	G. Aad <i>et al.</i>	(ATLAS Collab.)	REFID=56619
AAD	15AQ	JHEP 1508 137	G. Aad <i>et al.</i>	(ATLAS Collab.)	REFID=56647
AAD	15AX	EPJ C75 231	G. Aad <i>et al.</i>	(ATLAS Collab.)	REFID=56665
AAD	15B	PRL 114 191803	G. Aad <i>et al.</i>	(ATLAS and CMS Collabs.)	REFID=56434
AAD	15BC	EPJ C75 349	G. Aad <i>et al.</i>	(ATLAS Collab.)	REFID=56670
AAD	15BD	EPJ C75 337	G. Aad <i>et al.</i>	(ATLAS Collab.)	REFID=56671
AAD	15BE	EPJ C75 335	G. Aad <i>et al.</i>	(ATLAS Collab.)	REFID=56672
AAD	15CE	PR D92 092004	G. Aad <i>et al.</i>	(ATLAS Collab.)	REFID=56909
AAD	15CI	EPJ C75 476	G. Aad <i>et al.</i>	(ATLAS Collab.)	REFID=56936
Also		EPJ C76 152 (errat.)	G. Aad <i>et al.</i>	(ATLAS Collab.)	REFID=57367
AAD	15CX	JHEP 1511 206	G. Aad <i>et al.</i>	(ATLAS Collab.)	REFID=59980
AAD	15F	PR D91 012006	G. Aad <i>et al.</i>	(ATLAS Collab.)	REFID=56421
AAD	15G	JHEP 1501 069	G. Aad <i>et al.</i>	(ATLAS Collab.)	REFID=56424
AAD	15I	PRL 114 121801	G. Aad <i>et al.</i>	(ATLAS Collab.)	REFID=56444
AAD	15P	PRL 115 091801	G. Aad <i>et al.</i>	(ATLAS Collab.)	REFID=56492
AAD	15T	PL B749 519	G. Aad <i>et al.</i>	(ATLAS Collab.)	REFID=56546
AALTONEN	15	PRL 114 151802	T. Aaltonen <i>et al.</i>	(CDF and D0 Collabs.)	REFID=56464
AALTONEN	15B	PRL 114 141802	T. Aaltonen <i>et al.</i>	(CDF Collab.)	REFID=56465
KHACHATRY...	15AM	EPJ C75 212	V. Khachatryan <i>et al.</i>	(CMS Collab.)	REFID=56657
KHACHATRY...	15AN	EPJ C75 251	V. Khachatryan <i>et al.</i>	(CMS Collab.)	REFID=56658
KHACHATRY...	15BA	PR D92 072010	V. Khachatryan <i>et al.</i>	(CMS Collab.)	REFID=56895
KHACHATRY...	15H	PL B744 184	V. Khachatryan <i>et al.</i>	(CMS Collab.)	REFID=56505
KHACHATRY...	15Q	PL B749 337	V. Khachatryan <i>et al.</i>	(CMS Collab.)	REFID=56530
KHACHATRY...	15Y	PR D92 012004	V. Khachatryan <i>et al.</i>	(CMS Collab.)	REFID=56538
KHACHATRY...	15Z	PR D92 032008	V. Khachatryan <i>et al.</i>	(CMS Collab.)	REFID=56539
AAD	14AR	PL B738 234	G. Aad <i>et al.</i>	(ATLAS Collab.)	REFID=56125

AAD	14AS	PL B738 68	G. Aad <i>et al.</i>	(ATLAS Collab.)	REFID=56127
AAD	14BC	PR D90 112015	G. Aad <i>et al.</i>	(ATLAS Collab.)	REFID=56286
AAD	14BJ	JHEP 1409 112	G. Aad <i>et al.</i>	(ATLAS Collab.)	REFID=57146
AAD	14J	PL B732 8	G. Aad <i>et al.</i>	(ATLAS Collab.)	REFID=55769
AAD	14O	PRL 112 201802	G. Aad <i>et al.</i>	(ATLAS Collab.)	REFID=55849
AAD	14W	PR D90 052004	G. Aad <i>et al.</i>	(ATLAS Collab.)	REFID=55885
ABAZOV	14F	PRL 113 161802	V.M. Abazov <i>et al.</i>	(D0 Collab.)	REFID=56106
CHATRCHYAN	14AA	PR D89 092007	S. Chatrchyan <i>et al.</i>	(CMS Collab.)	REFID=56033
CHATRCHYAN	14AI	PR D89 012003	S. Chatrchyan <i>et al.</i>	(CMS Collab.)	REFID=56422
CHATRCHYAN	14AJ	NATP 10 557	S. Chatrchyan <i>et al.</i>	(CMS Collab.)	REFID=56423
CHATRCHYAN	14B	EPJ C74 2980	S. Chatrchyan <i>et al.</i>	(CMS Collab.)	REFID=55703
CHATRCHYAN	14G	JHEP 1401 096	S. Chatrchyan <i>et al.</i>	(CMS Collab.)	REFID=55713
CHATRCHYAN	14K	JHEP 1405 104	S. Chatrchyan <i>et al.</i>	(CMS Collab.)	REFID=55733
KHACHATRY...	14D	PL B736 64	V. Khachatryan <i>et al.</i>	(CMS Collab.)	REFID=55758
KHACHATRY...	14H	JHEP 1409 087	V. Khachatryan <i>et al.</i>	(CMS Collab.)	REFID=56014
KHACHATRY...	14P	EPJ C74 3076	V. Khachatryan <i>et al.</i>	(CMS Collab.)	REFID=56183
AAD	13AJ	PL B726 120	G. Aad <i>et al.</i>	(ATLAS Collab.)	REFID=55095
AAD	13AK	PL B726 88	G. Aad <i>et al.</i>	(ATLAS Collab.)	REFID=55096
Also		PL B734 406 (errat.)	G. Aad <i>et al.</i>	(ATLAS Collab.)	REFID=57144
AALTONEN	13L	PR D88 052013	T. Aaltonen <i>et al.</i>	(CDF Collab.)	REFID=55191
AALTONEN	13M	PR D88 052014	T. Aaltonen <i>et al.</i>	(CDF and D0 Collabs.)	REFID=55192
ABAZOV	13L	PR D88 052011	V.M. Abazov <i>et al.</i>	(D0 Collab.)	REFID=55189
CHATRCHYAN	13BK	PL B726 587	S. Chatrchyan <i>et al.</i>	(CMS Collab.)	REFID=55436
CHATRCHYAN	13J	PRL 110 081803	S. Chatrchyan <i>et al.</i>	(CMS Collab.)	REFID=54942
CHATRCHYAN	13X	JHEP 1305 145	S. Chatrchyan <i>et al.</i>	(CMS Collab.)	REFID=55031
CHATRCHYAN	13Y	JHEP 1306 081	S. Chatrchyan <i>et al.</i>	(CMS Collab.)	REFID=55035
HEINEMEYER	13A	arXiv:1307.1347	S. Heinemeyer <i>et al.</i>	(LHC Higgs CS Working Group)	REFID=57159
AAD	12AI	PL B716 1	G. Aad <i>et al.</i>	(ATLAS Collab.)	REFID=54198
AAD	12DA	SCI 338 1576	G. Aad <i>et al.</i>	(ATLAS Collab.)	REFID=54986
AALTONEN	12Q	PRL 109 111803	T. Aaltonen <i>et al.</i>	(CDF Collab.)	REFID=54246
AALTONEN	12R	PRL 109 111804	T. Aaltonen <i>et al.</i>	(CDF Collab.)	REFID=54247
AALTONEN	12S	PRL 109 111805	T. Aaltonen <i>et al.</i>	(CDF Collab.)	REFID=54248
AALTONEN	12T	PRL 109 071804	T. Aaltonen <i>et al.</i>	(CDF and D0 Collabs.)	REFID=54249
ABAZOV	12K	PL B716 285	V.M. Abazov <i>et al.</i>	(D0 Collab.)	REFID=54187
ABAZOV	12O	PRL 109 121803	V.M. Abazov <i>et al.</i>	(D0 Collab.)	REFID=54211
ABAZOV	12P	PRL 109 121804	V.M. Abazov <i>et al.</i>	(D0 Collab.)	REFID=54212
CHATRCHYAN	12BY	SCI 338 1569	S. Chatrchyan <i>et al.</i>	(CMS Collab.)	REFID=54987
CHATRCHYAN	12N	PL B716 30	S. Chatrchyan <i>et al.</i>	(CMS Collab.)	REFID=54181
DITTMAYER	12	arXiv:1201.3084	S. Dittmaier <i>et al.</i>	(LHC Higgs CS Working Group)	REFID=57158
DITTMAYER	11	arXiv:1101.0593	S. Dittmaier <i>et al.</i>	(LHC Higgs CS Working Group)	REFID=57157